Nanostructured silver-based bacteriophobic surfaces against catheter-associated urinary tract infections

María Cristina García Bonillo

UNIVERSITAT RAMON LLULL

DOCTORAL THESIS

Title	Nanostructured silver-based bacteriophobic surfaces against catheter-associated urinary tract infections.
Presented by	Cristina García Bonillo
Centre	IQS School of Engineering
Department	Bioengineering
Directed by	Dr. Salvador Borrós Gómez

This page left blank intentionally

A mi abuelo,

ojalá y este catéter te hubiese llegado a tiempo.

This page left blank intentionally

ACKNOWLEDGMENTS

The following paragraphs have been written in Spanish with *manchego* feelings, for a better expression of the author. Sorry for the local expressions, they come from my heart.

El primero en aparecer en estas líneas es, y debe ser, el Dr. Borrós. **Salvador**, muchísimas gracias por regalarme la entrada a DisneyLand. No tengo suficientes palabras para poder agradecerte la confianza que depositaste en mí, la niña de Tractivus que decía que quería hacer el doctorado, hace ya unos cuantos años. De ti me llevo mucho más que la dirección de una tesis apasionante, me llevo el espíritu emprendedor y el saber confiar en las personas, la honradez y dedicación, la resolución de conflictos infantiles sin perder la ilusión por el trabajo, el levantarse cada día con ganas de ayudar a otros a formarse, a realizarse y a vivir investigando, pero, sobre todo, enseñando. Me llevo broncas, merecidas y formadoras, pero también risas y mucho mucho *micromanagement*. Sé que has peleado por mí lo indecible, lo sé sin que me lo hayas dicho jamás, porque nunca cuentas lo mucho que te desvives por tus doctorandos y los dolores de cabeza (y cantidad de papeleo) que te damos, GRACIAS en mi nombre y en el del resto. Espero que el camino que vas a recorrer como Director te traiga todo lo bueno que mereces. He sido muy afortunada de encontrarte y de que me dejases pertenecer a GEMAT.

GEMAT no es un grupo de investigación, es una casa y una gran, atemporal y dispersa familia. El primer día bajas a la salita y encuentras un montón de gente que te mira preguntándose qué frikada vas a emprender. Estoy muy orgullosa de mi *familia del lab*, porque, aunque sepan que la vas a liar, aunque tengan cientos de cosas que hacer, estén a mitad de escribir un *paper*, la tesis o con tres centrífugas puestas a la vez, dejan a un lado sus tareas y te ayudan. Te ayudan a entender, a encontrar, a pedir, a organizar o a reír, te dan un abrazo cuando te hace falta. Este párrafo no es para nadie, esto es para GEMAT. **Que jamás se pierda este espíritu en el grupo**.

Robert, Joan, me habéis apoyado en todo desde mis inicios, me habéis educado y lanzado, me habéis visto llorar de pena, de ansiedad y de emoción, pero mucho más hemos reído. Juntos hemos ganado concursos, hemos dado charlas, hemos corrido muchísimo para llegar y hemos llegado. Hemos publicado, no hemos dormido y nos han dado ataques de corazón. Hemos trasladado cerdos juntos. Vosotros dos no lo sabéis, pero me habéis acompañado en dos de los peores momentos que he pasado en mi corta vida. Me disteis un beso y un abrazo largo y de corazón cuando mis padres estaban demasiado lejos como para hacerlo, todo sin dejar de hacerme reír y olvidar. Y esto son cosas que no podré pagar jamás, ni siquiera con manolitos.

Robert, mereces ser el primero solo por las horas de psicólogo gratuito que me has ofrecido. Años volviendo del lab juntos han hecho que las conversaciones que siempre empiezan con comida y restaurantes deriven en confesiones de vida bastante profundas y planes de futuro. Gracias por enseñarme tanto sobre química, clases y pasión, humor productivo, juegos y amistad. Gracias por ayudarme a elegir las batallas que debo luchar y por darme el empujón que me hace falta siempre. Gracias por esa empatía que te obliga a no descansar hasta que yo, y todos los demás, estamos bien. Gracias por luchar esta tesis. Gracias por ser mi mentor.

Joan, eres mi referente de esfuerzo y dedicación pasional. De la consecución de un objetivo sin importar los obstáculos y las noches en vela. Gracias por brindarme la oportunidad de formar parte de tu ilusión, de esta empresa que has construido proyecto a proyecto, drama a drama. Gracias por enseñarme tanto sobre lo *cutre* de la vida, de catalán, del trabajo y del *down Diagonal*. Siempre tendré todo tu refranero en la cabeza, para cada situación de la vida en la que necesite ser valiente, ser más fuerte o ser políticamente incorrecta. Gracias por todas las oportunidades que me has regalado, espero haberlas aprovechado bien.

A **Tractivus** y toda la gente que ha pasado por él; Coral, tú siempre serás mi compañera, aunque cambies de trabajo y de tesis veinte veces. Aunque me llames vieja y sosa, te he cogido un cariño brutal. Te admiro muchísimo, tanto científica como personalmente. Tienes que enseñarme a sacar ese genio consiguiendo que así te quieran más. Eres la heredera, tenlo en mente y sigue luchando mucho. Elena, gracias por ser mi compañera *marketiniana*, las mejores rrpp de la historia. Gracias por las conversaciones sinceras y por aguantarme tanto los dramas. Me has enseñado muchísimo, admiro mucho tu paciencia laboral y ética. Espero poder reírme muchos años más a tu lado. Ari, gracias por las charlas de campana y la sincera amistad que surgió entre galletas y bacterias. A Peri, porque fue *Tractiboy* brevemente y en qué mejor párrafo podría darle yo las gracias por sus consejos científicos y de vida, sus bromas, sus bailes en Rumanía y sus *solo una copita después de cenar y nos vamos ¡oh, son las 6!* Gracias por hacerme sentir parte de todo. A Xavi, gracias a *tu paso por Tractivus* me reí mucho contigo, pero aún hoy te mataba. Y, por último, al *summer camp* y todos los prácticum porque, pese a que los buenos se iban con Robert, disfruté mucho de la experiencia de hacer entender la importancia de la investigación a los chavales.

Dentro de la ***GEMATOfamily*** no pueden faltar las *tietas.* Gracias Nuria, gracias Marina por vuestra santa paciencia conmigo. He disfrutado muchísimo de las charlas que comenzaban con un problema, pasan por una queja y acababan arreglando el mundo (o arrasando con todo él).

Me habéis ayudado siempre en todo lo que ha estado en vuestra mano y no me refiero sólo a equipos y materiales. Muchas gracias por todo el apoyo, las risas y el cariño. Gracias Cris F., por estar siempre dispuesta a ofrecer ayuda, consejo y probar cualquier cosa que se nos pasa por la cabeza, a ver qué sale. Por los cafés y cotilleos, por los dramas bien resueltos y los vinos, por bailar y demostrar a todas las niñas que pasan por el grupo que se tiene que decir *aquí estoy yo*. Gracias por tu tiempo, es valiosísimo para mí que lo gastes conmigo.

Gracias a mis **compañeras** de tesis y de cerves para respirar, a mis compis de tarima. Me acogisteis con los brazos abiertos desde el primer día y me enseñasteis IQS con una sonrisa. Alba, gracias por poner a todos los demás, su bienestar y felicidad, por delante de ti. Gracias por no echarme de tu sitio el día que llegué. Gracias por cada una de las charlas y de los bailes. Gracias por hacernos ir a Rumanía, qué escalera, qué parques y qué risa. Cuando te fuiste se nos apagó la lucecita más pequeña y que más brillaba de todo GEMAT. Laura B., gracias por enseñarme a luchar con cabezonería cada una de las metas que nos propongamos. Por mostrarme que se puede ser fuerte, tener genio, dejar las cosas *claritas* y ser muy muy querida. Eres la cotilla con más talento que he conocido jamás, gracias por los cuchicheos. Nunu, nos ha quedado pendiente la *performance* pero sé que volveremos a vernos y reivindicaremos como nunca contra todas las injusticias del mundo. Gracias por todos los consejos y las horas de psicología, siempre tendrás mi ayuda para lo que sea. Mire S., gracias por sacarme del sótano, por los bailes con muleta, los bailes con botella y los bailes con abrazo. Patri, me he reído tanto contigo y todas las locuras que te rodean que no sabría ni por dónde empezar. Gracias por compartir con nosotros tus experiencias y por dejar que te saquemos de los sitios antes de que nos peguen. Anna Mas, gracias por haber sido mi referente en tantas cosas, por ayudar en todo siempre; en papeleos, en experimentos, en experiencias. Sentaste las bases de cómo debía ser este matriarcado que es biomat, es un honor haber heredado tu silla.

A los **chicos** de mi vida doctoral, a mis compañeros de salita, Torreta, gallego y Fira, en ese orden. Tito y Germán, debéis ir en pack porque en pack os conocí y así os sigo viendo. Gracias por enseñarme que la ciencia tiene más de ingenio y creatividad de lo que muchos creen. Que los problemas se solucionan cantando, bailando y abrazando. Tito, me debes una barbacoa. Germán, siempre serás un admirable artesano y artista para mí. Pol, siempre serás mi presidente. Muchas gracias por arrancarnos de la silla para aportar algo a IQS, mover a los doctorandos y ayudarme a crear amistades. Gracias por estar siempre dispuesto a *hacer cosas de ciencia y a ver qué sale* con nosotros. Aunque no salga. Mario, creo que no hemos coincidido ni tres horas en el laboratorio, pero las horas de fuera nos han cundido. Gracias por las charlas

y tu visión del mundo, por los futbolines y la bachata. Por tirarme al suelo tantas veces (y luego ir a recogerme). A Toni, Antonio, gracias por traerme el espíritu manchego cuando más falta me hace recordar mi casa. Gracias por compartir tanto conmigo, por las conversaciones y el intento de arreglar el mundo, espero que algún día podamos aportar algo para mejorarlo un pelín. No pierdas a la gitana que llevas dentro nunca. Quizá debí ponerte en el párrafo Tractivus.

Gracias a *las noches con Peri* no he salido loca.

Y por último las recientes incorporaciones. Gracias a todos los que hacéis que GEMAT continúe su camino. Grazie Roberta, por tus bizcochos de los lunes, nos haces a todos la semana más fácil. Por haber traído la biotecnología al grupo y haberla puesto a la altura, *anche se non ti piacciono le donne grasse*. Laura O., Gloria y Mónica, bienvenidas al grupo. Estoy muy contenta de teneros conmigo y espero que disfrutéis de estos años tanto como lo he hecho yo. Disfrutad cada ratito allí arriba o aquí abajo, que luego toca escribir.

A los **seniors** del grupo, Víctor Ramos, Marta G., Benjamí y Martí, gracias por enseñarnos los pasitos que hay que dar para llegar a ser todo lo que las palabras *científico y profesor* suponen. Gracias a todo Sagetis, a Elena, Miguel Ángel e Irene sobre todo, por las horas y consejos de la experiencia. Gracias a la Dra. Agut por dejarme utilizar sus instalaciones con tanto cariño durante años, al Dr. Colominas por las horas de ICP (interminables) al Dr. Abellà por acceder a meter en su SEM cualquier cosa que le lleváramos, al Dr. Gulías por acogerme en sus laboratorios y asignaturas y formarme como pseudoprofe y a la Dra. Verdaguer por enseñarnos a hacer rectas como Dios manda. Gracias también al personal técnico que ha ayudado en esta tesis, porque, aunque *sea su trabajo*, existen las personas que te reciben con una sonrisa, con emoción y cariño y las que sólo *hacen* su trabajo. A Emma Rossinyol, por las horas de FE-SEM y a Estefanía Contreras, por el cuidado de los animales del *in* vivo con tanto amor y respeto.

A *mis* cerdas, especialmente a Bimba y Lola, por dar su vida por esta tesis. Gracias a todas las cerditas que fueron sacrificadas para que la ingeniería de materiales avanzase un pasito y estemos un poquito más cerca de olvidar las CAUTI. Me acordaré toda la vida de ese *in vivo*, de los nervios, del querer hacerlo todo perfecto, del traslado de cerdos, de soñar que no sale, del chorro de pis, del coser y cateterizar en tiempo récord, de las 876 placas y del pensar que la vida de estos animales tuviese un significado. Gracias muy sinceras a todos los animales que sirven a la ciencia.

To Alexandra Asanovna Elbakyan, for giving me the tool to access knowledge, which should be free and accessible to the entire planet. This thesis would not be possible without her work.

Pese a que este trabajo ha sido realizado en este ambiente y gracias a toda esta gente, fuera de IQS he tenido apoyos gigantes que no podía dejar de mencionar. Gente que he tenido la increíble suerte de conocer a lo largo de los años y que me han hecho llegar hasta Barcelona y hasta este centro, a empujones y tirones, y que han hecho que me quede en él hasta poder estar orgullosa de mi trabajo.

A los **Hulios**, la familia catalana. Gracia a todos por hacerme sentir parte vuestra locura. Por las cenas y los encuentros en las terrazas, los juegos cooperativos, y esos desnudos espontáneos tan vuestros. A Ale, Geno, Sara, Óscar, Sergio, Gala, Pedro y Eva, gracias por todos los Viñas y perreos del mundo. Gracias a Sandra y Álvaro especialmente, por hacerme sentir amiga y comprendida.

A la **Xixofamily**, por hacerme sentir la acoplada más querida del mundo. Gracias por cada navidad, por cada baile, cada limbo y cada copa. Por tener conversaciones cada día, por sabernos amigos eternos pese a la distancia y los meses sin vernos. Sergio, gracias por escucharme, por animarme a todo pese a ese espíritu derrotista nuestro que a la vez es tan creativo. Gracias Luis, por ser mi vecino favorito, por abrazarme cuando hueles que lo necesito y arrancarme una sonrisa siempre. A mi Antón, no te daré las gracias por los audios, pero sí por tus conversaciones. Gracias por poner palabras a lo que ambos hemos sentido más de una vez. Sara, gracias por estar siempre siempre siempre dispuesta por y para todos. Te admiro muchísimo. Gracias Bea, por transmitirme tu pasión por esta profesión pese a todo lo que se deba sacrificar. Sois el ejemplo de mujer científica que querría dar a mis hijas.

A **Andrea** y **Jose**, porque sin ellos dos y sin aquellas tardes de biblioteca riéndonos, llorando y comiendo yo no estaría hoy a punto de defender esta tesis. Gracias por vuestros empujones y confianza. Gracias por cada viaje, por saber mantener la amistad pese a todo lo que se nos ha puesto en contra. Aquella *hasienda* sigue viva.

A **mis amigas**, sin nombre de grupo, sin apellidos ni motes porque fueron las primeras, las que siempre han estado ahí, las del pueblo, las de toda mi vida. Esta tesis es para Caribel, Eva, Bea, Carmen, Ángela, María y Graciela. Porque desde los 13 años (incluso desde los 3) habéis sido mi refugio y mi confesionario. Habéis sufrido cada drama de esta tesis conmigo, habéis escuchado y leído mis discursos con amor y paciencia. Siempre me habéis dado ánimos, siempre

habéis tenido detallazos conmigo, siempre me habéis abrazado y sonreído al verme volver. Os habéis alegrado de mis logros y habéis amortiguado mis fracasos. Habéis estado conmigo en hospitales, en fiestas y en todos mis pisos. Habéis brindado conmigo y lo seguiremos haciendo muchos años más. Os he sentido muy cerca pese a estar dolorosamente lejos. Gracias chicas, sois de lo mejor que tengo.

Por último, esta tesis es para las personas más importantes que tengo la suerte de tener en mi vida.

A **Manu**. Éstos han sido años raros, difíciles en ciertos momentos y súper felices en otros. Hemos construido dos tesis doctorales a base de horas y esfuerzo común en mitad de una vida un poco truculenta y noticias inesperadas. Hemos escuchado, comentado y debatido cada uno de los experimentos del otro, con mayor o menor dosis de drama, pero siempre con mucho amor de por medio. Has sabido hacerme sonreír cada día y darme un abrazaco cuando hacía falta. Gracias por ser mi compañero en todo momento, por los saltitos felices y los bailes, por las cañas, los sushis y las series. Vamos a por nuestra siguiente etapa, nuestra siguiente aventura y nuestra vida juntos.

A mi **hermana**. Ana, siempre has estado para compartir conmigo todos *los dramas de nuestras vidas*, echarnos una cerveza y reírnos un rato. Has aguantado y apoyado mis eternas chapas científicas sin dormirte, me has visto ensayar todas mis presentaciones sin queja y te has leído mis *papers* sin entenderlos. Tengo una suerte infinita de tenerte y espero que los años nos acerquen mucho más territorialmente, porque de corazón siempre estás conmigo.

Finalmente, **a mis padres**, porque me lo habéis dado todo siempre. Si hoy estoy a punto de defender esta tesis es porque jamás me habéis frenado. Desde que leíamos los primeros comics en el sofá pasando por la PAU y toda la carrera, habéis estado siempre apoyando mis decisiones, trabajando sin descanso para que no me faltase nada y pudiese conseguirlo todo. Habéis llevado mis logros por bandera, como vuestros, felices de que nosotras seamos felices. Sois mi ejemplo de trabajo, esfuerzo y honradez. Sois mi meta por superar. Muchas gracias por estar cerca de mí, aguantando mis monólogos y participando de este trabajo. Espero que siempre estéis orgullosos de vuestras chicas.

This thesis has been made with the support of the Secretariat of Universities and Research of the Business and Knowledge Department of the Government of Catalonia (DI-2016-073), and the support of Laboratorios Rubió, IQS School of Engineering and Tractivus.

This page left blank intentionally.

ABSTRACT

In this thesis, a bacteriophobic urinary Foley catheter has been developed. The bacteriophobic effect is based on a homogeneous super-hydrophobic coating with a specific micro- and nanostructure covered by a homogeneous metallic silver film, which create an uncomfortable environment for bacteria, avoiding bacterial attachment to the surface but without causing any effect on bacterial growth.

To achieve this, a set of super-hydrophobic nanostructured coatings based on different polymers has been developed. Plasma-polymerized pentafluorophenyl methacrylate (pp-PFM) and Polydopamine (PDA) have been used as base polymers, being coated with a thin film of metallic silver. All of them showed a reduction in bacterial adhesion between 4 and 6 orders of magnitude regarding the uncoated PDMS, as well as the ability to repel protein adhesion in *in vitro* tests.

The PDA-silver coating was selected to be implemented on the urinary catheter. This urinary catheter has been shown to maintain the bacteriophobic effect for 30 days *in vitro*, tested with simulation-use tests in flow and static conditions, using uropathogenic bacterial strains and clinical isolates. Moreover, the catheter has been validated *in vivo* using catheterized pigs as animal model for 15 days. During this period, the catheter has been able to maintain bacterial adhesion 2 orders of magnitude lower than commercial standard or antimicrobial catheters.

RESUMEN

En esta tesis se ha desarrollado un catéter urinario tipo Foley bacteriofóbico. El efecto bacteriofóbico se basa en un recubrimiento super-hidrofóbico micro- y nanostructurado con una topografía específica, recubierto por una película de plata metálica homogénea, que crea un ambiente incómodo para las bacterias, evitando la adhesión bacteriana a la superficie, pero sin provocar ningún efecto sobre el crecimiento bacteriano.

Para conseguirlo, se ha generado un conjunto de recubrimientos nanoestructurados super-hidrofóbicos basados en diferentes polímeros. Se han utilizado como polímeros base el metacrilato de pentafluorofenilo polimerizado por plasma (pp-PFM) y la polidopamina (PDA), recubiertos con una fina película de plata metálica. Todos ellos mostraron una reducción en la adhesión bacteriana de entre 4 y 6 órdenes de magnitud con respecto al PDMS sin recubrir, así como la capacidad de repeler la adhesión de proteínas en ensayos in vitro.

El recubrimiento basado en PDA-plata fue seleccionado para ser implementarlo en el catéter urinario. Este catéter urinario ha demostrado mantener el efecto bacteriofóbico durante 30 días in vitro, probado con ensayos de uso simulado en condiciones de flujo y estáticas, utilizando cepas bacterianas uropatógenas y aislados clínicos. Además, el catéter ha sido validado in vivo utilizando cerdos cateterizados como modelo animal durante 15 días. Durante este período, el catéter ha podido mantener la adhesión bacteriana 2 órdenes de magnitud por debajo de los catéteres estándar comerciales y los antimicrobianos.

RESUM

En aquesta tesi s'ha desenvolupat un catèter urinari tipus Foley bacteriofòbic. L'efecte bacteriofòbic es basa en un recobriment superhidrofòbic micro- i nanostructurat amb una topografia específica, recobert per una pel·lícula de plata metàl·lica homogènia, que crea un ambient incòmode per a les bactèries, evitant l'adhesió bacteriana a la superfície, però sense provocar cap efecte sobre el creixement bacterià.

Per aconseguir-ho, s'ha generat un conjunt de recobriments nanoestructurats superhidrofòbics basats en diferents polímers. S'han utilitzat com a polímers base el metacrilat de pentafluorofenil polimeritzat per plasma (pp-PFM) i la polidopamina (PDA), recoberts amb una fina pel·lícula de plata metàl·lica. Tots ells van a mostrar una reducció en l'adhesió bacteriana d'entre 4 i 6 ordres de magnitud respecte a PDMS sense recobriment, així com la capacitat de repel·lir l'adhesió de proteïnes en assajos *in vitro*.

El recobriment basat en PDA-plata va ser seleccionat per implementar-lo en el catèter urinari. Aquest catèter urinari ha demostrat mantenir l'efecte bacteriofòbic durant 30 dies *in vitro*, provat amb assajos d'ús simulat en condicions de fluix i estàtiques, utilitzant ceps bacterians uropatògenics i aïllats clínics. A més, el catèter ha estat validat *in vivo* mitjançant porcs cateteritzats durant 15 dies. Durant aquest període, el catèter ha pogut mantenir l'adhesió bacteriana 2 ordres de magnitud per debat dels catèters estàndard comercials i els antimicrobians

This page left blank intentionally.

TABLE OF CONTENTS

LIST OF FIGURES

LIST OF TABLES

LIST OF EQUATIONS

LIST OF PUBLICATIONS

García-Bonillo, C.; Texidó, R.; Reyes-Carmenaty, G.; Gilabert-Porres, J.; Borrós, S. Study of the Human Albumin Role in the Formation of a Bacterial Biofilm on Urinary Devices Using QCM-D. *ACS Appl. Bio Mater.* **2020**, *3* (5), 3354–3364. https://doi.org/10.1021/acsabm.0c00286.

Garcia-Bonillo, C.; Texido, R.; Gilabert-Porres, J.; Borrós, S. Matar o repel·lir? Superfícies antimicrobianes basades en plata Kill or repel? Silver-based antimicrobial surfaces *Rev. la Soc. Catalana Química* **2020**, *19*, 46.

García-Bonillo, C; Texidó, R; Gilabert-Porres, J; Borrós, S. Nanostructured metallic silver surfaces: Study of bacteriophobic and bacteriostatic effect to avoid bacterial adhesion on medical devices. *Mater Sci Eng C Mater Biol Appl* **2021** (submitted)

LIST OF CONFERENCES

PhD Day GenMicEst (Universitat de Barcelona, 2018) Poster presentation and short talk.

I Jornadas de Doctorands (Insitut Químic de Sarrià, 2019) Poster presentation and short talk, member of organizing committee.

5th International Congress of Bacteria-Material interactions (Stevens Institute of Technology, USA, 2019) Poster presentation, 3rd place best poster award.

Onzena Trobada de Joves Investigadors (EPS, Vilanova i la Geltrú, 2019) Short talk, best conference talk award.

Science outreach talks “Novel antimicrobial surfaces” and “Superbugs, the uncertain future of humanity” with ABSTEC (2019).

LIST OF ABREVIATIONS

AU – Artificial urine

BA – Blood agar medium

BSA – Bovine serum albumin

CA – Chocolate agar medium

CAUTI – Catheter-associated urinary tract infection

CFU – Colony forming unit

D – Dissipation

DA - Dopamine

F – Frequency

FE-SEM – Field Emission Scanning Electron Microscopy

FFT - Fast Fourier Transform

HA – Human albumin

HPLC - High performance liquid chromatography

LB / LB-A – Luria-Bertani broth / agar

MALDI-TOF - Matrix-Assisted Laser Desorption/Ionization with Time-off-flight

MC – MacConkey medium

OD – Optical Density

PBS - Phosphate-Buffered Saline

PDA - Polydopamine

PDMS – Polydimethylsiloxane

PFM – Pentafluorophenyl methacrylate

pp-PFM – plasma polymerized Pentafluorophenyl methacrylate

PS – Polystyrene

PU - Polyurethane

PVC – Poly-vinyl chloride

QCM-D – Quartz Crystal Microbalance with Dissipation monitoring

S / V – Sonication / Vortexing

TSB / TSA – Tryptic soy broth / agar medium

UTI – Urinary Tract Infection

This page left blank intentionally.

Chapter I. Introduction

1.1 MOTIVATION AND AIMS

The development and use of medical devices throughout history has allowed humanity to increase its health and life expectancy. These instruments are used in all fields of medicine, correcting or modifying the structure or function of the body for some health purpose[1]. One of the oldest and most used medical devices are urinary catheters. Urinary catheters, basically, are tubes placed into the body through the urethra to drain and collect urine from the bladder.

For more than 3.500 years, urinary catheters have been used in virtually every healthcare setting and contribute to improvements in patient care by relieving urinary retention[2,3]. The most known design of an urinary catheter is the Foley catheter, which consists in a tube that is inserted through the urethra and is held in the bladder by an inflatable balloon3 (

Figure I. 1).

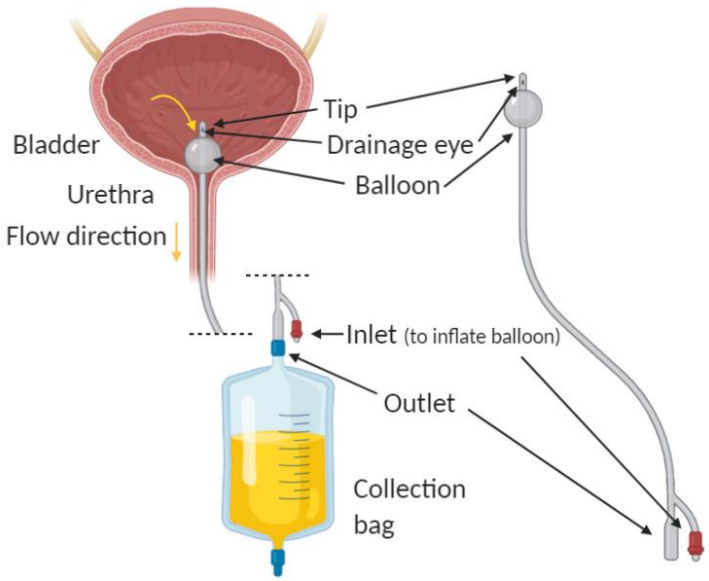

Figure I. 1. Foley catheter. Diagram of two-way Foley catheter inserted through urethra into the bladder. The yellow arrows represent urine flow through the catheter into the external collection bag. Image prepared by the author.

Foley catheters are usually made by materials such as gum-elastic, plastics as poly-vinyl chloride (PVC), polyurethanes (PU), medical silicones (MS) and latex rubbers[4]. These materials have been developed over the years to include most of the desirable characteristics in a urinary

catheter. These characteristics include high tensile strength, soft and pliable in order to provide a high resistant structure to the catheters that being able to resist big weights and torsions without losing their form. Also, an inherently chemical resistant to diverse compounds such as nitrogen or phosphate salts, proteins and cell debris to avoid the catheter occlusion. Finally, the most important urinary catheter's characteristics are the biocompatibility and the ability to meet flow requirements while maintaining a minimally invasive circumference[4,5]. Currently, latex and silicone Foley urinary catheters are most used medical devices and urinary catheterization is probably the most frequent medical act performed in hospitals[6,7]. It is estimated that up to 20 % of patients need this intervention during hospitalization and this number is even higher on surgical wards[6]. Moreover, 4 % in the community have urinary catheters in situ at any given time and its use is gradually growing, due to the increasing elderly, obese and diabetic populations[7,8].

Not surprisingly, catheter-associated urinary tract infection (CAUTI) is the most important disease associated with these devices and the most prevalent cause of hospital-acquired infection with an incidence of 40 % of nosocomial infection[9–11]. Moreover, in the United States 70 to 85 % of complicated urinary tract infections outside of a medical environment are attributable to indwelling catheters, accounting for 1 million cases per year[12]. CAUTI are associated with increased morbidity and mortality, and are collectively the most common cause of secondary bloodstream infections[12]. Although most CAUTIs are asymptomatic becoming in a chronic urinary infection, it is important to highlight the close relationship between symptomatic expression of CAUTI and the increased rate of mortality and morbidity in diabetic, immunocompromised or frail elderly patients[12,13].

Adherence and colonization of urinary catheters is the key event to initiating CAUTI pathogenesis. A urinary infection usually starts with periurethral contamination by an uropathogenic bacteria, followed by colonization of the urethra and subsequent migration of the pathogen to the bladder, an event that requires appendages such as flagella[12]. Uropathogens that cause CAUTI follow the same initial steps. The major route of infection is ascending at the time of insertion of a catheter through the urethra, via mucosal layer. After uropathogens reach the bladder, they can colonize the urothelium and the urinary catheter lumen[10]. Bacteria get a successful colonization owing to the fibrinogen accumulates on the catheter providing an ideal environment for the attachment of uropathogens that express fibrinogen-binding proteins, due to robust immune response induced by catheterization[12–17]. After their initial attachment on catheter surface, bacteria forms biofilm and promotes epithelial damage[12]. The urinary infection is able to reach to kidneys, producing pyelonephritis[16] and, if left untreated, the infection progresses to

sepsis by crossing the tubular epithelial cell barrier[17] normally between 3 to 10 days after catheterization[18] (Figure I. 2). Risk factors to develop early CAUTI, regardless of the patient's main medical condition, are paraplegia, incontinence, cerebrovascular diseases and female sex[19].

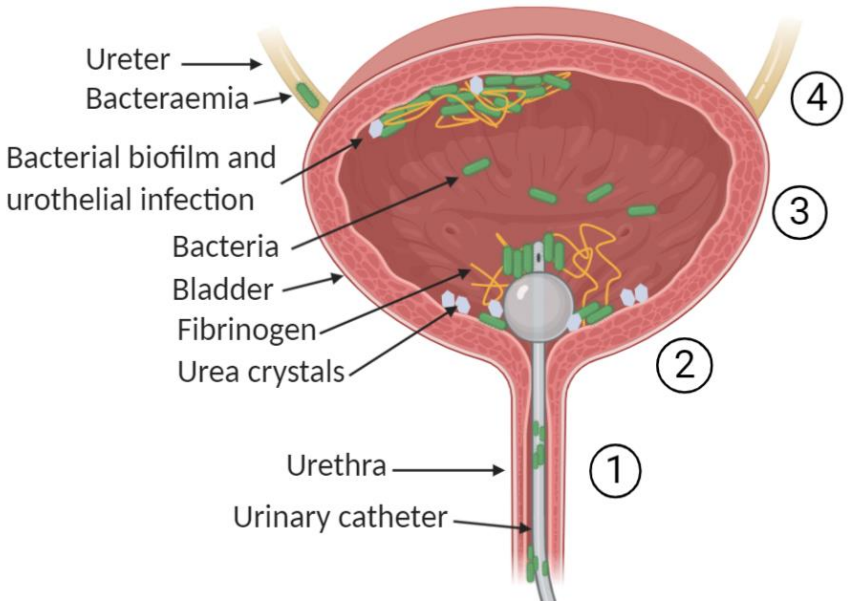

Figure I. 2. Process and pathogenesis of urinary tract infections. 1) Contamination of the periurethral area by catheterization, colonization of the urethra and migration to the bladder. 2) Inflammatory response in the bladder and fibrinogen accumulation in the catheter surface. Colonization of the bladder and catheter surfaces. 3) Urothelial damage and infection. Bacterial multiplication and biofilm formation, catheter lumen obstruction. 4) Bacteraemia. Ascension to the kidneys, sepsis and general infection. Image prepared by the author.

Watching this critical medical situation, CAUTI poses a risk to public health that cost to the health system $ 5.418 per patient on average considering a medium-size hospital, reaching $ 10.197 in patients admitted in intensive care units[20,21]. The cost of treating this infection is due to lengthening the patient's stay in the hospital, incrementing the possibilities to acquire other nosocomial infection or a complication[22].

Actual treatments to fight CAUTI are almost entirely based on antibiotic therapies[17], which are molecules that attack to bacteria by disrupting outer membranes, blocking receptors or dysregulate ion bombs as an example[23,24]. To fight CAUTI, trimethroprim sulfamethoxazole, β-lactamases such as cefotaximases and oxacillinases, ampicilin C-type and carbapenemases are

the most used antibiotics[25]. These antibiotics can be oral or intravenous and treatments last a week at least.

The exclusive use of antibiotics has a problematic issue. Antibiotic resistant is on the rise. Antimicrobial resistance in bacterial pathogens are associated with high morbidity and mortality, especially in gram-negative uropathogenic bacteria[26,27]. Uropathogenic strains are becoming increasingly difficult to treat owing to the widespread emergence of an array of antibiotic resistance mechanisms and the rapid expansion of these genetic elements in hospital enviroments[28–30]. Focusing only in CAUTI, amoxicillin with clavulanic acid, a commonly used antibiotic, showed a high resistance (87.5 %) in treatments carried out in 2013 in catheterized patients, adults or children without discrimination[31]. Treatment failure implies a relapse of the infection. Patients need new treatments and suffer a worsening of their quality of life, involving numerous adverse effects. As there is a shortage of effective therapies, lack of successful prevention measures, and only a few new antibiotics per decade, it is necessary the development of novel treatment or prevention options.

Options to prevent the antibiotics use are currently explored, trying to find new therapies to fight CAUTIs. Some of these new techniques involve antimicrobial peptides[32] or lytic enzymes[33] as direct urethral treatments or embedded into a hydrogel covering urinary devices. In addition, current proposed solutions are based on nanoparticles as antibacterial treatment or attached on catheters surfaces as antibacterial coatings[34–36]. Finally, phagetherapy[37] and vaccination[38] as control or treat CAUTIs are promising strategies but, currently, all of them are in seed-state or they have not been considered general solutions and their use is reduced to specific applications or for research purposes[33,39].

A seductive alternative to CAUTI treatment is to prevent the infection by antimicrobial urinary catheters. One of the most explored strategies consists of immobilizing antibiotic substances on the catheter surface. The release of these substances to the environment can be controlled using degradable hydrogels. These antimicrobial substances are released until exhaustion, when the urinary catheter loses its antimicrobial effect and is vulnerable to bacterial colonization. Urinary catheters coated with hydrogel and antibiotics inside were proposed and leaved to the market as antimicrobial urinary catheters around 2001[40] but, they has not been shown to be a clear advantage over conventional silicone-based catheters. So, their use is associated with research proposes due to the low effectivity and the non-solution to antibiotic resistance problem compare with their manufacture cost. Close to these catheters, there are urinary catheters on the market

with antimicrobial properties, based on the release of silver salts from a hydrogel instead of antibiotics[41]. However, these catheters also have the problem of exhaustion and the loss of its antimicrobial properties. As an example, Lubri-sil® are silicone Foley catheters coated with a hydrogel containing and releasing silver salts. This catheter has a useful life of less than 28 days, showing a reduction of infections in the first 5 days of implantation, reaching the infection rate of a common urinary catheter after that. Also, in randomized clinical trials, low urinary tract infections were observed in the silver impregnated catheters with not significant differences between silver and non-treated catheter groups[42]. This effect may be due to the depletion of the catheter silver or its blockage by mucosa and cellular debris, losing the antimicrobial silver effect.

As seen, technologies for releasing antimicrobial substances locally from the surface have proven to be ineffective or short-lived. An interesting approach is to use structures, micro- and nanostructures, that are found in nature with an interesting antimicrobial effect. These topographies on different surfaces (legs, wings…) can avoid bacterial colonization by a natural bactericidal physical mechanism, without the release of any substance. An extended study of this phenomenon is the cicada wings (*Psaltoda claripennis*)[43], whose ordered nanopillars prevent bacterial deposition (Figure I. 3A). The general idea is to be able to replicate this physical antibacterial mechanism and create inert surfaces that can avoid bacterial colonization without releasing any type of antimicrobial substance.

In light of this, biophysical manipulation of material surface topography to mimic natural structures present in some insects and plants, can confer interesting physical and chemical characteristics to surfaces[44]. Some authors have created structures such as nanopillars, patterns or pyramids[45], managing to avoid colonization of the surface with some effectiveness. These structures can affect the bacterial adhesion mechanisms and the permanent establishment of bacteria on the surface, through a physical effect of repulsion. Some of these structures can even cause physical damage to bacterial structures such as membranes, being considered bactericidal surfaces[46]. Most studied nanostructures have a diameter between 50 to 80 nm, 10 times smaller than medium-size bacteria, with average density at 40 structures/μm^2 and roughness of 40 nm[44,47]. With appropriate density, the cell membrane covers the top cap and also part of the vertical structure wall, leading to large stretching degree[44,48]. However, specific conditions present the highest bactericidal efficiency against *Staphylococcus aureus*[44] and others conditions affect to other bacterial species. This kind of biophysical models reveal that the bactericidal effect depend on the bacterial species, the membrane type, the bacterial size and the attachment conditions[45,48,49], being a partial solution to colonization problem.

Recent systematic studies of the topographical effect on bacterial activity and biofilm development are focused in nanopillar, nanosphere and microneedle structures as the most promising structures to avoid bacteria colonization (Figure I. 3) [45,47,48,50–52]. Some examples of these technologies are the nanopillars presented in the work of Watson et. al (2019)[48], where the authors explained the physical action of attack on bacteria (deformation/rupture) by nanopillar surfaces or the work of Serrano et. al (2015)[53], who described a method for generating nanostructures at the surface of commercial sutures and their potential for preventing biofilm formation. But, nowadays, there are not medical devices with modified surfaces by nanostructures into the market, specially, there are not urinary catheters based on these technologies.

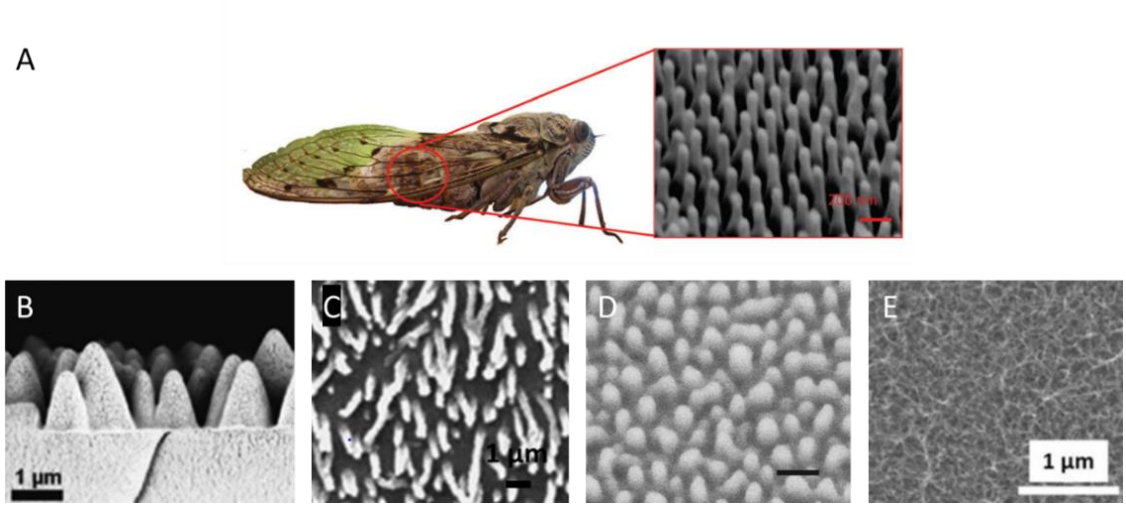

Figure I. 3. Field emission scanning electron microscopy images of different bio-inspired nanostructured surfaces. Image of bio-nanopillars in cicada wings43,50 (A), to inspire the modification of different substrates with polymer micro-cones or microneedles fabricated using a templating method50 (B), titanium nanotubes grown via anodic oxidation50 (C), nanopillars fabricated by UV nano-replication technology44 (D) or titanium nanowires by hydrothermal manufacture process (E)54. Red bar: 200 nm, black bars: 1 µm. Figure extracted and modified from previously cited works with academic purposes.

One of the reasons why these technologies are not taken to *in vivo* studies or even to the actual application is that, on numerous occasions these technologies are not suitable to real medical devices because their complex fabrication process or its low scalability, remaining as proofs of concept in the laboratory. Furthermore, one of the most complex problems to overcome is the application of these nanostructures on flexible surfaces, specifically medical silicones. The nanostructures and their components must be able to adapt to the shape of the medical device, in our case the urinary catheters, and not suffer tears, breaks or cracks when the device deforms,

moves or twists. But, overcoming the scalable manufacturing barrier and achieving a flexible and resistant nanostructured coating on silicone, these technologies could represent the future of anti-infective biomaterials.

For these reasons, to find a complete solution to avoid bacterial colonization must be a synergic technique, combining nanostructure technology easily to manufacture and an element to help it to promote the bacterial repulsion from surfaces.

Collectively, the use of modified surfaces to combat bacterial colonization and infection is a promising solution to the growing problem of nosocomial infections associated to medical devices[51]. Micro and nano-topographies and non-fouling chemistries represent a promising combination for long-term antibacterial activity.

At this point, antimicrobial metals have enjoyed a rich history of use in medicine and could be an appropriate tool to our purpose. The Edwin Smith papyrus, an ancient egyptian medical text, is one of the first written works that documents the use of a copper salts as astringent[55], also, there are many historical applications of silver (Ag) in medicine, including the use of silver nitrate ($AgNO_3$) to prevent gonorrhoeal eye infections in new-borns[56] , Ag foils to prevent infections in surgical wounds[53,57] or silver salts impregnated in urinary catheters, as previously mentioned[58]. Medicinal use of metals was prevalent until the discovery of antibiotics in the 1920s. Now, at the end of second decade of the twenty-first century, with the burgeoning threat of multidrug resistance and the dearth of new antibiotics in the pipeline, the use of antimicrobial metals is undergoing a renaissance[55]. Silver is an excellent agent to fight bacterial infections. The mechanism of action against bacteria is not clearly defined but, there is some evidence of silver ions interacting with sulfhydryl groups of proteins[59]. Also, silver ions are deposited in the cell wall as granules damaging it, and consequently, the electron transport chains losing their activity in bacterial respiratory process, components of DNA replication, and outer cell layers exhibit structural abnormalities[57,59,60] . The antibacterial process depends on the concentration of silver ion available in media and the bacterial capacity to process silver ion by proton-bombs[61]. This resistance to silver ions is determined by sensor/responder genomic system (SilRS)[62], located in some plasmids in gram-negative bacteria such as *Pseudomonas aeruginosa*[61,63]. However, chromosomally silver resistant mechanism has not been identified at that time and, perhaps it is a mutation in outer membrane porin proteins that conferee a deficient cation flux that not provide of advantages to bacteria and it is poorly diseminate[57]. Thus, silver stills one of most useful metals to avoid bacterial activity.

For all these reasons, synergic strategies between silver compounds and nanostructures to avoid bacterial colonization in medical devices could be the solution. This work proposes avoiding bacterial infection modifying medical device surfaces by a complex nanostructure with a metallic silver coating, demonstrating a controlled bacteriophobic, bacteriostatic or bactericide effect.

Based on previous work of Dr. Gilabert, Dr. Texidó and Prof. Borrós[64] in GEMAT group, different nanostructures applied to materials commonly used in medical devices, such as medical-grade silicone, will be explored. Playing with the shape and roughness, nanostructures will provide an effective antimicrobial surface in different bactericide grades. To obtain the nanostructure, two polymer coating strategies will be proved, using pentafluorophenyl methacrylate (PFM) and dopamine (DA) monomers as base films.

The final objective to this technology is to be applied on Foley urinary catheters. The modified catheters will be physically and chemically characterized according to standard guides and its bacteriophobic effect will be proven. Tests will be carried out *in vitro* and *in vivo,* to verify its efficacy as close as possible to reality.

To test the modified urinary catheter characteristics and its new bacteriophobic properties *in vitro,* biofilm methods and techniques to study bacterial attachment on surfaces will be revised. Currently, one of the biggest issues for biomaterials development is the study of their functionality in approximate real environments. Since the term *biofilm* was introduced in 1978, research is focused on the formation mechanism and how to eliminate it[65]. Several methodologies have been developed for study biofilm physiology, structure and composition by testing biomass[66] or bacterial viability[67]. However, there is a lack of consensus among the diversity of techniques used to grow and study biofilms, especially on biomaterial surfaces[65,68]. Clear example are ISO standards to test biofilm, focus on food industry and metal or plastic materials as polyethylene. ISOs 22196:2011 and 846:2019 evaluate the antibacterial activity of antibacterial-treated plastics. Protocols are designed to test the ability of treated plastics to kill microorganisms over 24 h period of direct contact in static conditions. At present time, an official protocol to study bacterial interaction with surfaces and how surfaces can avoid bacterial colonization at long times does not exist. Because of this, the present work will explore different techniques to study bacterial interactions with medical surfaces, how biofilm starts to grow using systems, bacteria and conditions near to reality and how quantify and show the bacteriophobic properties of different modified medical materials *in vitro* and *in vivo.*

Considering the above-mentioned failures in the current prevention of urinary catheters colonization and the limitations to study bacterial interaction and attachment with biomaterials used in medical devices, the main objective of this thesis is the development of new urinary catheter with bacteriophobic properties and the techniques to understand bacterial interaction with it, mimicking an environment as closely as possible to reality.

Therefore, to accomplish the main objective of this work, this thesis has been separated into the following goals:

Chapter II; Development and optimization of different protocols to study bacterial interaction with medical devices *in vitro* and *in vivo*.

- Traditional techniques and new ones were compared to understand the importance to use the correct materials and bacterial strains to study and extrapolate bacterial interactions and biofilm development on surfaces. Also, a new *in vitro* model to study biofilm growth on surfaces simulating urinary catheterization conditions was developed. The use of real and artificial urine, uropathogenic bacterial strains and different times of exposition in continuous flux, mimicking urinary flow, provided new tools to understand the formation of biofilm in urinary devices and what factors influence it. By last, the techniques were adapted to study the development of biofilm on medical devices *in vivo*, obtaining highly sensitive protocols.

Chapter III; Design and characterization of a set of nanostructured surfaces functionalized with metallic silver coating on medical-grade silicones.

- Based on previous work in GEMAT group, four new bacteriophobic or bacteriostatic surfaces were developed. Samples were manufactured by PFM and DA using different methodologies. Controlling the polymerization during the manufacture process, surfaces showed different levels of complexity and shapes in their nanostructure, which were enhanced by the silver coating applied on the polymers by two different Tollen's reactions. The coatings were characterized and their behaviour on contact with bacteria were tested. Synergic effects between silver coating and nanostructures to avoid bacterial colonization were studied with the objective to select the one that was implemented in the urinary catheter. To apply the technology to urinary catheters various criteria were considered: industrial scalability, reproducibility and cost.

Chapter IV; Implementing selected technology to real urinary catheters.

- Chemical and physical characterization of the device were carried out in this chapter. It was necessary to ensure that the coating is stable in real-life situations, with special attention on usage time and chemical conditions. To do this, urinary catheters were studied under flow conditions using different media, temperature and times to characterize the technical features of the new device. Also, *in vitro* tests to ensure that the bacteriophobic effect developed previously was transferred to the urinary catheter were done.

- In the second part of the chapter IV, the bacteriophobic silver-coated urinary catheters were tested *in vivo* with pigs as animal model. Protocols to implant the devices and to test their impact in pigs was created. Also, a complete study to test the efficacy of new silver-coated urinary catheters avoiding bacterial colonization was realized, using the protocols obtained in chapter II.

1.2 REFERENCES

(1) Asanuma, K. Global Harmonization Task Force Study Group 1: Definition of the Terms 'Medical Device' and 'In Vitro Diagnostic (IVD) Medical Device.' *Glob. Harmon. Task Force* **2012**, No. Ivd, 6. https://doi.org/GHTF/SG1/N071:2012.

(2) Feneley, R. C. L.; Hopley, I. B.; Wells, P. N. T. Urinary Catheters: History, Current Status, Adverse Events and Research Agenda. *J. Med. Eng. Technol.* **2015**, *39* (8), 459–470. https://doi.org/10.3109/03091902.2015.1085600.

(3) Williams, D. L. *Targeting Biofilms in Translational Research, Device Development and Industrial Sectors*; 2019.

(4) Singha, P.; Locklin, J.; Handa, H. A Review of the Recent Advances in Antimicrobial Coatings for Urinary Catheters. *Acta Biomater.* **2017**, *50* (November), 20–40. https://doi.org/10.1016/j.actbio.2016.11.070.

(5) Beiko, D. T.; Knudsen, B. E.; Denstedt, J. D. Advances in Ureteral Stent Design. *J. Endourol.* **2003**, *17* (4), 195–199. https://doi.org/10.1089/089277903765444294.

(6) Shackley, D. C.; Whytock, C.; Parry, G.; Clarke, L.; Vincent, C.; Harrison, A.; John, A.; Provost, L.; Power, M. Variation in the Prevalence of Urinary Catheters: A Profile of National Health Service Patients in England. *BMJ Open* **2017**, *7* (6), 1–8. https://doi.org/10.1136/bmjopen-2016-013842.

(7) Garg, S.; Prakash, S.; Bhatia, N.; Daga, M. Urinary Catheterization in Medical Wards. *J. Glob. Infect. Dis.* **2010**, *2* (2), 83. https://doi.org/10.4103/0974-777x.62870.

(8) Medical Devices Industry and Market Prospects 2013-2023.

(9) Khan, H. A.; Ahmad, A.; Mehboob, R. Nosocomial Infections and Their Control Strategies. *Asian Pac. J. Trop. Biomed.* **2015**, *5* (7), 509–514. https://doi.org/10.1016/j.apjtb.2015.05.001.

(10) Ha, U.-S.; Cho, Y.-H. Catheter-Associated Urinary Tract Infections: New Aspects of Novel Urinary Catheters. *Int. J. Antimicrob. Agents* **2006**, *28* (6), 485–490. https://doi.org/10.1016/j.ijantimicag.2006.08.020.

(11) Sabir, N.; Ikram, A.; Zaman, G.; Satti, L.; Gardezi, A.; Ahmed, A.; Ahmed, P. Bacterial Biofilm-Based Catheter-Associated Urinary Tract Infections: Causative Pathogens and Antibiotic Resistance. *Am. J. Infect. Control* **2017**, *45* (10), 1101–1105. https://doi.org/10.1016/j.ajic.2017.05.009.

(12) Flores-Mireles, A. L.; Walker, J. N.; Caparon, M.; Hultgren, S. J. Urinary Tract Infections: Epidemiology, Mechanisms of Infection and Treatment Options. *Nat. Rev. Microbiol.* **2015**,

13 (5), 269–284. https://doi.org/10.1038/nrmicro3432.

(13) Pigrau, C. Infecciones Del Tracto Urinario Nosocomiales. *Enferm. Infecc. Microbiol. Clin.* **2013**, *31* (9), 614–624. https://doi.org/10.1016/j.eimc.2012.11.015.

(14) Trautner, B. W.; Darouiche, R. O. Catheter-Associated Infections. *Arch. Intern. Med.* **2004**, *164* (8), 842. https://doi.org/10.1001/archinte.164.8.842.

(15) Reisner, A.; Maierl, M.; Jörger, M.; Krause, R.; Berger, D.; Haid, A.; Tesic, D.; Zechner, E. L. Type 1 Fimbriae Contribute to Catheter-Associated Urinary Tract Infections Caused by Escherichia Coli. *J. Bacteriol.* **2014**, *196* (5), 931–939. https://doi.org/10.1128/JB.00985-13.

(16) Hooton, T. M. Uncomplicated Urinary Tract Infection. *New Engl. J. Med.* **2012**, *366* (11), 1028–1037. https://doi.org/10.1056/NEJMcp1104429.

(17) Terlizzi, M. E.; Gribaudo, G.; Maffei, M. E. UroPathogenic Escherichia Coli (UPEC) Infections: Virulence Factors, Bladder Responses, Antibiotic, and Non-Antibiotic Antimicrobial Strategies. *Front. Microbiol.* **2017**, *8* (AUG). https://doi.org/10.3389/fmicb.2017.01566.

(18) Verleyen, P.; De Ridder, D.; Van Poppel, H.; Baert, L. Clinical Application of the Bardex IC Foley Catheter. *Eur. Urol.* **1999**, *36* (3), 240–246. https://doi.org/10.1159/000068005.

(19) Letica-Kriegel, A. S.; Salmasian, H.; Vawdrey, D. K.; Youngerman, B. E.; Green, R. A.; Furuya, E. Y.; Calfee, D. P.; Perotte, R. Identifying the Risk Factors for Catheter-Associated Urinary Tract Infections: A Large Cross-Sectional Study of Six Hospitals. *BMJ Open* **2019**, *9* (2), 1–7. https://doi.org/10.1136/bmjopen-2018-022137.

(20) Klevens, R. M.; Edwards, J. R.; Richards, C. L.; Horan, T. C.; Gaynes, R. P.; Pollock, D. A.; Cardo, D. M. Estimating Health Care-Associated Infections and Deaths in U.S. Hospitals, 2002. *Public Health Rep.* **2007**, *122* (2), 160–166. https://doi.org/10.1177/003335490712200205.

(21) Hollenbeak, C. S.; Schilling, A. L. The Attributable Cost of Catheter-Associated Urinary Tract Infections in the United States: A Systematic Review. *Am. J. Infect. Control* **2018**, *46* (7), 751–757. https://doi.org/10.1016/j.ajic.2018.01.015.

(22) Haque, M.; Sartelli, M.; McKimm, J.; Bakar, M. A. Health Care-Associated Infections – An Overview. *Infect. Drug Resist.* **2018**, *11*, 2321–2333. https://doi.org/10.2147/IDR.S177247.

(23) Pallasch, T. J. Antibiotic Resistance. *Dent. Clin. North Am.* **2003**, *47* (4), 623–639. https://doi.org/10.1016/S0011-8532(03)00039-9.

(24) Donowitz, Gerald R.; Mandell, G. L. DRUG THERAPY: Beta-Lactam Antibiotics. *N. Engl.*

J. Med. **1990**, *322* (20), 1405–1411.

(25) Flores-Mireles, A. L.; Walker, J. N.; Caparon, M.; Hultgren, S. J. Urinary Tract Infections: Epidemiology, Mechanisms of Infection and Treatment Options. *Nat. Rev. Microbiol.* **2015**, *13* (5), 269–284. https://doi.org/10.1038/nrmicro3432.

(26) Tacconelli, E.; Carrara, E.; Savoldi, A.; Harbarth, S.; Mendelson, M.; Monnet, D. L.; Pulcini, C.; Kahlmeter, G.; Kluytmans, J.; Carmeli, Y.; et al. Discovery, Research, and Development of New Antibiotics: The WHO Priority List of Antibiotic-Resistant Bacteria and Tuberculosis. *Lancet Infect. Dis.* **2018**, *18* (3), 318–327. https://doi.org/10.1016/S1473-3099(17)30753-3.

(27) Ghouri, F.; Hollywood, A.; Ryan, K. A Systematic Review of Non-Antibiotic Measures for the Prevention of Urinary Tract Infections in Pregnancy. *BMC Pregnancy Childbirth* **2018**, *18* (1). https://doi.org/10.1186/s12884-018-1732-2.

(28) Pendleton, J. N.; Gorman, S. P.; Gilmore, B. F. Clinical Relevance of the ESKAPE Pathogens. *Expert Rev. Anti. Infect. Ther.* **2013**, *11* (3), 297–308. https://doi.org/10.1586/eri.13.12.

(29) Altaf, I. U. K.; Khan, A.; Mahboob, A. Antimicrobial Resistance and a Diminishing Pool of Reserved Antibiotics. *Sao Paulo Med. J.* **2019**, *137* (4), 384–385. https://doi.org/10.1590/1516-3180.2019.0368120619.

(30) Tan, X.; Pan, Q.; Mo, C.; Li, X.; Liang, X.; Li, Y.; Lan, Y.; Chen, L. Carbapenems vs Alternative Antibiotics for the Treatment of Complicated Urinary Tract Infection: A Systematic Review and Network Meta-Analysis. *Med. (United States)* **2020**, *99* (2). https://doi.org/10.1097/MD.0000000000018769.

(31) Polanco Hinostroza, F.; Loza Munarriz, R. Antibiotic Resistance of Pathogens Causing Urinary Tract Infections in Children Attended at a Private Institution from 2007-2011. *Rev. Medica Hered.* **2013**, *24* (3), 210–216.

(32) Ageitos, J. M.; Sánchez-Pérez, A.; Calo-Mata, P.; Villa, T. G. Antimicrobial Peptides (AMPs): Ancient Compounds That Represent Novel Weapons in the Fight against Bacteria. *Biochem. Pharmacol.* **2016**. https://doi.org/10.1016/j.bcp.2016.09.018.

(33) Beloin, C.; Renard, S.; Ghigo, J. M.; Lebeaux, D. Novel Approaches to Combat Bacterial Biofilms. *Curr. Opin. Pharmacol.* **2014**, *18*, 61–68. https://doi.org/10.1016/j.coph.2014.09.005.

(34) Mikhailov, O. V.; Mikhailova, E. O. Elemental Silver Nanoparticles: Biosynthesis and Bio Applications. *Materials (Basel).* **2019**, *12* (19). https://doi.org/10.3390/ma12193177.

(35) Wang, H.; Liu, Y.; Li, M.; Huang, H.; Xu, H. M.; Hong, R. J.; Shen, H. Multifunctional TiO2

Nanowires-Modified Nanoparticles Bilayer Film for 3D Dye-Sensitized Solar Cells. *Optoelectron. Adv. Mater. Rapid Commun.* **2010**, *4* (8), 1166–1169. https://doi.org/10.1039/b000000x.

(36) Wang, J.; Li, J.; Guo, G.; Wang, Q.; Tang, J.; Zhao, Y.; Qin, H.; Wahafu, T.; Shen, H.; Liu, X.; et al. Silver-Nanoparticles-Modified Biomaterial Surface Resistant to Staphylococcus: New Insight into the Antimicrobial Action of Silver. *Sci. Rep.* **2016**, *6* (March), 1–16. https://doi.org/10.1038/srep32699.

(37) Rossmann, F. S.; Racek, T.; Wobser, D.; Puchalka, J.; Rabener, E. M.; Reiger, M.; Hendrickx, A. P. A.; Diederich, A. K.; Jung, K.; Klein, C.; et al. Phage-Mediated Dispersal of Biofilm and Distribution of Bacterial Virulence Genes Is Induced by Quorum Sensing. *PLoS Pathog.* **2015**, *11* (2), 1–17. https://doi.org/10.1371/journal.ppat.1004653.

(38) Hagan, E. C.; Donnenberg, M. S.; Mobley, H. L. T. Uropathogenic Escherichia Coli. *EcoSal Plus* **2009**, *3* (2). https://doi.org/10.1128/ecosalplus.8.6.1.3.

(39) Ribeiro, S. M.; Felício, M. R.; Boas, E. V.; Gonçalves, S.; Costa, F. F.; Samy, R. P.; Santos, N. C.; Franco, O. L. New Frontiers for Anti-Biofilm Drug Development. *Pharmacol. Ther.* **2016**, *160*, 133–144. https://doi.org/10.1016/j.pharmthera.2016.02.006.

(40) Zhu, Z.; Wang, Z.; Li, S.; Yuan, X. Antimicrobial Strategies for Urinary Catheters. *J. Biomed. Mater. Res. - Part A* **2019**, *107* (2), 445–467. https://doi.org/10.1002/jbm.a.36561.

(41) Srinivasan, A.; Karchmer, T.; Richards, A.; Song, X.; Perl, T. M.; Srinivasan, A.; Karchmer, T.; Richards, A.; Song, X.; Perl, T. M. A Prospective Trial of a Novel , Silicone-Based , Silver-Coated Foley Catheter for the Prevention of Nosocomial Urinary Tract Infections. **2014**, *27* (1), 38–43.

(42) Al-Qahtani, M.; Safan, A.; Jassim, G.; Abadla, S. Efficacy of Anti-Microbial Catheters in Preventing Catheter Associated Urinary Tract Infections in Hospitalized Patients: A Review on Recent Updates. *J. Infect. Public Health* **2019**, *12* (6), 760–766. https://doi.org/10.1016/j.jiph.2019.09.009.

(43) Jaggessar, A.; Shahali, H.; Mathew, A.; Yarlagadda, P. K. D. V. Bio-Mimicking Nano and Micro-Structured Surface Fabrication for Antibacterial Properties in Medical Implants. *J. Nanobiotechnology* **2017**, *15* (1), 1–20. https://doi.org/10.1186/s12951-017-0306-1.

(44) Wu, S.; Zuber, F.; Weber, K. M.; Brugger, J.; Ren, Q. Nanostructured Surface Topographies Have an Effect on Bactericidal Activity. *J. Nanobiotechnology* **2018**, 1–9. https://doi.org/10.1186/s12951-018-0347-0.

(45) Modaresifar, K.; Azizian, S.; Ganjian, M.; Fratila-Apachitei, L. E.; Zadpoor, A. A.

Bactericidal Effects of Nanopatterns: A Systematic Review. *Acta Biomater.* **2019**, *83*, 29–36. https://doi.org/10.1016/j.actbio.2018.09.059.

(46) Yi, G.; Riduan, S. N.; Yuan, Y.; Zhang, Y. Microbicide Surface Nano-Structures. *Crit. Rev. Biotechnol.* **2019**, *39* (7), 964–979. https://doi.org/10.1080/07388551.2019.1641788.

(47) Singha, P.; Locklin, J.; Handa, H. A Review of the Recent Advances in Antimicrobial Coatings for Urinary Catheters. *Acta Biomater.* **2017**, *50* (November), 20–40. https://doi.org/10.1016/j.actbio.2016.11.070.

(48) Watson, G. S.; Green, D. W.; Watson, J. A.; Zhou, Z.; Li, X.; Cheung, G. S. P.; Gellender, M. A Simple Model for Binding and Rupture of Bacterial Cells on Nanopillar Surfaces. *Adv. Mater. Interfaces* **2019**, *6* (10), 1–8. https://doi.org/10.1002/admi.201801646.

(49) Elbourne, A.; Chapman, J.; Gelmi, A.; Cozzolino, D.; Crawford, R. J.; Truong, V. K. Bacterial-Nanostructure Interactions: The Role of Cell Elasticity and Adhesion Forces. *J. Colloid Interface Sci.* **2019**, *546*, 192–210. https://doi.org/10.1016/j.jcis.2019.03.050.

(50) Linklater, D. P.; Juodkazis, S.; Ivanova, E. P. Nanofabrication of Mechano-Bactericidal Surfaces. *Nanoscale* **2017**, *9* (43), 16564–16585. https://doi.org/10.1039/C7NR05881K.

(51) Mi, G.; Shi, D.; Wang, M.; Webster, T. J. Reducing Bacterial Infections and Biofilm Formation Using Nanoparticles and Nanostructured Antibacterial Surfaces. *Adv. Healthc. Mater.* **2018**, *7* (13), 1–23. https://doi.org/10.1002/adhm.201800103.

(52) Hasan, J.; Chatterjee, K. Recent Advances in Engineering Topography Mediated Antibacterial Surfaces. *Nanoscale* **2015**, *7* (38), 15568–15575. https://doi.org/10.1039/c5nr04156b.

(53) Serrano, C.; García-Fernández, L.; Fernández-Blázquez, J. P.; Barbeck, M.; Ghanaati, S.; Unger, R.; Kirkpatrick, J.; Arzt, E.; Funk, L.; Turón, P.; et al. Nanostructured Medical Sutures with Antibacterial Properties. *Biomaterials* **2015**, *52* (1), 291–300. https://doi.org/10.1016/j.biomaterials.2015.02.039.

(54) Tripathy, A.; Sen, P.; Su, B.; Briscoe, W. H. Natural and Bioinspired Nanostructured Bactericidal Surfaces. *Adv. Colloid Interface Sci.* **2017**, *248*, 85–104. https://doi.org/10.1016/j.cis.2017.07.030.

(55) Lemire, J. A.; Harrison, J. J.; Turner, R. J. Antimicrobial Activity of Metals: Mechanisms, Molecular Targets and Applications. *Nat. Rev. Microbiol.* **2013**, *11* (6), 371–384. https://doi.org/10.1038/nrmicro3028.

(56) Groenouw. Die Augenentztindung Der Neugeborenen in Klinischer Und Bakteriologiseher Hinsicht. **1900**.

(57) Silver, S.; Phung, L. T.; Silver, G. Silver as Biocides in Burn and Wound Dressings and

Bacterial Resistance to Silver Compounds. *J. Ind. Microbiol. Biotechnol.* **2006**, *33* (7), 627–634. https://doi.org/10.1007/s10295-006-0139-7.

(58) Hachem, R.; Reitzel, R.; Borne, A.; Jiang, Y.; Tinkey, P.; Uthamanthil, R.; Chandra, J.; Ghannoum, M.; Raad, I. Novel Antiseptic Urinary Catheters for Prevention of Urinary Tract Infections: Correlation of in Vivo and in Vitro Test Results. *Antimicrob. Agents Chemother.* **2009**, *53* (12), 5145–5149. https://doi.org/10.1128/AAC.00718-09.

(59) Jung, W. K.; Koo, H. C.; Kim, K. W.; Shin, S.; Kim, S. H.; Park, Y. H. Antibacterial Activity and Mechanism of Action of the Silver Ion in Staphylococcus Aureus and Escherichia Coli. *Appl. Environ. Microbiol.* **2008**, *74* (7), 2171–2178. https://doi.org/10.1128/AEM.02001-07.

(60) Dakal, T. C.; Kumar, A.; Majumdar, R. S.; Yadav, V. Mechanistic Basis of Antimicrobial Actions of Silver Nanoparticles. *Front. Microbiol.* **2016**, *7* (NOV), 1–17. https://doi.org/10.3389/fmicb.2016.01831.

(61) Silver, S. Bacterial Silver Resistance: Molecular Biology and Uses and Misuses of Silver Compounds. *FEMS Microbiol. Rev.* **2003**, *27* (2–3), 341–353. https://doi.org/10.1016/S0168-6445(03)00047-0.

(62) Gupta, A.; Matsui, K.; Lo, J. F.; Silver, S. Molecular Basis for Resistance to Silver Cations in Salmonella. *Nat. Med.* **1999**, *5* (2), 183–188. https://doi.org/10.1038/5545.

(63) Haefeli, C.; Franklin, C.; Hardy, K. Plasmid-Determined Silver Resistance in Pseudomonas Stutzeri Isolated from a Silver Mine. *J. Bacteriol.* **1984**, *158* (1), 389–392. https://doi.org/10.1128/jb.158.1.389-392.1984.

(64) Gilabert-Porres, J.; Martí, S.; Calatayud, L.; Ramos, V.; Rosell, A.; Borrós, S. Design of a Nanostructured Active Surface against Gram-Positive and Gram-Negative Bacteria through Plasma Activation and in Situ Silver Reduction. *ACS Appl. Mater. Interfaces* **2016**, *8* (1), 64–73. https://doi.org/10.1021/acsami.5b07115.

(65) Azeredo, J.; Azevedo, N. F.; Briandet, R.; Cerca, N.; Coenye, T.; Costa, A. R.; Desvaux, M.; Di Bonaventura, G.; Hébraud, M.; Jaglic, Z.; et al. Critical Review on Biofilm Methods. *Crit. Rev. Microbiol.* **2017**, *43* (3), 313–351. https://doi.org/10.1080/1040841X.2016.1208146.

(66) Alexander, T. E.; Lozeau, L. D.; Camesano, T. A. QCM-D Characterization of Time-Dependence of Bacterial Adhesion. *Cell Surf.* **2019**, *5* (January), 100024. https://doi.org/10.1016/j.tcsw.2019.100024.

(67) Merritt, J. H.; Kadouri, D. E.; O'Toole, G. A. Growing and Analyzing Static Biofilms. *Curr. Protoc. Microbiol.* **2011**, No. SUPPL. 22, 1–18. https://doi.org/10.1002/9780471729259.mc01b01s22.

(68) Sjollema, J.; Zaat, S. A. J.; Fontaine, V.; Ramstedt, M.; Luginbuehl, R.; Thevissen, K.; Li, J.; van der Mei, H. C.; Busscher, H. J. In Vitro Methods for the Evaluation of Antimicrobial Surface Designs. *Acta Biomater.* **2018**, *70*, 12–24. https://doi.org/10.1016/j.actbio.2018.02.001.

Chapter II. Study of biofilm development in medical materials

ABSTRACT

In this chapter, different strategies have been proposed for the development and the evaluation of bacterial biofilms on materials commonly used in medical devices. Tests *in vitro*, in complex environments simulating normal use of the devices, and tests *in vivo* were used to understand the formation of biofilm on medical silicones.

2.1 INTRODUCTION

As explained in the previous chapter, the aim of this work is to develop new antibacterial urinary catheters to fight CAUTIs. For this purpose, different strategies to obtain antibacterial surfaces have been developed and tested in different ways. But, to apply these strategies to real medical devices and evaluate their functionality, the bacterial behaviour in contact with materials present on medical devices must be studied. Nowadays, identifying and studying bacterial adhesion in materials used in medicine present a great technical challenge. This chapter introduces the current techniques to study bacterial biofilms and their drawbacks. In order to solve it, a new methodology have been developed to determine bacterial adhesion and biofilm formation on the surface of materials used in medicine and real medical devices. Techniques have been validated both *in vivo* and *in vitro* tests, being sensitive enough to observe from punctual bacterial adhesion to mature biofilms formed by mixed populations.

To define these new methodologies to study bacteria on medical materials, it is necessary to understand how a biofilm develops on surfaces. Bacteria exist in two states, planktonic or sessile cells. Planktonic bacteria can growth exponentially and colonize new niches. These bacteria express adhesion structures and they are metabolically active whereas sessile bacterial populations are focused on perseverance, forming protective structures known as biofilms, usually attached on surfaces[1].

Biofilms are defined as *structured communities of microbial species embedded in a biopolymer matrix on either biotic or abiotic substrata*[2,3]*.* Most relevant characteristic of biofilms is its resistance to biocides, antibiotic chemotherapy and clearance by humoral or cellular host defence mechanisms[1,2,4], becoming a reservoir of active bacteria that can develop serious infections in case of colonize healthcare environments. Biofilm formation is a complex process which depends

on multiple variables, including the bacterial specie involve, surface characteristics, nutrient availability, hydrodynamics and quorum sensing[5–7]. Briefly, there are at least three phases involved in the biofilm formation process[2,8,9]: Attachment of bacteria to surfaces by different appendages, division of attached cells on surfaces and aggregation of bacteria from the bulk fluid to the developing biofilm (Figure II. 1). This last accumulation step requires coordinated efforts from the biofilm community to produce a viable mature biofilm, ensuring the oxygenation and distribution of nutrients to the different bacterial strata.

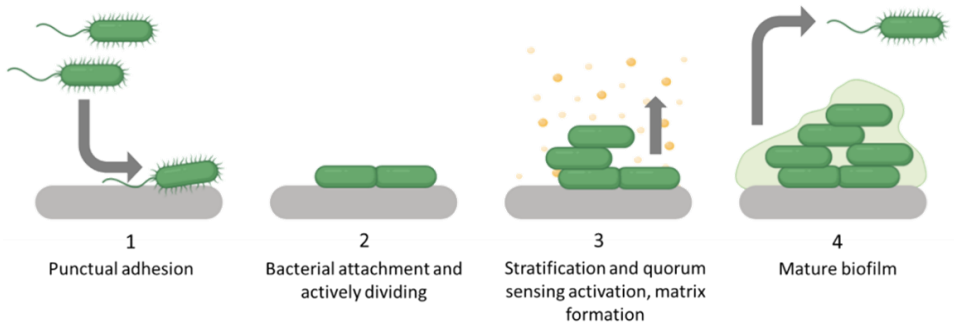

Figure II. 1. Developmental stages in biofilm formation. (1) One or more planktonic bacterial species adhere to a biotic or abiotic surface by different mechanisms or appendages. (2) Attached bacteria loss their appendages and start to duplicate, forming microcolonies. (3) Bacteria change their metabolism, bacteria start to send different signals (sRNAs, pDNA and different molecules of quorum sensing), matrix formation begins. (4) The matrix is a complex environment, water and nutrient-exchange channels are formed, bacterial division slows down and the set is resistant to external microbicidal agents. Image prepared by the author.

In last two decades, the knowledge about biofilms has increased due to the advances in molecular and imaging tools, revealing that biofilms are complex and dynamic structures. A clear example of the complexity of biofilm matrix was presented in 2001 for the first time, when observing biofilm was possible by a confocal laser scanning microscope, shown living biofilms of *Pseudomonas aeruginosa* by staining process with fluorescent probes[10]. After that, biofilms were considered highly hydrated open structures constituted of 73 to 98 % of extracellular substances and large void spaces, allowing the circulation of nutrients and signalling molecules and catabolites. This view changed the idea of biofilms like rigid structures and showing the need of create new strategies to visualize bio-structures completely[7,11].

The new vision of bacteria-surface interactions has made to rethink the tools to study biofilm development. However, nowadays, there is a lack of consensus among the diversity of techniques to visualize and quantify bacteria or biofilms[12,13], and not only in the scientific community. A clear example are the standards guides, such as ISOs 22196 and 846, that evaluates the antibacterial activity of antibacterial-treated plastics in food industry. Currently, an official protocol to study bacterial interaction with surfaces and how surfaces can avoid bacterial colonization does not exist. Bringing the biofilm study problem to medical devices, there is a giant lack of standard protocols and information of how to study the behaviour of bacteria on materials used in medical industry. None of the available standard protocols are indicated to study surface colonization, biofilm formation, or the effect of materials on bacterial attachment.

For this reason, the study of the development of a biofilm on materials for medical use, such as plastics and silicones, is currently a technical challenge. To understand biofilms in all their complexity, how bacteria interact and adhere to materials should be studied first. For this, testing their interaction with the material by techniques that allow a direct visualization of the bacteria and the surface, without neglecting the state of these bacteria (live, metabolically active, latent, or dead) is necessary. Currently, there are few tools that allow the visualization of this process directly, without intermediaries that camouflage the real behaviour of the bacteria or its state. Microscopy and bacterial counts, in combination, offer certain information that is often incomplete and losing the overall bacterial-surface vision, focusing only on the biofilm as an independent structure and not as the result of an interaction between the material and the bacteria.

Along with the techniques, another critical factor is the parameters commonly used in biofilm tests that influences the understanding of biofilm development. Currently, biofilms developed *in vitro* are studied for short times, under controlled conditions and in complete media, not in a real infection environment. Also, one of the major problems of these standards is the use of materials such as polystyrene or glass for tests, rare materials in medicine, instead of real medical devices. This supposes a loss of complexity of the tests, misunderstanding which parameters can be key in the development of a mature biofilm. For all that, this scenario represents an added problem when designing strategies to avoid bacterial colonization and biofilm formation.

Seeing the biofilm formation process entirely and, furthermore, being able to interfere in the biofilm formation process, it is necessary to carry out the tests aimed at it. Directly or indirectly, the most used techniques are extensively shown in the annex, Table II. 1. However, in this

chapter, the most common techniques have been commented and summarized below and in Figure II. 2.

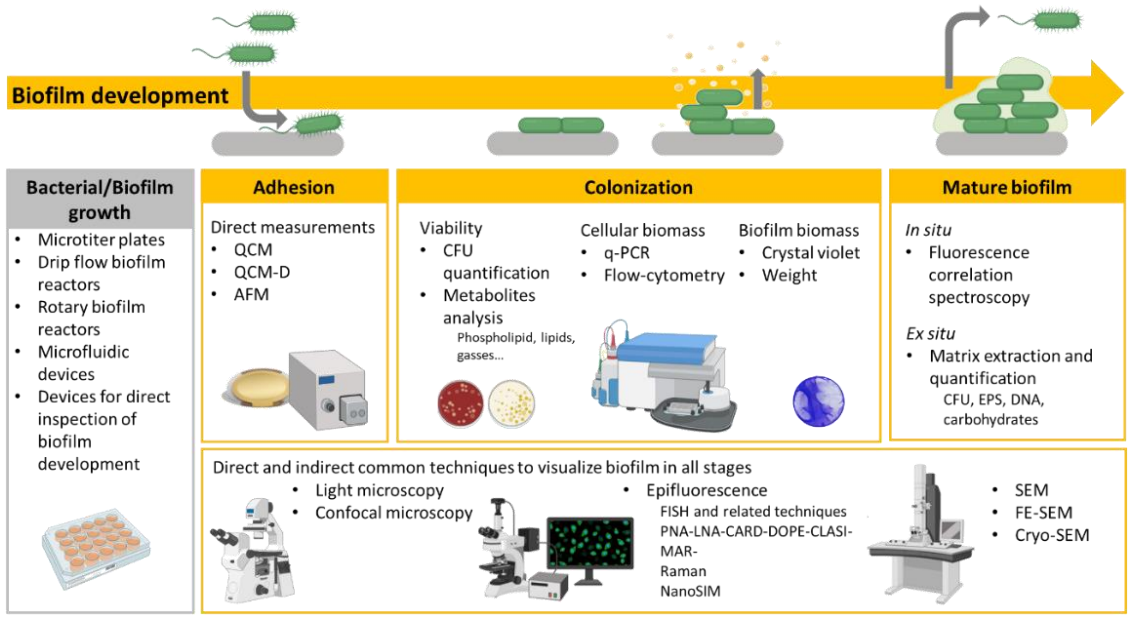

Figure II. 2. Overview of methods to grow and characterize biofilms. It includes different biofilm devices, methods to assess adhesion extent and strength, techniques to measure biofilm biomass, viability and matrix composition and visualize the biofilm structure. Techniques are divided into groups according to the stage of biofilm development when are used. *In situ* techniques are subject to the material and the morphology of the surface to be studied (silicones, plastics, sheets, tubes, spheres…). Different microscopy techniques to visualize biofilm matrix and bacteria can be used in any moment of biofilm development. Image prepared by the author based on the information obtained from different reviews[14–21].

Different qualitative parameters are usually considered when evaluating and studying biofilms by visualization techniques using different microscopy tools. These parameters are the physical structure of a mature biofilm, such as the types of nutrient and gasses transport channels, as well as the integrity and shape of the individual bacteria that compose the biofilm (if they are not embedded in the matrix) or, in case of studying the adhesion of bacteria to a surface, the integrity of their membranes, shape, volume and their distribution on the surface[17,22]. To test antibacterial surfaces, it is interesting to focus efforts on studying two processes: how the bacteria interact with the surface and the development of a complex biofilm on it[12–14,17]. The evaluation and visualization of these phenomena serves to identify the antibacterial mechanisms of the surface: bacteriostatic, bacteriophobic or bactericide. But, showing biofilm physiology and structure on a specific material,

especially in *in vivo* studies where bacteria usually are mixed species with different conformations, is of special interest[23–25].

Most used techniques are based on Scanning Electron Microscopy (SEM) or confocal imaging microscopy. Microscopy has the advantage of producing fascinating images that can be used directly as general information source of biofilm. As example of the use of microscopy to study the biofilm structure, Field Emission Scanning Electron Microscopy (FE-SEM) has been widely used (Figure II. 3). Pompilio et. al[26]. visualized *Staphylococcus aureus* biofilm onto polystyrene after three day of incubation in 2015, one of the first *in vitro* studies of biofilm beyond 48 h. However, the provided images showed a partial-biofilm developed, breaks in the biofilm structure and the stratification were not appreciated despite being gram-positive bacteria, who better withstand the stress of preparing the samples for FE-SEM. To increase the clarity of the images, Transmission Electron Microscopy (TEM) and cryo-SEM were used for the determination of the *Proteus mirabilis* biofilm structure and composition on infected urinary catheters. But, despite of a high level of resolution and detail, concluding remarks were not obtained. One of the main causes was the destruction of the exopolymer matrix during sample preparation[16]. If the objective of the study is to verify the efficacy of an antimicrobial surface, the loss of the matrix is especially important and generates a lot of extra considerations. The visualization techniques must ensure the integrity of the structure of the biofilm, since the rupture of the matrix may be because of the surface and to learn how biomass interacts with the surface.

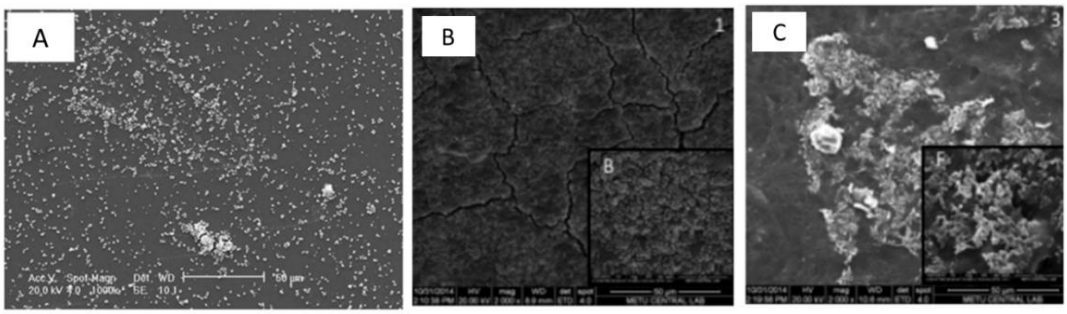

Figure II. 3. FE-SEM images of *S. aureus* at 3 days of incubation on polystyrene by Pompilio et. al (2015) (A) and images from colonized urinary catheters by *E. faecalis in vitro* from the study of Kart et. al (2017) (B and C). Images modified and reproduced with academic purposes.

The problem of correctly visualizing biofilm on a surface is increased when studying complex surfaces, such as those of medical devices. The use of imaging to study biofilm formation in real medical devices has been rarely used and few studies have been carried out. The major problem

to obtain information directly from urinary devices are the shape of the device, usually tubes with a narrow lumen where bacteria are. The shape amplifies the problem of losing the biofilm matrix by natural detachment due to the sample-overtreat. One of the most recent works in this field is the study of the colonization of urinary catheters by *Enterococcus faecalis* by Kart et. al (2017)[27] (Figure II. 3 B and C). In this work, a SEM images of bacteria on silicone catheters are shown but, it is necessary to emphasize that the culture of the bacteria was not carried out in the whole device but in a fragment for 1 to 5 days. Moreover, many of the problems described above were found: biofilm breakage, biomass loss and ultimately and loss of structural information.

Conversely, confocal laser scanning microscopy is a valuable tool for the study of biofilms, as it allows real-time visualization of fully hydrated, living specimens[19,28]. Various extracellular compounds can be labelled fluorescently and visualized. As an example of the molecule visualization and quantification is the use of the staining TOTO-1 to stain extracellular DNA in *Staphylococcus epidermidids* biofilms *in vitro* (Figure II. 4). The biggest drawback of the use of confocal microscopy images is the limitation given by the probes. It is necessary to use a fluorophore for each element to be visualized, either direct or non-specific. Currently, there are probes for any element to study: bacterial membranes, genetic material, proteins (or a single specific protein), polysaccharides ... but with a big limitation: it is necessary to use fluorophores that emit signal at sufficiently separated lengths to properly observe the set of elements, otherwise, cannot be distinguished.

In case of studying antimicrobial surfaces, applying confocal techniques is complicated. Being able to visualize the surface under the bacteria or the biofilm is key to understanding the interaction between the elements. Furthermore, in the case of applying this technique to complex medical devices, especially curved ones, focusing biofilm layers is extremely difficult[22,28].

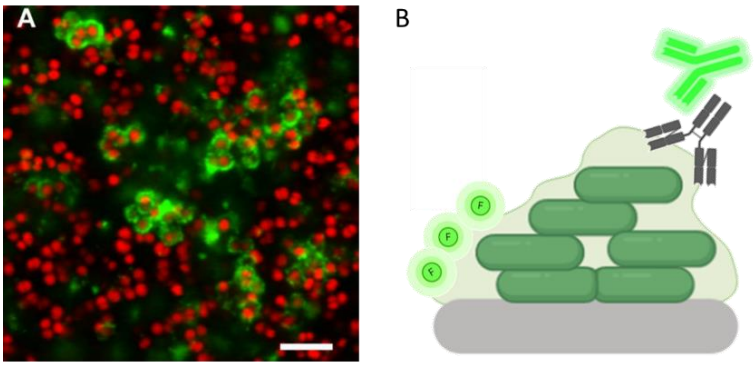

Figure II. 4 A. Confocal microscopy image using TOTO-1 syto to stain extracelluar DNA of *S. epidermidis* biofilms *in vitro*. Image from the work of Schlafer and Rikke (2017)[15], reproduced with academic purposes. Bars: 5 µm. B. Classical sample preparation to visualize different elements of biofilm, bacteria or matrix: single-probe preparation marked as F and *sandwich* preparation scheme.

One of most mentioned advantage of microscopy is the ability to quantitatively analyse biofilms[11,29]. This method of quantification is usually applied to punctual bacterial adhesion on modified surfaces, counting bacteria in a specific area and assuming the rate bacteria per area. Biofilm quantification is too complicated because the multiple layers of bacteria and the complex matrix around them camouflaging the total number of bacteria attached on surfaces. This methodology has serious problems, including the impossibility of distinguish between life or dead bacteria attached (or casual deposited) on surface. Few authors can show structural damage on bacterial membrane, assuming that bacteria are dead, but this technique is subject to subjective interpretation.

Considering the limitations of microscopy as a counting tool, a lot of authors have tried to quantify the bacteria embedded in biofilms. Many of the reported *in vitro* methods use flat surfaces to grow biofilms[16] but curved surfaces, as urinary catheters, cannulas, stents or tubes used in medicine, present a different set of challenges. Complex structures such as presented in medical devices are also difficult to visualize under microscope, therefore, quantification techniques gain importance. Different methodologies to disrupt and extract biofilm from surfaces and medical devices were tuning to quantify bacteria. Notable among these, is the use of sonication and vortex agitation are relatively successful[21,27,30]. But most of the techniques to disrupt biofilms are applied on biofilms that have grown only for 18 to 48 h. In clinical settings, where medical devices remain *in situ* for weeks, biofilms develop over a longer period and are much harder to disrupt. In urinary catheters case, crystalline biofilms responsible for catheter associated urinary tract infections

(CAUTI) are known to be often caused by mixed pathogens with complex salt-biological matrix structures strongly attached to catheter's lumen[31]. In this context, Mandakhalikar et. al (2018)[32] studied the optimization of biofilm-extraction method from catheterized mices, revealing very significant differences between methodologies. Therefore, the application of different techniques to visualize and quantify the biofilm can offer different information about its status, leading to confusion.

In addition to all explained above, there is a problem with the duration of the experiments to test biofilm development in a surface. *In vitro* studies that analyze the behavior of bacteria and the development of biofilms on surfaces are carried out in short periods of time (commonly 4 to 24 hours and a maximum of 48 hours)[33–35]. In case of studying surfaces with bactericidal, bacteriostatic or bacteriophobic effects, the study time is more significant. The duration of the effect of these antimicrobial surfaces cannot be corroborated beyond the hours in which they have been in contact with bacteria. Techniques that can study the bacterial interaction with the surface for long periods will be very useful. In this area, the Quartz Crystal Microbalance with Dissipation monitoring (QCM-D) stands out as a powerfull tool to test bacterial interactoin with surfaces and how biofilm develops[14,36]. However, techniques such as QCM or QCM-D can be applied *in vitro* in very specific systems, not on medical devices.

Despite of medical devices are the target of the studies, generally, they are not the platform of choice for researchers to study biofilm due to the complexity involved in developing biofilms on medical devices. The size of the medical devices, their design and their shape are usually the main drawbacks. Developing biofilm *in vitro* on complete medical devices by making bacteria interact with the areas of interest involves a complex optimization process. Because of this, a significant gap exists in this field. As surface-associated biofilms are highly dependent on the topography of the substrate, its chemical characteristics and the level of exposure to gasses and water[11], testing biofilm development in real medical devices is a point to achieve.

Furthermore, biofilms can take up nutrients directly from the material where bacteria are adhered, especially, important feature when studying antibacterial surfaces[23]. Because of this, the same bacterial biofilm can vary depending on the selection of the base material where biofilm is growing[43]. So, an interesting approach is to study biofilm on materials used in medical devices manufacture. These materials are commonly plastic and rubber with generally lightweight, an excellent flexibility and an inexpensive manufacturing cost[37]. Also, they present low levels of cytotoxicity, used for short or long times on patients. However, because of they are the most

widely used materials in single-use or implantable medical devices, they have the highest levels of bacterial colonization, especially on silicones and polyurethanes[38,39], despite of the fact of they are considered *low-colonizable materials*[40,41]*.* Moreover, the natural topography of materials, its micro- and nanostructure, plays a fundamental role in bacterial adhesion and biofilm development[23,42,43]. Therefore, it would be interesting to study materials that show the same micro- and nanostructure than the real products.

The last parameter to consider when studying biofilm is the bacterial strain used to develop it. To test biomedical materials are usually used laboratory models whose results cannot be extrapolated to the rest of bacterial species[33]. Model bacteria are very different from pathogenic clinical isolates. Ideally, the most common bacterial clinical-isolate strains should be used to test the surface where these bacterial infections develop. As an example, in catheter associated urinary tract infections (CAUTI) would be interesting to use uropathogenic bacteria with specific adhesion mechanisms for urinary epithelium and with a process of biofilm formation that includes urease in its matrix[44–46].

Therefore, this chapter reviews traditional methodologies and parameters usually tested to understand biofilms, highlighting the need to bring them closer to the real medical devices. Furthermore, current protocols were discussed, noting the need to find simple and versatile techniques that can be extrapolated from *in vitro* tests to *in vivo* tests, without varying reproducibility and reliability.

With the above goals in mind, this chapter proposes an easy-to-use methodology to visualize and quantify, with high sensitivity, attached bacteria to silicone surfaces and real medical devices silicone-based. Developed techniques must be sensitive enough to study antibacterial surfaces, with low attached bacteria, avoiding general results such as *black photo results.* The big goal is to show the real behaviour of bacteria on antibacterial (or not) surfaces, bringing the conditions as close as possible to reality. Also, one method to study bacterial attachment and early biofilm mimicking urinary devices *in vitro* has been proposed. The method consists of simulating environmental and physical conditions of urinary tract using QCM-D and a clinical isolate uropathogenic strain as infective strain model. To probe this model, the role of human albumin present in urine on biofilm formation has been studied.

Finally, as the real problem is to study biofilm development beyond *in vitro* tests, in real medical devices, the techniques should be able to perform the biofilm evaluation in real environments. The methodologies proposed will be applied in *in vivo* studies, testing its versatility to visualize

multi-specie biofilm structures on real medical devices at long times (> 20 days), identifying the bacterial strains which form part on it.

Pages have been removed from this version of the thesis as are protected under industrial property rights

2.3 RESULTS and DISCUSSION

2.3.1 Evaluation of conventional techniques, materials and bacterial strains to study the development of biofilms on surfaces.

In this section, conventional techniques to grow and study biofilms on surfaces will be evaluated to establish a reproducible method, sensitive enough and as close as possible to real conditions. These techniques should be used to study the biofilm development on medical devices both *in vitro* and *in vivo*, considering all the drawbacks and challenges explained above (Figure II. 7 A-D).

To evaluate the importance of bacterial culture technique on materials and to determine how put in contact bacteria with surfaces for future experiments, two common bacterial set ups were tested: placing the sample at the bottom of the container where the culture medium is located or placing the sample on the side or floating with the face of interest in contact with the medium. To prove this phenomenon, counts of colony forming units (CFU) per cm^2 of *E. coli* CFT073 and *P. aeruginosa* PAO1 were made in PDMS placed at the bottom or the top of the well (Figure II. 7 A).

As can be noted in Figure II. 7 A, important differences in the counts of adhering bacteria were observed regardless of the bacterial strain used. Bottom samples presented massive deposition of dead bacteria, bacterial debris and bacterial secretions nonrelated with biofilm matrix on surface, disrupting the bacterial interaction with surface and creating partial biofilm mixed with biological waste. Placing material at bottom of wells produced unstable bacterial adhesion. Biofilms formed with this procedure were unstable and heterogeneous, losing principal characteristics of biofilm on surfaces: be anchored to the surface resisting washes. This could be due to the limitation of using media in static conditions, without refill, and an inoculum that reaches a stationary phase. By contrast, surfaces that were put in contact with the media by floating or on the side of well, showed a well strong biofilm, wash resistant. Samples were easy to manipulate, and biofilm held homogeneously on the surface. All bacterial debris, waste substances and biological residues fell into the bottom of the well. This situation leaved the surface in contact with bacteria free of debris. Only bacteria and biological remains that actively interact with surface, were deposited on it. This experiment remarks the importance of the design and the setup of the tests for the study of bacterial adhesion to materials.

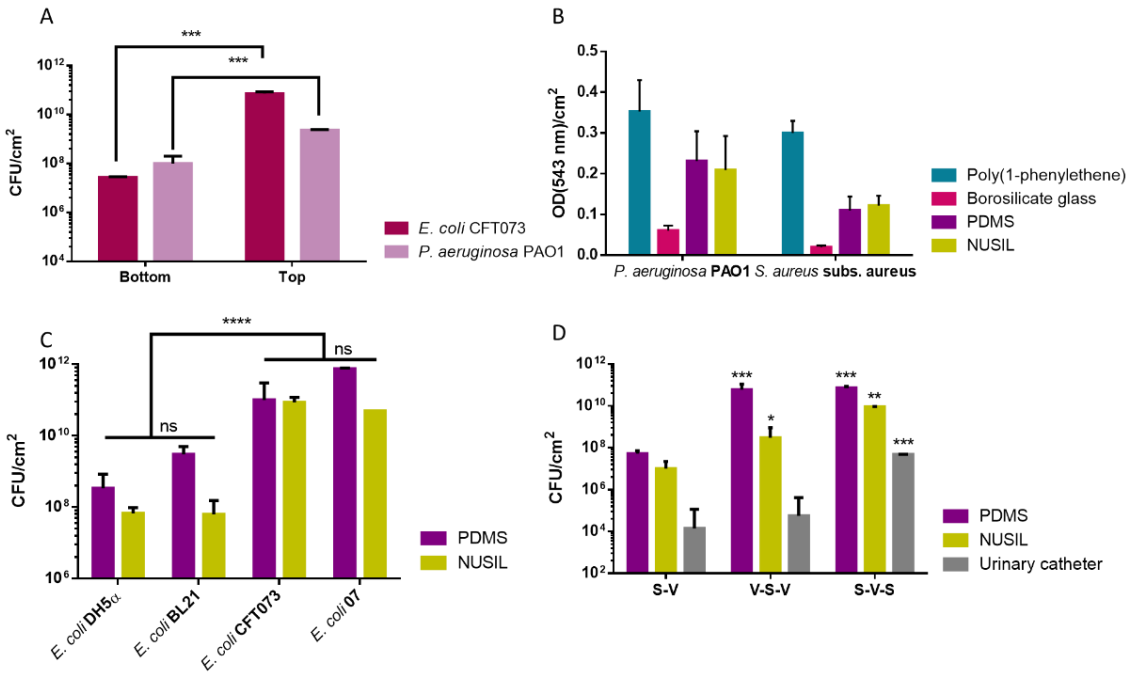

Figure II. 7. A. Bacterial counts per cm^2 of *E. coli* CFT073 and *P. aeruginosa* PAO1 attached to the surface of PDMS. PDMS was placed at the base of the well (bottom) or on the surface, floating (top). B. Crystal violet stain of biofilm formed on different surfaces. *P. aeruginosa* PA01 and *S. aureus subs. aureus* strains were used as model. Measures were taken at 543 nm and normalize per cm^2 to compare between surfaces. The test was carried out 3 times with 3 to 5 replicates per surface. C. Different strains of *Escherichia coli* attached differentially to PDMS and NUSIL. D. Colony forming units per cm^2 extracted from PDMS, NUSIL and urinary catheters using different protocols based on vortexing and sonication. Vortexing (V) was applied during 2 min and sonication (S) was applied during 10 min in water bath. *Escherichia coli* CFT073 was used as adhesion model. Statistical analysis was performed with multiple comparations between materials and protocols. Protocol S-V was used as reference. P-values correspond to: (*) p-value < 0.05, (**) p-value < 0.01, (***) p-value < 0.001, (****) p-value < 0.0001

Next steps were understanding the importance of the right selection of the material on which studying the development of a biofilm, as conventional biofilm-study materials were tested (poly(1-phenylethene, PS) and borosilicate glass). As implantable medical device materials, polydimethylsiloxane (PDMS) and medical silicone (NUSIL) were used in this chapter (Figure II. 7 B). After growing biofilm on selected materials, in order to evaluate biomass deposited on materials, as a reference of biofilm formation, crystal violet staining was used.

Results present in Figure II. 7 B reflects the common drawback of crystal violet staining[17,53]. Four problems stand out: the poor reproducibility shown in the high deviation values, the loss of biofilm mass attached on surfaces due to the high manipulation of samples, the impossibility of

distinguish between live and dead bacteria and the ignorance of the stage of the biofilm. However, tested materials were compared using crystal violet stain standard protocol to quantify biomass adhered to each surface in this case. As shown in Figure II. 7 B, two different bacterial strains was used. Pseudomonas aeruginosa and Staphylococcus aureus were adhered with different values to each material. PS had higher level of bacterial adhesion, as previously reported in bibliography[54]. Considering the differences between silicone-based materials and PS, PS should not be use as reference despite of its extended use in the research community, if possible. Furthermore, despite being one of the standards, borosilicate glass did not reflect in any case the real behaviour of biofilm formation and biomass deposition to surfaces, offering poor data that cannot be extrapolated to other materials.

Lastly, PDMS and NUSIL were compared in biomass-attachment field using different bacterial strains (Figure II. 7 C). Four strains were used: *Escherichia coli* DH5α (laboratory model for cloning), *Escherichia coli* BL21 (laboratory model for protein expression and purification, proteases deficient), *Escherichia coli* CFT073 (urological clinical isolate, uropathogenic and drug resistant model from USA, purchased in ATCC®), and *Escherichia coli* 07 (uropathogen clinical isolated from infected urinary catheters). The most notable differences are due to the adhesion systems expressed by these strains (adhesins, pili, fimbriae and flagella) directly related with their pathogenicity[46,55,56]. As shown in Figure II. 7 C, different bacterial strains presented different adhesion on PDMS and NUSIL, being significant the difference between strains and not between materials. Specifically, differences between *E. coli* strains were proven. Clinical isolate *E. coli* CFT073 and 07, uropathogenic strains, possess a plethora of both structural (fimbriae, pili, curli and flagella) and secret toxins or virulence factors that contribute to their capacity to attach on surfaces (and cells) causing infections[46]. Laboratory model *E. coli* DH5α and BL21 showed less adhesion and biofilm formation to surfaces, as expected. In addition, the differences in adhesion counts between PDMS and NUSIL were more important using these bacterial strains. The use of strains that naturally do not have adhesion mechanisms to surfaces should not be recommended to study how bacteria interact with surfaces, due to test will offer non-real data. It has been shown that it is necessary to carry out studies of interaction between surfaces of interest with key bacteria, lay assay laboratory models.

It is not only important the material, the bacterial strain and the culture conditions to understand biofilm development. Quantification methods provide key information to understand material-bacteria interactions, as well as the metabolic status of adhered bacteria and the grade of maturity of the tested biofilm. But bacterial quantification methods on medical devices have a problem: in

clinical settings, medical devices remain in situ for days or weeks, where biofilms develop over a longer period. This biofilm is much sturdier and more challenging to dislodge to quantify the bacterial content. Because of this, many of reported in vitro methods use flat surfaces to growth biofilms[17,36,57] but medical devices are usually curved tubes with a lumen section where biofilm develops. These complex structures make biofilm extraction even more difficult.

Looking for a sensitive-enough method to ensuring the extraction of all biofilm and bacteria attached to a surface, various protocols had carried out with few variations, based on the work of Mandakhalikar et. al.[32]. Using simple techniques to biofilm disruption: vortexing (V) and sonication (S), bacterial extraction were tested on PDMS and NUSIL coupons and urinary catheters 100 % silicone based (sizes from 10 to 20 Fr), shown in Figure II. 7 D. As can be noted, biofilm was extracted from surfaces using three different protocols and then, colony forming unites (CFU) per cm2 were plated and counted. All these methods allowed quantify adherent and metabolically active bacteria but, it was necessary to find the most sensitive protocol in order to recover all bacteria from the complex medical devices. S-V-S protocol showed the highest number of CFUs recovered per cm2, with the smallest deviation. However, all three techniques represent an increase in the sensitivity of biofilm extraction, compared to what is usually used[7,32]. But, the statistically significant differences shown between extraction protocols were evident, so S-V-S protocol will be the method used to extract bacteria and biofilm throughout this work. This protocol was used to quantify attached bacteria to PDMS and NUSIL using different bacterial strains for the rest of the tests made in the Figure II. 7.

Thus, in this section we have analysed and discarded the traditional techniques of growth and study of biofilm. Crystal violet stain test is a not useful tool to study bacterial adhesion on surfaces. It will also not be useful for the study of antibacterial surfaces, due to its high variability and low sensitivity. However, this technique has been used to highlight the need to study the biofilm formation on the surfaces of interest and not on materials for standard use. Furthermore, material and bacterial strain used in the tests play an important role in the study of bacteria-material interactions and biofilm development. From now on, bacterial strains from clinical uropathogenic isolates, biofilm formation models or bacteria with clinical relevance will be used. Also, bacteria will be grown on surfaces of interest (NUSIL, PDMS or urinary catheter) to test these materials and their physical or chemical properties regarding bacterial attachment.

In order to quantify live bacteria adhered to surfaces, specifically in urinary catheters, the third proposed protocol (S-V-S) will be used. However, these techniques offer indirect information

about the material and the interaction of bacteria on it. That is why it is necessary to develop visualization techniques for testing antimicrobial surfaces, to know the surface-infection relationship closely.

2.3.2 Microscopy techniques to observe bacterial attachment and biofilm formation on surfaces.

As explained in the Introduction section, microscopy techniques present a several problems when studying interactions between bacteria and materials. Different strains of *P. aeruginosa* have been grown on PDMS and visualized under confocal microscopy to study the bacterial adhesion phenomena to silicones. Figure II. 8 A and B show images of the same surface colonized by *P. aeruginosa* PAO1. These tests highlighted the need to generate a large image library to obtain robust statistics due to the difference in bacterial colonization on the same sample. Furthermore, the images shown in Figure II. 8 C and D correspond to clinical isolates of *P. aeruginosa* grown on PDMS at different times which showed an intermediate level of bacterial adhesion. The images show bacteria on a plane, but it is more difficult to see how bacteria are on the surface because the loss of visualization of the material under them. Using this technique, it was not possible to obtain information on how bacteria had adhered to the surface: randomly or following a pattern given by the material. The maturity of the biofilm, the presence of strata or its shape neither could be observed. Therefore, confocal fluorescence microscopy was used in this work to provide complementary information to the study but not as a main tool.

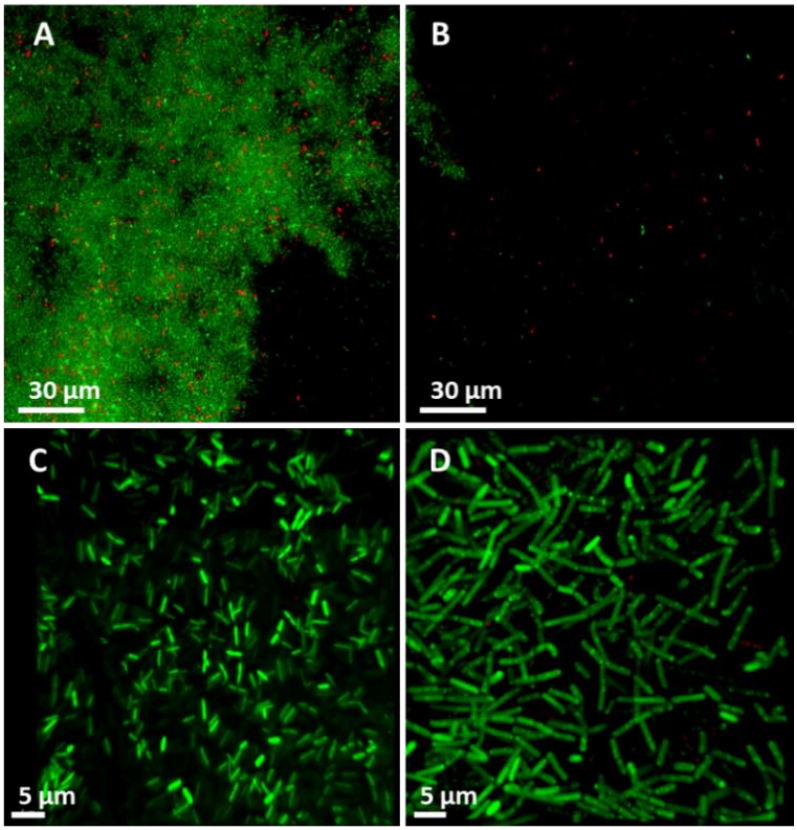

Figure II. 8. Confocal microscopy of *P. aeruginosa* on PDMS surfaces. Images were taken after stain with Live-Dead cell staining kit. Biofilm is not homogeneous and depending on the area targeted, may give biased information. Also, surface under biofilm is camouflaged by the technique and the topography cannot be appreciated.

Similarly, Scanning Electron Microscopy (SEM) or Field-Emission Scanning Electron Microscopy (FE-SEM) offer information about bacterial colonization and their interaction with surfaces[22]. This information can be useful determining how bacteria interact with surfaces and even understanding how antimicrobial materials affect bacterial adhesion. FE-SEM have been widely used in studies although they cannot provide reliable information about the state (living or dead) of bacteria.

However, SEM techniques have other difficulties in obtaining bacterial images from surfaces. One of them is the need to fix the sample to the surface before viewing. Standard protocols to fix bacteria and biofilm are based on serial dehydrations of matrix using water and ethanol[11]. In this part, a protocol was developed to fix natural biofilms of mixed bacterial species, formed on silicone-based medical devices to visualization with FE-SEM. This protocol tries to keep the 3D

structure of biofilm matrix intact and the integrity of bacteria attached on surface, avoiding the loss of biofilm texture or the bacterial form. In addition, avoiding the cracking of biofilm, on the entire surface, was a goal.

Two protocols to fix bacteria were created. Figure II. 9 shows FE-SEM images obtained using the two protocols explained in materials and methods section. Briefly, first one uses 2.5 % glutaraldehyde solution and ethanol diluted in water to fix bacteria. Modified protocol uses 4 % formaldehyde solution and ethanol diluted in PBS or water to fix bacteria.

First protocol was used on samples what are shown in Figure II. 9 A, C and E, and the second one was used on Figure II. 9 B, D and F.

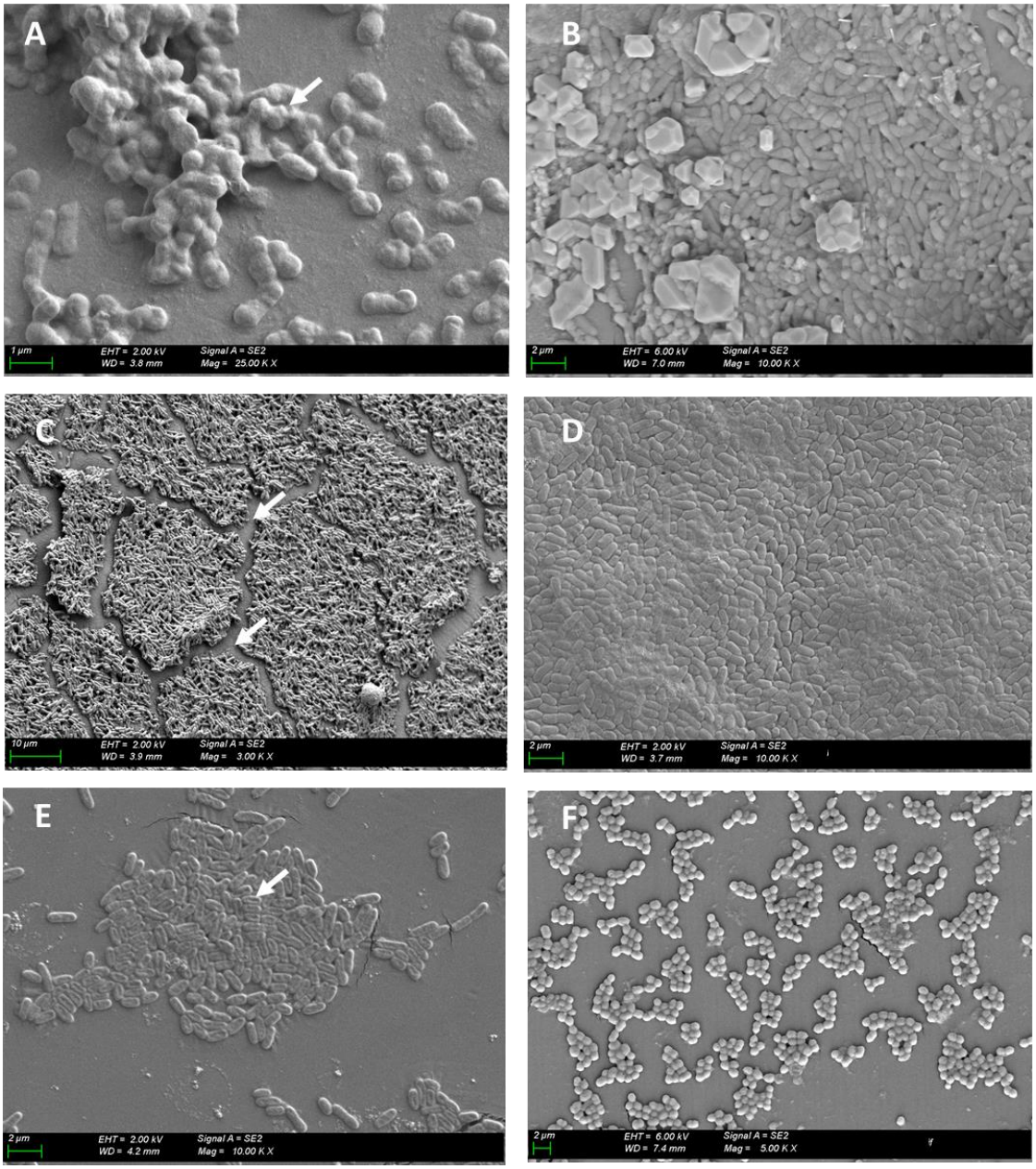

Figure II. 9. FE-SEM images of a biofilm or bacterial adhesion on PDMS coupons. Homogeneous layer of adhered bacteria. Different fixation protocols were applied to surfaces to fix bacteria and biofilm structures. First described protocol was applied to A, C and E samples and the second one was applied to B, D and F samples. White arrows remark the interesting points of each image.

As can be seen in Figure II. 9 A, bacteria presented a diffused morphology without any appreciation of matrix or structure, as well as Figure II. 9 C, where crushed bacteria can be seen,

having lost their volume and shape, drawing small craters in their centre. This poses a problem when analysing the morphology of bacteria and how they can be affected by the surface. In studies on antimicrobial surfaces respecting the bacterial morphology is essential, to know if the surface influences them. On the other hand, Figure II. 9 E showed adhered bacteria on the surface, homogeneously in monolayer, but the film was broken and lifted. This loss of film can occur throughout the sample, giving incomplete information about the true bacterial behaviour on that surface.

In contrast, second protocol applied on the images of Figure II. 9 B, D and F, showed the monolayers of bacteria adhered clearly without open, broken or raised areas. In case of image F, the shape, volume and structure of the individual bacteria could be fully appreciated. This protocol maintained the structure and texture of microcolonies and the connections between them. So, this protocol makes it possible to study how the bacteria are attached to the surface as well as the integrity of their membranes. These images provide much more information of bacterial adhesion on surfaces and offer a real scenario on which studying the effect of external agents, such as antimicrobial ones. So, protocol 2 has been used in this work to visualize single strain bacteria, mix populations and *in vitro* or *in vivo* biofilms on 2D samples or real medical devices.

According to the information obtained and discussed for the visualization of biofilm on silicone-based surfaces, and once the extraction and quantification of the bacteria adhered to the surfaces have been optimized, the guidelines are established to study biofilm and bacterial adhesion on the surface in a reproducible and sensitive-enough way, using different techniques such as FE-SEM or bacterial quantification protocols.

2.3.3 *In vitro* study of bacterial adhesion and biofilm development on simulated complex environments.

Previous section highlights the need to create standardized methodologies to growth and analyse biofilm on surfaces. The above methods provide very valuable information about the state of the attached bacteria on surfaces, the number of bacteria interacting with the material and the shape and mature level of biofilm developed on surfaces. However, to study the interaction of bacteria with antimicrobial materials in depth, knowing about the bacteria-material adhesion mechanism and the interactions with material structures, it is necessary to find much more precise tools.

Studying urinary infections, there are elements which is rarely taken into account, such as the media composition on biofilm develops, the flow conditions and the bacterial strain[58]. In a real infection, media varies with the evolution of the infection and the environment response. The presence of biomolecules, salts or waste proteins can interact with surfaces and affect bacterial adhesion, growth and biofilm development, creating a complex system where infection is developed[18]. If the purpose is to study the interaction of bacteria with medical device surfaces, it is necessary to recreate as close as possible the conditions where biofilm will develop.

As previously mentioned, recreating the environmental conditions in which a biofilm develops on a surface is necessary to understand it. In case of urinary catheters, to recreate an urinary infection is extremely complex because bacteria grows in a continuous flow in urine, which is an aqueous medium composed mostly of water with dissolved salts, short peptides, free amino acids, cell debris from the bladder epithelium, and waste proteins[47,59].

In this sense, one of the main proteins that it can find in urine derived from previous pathologies is human albumin (HA). HA could play a critical role during biofilm formation. Excreted HA is used as a diagnostic value in the initial detection of renal disease because is an indication of proteinuria[60], which is also a predictor of progressive kidney damage, and a cardiovascular risk marker and predictor[61–64]. These dissolved molecules can play and important role during the bacterial attachment because it is well known that molecules, such as fibrinogen or urea crystals, can interact with hydrophobic surfaces, as urinary catheters, providing new anchor points where bacteria can attach and grow[65,66]. Also, HA can interact with different surfaces as silicone or polystyrene[67], forming a layer which can cover urinary medical devices facilitating the bacteria anchoring. However, there is a lack of information on biofilm models that do not study the relationship between the presence of HA dissolved in urine and the bacterial attachment on urinary catheters, the development of biofilm and the further development of an urinary infection.

In addition to the above, select the strain model is a key factor. To understand urinary infections on urinary catheters, an uropathogenic strain, clinical isolate *Escherichia coli* CFT073 was used, which produce bacteriuria and other catheter associated urinary tract infections[45,68]. Uropathogenic strains possess unique structural and virulence factors[44] that contribute to their capacity to adhere to catheters surface forming biofilm[45,46].

Taking all these into account, a model will be developed to study *E. coli* CFT073 adhesion to surfaces in conditions close to reality. This model has been explained briefly in Figure II. 10.

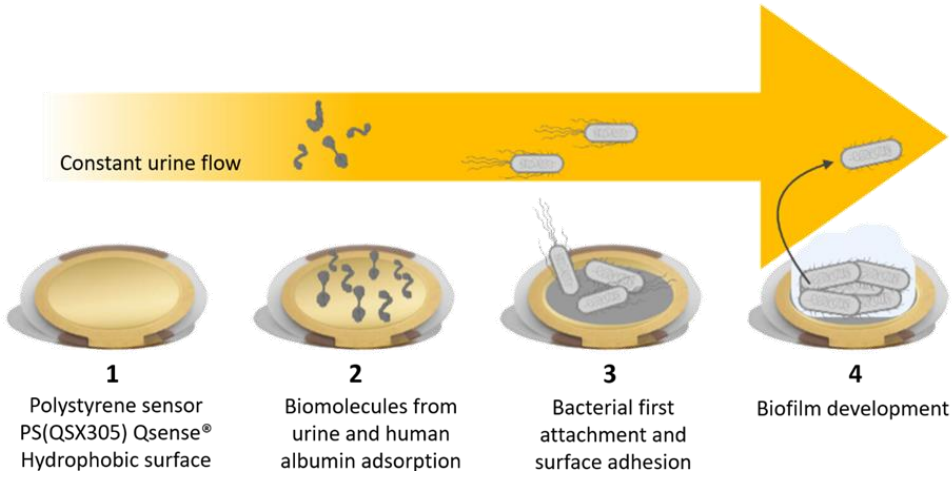

Figure II. 10 Model to study biofilm formation on QCM-D chamber for hydrophobic surfaces. Under constant flow, artificial urine with human albumin and other biomolecules was circulated through the QCM-D chamber. Elements present in artificial urine were adhered on the sensor, creating a layer of biomolecules where bacteria can be anchored (2). After that, bacteria were circulated to observe how interacts with the created layer of biomolecules in different ways (3). Finally, attached bacteria developed a biofilm under flow conditions using artificial urine as a growth media (4).

First, for the creation of a suitable model to study the influence of HA dissolved in patients' urine, two types of urine (artificial urine and urine from healthy donors) have been evaluated with the QCM-D. The experiment procedure was designed to evaluate the QCM-D output signal complexity for selected media. The output signal must present simple frequency and dissipation shifts that reflect the real behaviour of urine through urinary catheter but without noise or complex signals that mask HA contribution on the hydrophobic surface.

Changes in both frequency and dissipation signals were recorded by QCM-D using a polystyrene-gold (PS-gold) sensor during 12 hours in continuous media flow without recirculation. The results of the evaluation of artificial urine, the frequency and dissipation changes, are shown in Figure II. 11. As expected, the artificial urine through the QCM-D chamber caused a frequency shift due to the adhesion of mass onto the sensor surface. More specifically, it is possible to identify two stages in the QCM-D signal evolution profile: the first one corresponds with the first 4 hours of experiment (Figure II. 11 zone I) and the second one, from 4 to 12 hours of incubation (Figure II. 11 zone II).

During the first stage it can be observed a slight mass increase that may be attributed to the adsorption of peptides and proteins present in the artificial urine on the hydrophobic surfaces of

the QCM-D sensor[69]. The second stage reveals a progressive and slower frequency and dissipation shift until it reaches a plateau as most binding sites were occupied in the first phase, improving the layer uniformity by the molecule ordering and packing in this phase[65,70].

In addition, changes in the dissipation, Figure II. 11 A, revealed that the mass adsorbed on the sensors surface during the second stage became softer and dissipative. This may indicate that the layer of biomolecules adsorbed in the surface is stable and other molecules from urine start to interact and form complexes with them, forming a soft structure[71,54]. Microscopy images of QCM-D sensor during the circulation of artificial urine to observe changes on surface are shown in Figure II. 11 C. After 2 hours of circulation, small structures appeared heterogeneously on the surface of the sensor which are clearly visible at the endpoint of incubation. The formation of these structures fits with the observed changes in frequency and dissipation of the QCM-D signal output.

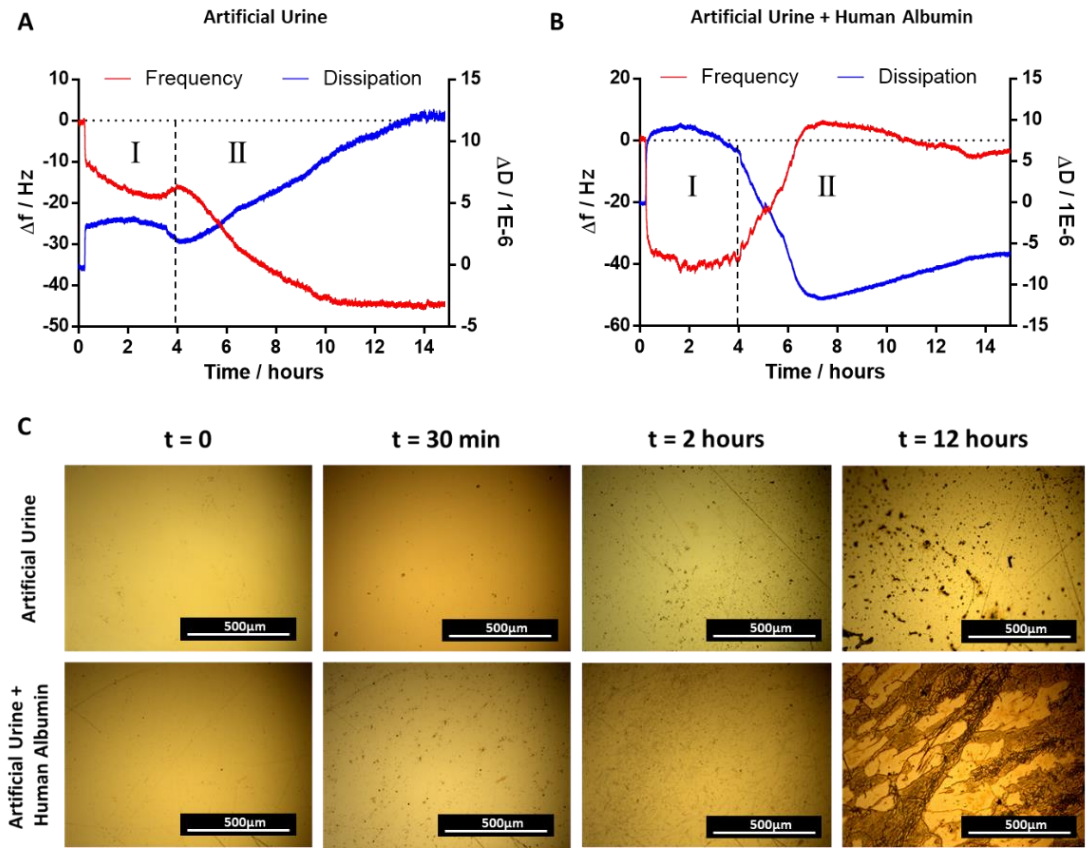

Figure II. 11 Frequency and Dissipation changes monitored using QCM-D during the circulation of artificial urine (A) and artificial urine with 0.3 mg/mL of human albumin (B). Data was obtained using a polystyrene – gold sensor. Overtone 7th

is shown. Time lapse of the sensor surface using QCM-D window module (C). Microscopy images were taken at time 0, 30 min, 2 hours and 12 hours during the circulation of artificial urine and artificial urine with 0.3 mg/ml of human albumin.

For the evaluation of artificial urine with HA, 0.3 mg/mL HA in artificial urine was circulated through QCM-D chamber, monitoring differences in the output signal. It is widely described the adsorption behaviour and conformational dynamics of HA on hydrophobic surfaces[70,72,73]. Thus, it should be expected a similar two-phase adsorption behaviour in aqueous solution, like the one described for bare artificial urine in Figure II. 11 A. As anticipated, the first stage of artificial urine circulation with HA (Figure II. 11 B) presented a dramatic shift in frequency and dissipation indicating a rapid adsorption of HA on the surface of the sensor. However, after 4 hours of circulation, a second stage of adsorption events can be observed, reflected in an increase of frequency values. As previously described, frequency shifts should indicate a loss of mass from the sensor surface[74] or a water desorption[75] from HA layers. However, in this case, positive frequency values can be explained as a result of a collapse and a saturation of the sensor surface. This can be directly related to the formation of amorphous HA aggregates or biomolecules complexes as well as HA fibers[72,76] due to the high concentrations of HA used. These structures under flow may change the sensor oscillation increasing the frequency signal output. The time lapse obtained through QCM-D window module to monitor the mass deposition on the sensor provided evidences validating this hypothesis. Images taken at 12 hours (Figure II. 11 C) reveal the formation of a higher number of fibbers attached to sensor surface than the ones formed when artificial urine was recirculated without HA.

To that extent, the ability of the QCM-D technique to provide information of artificial urine behaviour and HA deposition on hydrophobic surface under constant flow has been demonstrated and, in the light of these discussions, we propose a model to study the effect of high concentrations of HA dissolved in artificial urine by QCM-D whose times of incubation do not exceed 2 h.

As previously mentioned, biomolecules such as protein and short peptides adsorbed on sensor surface are responsible of shifts and variations on frequency signals during artificial urine circulation. To validate this behaviour on our model during the QCM-D assay, total amount of protein was quantified through microBSA assay at different times (Figure II. 12). Moreover, the same quantification was performed on silicone (PDMS) coupons incubated with the same conditions, to verify that PS-gold QCM-D sensors work as a representative platform to study

adhesion on hydrophobic surface. Thus, the results may be equivalent to urinary catheter systems, which are manufactured using silicone as main material.

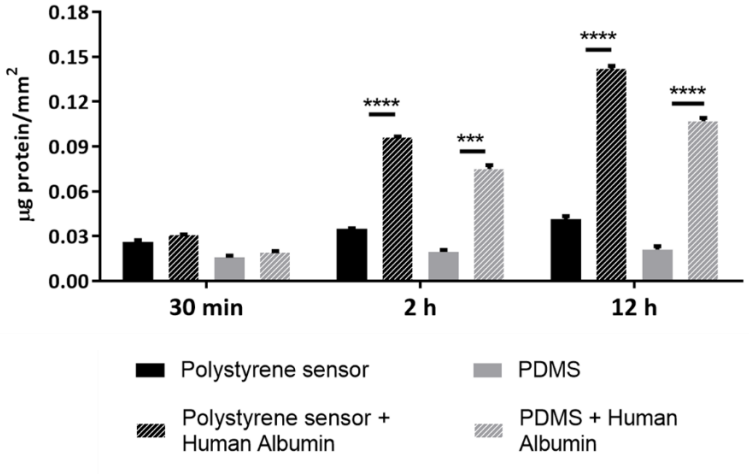

Figure II. 12 Protein quantification of QCM-D sensor on Polystyrene – gold sensor and PDMS coupons for different incubation times (30 min, 2 hours and 12 hours). Samples were incubated with artificial urine and artificial urine with 0.3g/ml of HA.

Reflecting the behaviour monitored through QCM-D, adding HA to urine increases the protein adsorbed on surface, reaching its maximum value at 12h an increase on deposited protein was observed at 2 and 12 hours, but not in the first 30 minutes, which remarks the importance of performing long-time studies to understand the role of HA in the studied system.

The higher amount of protein adsorbed at 12 h match with sensor saturation phenomenon observed in Figure II. 11 B, supporting the hypothesis and validating the suitability of our model.

For the studied time interval, the amount of deposited protein increases with the time of circulation for both surfaces. It is interesting to note that both graphs presented a similar profile for protein quantification values, indicating a certain degree of similarity between both hydrophobic surfaces. As a result, HA adhesion on hydrophobic surface can be monitored through QCM-D, providing an explanation of the biomolecules adhesion behaviour.

Next step was to validate the model using real urine to approximate it as close as possible to reality. Circulation of real urine with and without HA for 12 hours revealed different frequency and dissipation profiles in the QCM-D monitoring output, especially when profiles are compared with

the same test performed with artificial urine (Figure II. 11 A and B). After 1 hour of real urine circulation, a sudden drop of the frequency value was observed indicating a mass increase on the surface of the sensor. This fact indicates that in real urine, the higher number of biomolecules present in media interact with the surface[59], being adsorbed in less time than the biomolecules from artificial urine and forming a rigid layer. After 2 h of test, the QCM-D output signal became erratic in the frequency and dissipation values. This effect can have been caused by a precipitation of big clusters of molecules from real urine that interacted with HA. QCM-D window module images revealed the early formation of aggregates after 30 min of circulation, supporting the idea (Figure II. 13). As can be seen in supplementary materials, real urine with HA at high concentrations form a precipitate after 24 h at room temperature. This phenomenon may indicate that HA creates complex aggregates with some biomolecules present in real urine that are not present in artificial urine[76]. These results showed that unfortunately, real urine cannot be used to study bacterial adhesion on surfaces and how dissolved HA can favour or not the bacterial attachment and biofilm development.

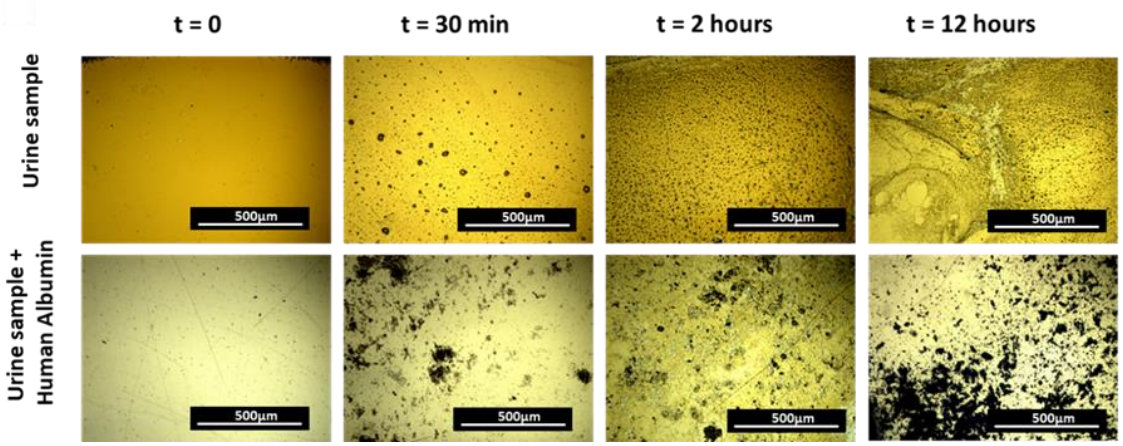

Figure II. 13 Microscopy images from sensor surface. Images were taken during real urine circulation at time 0, 30 min, 2 hours and 12 hours with or without 0.3 mg/ml of HA dissolved. Heterogenous aggregates are shown in early stages of the study.

2.3.3.1 Effect of dissolved human albumin in urine in first bacterial attachment and biofilm development

To evaluate the effect of HA over the bacteria attachment it has been used the previous developed model to study *Escherichia coli* CFT073 (uropathogenic model strain) behaviour under different conditions to recreate CAUTI conditions. First, artificial urine with and without HA was

circulated through QCM-D chamber during 2 h (Figure II. 14) forming a thin film of biomolecules onto the sensor surface. After circulation of urine with and without HA, bacteria were inoculated for 1 h in continuous flow. After that, artificial urine without HA in all cases, was used as a bacterial growing media to study biofilm formation.

Regarding the biofilm formation in absence of HA, it can be seen in Figure II. 14 A, that in the first stage of the test, artificial urine behaved as previously studied in the model (Figure II. 14 A). In a second stage, bacteria came into the QCM-D chamber and a frequency decrease was observed, indicating, that can be easily associated with the bacteria attachment phenomenon. After the stabilization of bacteria, artificial urine provided the bacterial growing substrate, bacteria replicated and produced a progressive decrease on frequency values until 11 h of test, revealing again a mass increase on the sensor surface. At 11 h of experiment the QCM-D profile changed by increasing the frequency and showing little mountains and valleys until endpoint. This indicated a loss of mass from sensor surface or a stagnation of bacteria development. However, as previously reported by Lubarsky et. al[75], this profile, showing a film hydration and dehydration may be related with biofilm development and maturation. As explained in literature, this phenomenon takes place during the multi-layered structure related to a mature biofilm. In addition, frequency values were staged and maintained over time while dissipation increased notably. These values showed that the film deposited on surface became much more viscoelastic, one of the principal characteristics of biofilms[77]. Additionally, using microscopy images it was possible to confirm the different stages of the biofilm development (Figure II. 14 C), resulting in a mature biofilm completely attached at 18 h.

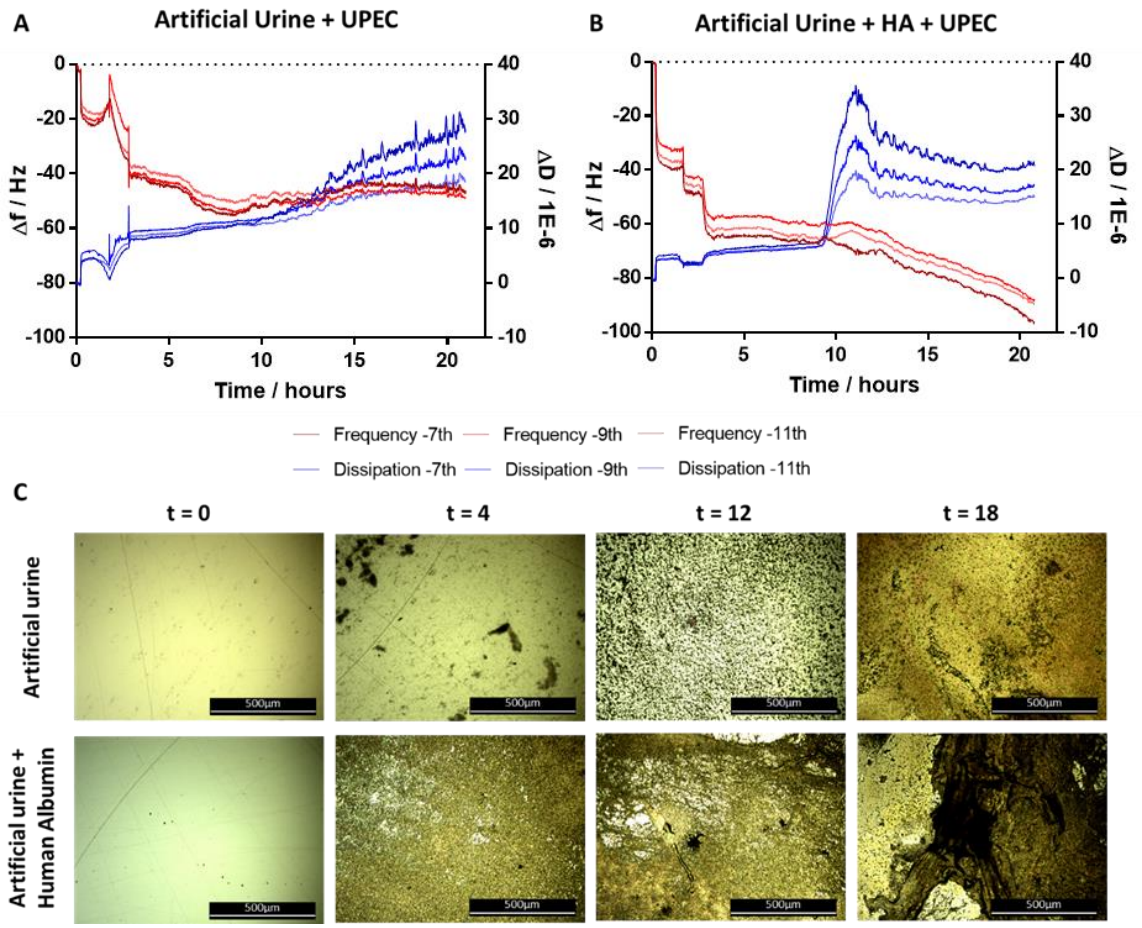

Figure II. 14 Study of influence of HA dissolved in artificial urine in first bacterial attachment and biofilm development. QCM-D profile of artificial urine (A) and artificial urine with HA (B). After 2 h incubating with artificial urine with or without HA, *E. coli* CFT073 in PBS was circulated through the sensor during 1 h, followed by artificial urine sterile without HA in all cases during 18 h. Values of frequency (red lines) and dissipation (blue lines) were taken by QCM-D. Only three overtones are represented on graphs: 7th, 9th and 11th. Images obtained by microscopy with X 10 magnification (C).

After the analysis of biofilm formation on sensor surface using artificial urine, we studied the contribution of HA to the biofilm growth. Urine with HA was led through the QCM-D chamber and HA interacted with sensor surface during 2 h forming a rigid layer[78], as can be noted in the dissipation values. (Figure II. 14 B). Once *E. coli* CFT073 was introduced, in contrast with the profile of Figure II. 14 A, no washing effect was observed, and the circulation of bacteria caused the frequency values drop quickly. After 8 h of test, frequency values decreased more sharply, coinciding with a pronounced rise in dissipation values, showing that the formed film on surface becomes more viscoelastic, indicating a more structured and developed biofilm than the one

tested without HA[77]. Comparing microscopy images between both conditions (Figure II. 14 C), the adhered mass of the test with HA is bigger, homogeneous and stratified than the one shown in the test without HA. These results indicate that HA plays a critical role in the first stages of bacterial attachment, allowing more attached bacteria and producing a rapid biofilm development and maturation.

2.3.3.2 Analysis of bacterial motility on surface and biofilm flow by FFT.

Planktonic bacteria attach to the surface using their appendages as anchoring points. Once bacteria are bonded to the surface, the interaction between them is promoted. Hence in the interphase bacteria-surface act physical forces that include van der Waals forces, steric interaction and electrostatic interaction, as well as interaction produced by bacteria appendages which entangles bacteria with the biomolecules present on the surface[20,79]. During the formation of stable biofilm, bacteria present a characteristic flagellar movement that produces a fluctuation originated from the dynamic activity of bacteria interacting with the surface of the substrate[80,81]. Once the biofilm is consolidated, the bacterial motility is drastically attenuated because bacteria are embedded into the biofilm structure losing their appendages[81] (Figure II. 15). Changes present in motility during previous stages of biofilm consolidation may provide information about how biofilm has been developed and its maturation grade.

According with the mentioned mechanism, we studied *E. coli* CFT073 bacteria motility using QMC-D in artificial urine model to study the role of HA promoting biofilm formation and the impact on the kinetics of biofilm consolidation. Hence, characteristic fluctuations on the resonance frequency were analysed, which represent a quantitative indicator of dynamic activities performed by adhered bacteria on a surface. The study of these fluctuations using fast Fourier transformation (FFT) is able to evaluate the response of bacterial cell to environment changes[51]. FFT is a useful tool to study fluctuating time series providing the corresponding power spectrum plots, which reflects the contribution of individual harmonics function of specific frequency to overall time series as function of frequency. Hence, a peak in the power spectrum corresponds to a characteristic frequency indicating a periodicity on the experimental data. This periodicity during cell environments analysis is easily associated with cell motility as it has been described in bibliography[51].

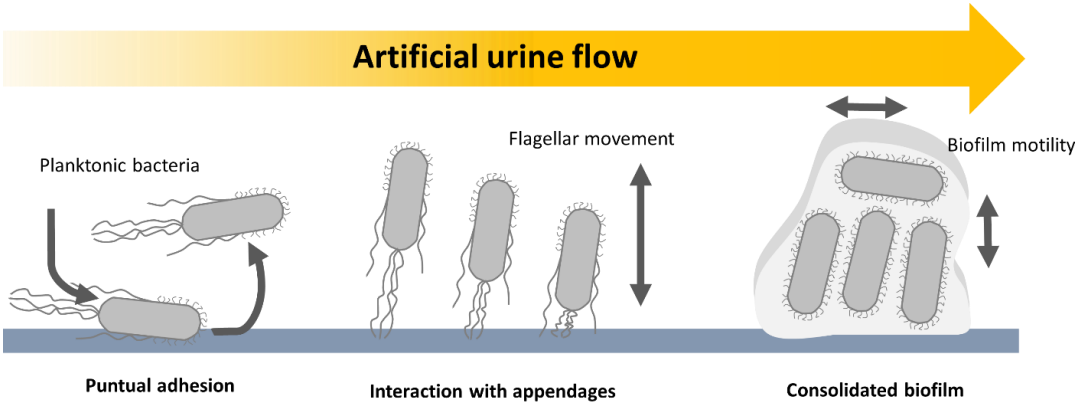

Figure II. 15 Bacterial interactions with surfaces. Bacterial interactions with surfaces. First, bacteria are adhered to substrate due to the interactions of their appendages and the electrostatic forces. Flagellum may interact with surface and a flagellar movement is produced, which is attenuated at the end of biofilm consolidation. Bacteria inside a mature biofilm can move by Brownian movement and biofilm mass swings.

Based on frequency changes monitored through QCM-D for artificial urine with and without HA in presence of *E. coli* CFT073 (Figure II. 14 A and B), we focused on the motility study in three stages of interest. First, the stage when artificial urine (or artificial urine with HA) was introduced in QCM-D chamber. Next, the stage when *E. coli* CFT073 inoculum was circulated into the system and finally, the frequency shift during biofilm development (Figure II. 16).

The motility study was performed comparing the power graphs of the three studied stages, with and without HA (Figure II. 16 A-H). All stages were studied under physiological urine flow revealing a characteristic functionality in all power graphs as observed in bibliography[51]. Although the urine flow may cause an additional fluctuation in monitored data, FFT analysis was carried out under those conditions to evaluate the model in a medium as close as possible to that existing in urinary catheters.

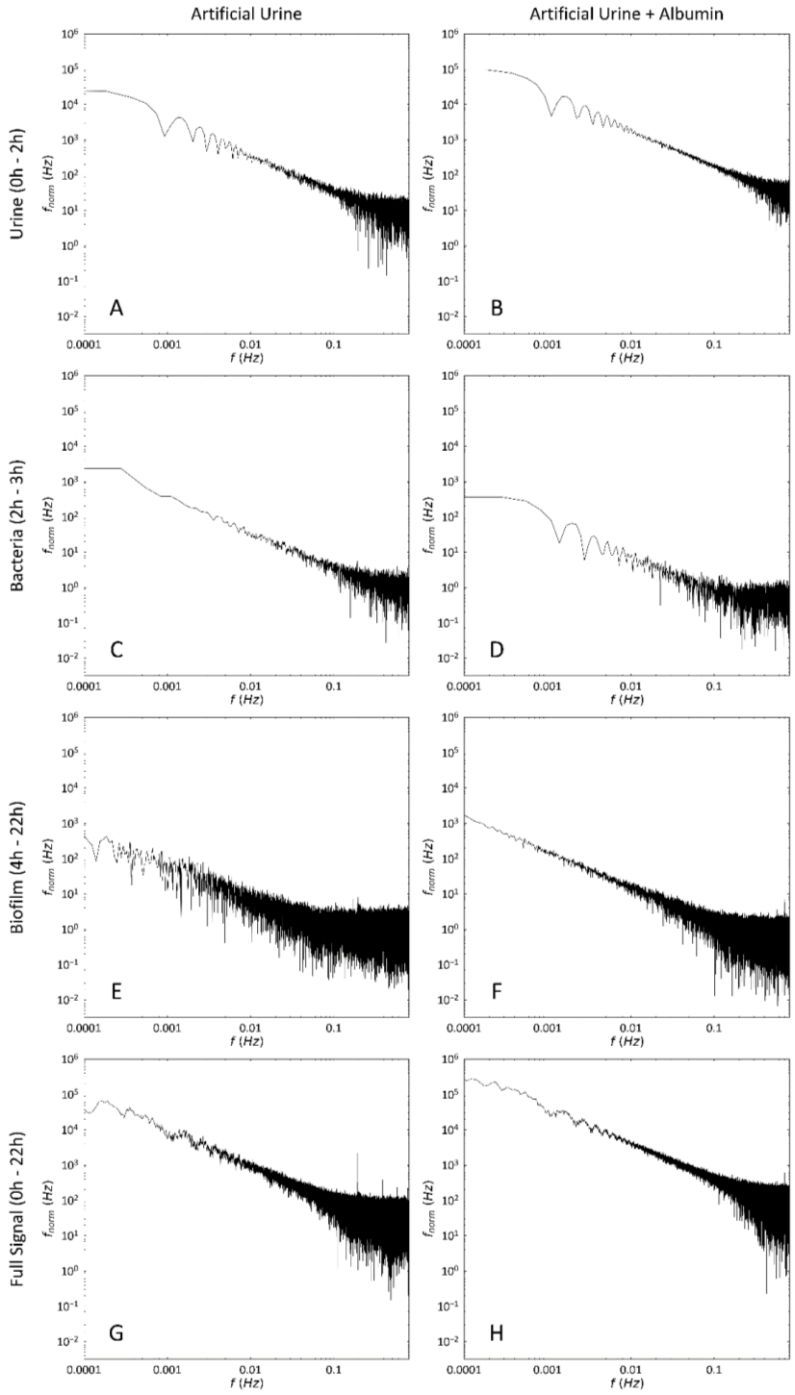

Figure II. 16 Power density spectra obtained after applying FFT algorithm to sections of interest of the QCM-D monitoring output signal. The studied stages were: A first stage with urine circulating on the sensor surface before *E. coli* CFT073 incubation without HA (A) and with HA (B) (2 hours). A second stage with *E. coli* CFT073 incubation on surface without

HA (C) and with HA (D). Bacterial biofilm development during test (18 h) after *E. coli* CFT073 attachment on surfaces without HA (E) and with HA (F). And finally, the complete profile of tested surfaces without HA (G) and with HA (H).

Figure II. 16 A and B show the power density spectra of the resonance frequency for the first stage of urine circulation with and without HA respectively. The profile shape revealed the attenuation of peaks at ~ 0.02 Hz and 0.1Hz in the power density spectrum of artificial urine with HA (Figure II. 16 B) indicating small changes in the surface dynamic activity attributed to the formation of HA structures adhered on the sensors surface, supporting the behaviour previously observed with QCM – D monitoring.

When bacteria were circulated in QCM-D chamber for one-hour, different profiles were observed depending on if the urine circulated containing HA. As can be shown in Figure II. 16 C, the power density spectra of artificial urine during bacteria addition revealed the presence of different frequency fluctuations in the 0.001 – 0.1 Hz zone as well as the presence of resonance features in the zone of 0.1 – 1 Hz, where the peak at 0.2 Hz was especially significative. These changes in the dynamic activity on the sensor surface indicated that bacteria were interacting with the surface bioenvironment formed in the previous part. The changes on the motility of the surface may be attributed to the flagellar movement of the adhered bacteria. However, Figure II. 16 D revealed an attenuated power density profile indicating a reduction of the dynamic activity. It may be considered that this reduction was produced by the fact that bacteria were not being attached to the surface of the sensor. However, frequency shift on QCM -D profiles as well as QCM-D chamber time-lapse images performed during this stage, clearly demonstrate the adhesion of bacteria and the formation of different structures attributed to HA. Our hypothesis is that bacteria presented a high degree of affinity for HA structures, being strongly integrated on these structures or even embedded on them. Bacteria – substrate anchorage and posterior bacteria flagellar movement were mainly determined by the static and dynamic properties of the HA structures.

The power density spectra of the biofilm development (Figure II. 16 E and F) is of relevance. *E. coli* CFT073 biofilm formation with HA in sensor surface (Figure II. 16 F) presented a higher attenuation of the frequency amplitudes compared with the same test performed with artificial urine without HA (Figure II. 16 G). It was also observed the suppression of resonance features, specifically a high resonance frequency near 0.1 Hz. That attenuation indicates that the reduction of the general motility of the elements present in the sensor surface occurred not only during the bacteria adhesion stage but also during the whole test. This motility reduction indicates that the biofilm produced in HA is more stratified and matured than the one produced at low HA

concentrations. The power density spectra of the complete test (Figure II. 16 G and H) support the previous statements, where plot for artificial urine with HA presented a more attenuated profile and the loss of predominant peaks from artificial urine without HA.

In this section, not only a biofilm has been generated in environmental conditions similar to observed during the development of a CAUTI, but also this model has been used in order to find the role of HA present in urine at high concentrations in bacterial attachment and medical devices colonization. It has been found that dissolved HA in urine produces complex structures allowing the immobilization of bacteria on surfaces. This early and strong bacterial attachment accelerates the formation of mature biofilm on surface.

The QCM-D technique allowed understanding the importance of proteins present in complex media in bacterial adhesion to surfaces process. The dynamic model allowed the study of bacterial adhesion at long times and how adhesion phenomenon varied according to the presence of proteins capable of interacting with the material. For future proposals for antimicrobial materials, it will be necessary to consider that the material not only repels the bacterial interaction, but it would be interesting that the material repels the protein interaction as well. Despite the results obtained, QCM-D can only be used to obtain *in vitro* approximations. These methodologies can approach real situations by mimicking flows or infection times, but they cannot be extrapolated to analyse the formation of biofilms in situations of real infections or *in vivo* studies. Therefore, this technique is relegated to studies of material-bacteria interaction *in vitro*.

2.3.4 *In vivo* study of biofilm formation on medical devices

The techniques developed in the previous sections presented good results applied in vitro. However, the biofilm to be studied is formed on medical devices under real conditions. Real biofilms are more complex than in vitro ones, affecting their characterization. Biofilms formed on medical devices are usually matrices of mixed bacterial populations and species. These bacteria build mixed biofilms by synergies or compete to occupy the niches. In addition, these biofilms are much more mature and stratified than the laboratory-developed ones, so, their visualization is much more complex, even though a correct evaluation gives a lot of information. The techniques to visualize and quantify these biofilms must be sensitive enough. Because of this, the techniques developed in previous sections will be reviewed to verify their adaptation to in vivo tests.

For evaluation of the developed methods, a study of biofilm development on tracheal stents was made. After 30 days of implantation, tracheal stents were extracted from pigs. Three tests

were performed, illustrated in Figure II. 17: (1) an extraction and quantification of the live bacteria embedded in the biofilm via the sonication and vortex protocol using different media and culture conditions, (2) an isolation of the extracted bacterial species and their identification by MALDI-TOF and (3) a visualization of the biofilm by FE-SEM.

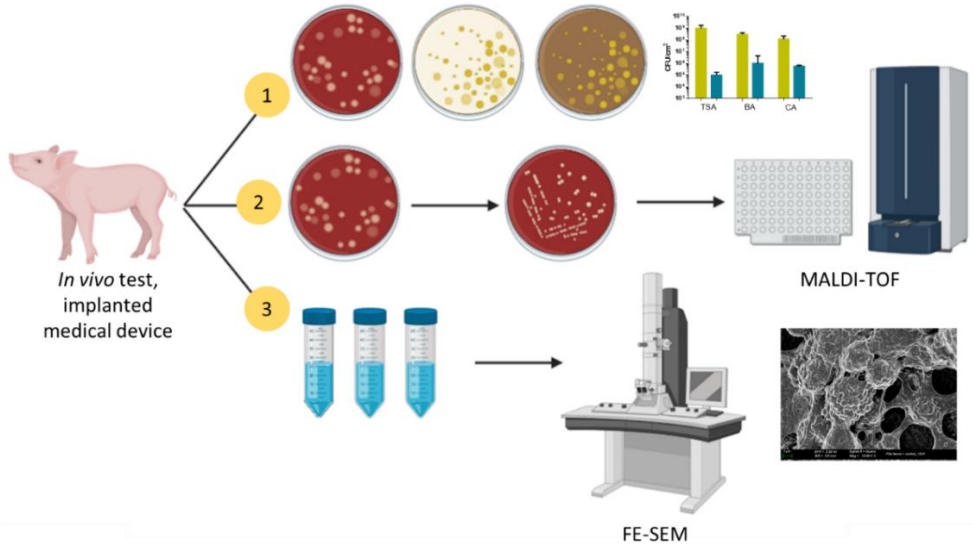

Figure II. 17 Scheme of techniques for biofilm visualization, quantification, and bacterial identification from real medical devices in *in vivo* studies, specifically, in tracheal stent implanted during 30 days in mini pigs. 1) Bacterial quantification in different media (complete media such as blood agar or chocolate agar and regular media such as TSA or LB-agar) using the protocol of biofilm extraction and quantification previously studied. 2) Bacterial isolation from cultures and identification by MALDI-TOF technique. 3) Visualization of biofilm structure by FE-SEM, previously fixed and dehydrated on the medical device studied according to the protocols developed.

First, samples were gently washed in sterile PBS and kept there for no more than 2 h after its extraction. This step prevented that bacteria dyed and eliminated biological debris not adhered to the stent, such as mucosa and blood. After that, the tracheal stent was cut into two fragments; one of them was treated to visualize biofilm by FE-SEM. Biofilm was extracted and quantified from the other fragment. After quantification of the bacteria extracted, each different specie was isolated and identified by MALDI-TOF.

Bacterial quantification was made according to the protocol S-V-S described in previous section. To ensure the correct growth of bacteria complex and standard media were used and bacteria were grown during 48 h (Figure II. 18).

As can be noted, it was possible to extract the biofilm formed on the tracheal stents using S-V-S protocol. After that, bacteria were quantified. The average number of bacteria adhere to stent per cm^2 was 10E09. The technique was sensitive enough to extract and quantify from 100 ± 30 CFU/cm^2. Different species were observed depending on the medium used, so, the identification of the bacterial species was done for each of isolated specie.

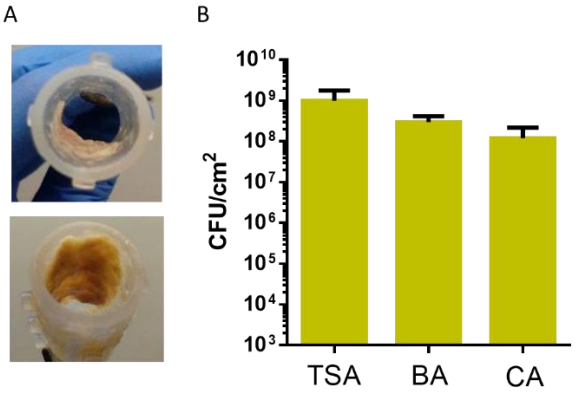

Figure II. 18 Biofilm images and bacterial quantification on tracheal stent. A) Image of tracheal stent after 30 days of implantation in pigs after washing. B) Bacterial quantification from tracheal stent after 30 days of implantation in pigs. Bacterial cultures were made in complete media (blood agar, BA and chocolate agar, CA) and regular media (TSA). The cultures were growth in atmospheric conditions and in an incubator with 5 % of CO_2 atmosphere at least 48 h.

Once the extraction was carried out, different bacterial species were isolated and cultivated in appropriated medium and growth conditions. After, these bacterial species were identified using MALDI-TOF technique (Figure II. 19). Bacteria were classified into three ranges, according to their relationship with respiratory infection. Bacteria belonging to the natural respiratory microbiota were classified as non-pathogenic, in green. Bacteria that are commonly found in the respiratory tract but can trigger respiratory infections as opportunistic pathogens were classified in yellow. In addition, these bacteria were found in higher numbers than those established as normal due to their high presence in the extracts, despite of the difficulty of culturing. Respiratory pathogenic bacteria were classified with red colour. As results shown, revealed bacterial strains can explain the infection progress of the pigs. Respiratory pathogenic bacteria were found in a much higher percentage than usual. In addition, MALDI-TOF offered the possibility of finding which pathogenic bacteria was causing the infection almost entirely and colonizing the device almost completely. In this case, *Klebsiella pneumoniae* was the most isolated bacterium from the tracheal stent (33 % of total bacterial counts (1E09 CFU/cm^2)).

The complete analysis of bacteria extracted from MALID-TOF test are able in supplementary information.

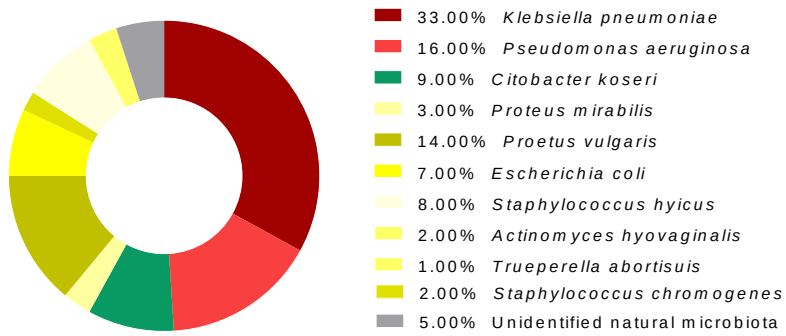

Figure II. 19 Bacterial identification by MALDI-TOF from tracheal stent after 30 days of implantation in pigs. Bacteria were classified according to their respiratory pathogenicity (red), opportunistic pathogens of respiratory, digestive or urinary tracts (yellow), natural microbiota (green) and unidentified microbiota of minipig (silver). The percentage indicate the number of bacteria of each specie isolated presented in the medical device compared to the total number of isolated bacteria.

After bacterial quantification and identification, biofilm was visualized by FE-SEM to observe the its maturity level and morphology. The images are showed in Figure II. 20, from A to I. Images correspond to the tracheal stents, showing a highly stratified mature biofilm in different ways. The images showed a complex, layered and mature biofilm formed on the tracheal stent (Figure II. 20 A-D). In the biofilm matrix, the formation of microcolonies (spheres) about 5 to 7 µm diameter connected and superimposed, could be observed. The connections between the spheres, the channels and the biomass are well stablished. In the biofilm it can see depth structures and details about the biofilm anchoring points to the surface. An example is the appearance of pillars, supposedly flexible and created from extracellular mucosa.

The biofilm was completely structured in layers, which had a complex system of channels. These channels are created to give way to water, gases and nutrients and thus prevent the loss or death of the deeper levels of the bacterial biofilm. Channels often appear in biofilms of very mature mixed populations. Therefore, a high level of colonization and infection is assumed in this medical device.

Figure II. 20 E and F showed a different tracheal stent, where biofilm seemed less structured. Individual bacteria (bacilli) can be seen embedded in a mucous matrix. However, this mucous

layer covering the tracheal stent was homogeneous and it seemed to be in an earlier stage of biofilm development than mentioned above. Furthermore, the images showed an uniform film, without breaks due to manipulation and without lifting of the bacterial matrix, its loss or blurring. It is evident that there are clear differences between the two biofilms studied, so the technique can preserve mature biofilms and biofilms in early stage of development without losing any detail.

Finally, biofilm thickness data were obtained using the FE-SEM measurement tool (Figure II. 20 G and I). The thickness was measured using a raised area of the biofilm just in the cutting area of the scalpel. As can be seen in the Figure II. 20, there is a thickness difference of almost 12 µm between them. The mature biofilm observed in images A to D corresponds to the thickness measurement of 15.30 µm, while the biofilm in early development had a measurement of 3.82 µm. Therefore, it is easy to relate the complexity and maturity of a biofilm with the thickness of the film shown. It is necessary to emphasize that, due to the dehydration techniques that were carried out to be able to visualize the samples in FE-SEM, the thickness of the film could vary considerably. However, we assume that the relation is maintained.

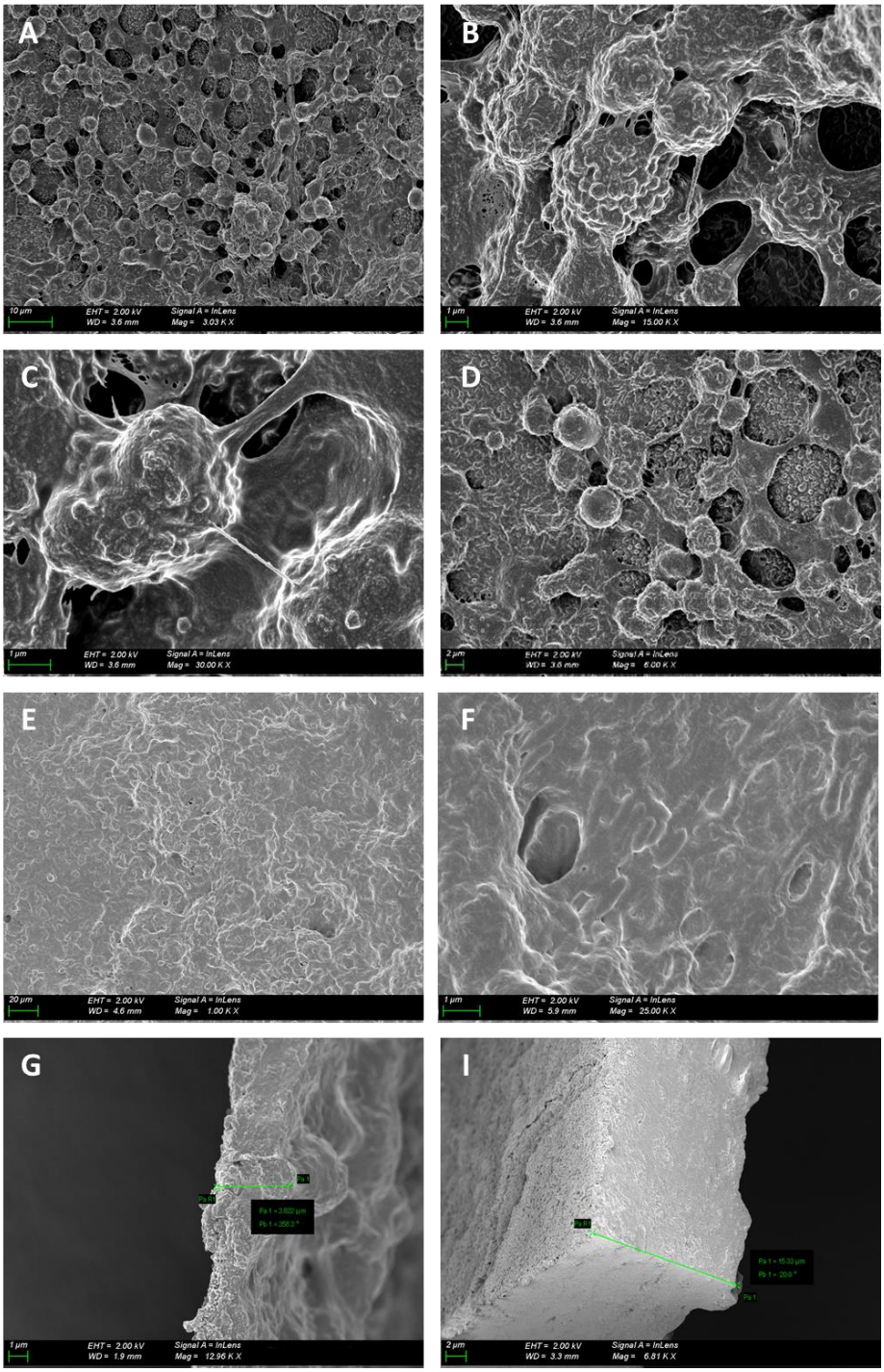

Figure II. 20 FE-SEM images from 100 % silicone-based tracheal stents after 30 days of implantation in pigs. Different zooms from tracheal stents are shown in images A to F. Biofilm thickness are shown in G and I images from two different tracheal stents.

The opportunity to participate in the *in vivo* analysis of tracheal stents infections, confirmed that the optimized protocols for quantifying bacteria and visualizing mature biofilms from mixed populations are applicable to real environments. The techniques to extract and quantify biofilm were sensitive enough to observe different degrees of bacterial interaction with the device. The formation of mature biofilm composed of different bacterial species on tracheal stents did not pose a problem for its quantification. In addition, the biomass fixation techniques allowed visualizing the adhered biofilm on the curved surface of the devices with a high level of detail. Thus, the tests allowed a better understanding of the development of a tracheal stent infection during the first month of implantation. So, these techniques may be useful during the study of biofilm in urinary catheters during the following chapters due to the similarities between the device

2.4 CONCLUDING REMARKS

In this chapter, protocols and techniques to study bacteria-material interactions have been developed. Different materials and techniques used to develop biofilms on surfaces, as well as the bacterial strain and medium, have been evaluated. Tests showed that these parameters must be as close as possible to reality to obtain remarkable results that can be extrapolated to real infective process. Furthermore, techniques have been defined successfully to study bacterial adhesion and biofilm formation on materials for medical use, such as silicones and on common medical devices, such as urinary catheters and tracheal stents. For that purpose, protocols for counting bacteria adhering to surfaces have been obtained. These protocols are sensitive enough to count and distinguish bacterial counts from punctual adhesion to mature biofilms.

Moreover, biofilm visualization techniques for medical devices have been developed using FE-SEM. It has been possible to observe from first stages of bacterial adhesion to mature biofilm structures formed on the surfaces of the medical devices. The images had a high rate of detail that provided information about the way bacteria were anchored to surfaces and their structure. Moreover, FE-SEM protocols offered information about biofilm structure and formation in *in vivo* environments without drawbacks. Furthermore, the bacterial population of the tracheal stent could be isolated and identified using MALDI-TOF.

In order to obtain more information about bacteria-material interactions and the parameters that could promote bacterial adhesion to surfaces, QCM-D has been used to evaluate the adhesion of bacteria in complex media like urine under flow conditions. The QCM-D studies showed a clear relationship between the presence of protein in the medium and the improvement of bacterial adhesion and the biofilm development in urine-like media.

In vitro and *in vivo* tests have been performed obtaining well established protocols to detect bacteria on surfaces in different environments and conditions. These techniques and protocols allow the evaluation of the antimicrobial materials developed in the following chapters and can be applied to the study of the bacterial interaction with urinary catheters.

2.5 REFERENCES

(1) Donné, J.; Dewilde, S. *The Challenging World of Biofilm Physiology*, 1st ed.; Elsevier Ltd., 2015; Vol. 67. https://doi.org/10.1016/bs.ampbs.2015.09.003.

(2) Place, J. L.; Rupp, M. E.; Finch, R. G. *Biofilms, Infection and Antimicrobial Therapy*; 2006. https://doi.org/10.1201/9781420028232.ch12.

(3) Gianfranco Donelli. *Microbial Biofilms IN Series Editor*; 2014.

(4) Vila, J.; Soriano, A.; Mensa, J. Bases Moleculares de La Adherencia Microbiana Sobre Los Materiales Protésicos. Papel de Las Biocapas En Las Infecciones Asociadas a Los Materiales Protésicos. *Enferm. Infecc. Microbiol. Clin.* **2008**, *26* (1), 48–55. https://doi.org/10.1157/13114395.

(5) Zaborowska, M.; Welch, K.; Branemark, R.; Khalilpour, P.; Engqvist, H.; Thomsen, P.; Trobos, M. Bacteria-Material Surface Interactions: Methodological Development for the Assessment of Implant Surface Induced Antibacterial Effects. *J. Biomed. Mater. Res. - Part B Appl. Biomater.* **2015**, *103* (1), 179–187. https://doi.org/10.1002/jbm.b.33179.

(6) Bryers, J. D. Medical Biofilms. *Biotechnol. Bioeng.* **2008**, *100* (1), 1–18. https://doi.org/10.1002/bit.21838.

(7) Donlan, R. M. Biofilms: Microbial Life on Surfaces. *Emerg. Infect. Dis.* **2002**, *8* (9), 881–890. https://doi.org/10.3201/eid0809.020063.

(8) Cheung, H. Y.; Chan, G. K. L.; Cheung, S. H.; Sun, S. Q.; Fong, W. F. Morphological and Chemical Changes in the Attached Cells of Pseudomonas Aeruginosa as Primary Biofilms Develop on Aluminium and CaF2plates. *J. Appl. Microbiol.* **2007**, *102* (3), 701–710. https://doi.org/10.1111/j.1365-2672.2006.03137.x.

(9) Feng, G.; Cheng, Y.; Wang, S. Y.; Borca-Tasciuc, D. A.; Worobo, R. W.; Moraru, C. I. Bacterial Attachment and Biofilm Formation on Surfaces Are Reduced by Small-Diameter Nanoscale Pores: How Small Is Small Enough? *npj Biofilms Microbiomes* **2015**, *1* (May). https://doi.org/10.1038/npjbiofilms.2015.22.

(10) Takenaka, S.; Iwaku, M.; Hoshino, E. Artificial Pseudomonas Aeruginosa Biofilms and Confocal Laser Scanning Microscopic Analysis. *J. Infect. Chemother.* **2001**, *7* (2), 87–93. https://doi.org/10.1007/s101560100014.

(11) Donelli, G. Microbial Biofilms, Methods and Protocols Edited. *Springer* **2014**, 13–15. https://doi.org/10.1007/978-1-4939-0467-9.

(12) Azeredo, J.; Azevedo, N. F.; Briandet, R.; Cerca, N.; Coenye, T.; Costa, A. R.; Desvaux, M.; Di Bonaventura, G.; Hébraud, M.; Jaglic, Z.; et al. Critical Review on Biofilm Methods.

Crit. Rev. Microbiol. **2017**, *43* (3), 313–351. https://doi.org/10.1080/1040841X.2016.1208146.

(13) Sjollema, J.; Zaat, S. A. J.; Fontaine, V.; Ramstedt, M.; Luginbuehl, R.; Thevissen, K.; Li, J.; van der Mei, H. C.; Busscher, H. J. In Vitro Methods for the Evaluation of Antimicrobial Surface Designs. *Acta Biomater.* **2018**, *70*, 12–24. https://doi.org/10.1016/j.actbio.2018.02.001.

(14) Alexander, T. E.; Lozeau, L. D.; Camesano, T. A. QCM-D Characterization of Time-Dependence of Bacterial Adhesion. *Cell Surf.* **2019**, *5* (January), 100024. https://doi.org/10.1016/j.tcsw.2019.100024.

(15) Schlafer, S.; Meyer, R. L. Confocal Microscopy Imaging of the Biofilm Matrix. *J. Microbiol. Methods* **2017**, *138*, 50–59. https://doi.org/10.1016/j.mimet.2016.03.002.

(16) Magana, M.; Sereti, C.; Ioannidis, A.; Mitchell, C. A.; Ball, A. R.; Magiorkinis, E.; Chatzipanagiotou, S.; Hamblin, M. R.; Hadjifrangiskou, M.; Tegos, G. P. Options and Limitations in Clinical Investigation of Bacterial Biofilms. *Clin. Microbiol. Rev.* **2018**, *31* (3), 1–49. https://doi.org/10.1128/CMR.00084-16.

(17) Wilson, C.; Lukowicz, R.; Merchant, S.; Valquier-Flynn, H.; Caballero, J.; Sandoval, J.; Okuom, M.; Huber, C.; Brooks, T. D.; Wilson, E.; et al. Quantitative and Qualitative Assessment Methods for Biofilm Growth: A Mini-Review. *Res. Rev. J. Eng. Technol.* **2017**, *6* (4).

(18) Achinas, S.; Charalampogiannis, N.; Jan, G.; Euverink, W. Applied Sciences A Brief Recap of Microbial Adhesion and Biofilms. **2019**, 1–15.

(19) Allan, V.; Claxton, N. S.; Fellers, T. J.; Davidson, M. W.; Diaspro, A.; Chirico, G.; Collini, M.; Glycotech; Ibidi; Kamenyeva, O.; et al. Fluorescence Microscopy. *PLoS One* **2005**, *8* (4), 910–919. https://doi.org/10.1038/nmeth817.

(20) Garrett, T. R.; Bhakoo, M.; Zhang, Z. Bacterial Adhesion and Biofilms on Surfaces. *Prog. Nat. Sci.* **2008**, *18* (9), 1049–1056. https://doi.org/10.1016/j.pnsc.2008.04.001.

(21) Zaborowska, M.; Welch, K.; Branemark, R.; Khalilpour, P.; Engqvist, H.; Thomsen, P.; Trobos, M. Bacteria-Material Surface Interactions: Methodological Development for the Assessment of Implant Surface Induced Antibacterial Effects. *J. Biomed. Mater. Res. - Part B Appl. Biomater.* **2015**, *103* (1), 179–187. https://doi.org/10.1002/jbm.b.33179.

(22) Donelli, G. Microbial Biofilms, Methods and Protocols Edited. *Springer* **2014**, *1147*, 73–84. https://doi.org/10.1007/978-1-4939-0467-9.

(23) Magana, M.; Sereti, C.; Ioannidis, A.; Mitchell, C. A.; Ball, A. R.; Magiorkinis, E.; Chatzipanagiotou, S.; Hamblin, M. R.; Hadjifrangiskou, M.; Tegos, G. P. Options and

Limitations in Clinical Investigation of Bacterial Biofilms. *Clin. Microbiol. Rev.* **2018**, *31* (3), 1–49. https://doi.org/10.1128/CMR.00084-16.

(24) Hall-Stoodley, L.; Costerton, J. W.; Stoodley, P. Bacterial Biofilms: From the Natural Environment to Infectious Diseases. *Nature Reviews Microbiology*. 2004, pp 95–108. https://doi.org/10.1038/nrmicro821.

(25) Merritt, J. H.; Kadouri, D. E.; O'Toole, G. A. Growing and Analyzing Static Biofilms. *Curr. Protoc. Microbiol.* **2011**, No. SUPPL. 22, 1–18. https://doi.org/10.1002/9780471729259.mc01b01s22.

(26) Pompilio, A.; De Nicola, S.; Crocetta, V.; Guarnieri, S.; Savini, V.; Carretto, E.; Di Bonaventura, G. New Insights in Staphylococcus Pseudintermedius Pathogenicity: Antibiotic-Resistant Biofilm Formation by a Human Wound-Associated Strain. *BMC Microbiol.* **2015**, *15* (1), 1–14. https://doi.org/10.1186/s12866-015-0449-x.

(27) Kart, D.; Kustimur, A. S.; Sağıroğlu, M.; Kalkancı, A. Evaluation of Antimicrobial Durability and Anti-Biofilm Effects in Urinary Catheters Against Enterococcus Faecalis Clinical Isolates and Reference Strains. *Balkan Med. J.* **2017**, *34* (6), 546–552. https://doi.org/10.4274/balkanmedj.2016.1853.

(28) Schlafer, S.; Meyer, R. L. Confocal Microscopy Imaging of the Biofilm Matrix. *J. Microbiol. Methods* **2017**, *138*, 50–59. https://doi.org/10.1016/j.mimet.2016.03.002.

(29) Wilson, C.; Lukowicz, R.; Merchant, S.; Valquier-Flynn, H.; Caballero, J.; Sandoval, J.; Okuom, M.; Huber, C.; Brooks, T. D.; Wilson, E.; et al. Quantitative and Qualitative Assessment Methods for Biofilm Growth: A Mini-Review. *Res. Rev. J. Eng. Technol.* **2017**, *6* (4).

(30) Colletta, A.; Wu, J.; Wo, Y.; Kappler, M.; Chen, H.; Xi, C.; Meyerhoff, M. E. S-Nitroso-N-Acetylpenicillamine (SNAP) Impregnated Silicone Foley Catheters: A Potential Biomaterial/Device to Prevent Catheter-Associated Urinary Tract Infections. *ACS Biomater. Sci. Eng.* **2015**, *1* (6), 416–424. https://doi.org/10.1021/acsbiomaterials.5b00032.

(31) Stickler, D. J.; Morgan, S. D. Observations on the Development of the Crystalline Bacterial Biofilms That Encrust and Block Foley Catheters. *J. Hosp. Infect.* **2008**, *69* (4), 350–360. https://doi.org/10.1016/j.jhin.2008.04.031.

(32) Mandakhalikar, K. D.; Rahmat, J. N.; Chiong, E.; Neoh, K. G.; Shen, L.; Tambyah, P. A. Extraction and Quantification of Biofilm Bacteria: Method Optimized for Urinary Catheters. *Nat. Sci. Reports* **2018**, *8* (1), 1–9. https://doi.org/10.1038/s41598-018-26342-3.

(33) Jones, J. F.; Feick, J. D.; Imoudu, D.; Chukwumah, N.; Vigeant, M.; Velegol, D. Oriented

Adhesion of Escherichia Coli to Polystyrene Particles. *Appl. Environ. Microbiol.* **2003**, *69* (11), 6515–6519. https://doi.org/10.1128/AEM.69.11.6515-6519.2003.

(34) Yang, Y. F.; Li, Y.; Li, Q. L.; Wan, L. S.; Xu, Z. K. Surface Hydrophilization of Microporous Polypropylene Membrane by Grafting Zwitterionic Polymer for Anti-Biofouling. *J. Memb. Sci.* **2010**, *362* (1–2), 255–264. https://doi.org/10.1016/j.memsci.2010.06.048.

(35) Regina, V. R.; Poulsen, M.; Søhoel, H.; Bischoff, C.; Meyer, R. L. Quantification of Bacteria on Abiotic Surfaces by Laser Scanning Cytometry: An Automated Approach to Screen the Antifouling Properties of New Surface Coatings. *J. Lab. Autom.* **2012**, *17* (4), 293–301. https://doi.org/10.1177/2211068212450013.

(36) Orgad, O.; Oren, Y.; Walker, S. L.; Herzberg, M. The Role of Alginate in Pseudomonas Aeruginosa EPS Adherence, Viscoelastic Properties and Cell Attachment. *Biofouling* **2011**, *27* (7), 787–798. https://doi.org/10.1080/08927014.2011.603145.

(37) Ratner, B. D.; Hoffman, A. S.; Schoen, F. J.; Lemons, J. E. *Introduction - Biomaterials Science: An Evolving, Multidisciplinary Endeavor*, Third Edit.; Elsevier, 2013. https://doi.org/10.1016/B978-0-08-087780-8.00153-4.

(38) Monteiro, D. R.; Gorup, L. F.; Takamiya, A. S.; Ruvollo-Filho, A. C.; Camargo, E. R. de; Barbosa, D. B. The Growing Importance of Materials That Prevent Microbial Adhesion: Antimicrobial Effect of Medical Devices Containing Silver. *Int. J. Antimicrob. Agents* **2009**, *34* (2), 103–110. https://doi.org/10.1016/j.ijantimicag.2009.01.017.

(39) Tipnis, N. P.; Burgess, D. J. Sterilization of Implantable Polymer-Based Medical Devices: A Review. *Int. J. Pharm.* **2018**, *544* (2), 455–460. https://doi.org/10.1016/j.ijpharm.2017.12.003.

(40) Verma, A. Differences in Bacterial Colonization and Biofilm Formation Property of Uropathogens between the Two Most Commonly Used Indwelling Urinary Catheters. *J. Clin. Diagnostic Res.* **2016**, 1–3. https://doi.org/10.7860/JCDR/2016/20486.7939.

(41) Lawrence, E. L.; Turner, I. G. Materials for Urinary Catheters: A Review of Their History and Development in the UK. *Med. Eng. Phys.* **2005**, *27* (6), 443–453. https://doi.org/10.1016/j.medengphy.2004.12.013.

(42) Elbourne, A.; Chapman, J.; Gelmi, A.; Cozzolino, D.; Crawford, R. J.; Truong, V. K. Bacterial-Nanostructure Interactions: The Role of Cell Elasticity and Adhesion Forces. *J. Colloid Interface Sci.* **2019**, *546*, 192–210. https://doi.org/10.1016/j.jcis.2019.03.050.

(43) Ramstedt, M.; Ribeiro, I. A. C.; Bujdakova, H.; Mergulhão, F. J. M.; Jordao, L.; Thomsen, P.; Alm, M.; Burmølle, M.; Vladkova, T.; Can, F.; et al. Evaluating Efficacy of Antimicrobial and Antifouling Materials for Urinary Tract Medical Devices: Challenges and

Recommendations. *Macromol. Biosci.* **2019**, *19* (5), 1800384. https://doi.org/10.1002/mabi.201800384.

(44) Wright, K. J.; Seed, P. C.; Hultgren, S. J. Uropathogenic Escherichia Coli Flagella Aid in Efficient Urinary Tract Colonization. *Infect. Immun.* **2005**, *73* (11), 7657–7668. https://doi.org/10.1128/IAI.73.11.7657-7668.2005.

(45) Hagan, E. C.; Donnenberg, M. S.; Mobley, H. L. T. Uropathogenic Escherichia Coli. *EcoSal Plus* **2009**, *3* (2). https://doi.org/10.1128/ecosalplus.8.6.1.3.

(46) Terlizzi, M. E.; Gribaudo, G.; Maffei, M. E. UroPathogenic Escherichia Coli (UPEC) Infections: Virulence Factors, Bladder Responses, Antibiotic, and Non-Antibiotic Antimicrobial Strategies. *Front. Microbiol.* **2017**, *8* (AUG). https://doi.org/10.3389/fmicb.2017.01566.

(47) Brooks, T.; Keevil, C. W. W. A Simple Artificial Urine for the Growth of Urinary Pathogens. *Lett. Appl. Microbiol.* **1997**, *24* (3), 203–206. https://doi.org/10.1046/j.1472-765X.1997.00378.x.

(48) Gilabert-Porres, J.; Martí, S.; Calatayud, L.; Ramos, V.; Rosell, A.; Borrós, S. Design of a Nanostructured Active Surface against Gram-Positive and Gram-Negative Bacteria through Plasma Activation and in Situ Silver Reduction. *ACS Appl. Mater. Interfaces* **2016**, *8* (1), 64–73. https://doi.org/10.1021/acsami.5b07115.

(49) Hohmann, S.; Neidig, A.; Kühl, B.; Kirschhöfer, F.; Overhage, J.; Brenner-Weiß, G. A New Data Processing Routine Facilitating the Identification of Surface Adhered Proteins from Bacterial Conditioning Films via QCM-D/MALDI-ToF/MS. *Anal. Bioanal. Chem.* **2017**, *409* (25), 5965–5974. https://doi.org/10.1007/s00216-017-0521-5.

(50) Bragazzi, N. L.; Amicizia, D.; Panatto, D.; Tramalloni, D.; Valle, I.; Gasparini, R. *Quartz-Crystal Microbalance (QCM) for Public Health: An Overview of Its Applications*, 1st ed.; Elsevier Inc., 2015; Vol. 101. https://doi.org/10.1016/bs.apcsb.2015.08.002.

(51) Sapper, A.; Wegener, J.; Janshoff, A. Cell Motility Probed by Noise Analysis of Thickness Shear Mode Resonators. *Anal. Chem.* **2006**, *78* (14), 5184–5191. https://doi.org/10.1021/ac060094g.

(52) Cooley, J. W.; Tukey, J. W. An Algorithm for the Machine Calculation of Complex Fourier Series. *Math. Comput.* **1965**, *19* (90), 297. https://doi.org/10.2307/2003354.

(53) Vesterlund, S.; Paltta, J.; Karp, M.; Ouwehand, A. C. Measurement of Bacterial Adhesion-in Vitro Evaluation of Different Methods. *J. Microbiol. Methods* **2005**, *60* (2), 225–233. https://doi.org/10.1016/j.mimet.2004.09.013.

(54) An, Y. H.; Friedman, R. J. Concise Review of Mechanisms of Bacterial Adhesion to

Biomaterial Surfaces. *J. Biomed. Mater. Res.* **2004**, *43* (3), 338–348. https://doi.org/10.1002/(SICI)1097-4636(199823)43:3<338::AID-JBM16>3.0.CO;2-B.

(55) Pratt, L. A.; Kolter, R. Genetic Analysis of Escherichia Coli Biofilm Formation: Roles of Flagella, Motility, Chemotaxis and Type I Pili. *Mol. Microbiol.* **1998**, *30* (2), 285–293. https://doi.org/10.1046/j.1365-2958.1998.01061.x.

(56) Totsika, M.; Kostakioti, M.; Hannan, T. J.; Upton, M.; Beatson, S. A.; Janetka, J. W.; Hultgren, S. J.; Schembri, M. A. A FimH Inhibitor Prevents Acute Bladder Infection and Treats Chronic Cystitis Caused by Multidrug-Resistant Uropathogenic Escherichia Coli ST131. *J. Infect. Dis.* **2013**, *208* (6), 921–928. https://doi.org/10.1093/infdis/jit245.

(57) Orgad, O.; Oren, Y.; Walker, S. L.; Herzberg, M. The Role of Alginate in Pseudomonas Aeruginosa EPS Adherence, Viscoelastic Properties and Cell Attachment. *Biofouling* **2011**, *27* (7), 787–798. https://doi.org/10.1080/08927014.2011.603145.

(58) Hachem, R.; Reitzel, R.; Borne, A.; Jiang, Y.; Tinkey, P.; Uthamanthil, R.; Chandra, J.; Ghannoum, M.; Raad, I. Novel Antiseptic Urinary Catheters for Prevention of Urinary Tract Infections: Correlation of in Vivo and in Vitro Test Results. *Antimicrob. Agents Chemother.* **2009**, *53* (12), 5145–5149. https://doi.org/10.1128/AAC.00718-09.

(59) Pieper, R.; Gatlin, C. L.; McGrath, A. M.; Makusky, A. J.; Mondal, M.; Seonarain, M.; Field, E.; Schatz, C. R.; Estock, M. A.; Ahmed, N.; et al. Characterization of the Human Urinary Proteome: A Method for High-Resolution Display of Urinary Proteins on Two-Dimensional Electrophoresis Gels with a Yield of Nearly 1400 Distinct Protein Spots. *Proteomics* **2004**, *4* (4), 1159–1174. https://doi.org/10.1002/pmic.200300661.

(60) Carter, J. L.; Tomson, C. R. V.; Stevens, P. E.; Lamb, E. J. Does Urinary Tract Infection Cause Proteinuria or Microalbuminuria? A Systematic Review. *Nephrol. Dial. Transplant.* **2006**, *21* (11), 3031–3037. https://doi.org/10.1093/ndt/gfl373.

(61) Sellers, E. A. C.; Blydt-Hansen, T. D.; Dean, H. J.; Gibson, I. W.; Birk, P. E.; Ogborn, M. Macroalbuminuria and Renal Pathology in First Nation Youth with Type 2 Diabetes. *Diabetes Care* **2009**, *32* (5), 786–790. https://doi.org/10.2337/dc08-1828.

(62) Newman, D. J.; Mattock, M. B.; Dawnay, A. B. S.; Kerry, S.; McGuire, A.; Yaqoob, M.; Hitman, G. A.; Hawke, C. Systematic Review on Urine Albumin Testing for Early Detection of Diabetic Complications. *Health Technol. Assess. (Rockv).* **2005**, *9* (30). https://doi.org/10.3310/hta9300.

(63) Shahbazian, H.; Rezaii, I. Diabetic Kidney Disease; Review of the Current Knowledge. *J. Ren. Inj. Prev.* **2013**, *2* (2), 73–80. https://doi.org/10.12861/jrip.2013.24.

(64) Kalantari, S.; Jafari, A.; Moradpoor, R.; Ghasemi, E.; Khalkhal, E. Human Urine

Proteomics: Analytical Techniques and Clinical Applications in Renal Diseases. *Int. J. Proteomics* **2015**, *2015*. https://doi.org/10.1155/2015/782798.

(65) Felgueiras, H. P.; Antunes, J. C.; Martins, M. C. L.; Barbosa, M. A. *Fundamentals of Protein and Cell Interactions in Biomaterials*; Elsevier Ltd., 2018. https://doi.org/10.1016/B978-0-08-100803-4.00001-2.

(66) Flores-Mireles, A. L.; Walker, J. N.; Caparon, M.; Hultgren, S. J. Urinary Tract Infections: Epidemiology, Mechanisms of Infection and Treatment Options. *Nat. Rev. Microbiol.* **2015**, *13* (5), 269–284. https://doi.org/10.1038/nrmicro3432.

(67) Brash, J. L.; Uniyal, S. Dependence of Albumin-Fibrinogen Simple and Competitive Adsorption on Surface Properties of Biomaterials. *J. Polym. Sci. Polym. Symp.* **2007**, *66* (1), 377–389. https://doi.org/10.1002/polc.5070660135.

(68) Haque, M.; Sartelli, M.; McKimm, J.; Bakar, M. A. Health Care-Associated Infections – An Overview. *Infect. Drug Resist.* **2018**, *11*, 2321–2333. https://doi.org/10.2147/IDR.S177247.

(69) Sevilla, P.; Gil, J.; Aparicio, C. Relevant Properties for Immobilizing Short Peptides on Biosurfaces. *Irbm* **2017**, *38* (5), 256–265. https://doi.org/10.1016/j.irbm.2017.06.003.

(70) Phan, H. T. M.; Bartelt-Hunt, S.; Rodenhausen, K. B.; Schubert, M.; Bartz, J. C. Investigation of Bovine Serum Albumin (BSA) Attachment onto Self-Assembled Monolayers (SAMs) Using Combinatorial Quartz Crystal Microbalance with Dissipation (QCM-D) and Spectroscopic Ellipsometry (SE). *PLoS One* **2015**, *10* (10). https://doi.org/10.1371/journal.pone.0141282.

(71) Malmström, J.; Agheli, H.; Kingshott, P.; Sutherland, D. S. Viscoelastic Modeling of Highly Hydrated Laminin Layers at Homogeneous and Nanostructured Surfaces: Quantification of Protein Layer Properties Using QCM-D and SPR. *Langmuir* **2007**, *23* (19), 9760–9768. https://doi.org/10.1021/la701233y.

(72) Molino, P. J.; Higgins, M. J.; Innis, P. C.; Kapsa, R. M. I.; Wallace, G. G. Fibronectin and Bovine Serum Albumin Adsorption and Conformational Dynamics on Inherently Conducting Polymers: A QCM-D Study. *Langmuir* **2012**, *28* (22), 8433–8445. https://doi.org/10.1021/la300692y.

(73) Alkan, M.; Demirbaş, Ö.; Doğan, M.; Arslan, O. Surface Properties of Bovine Serum Albumin - Adsorbed Oxides: Adsorption, Adsorption Kinetics and Electrokinetic Properties. *Microporous Mesoporous Mater.* **2006**, *96* (1–3), 331–340. https://doi.org/10.1016/j.micromeso.2006.07.007.

(74) Mas-Vinyals, A.; Gilabert-Porres, J.; Figueras-Esteve, L.; Borrós, S. Improving Linking

Interface between Collagen-Based Hydrogels and Bone-like Substrates. *Colloids Surfaces B Biointerfaces* **2019**, *181* (June), 864–871. https://doi.org/10.1016/j.colsurfb.2019.06.046.

(75) Lubarsky, G. V.; Davidson, M. R.; Bradley, R. H. Hydration-Dehydration of Adsorbed Protein Films Studied by AFM and QCM-D. *Biosens. Bioelectron.* **2007**, *22* (7), 1275–1281. https://doi.org/10.1016/j.bios.2006.05.024.

(76) Wiggins, R. C.; Kshrisagar, B.; Kelsch, R. C.; Wilson, B. S. Fragmentation and Polymeric Complexes of Albumin in Human Urine. *Clin. Chim. Acta* **1985**, *149* (2–3), 155–163. https://doi.org/10.1016/0009-8981(85)90329-8.

(77) Peterson, B. W.; He, Y.; Ren, Y.; Zerdoum, A.; Libera, M. R.; Sharma, P. K.; van Winkelhoff, A. J.; Neut, D.; Stoodley, P.; van der Mei, H. C.; et al. Viscoelasticity of Biofilms and Their Recalcitrance to Mechanical and Chemical Challenges. *FEMS Microbiol. Rev.* **2015**, *39* (2), 234–245. https://doi.org/10.1093/femsre/fuu008.

(78) Feiler, A. A.; Sahlholm, A.; Sandberg, T.; Caldwell, K. D. Adsorption and Viscoelastic Properties of Fractionated Mucin (BSM) and Bovine Serum Albumin (BSA) Studied with Quartz Crystal Microbalance (QCM-D). *J. Colloid Interface Sci.* **2007**, *315* (2), 475–481. https://doi.org/10.1016/j.jcis.2007.07.029.

(79) Floyd, K. A.; Eberly, A. R.; Hadjifrangiskou, M. Adhesion of Bacteria to Surfaces and Biofilm Formation on Medical Devices. In *Biofilms and Implantable Medical Devices*; Elsevier, 2017; pp 47–95. https://doi.org/10.1016/B978-0-08-100382-4.00003-4.

(80) Gutman, J.; Walker, S. L.; Freger, V.; Herzberg, M. Bacterial Attachment and Viscoelasticity: Physicochemical and Motility Effects Analyzed Using Quartz Crystal Microbalance with Dissipation (QCM-D). *Environ. Sci. Technol.* **2013**, *47* (1), 398–404. https://doi.org/10.1021/es303394w.

(81) Kearns, S. B. G. and D. B. Regulation of Flagellar Motility during Biofilm Formation. *FEMS Microbiol. Rev. Rev.* **2013**, *23* (1), 1–7. https://doi.org/10.1038/jid.2014.371.

This page left blank intentionally.

Chapter III. Antibacterial nanostructured metallic-coated surfaces

ABSTRACT

In this chapter, a set of micro- and nanostructured surfaces based on different polymers coated with a metallic silver film has been applied on silicones. The effect of these coatings on bacterial growth and bacterial adhesion to surfaces has been studied, with the aim of selecting one of them to be implemented on urinary catheters.

3.1 INTRODUCTION

Previously, the early bacterial adhesion and biofilm development on surfaces was studied at different conditions. The elements and conditions that promote bacterial adhesion to materials related with medical devices were tested. Similarly, the main limitations of the techniques currently used have been exposed. Thus, sensitive-enough protocols have been implemented for the study of surface colonization on complex surfaces to detect different stages of bacterial attachment and biofilm maturation *in vitro* and *in vivo*.

As previously described, to reduce the impact of catheter-associated urinary tract infections (CAUTI) in healthcare system is critical to avoid the bacterial colonization on urinary catheters. CAUTIs can be originated from multiple bacterial species, which cause different severity grade of infections depending on diverse factors such as environmental, pathogenesis level, virulence of the strain and patient's previous symptomatology. Despite their intrinsic variability, CAUTI pathogens have common colonization mechanism[1–4], which open ups a windows of opportunity for generalist CAUTI prevention approaches.

To improve urinary catheters design to prevent CAUTIs, different strategies have been explored. A promising approach consist in the modification of the medical device surface to provide antibacterial properties[5]. This surface functionalization usually consists in antibacterial agents immobilized through weak interactions allowing the release from surfaces to bacteria. Most common strategies involve bactericide agents such as metallic ions[5–8] as silver, copper, zinc and chloride or iodine salts among others, e.g. antimicrobial peptides[9], when are released, they promote bacterial membranes degradation, interact with electron chain transport, proteins or DNA killing bacteria. Among them, metallic ions are generating special attention due to the fact that target simultaneously bacterial cell walls and intracellular targets via physical interactions, generating reactive oxygen species[10]. Thus, it is much more difficult for bacteria to develop

resistance against them[10,11]. The liberation of metallic ions from immobilized molecules on the surface of a medical device produces a burst release that ensure a high bacterial mortality[12,13]. Moreover, stopping bacterial growth by releasing bacteriostatic effectors in the first hours of medical device implantation can protect the device and the patient[14,15].

At this point, with the surge of multi-resistant bacteria and the shortage of new antibiotics, the use of metals with antimicrobial properties is on the rise. Silver has a long history, but it is a trend in all these forms: metallic silver, silver salts and colloidal silver, as antimicrobial metal. Silver has been used as an effective antibacterial agent for many centuries and has retained effective antibacterial activity throughout that period. The mechanism of action against bacteria is not clearly defined but, there is a discussion about the silver ions interacting with thiol groups of proteins[16]. Also, silver ions are deposited in the cell wall as granules damaging it, and consequently, the electron transport chains losing their activity in bacterial respiratory process, components of DNA replication, and outer cell layers exhibit structural abnormalities[16–18] (Figure III. 1). The antibacterial process depends on the concentration of silver ion available in media and the bacterial capacity to process silver ion by proton-bombs[19]. Yet, there have been no conclusive reports on the development of bacterial resistance to metallic silver. There are, however, some reports of bacterial resistance to ionic silver. Such resistance may involve reducing silver ions to the less toxic neutral oxidation state or active efflux of silver ions from the cell by P-type adenosine triphosphatases or chemiosmotic silver ions/H+ antiporters[20]. However, chromosomally silver resistant mechanism has not been identified at that time and, perhaps, it is a mutation in outer membrane porin proteins that conferee a deficient cation flux that not provide of advantages to bacteria and it is poorly disseminate, as explained in the introduction chapter[18]. Thus, silver stills one of most useful metals to avoid bacterial activity.

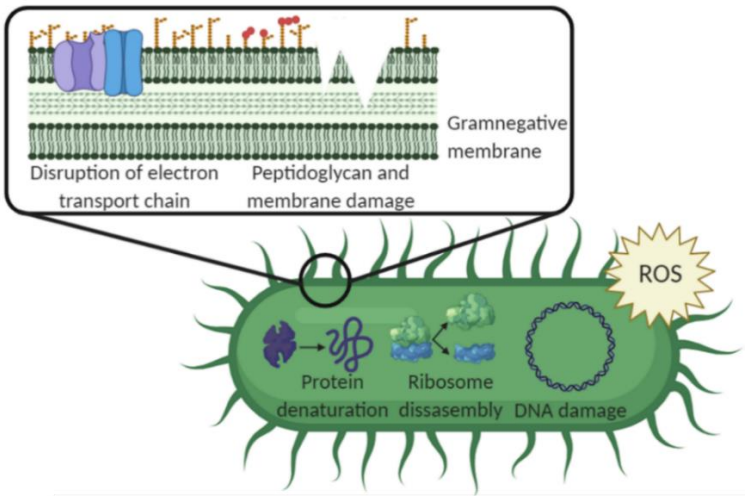

Figure III. 1. General mechanisms for antimicrobial mode of action of silver. Focusing on bacterial membrane, silver can disrupt the electron transport chain, affecting metabolically to bacteria and promoting a leakage of cellular ATP. Also, bacterial permeability can be altered, producing an osmotic imbalance and a impair transport activity. Adhesion mechanism and flagella can be destabilised. Inside bacteria, protein and enzyme denaturalization and ribosome disassembly promote a protein deficient metabolism, altering the signalling system and the duplication ratio. Reactive oxygen species are metabolized, promoting an oxidative stress. By last, interaction with DNA promote mutations and the inability to duplicate. Image made by the author.

The cytotoxicity studies carried out with silver offers an interesting point of view. If we want to standardize the use of silver-modified medical devices, it is necessary to know how silver can interfere with the metabolic processes of eukaryotic cells, just as it does in prokaryotes. Over the years, numerous cytotoxicity studies have been carried out on silver in all its forms, ionic, metallic and salt forms. Silver is present in human body and it can bioaccumulate in organs such as the liver or kidneys, however, the amounts necessary to suffer tissue damage or organ failures were recorded in works such as Lansdown, A. ("*Silver in health care: Antimicrobial effects and safety in use interactions between skin and biofunctional metals*" and "*A pharmacological and toxicological profile of silver as an antimicrobial agent in medical devices*")[21,22], where he indicated that the systemic toxicity of metallic silver was studied in 30 healthy volunteers who consumed silver leaf (oral, 50 mg / day) for 20 days. Apart from transitory changes in hepatic enzymes, the treatment was well tolerated without symptoms of argyria. This study laid the foundation for silver tolerance in the body and will be used as a reference in this work. However, the use of silver in medical devices has been relegated to its integration as a salt form in hydrogels. These hydrogels usually coat medical devices and release silver in ionic form, producing an effective short-term antimicrobial effect. Antimicrobial release strategies have disadvantages that once all the metal ions have been released, surfaces loss all their effectiveness, leaving the device and the patient

unprotected once the hydrogel has degraded or all available ions have been consumed. Furthermore, accumulation of biomass or biomolecules from bacteria or the environment on surfaces can block the release of ions and providing a new colonizable niche by bacteria, as is the case of urinary catheters[3,23,24].

To avoid all the drawbacks offered by releasing strategies, bacterial colonization can be avoided through a new approach: modifying the surface topography of the materials at micro and nanoscale which interferes with bacterial adhesion. Surface topography-based approaches prevent bacterial colonization without releasing any type of antimicrobial agent. Bacterial colonization is avoided creating surfaces with poor interaction with bacteria during firs steps of bacterial adhesion. This phenomenon of low bacterial interaction confers to surfaces the ability to repel bacteria, called bacteriophobic effect98. As a common way to improve the low-surface-energy properties in medical devices, the surface morphology or roughness could be further modified[25]. These surfaces were initially inspired by the specific nanotopographies of insect wings, and other surfaces found in nature, due to the presence of hierarchical nano-features, such as hairs, pillars, needles, plates, which endowed the surfaces with natural anti- wetting and antibiofouling characteristics[26]. Using micro and nanopatterns with different forms and structures, self-cleaning and low adhesion surfaces have been presented with different effects on bacteria[27,28]. The isolation of bacteria or the prevention of the adhesion by creating a bactericidal, bacteriostatic or bacteriophobic environment using nanostructures is considered the next generation of antimicrobial surfaces[26,27,29]. The mechanism is based on the deformation or break of the bacterial membrane when enters in contact with the surface morphology in the first steps of biofilm formation, during bacteria adhesion (Figure III. 2)[28,30].

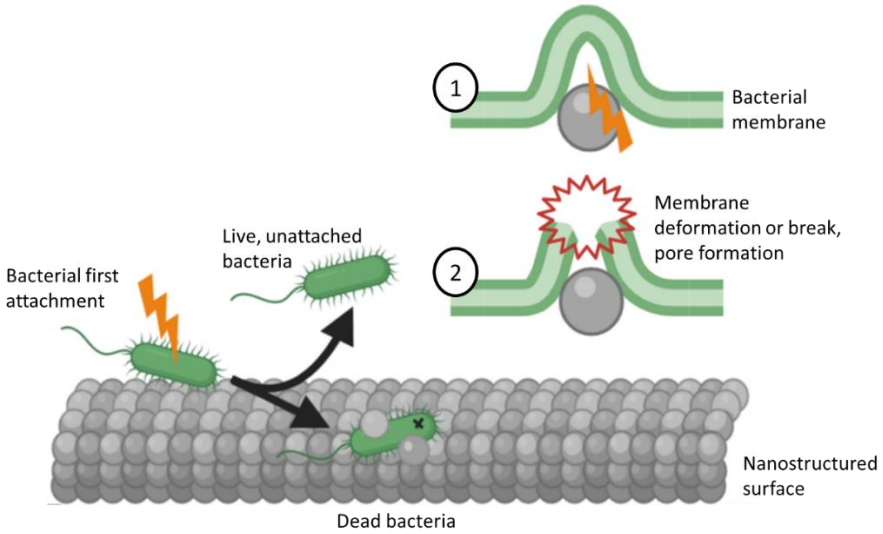

Figure III. 2. Scheme on the effect of a nanostructure surface on bacterial adhesion. Nanostructures affect the integrity of the bacterial membrane, subjecting it to stresses and deformations that it may not withstand. Image created by the author of this thesis based on the work of different authors28,29,31,32.

One of the most interesting characteristics of nanostructures as protection tools against bacterial infections is their long-lasting effect and their non-selective effect, perhaps providing a general solution to bacterial colonization. The discovery that the regular arrays of nanopillars found on cicada (*Psaltoda claripennis*) wings were also capable of lysing non-specific bacteria has led to a surge in the use of biomimicry to develop surfaces whereby the nanotopography is capable of mechanically inactivating bacteria[26,33]. Inspired on it, a lot of shapes and patterns have been explored. Among them, nanopillars and nano-needles are not the only ones capable of disrupting bacterial membranes by stress, although they seem to be the most obvious structures. But softer structures that generate microenvironments that repel bacteria through other strategies are also effective[28,34]. The main micro and nanostructures created and explored using the techniques mentioned above in recent years are shown in Figure III. 3, as a diagram.

There is a debate about the ideal size of these structures. Considering the size of bacteria, different structures can cause different effects: from massive generation of pores and nano-ruptures by needles, deformation and loss of functionality due to larger structures or complete membrane ruptures that make bacterial survival unviable. In addition, nanostructures can interrupt complex adhesion processes to the surface, interfering with the adhesion systems, adhesins and fimbriae, making bacteria uncomfortable in the surface. The homogeneity of microstructures and their separation also play an important role in the bacterial adhesion

prevention. The nanostructures must be close enough so that bacteria do not lodge in the valleys created, using it as a refuge (Figure III. 3). But these structures should not be so close that they do not offer any opposition to bacterial adhesion, allowing deformation of the bacterial wall.

Finding the balance between these parameters and the homogeneity in the construction of the surfaces are, nowadays, the greatest challenges in the manufacture of these structures.

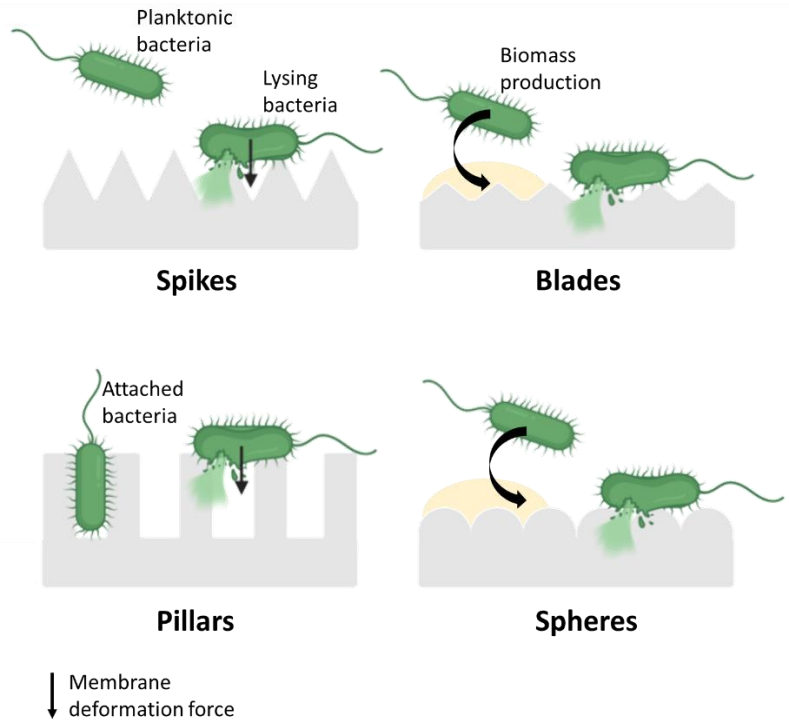

Figure III. 3. Diagram of the most common topographies that confer bacteriophobic properties to base materials. The diagram shows how different structures can interact in different ways with bacteria, causing different effects on them. Different topographies prevent the correct bacteria-surface interaction. Depending on the shape and size, the structures can cause from tension and rupture of the membranes to deformation of the bacterial wall, killing or inhibiting bacteria. Furthermore, topographies induce expression of different bacterial appendages, inhibit bacterial duplication, avoid or favour the adhesion of biomass to surfaces, create micro-currents that prevent adhesion or alter adhesion patterns, inhibiting bacterial communication[29,35–37]. Image prepared by the author.

Various strategies to create nanostructures with different patterns and shapes have been explored in recent years. The most used techniques are based on modifying the base material by erosion, using a mould to create a patterned material or generating a structure by polymerizing various compounds. Several examples include plasma etching, which uses non-hazardous and

process-stable gases, based usually on fluorine chemistry to earth surface structures. Etching has several advantages such as the capacity of achieving high aspect ratio structures but the difficulty to obtain uniform structures, the long reaction duration and the low scalability are its worst disadvantages[38,39]. Another of the most used methods to generate nano structures is based on the mechanical or chemical exfoliation of materials. The exfoliation of single layers of graphene by sonication generates crystals in a simple step, but this method is difficult to control[26]. More controlled methods are based on chemical vapor deposition[6,40], where the growth of the films on a substrate occurs through the vaporization of volatile precursors using gas flow and temperature control to favour chemical reactions. The advantages of these techniques are that they are not restricted to certain materials, but any substrate can be a candidate for modification. However, the use of these polymerization techniques and creation of nanostructures are a technical challenge, require a great deal of technical training for manufacturing personnel and require a large investment to be industrially scaled[38,41,42]. These disadvantages hold back the implementation of these technologies in real medical devices. An alternative may be creating nanostructures or modifying the surfaces using simpler and scalable chemical methods, based on reactions that do not require sophisticated equipment, such as water-based reactions or low-heat ones[43]. These polymerization reactions can usually be applied to various base materials and are easily adaptable to complex morphologies, such as those presented by current medical devices. The parameters that define these processes are easily modulable, creating different topographies with different characteristics just by playing with the polymerization parameters. The total control of the resulting morphology and the option to modify it later chemically to modulate its effect are the most valued features.

Both, nanostructures and antimicrobial coatings strategies can work together, avoiding their disadvantages and finding synergies to increase their antimicrobial potential. Thus, it is interesting to create a set of micro and nanostructures that provide a physical repulsion effect to bacteria, enhanced with a thin coating of metallic silver, which adapts to the structure and provides an uncomfortable environment to bacteria. To create nanostructured surfaces, the use of polymers that serve as a pattern to immobilize molecules of interests, such as metallic silver, in a controlled way, is explored[26,37]. Different surfaces based on two different polymer coating strategies applied on medical-grade silicones can be obtained. Using pentafluorophenyl methacrylate (PFM) and dopamine (DA) monomers as principal molecules, and controlling the parameters of the different polymerization methods, films with different topographies and roughness can be obtained. After that, the surfaces are coated with a metallic silver film by a well-known diamminesilver(I) ion reductive process. Modifying the shape and roughness, surfaces provided an antimicrobial effect from bacteriophobic to bactericidal grade. These coating structure can be made on silicone-based

materials: PDMS and NUSIL and they have been studied using all the techniques developed in the previous chapter to test the antimicrobial activity.

Pages have been removed from this version of the thesis as are protected under industrial property rights

3.3 RESULTS and DISCUSSION

Two methods based on PFM or Dopamine polymerization were proposed to obtain micro and nanostructured surfaces by polymerization of a polymeric patter for the immobilization of silver nanostructures on silicone-based surfaces. Subsequently, the structures were covered with a thin film of metallic silver by reduction, respecting the topography. Using these two strategies, four micro- and nanostructured silver-based surfaces was obtained and characterized in order to test their antimicrobial capacities for future applications.

3.3.1 Nanostructured silver surfaces based on plasma-polymerized pentafluorophenyl methacrylate.

Previously in GEMAT group, silver-nanostructured surfaces have achieved by immobilizing metallic silver on flexible substrates through plasma-polymerized pentafluorophenyl methacrylate (pp-PFM)[6,40,47]. PFM thin films offered highly reactive ester groups that allowed them to react with amine bearing molecules, such as amine sugar, to create reductive surfaces capable to reduce silver salts to metallic silver coatings[6,40,46]. These surfaces showed an interesting bactericidal behaviour through oxidation of the metallic silver coating, with a controlled release profile of bactericidal silver ions[55]. In addition, PFM polymerization processes are versatile to obtain films with different thickness, orientation, shape… creating different polymeric microstructures on silicones. By controlling the PFM polymerization parameters, the polymer structure on the base material can be modified, modifying the bacteria-surface interactions.

In this work, it was found that, depending on the conditions of plasma polymerization, the thickness and the tortuosity of pp-PFM thin film can be controlled and modulated. The capacity of control the polymerization process produced samples with different surface micro- and nanostructures. After polymerization process, silver was deposited on surface by reductive capacity of the polymer showing different silver morphologies depending on the pp-PFM structure.

Hence, it is possible to differentiate three nanostructures formed from the silver layer: *Sharp blades*, *thick blades* and *leaves,* which structure and their proposed mechanism against bacteria is showed in Figure III. 9.

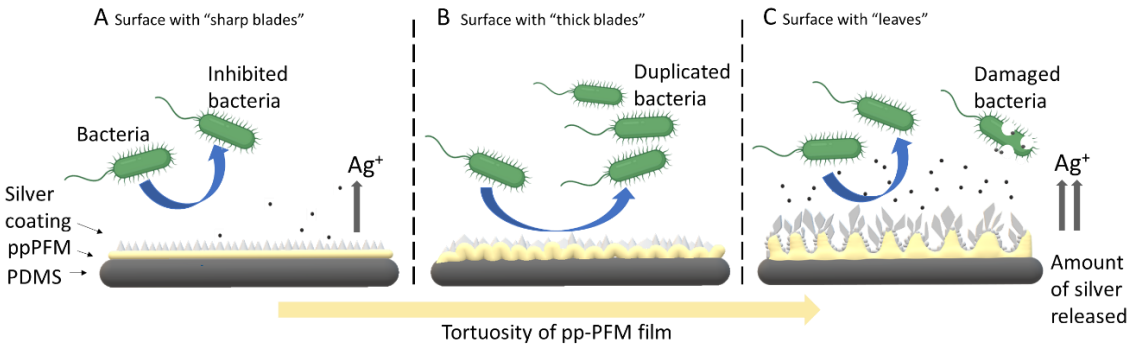

Figure III. 9. Graphical abstract of three different surfaces. Surfaces present different complexity grade according to their synthesis. Based on their visual macroscopic structures, samples were named as: "sharp blades" (A), "thick blades" (B) and "leaves" (C).

Among all the conditions that affect the polymerization of PFM, and therefore the conformation of the pp-PFM chains, the most critical were the polymerization time (time that PDMS samples were exposed to pp-PFM plasma) and the post-polymerization time (time that pp-PFM vapor were kept constant after the polymerization). The variation of these conditions to obtain the described structures is shown in

Table III 1.

It was found that low times (3 minutes each) in both, polymerization and post-polymerization process allow the obtention of a thin pp-PFM films, where the nucleation of silver created multiple sharp structures of 200 nm long and a about few nanometres wide ("Sharp blades" Figure III. 10 A.1 and A.2).

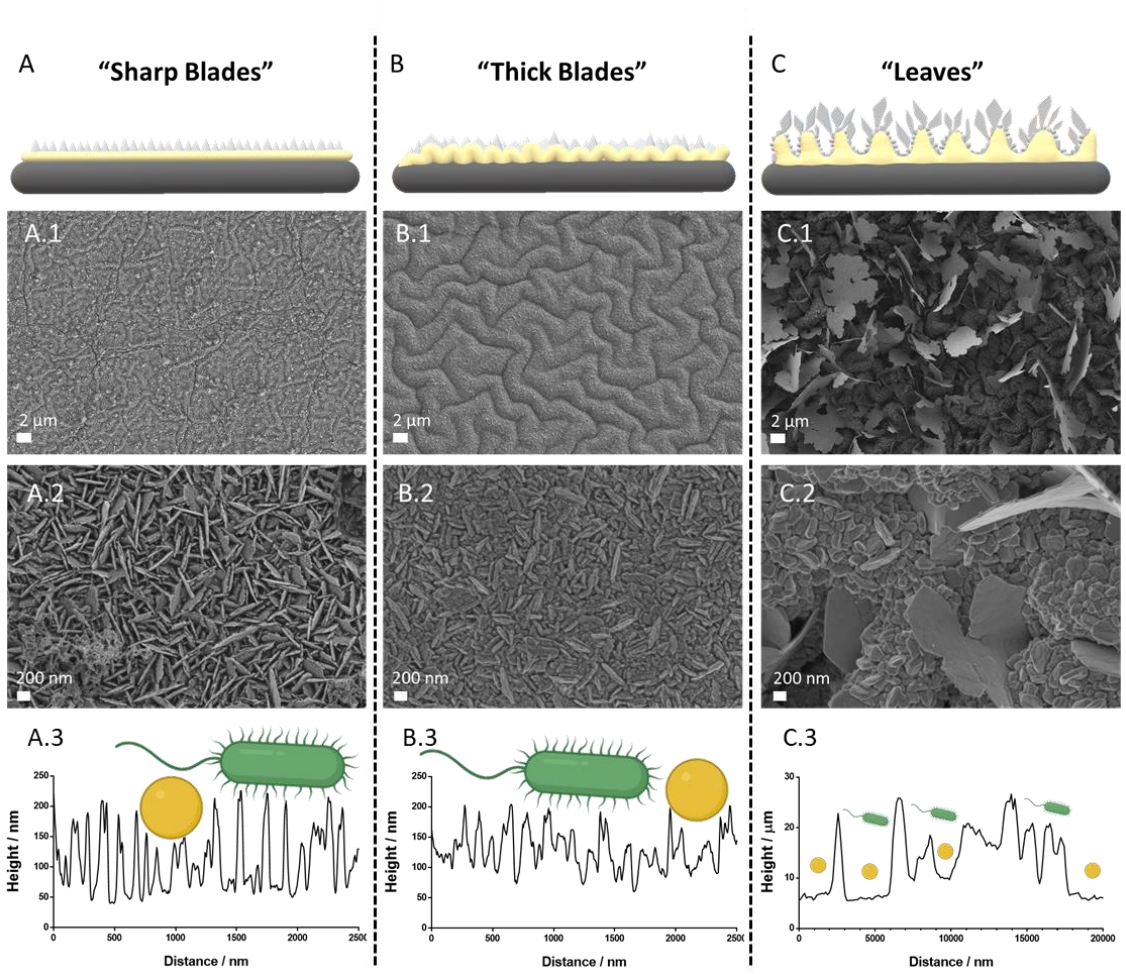

Figure III. 10. Field emission scanning electron microscopy of three silver surfaces. The graph represents the base silicone (PDMS, dark grey), the pp-PFM coating (yellow) with different shapes according to the tortuosity observed in the FE-SEM images and the silver coating with different morphologies (light grey). Samples were named according to the pp-PFM tortuosity and the nanostructure observed on their surface. Surface with "sharp blades" (A, A.1 and A.2), surface with "thick blades" (B, B.1and B.2) and surface with "leaves" (C, C.1, and C.2). Mechanism underlying the influence of surface morphology on bacteria adhesion based on the roughness profile of "sharp blades" (A.3), "thick blades" (B.3) and "leaves" (C.3) morphology. Scheme of the bacteria is represented to scale in relation to the roughness profile.

Increasing the post-polymerization time allows the termination of PFM chain growth after plasma process. This allows the reactive points of the plasma polymerized polymer chain to react with the vapour of the PFM and increases the "mountainous region morphology", where peaks and valleys are clearly more recognizable (Figure III. 10 B.1). The result after silver nucleation was similar to the showed in the previous surface but, in this case, the "blades" are obviously wider in comparation with the previous structure, naming them "thick blades" (Figure III. 10 B.2).

Table III 1: Plasma polymerization conditions for pp-PFM PDMS modification to obtain specific metallic silver structures.

	POLYMERIZATION TIME (MIN)	POST-POLYMERIZATION TIME (MIN)
A - SHARP BLADES	3	3
B - THICK BLADES	3	10
C - LEAVES	10	10

Higher polymerization and post-polymerization times (10 minutes) result in a more complex structure due to and increasing of pp-PFM chain tortuosity, where silver nucleation sites lead to the generation of silver leaves covering the main surface (Figure III. 10 C.1) with a thickness of less than 50 nm. Behind the leaves structures it can be found that the “mountainous region morphology” is maintained but, unlikely the leaves morphology, a significative particle growth was observed: nanoparticles present a size higher than 200 nm (Figure III. 10 C.2).

Roughness profile of studied surfaces was performed to evaluate the ability of the morphology to create unfavorable conditions for bacterial adhesion and to elucidate a hypothesis for the antibacterial – bacteriophobic mechanism. Figure III. 10 A.3 shows the roughness profile for a representative region of the sharp blades surface. The profile confirms the presence of blades with a height about 150 nm and a distance between blades less than 100 nm while thick blades present a similar roughness profile (Figure III. 10 B.3) with blades about 100 nm height separated less than 80 nm. Previous reports indicated that physical impediments leaded by the roughness of the surface topography may play an interesting role avoiding bacteria interaction and attachment[56]. Figure III. 10 A.3 and B.3, shows a schematic of the bacteria-surface interaction indicating how multiscale wrinkled surfaces can difficult the bacterial attachment due to limited surface area available.

The characterization of the “leaves” structure is much more complex due to its random morphology leaded by silver nucleation, showing a micro- and nano-roughness formed by a slender “leave” of 10 µm of height and a thickness of less than 50 nm with a separation between the leaves that can be higher than 2 µm (Figure III. 10 C.3). Initially, in this case, bacterium can easily interact with the surface due to the separation between the leaves however, the once the bacteria reach the surface the effect of the nanostructure must be evaluated.

Surface hydrophobicity was studied due to its role in the bacterial adhesion mechanism. It is known that rough surfaces with low hydrophobicity present more sites for bacterial attachment [11,57] providing protection from the shear forces produced by the exposition to biological medium[32].

With this phenomenon in mind, water contact angle (WCA) of the silver surfaces was measured using uncoated PDMS coupon as control (Figure III. 11 A). PDMS samples showed a characteristic WCA around 95º indicating a well described hydrophobic behaviour of silicones. However, the modified surfaces revealed a WCA around 150º indicating that these surfaces are in the range of super-hydrophobicity.

The nano-structuration of the silver surfaces present a high accentuated roughness that contributes increasing the hydrophobicity to super-hydrophobic range. As described in literature, the combination of nanostructured rough surface with super-hydrophobic behaviour may act as an antifouling surface and/or promote the air entrapped beneath the liquid in the topography and therefore, reducing the bacterial adhesion and obtaining a bacteriophobic effect [57–60].

Once hydrophobicity was studied, the amount of total silver deposited on surfaces was evaluated. It is interesting to highlight that the developed surfaces present the same amount of silver as shown in Figure III. 11 B, regardless of the complexity of their structure. These results indicate that super-hydrophobicity behaviour is not achieved due to an increase of the amount of silver in the surface but by a redistribution of how this silver has been anchored to it. Considering that, all changes produced by the surfaces on bacterial adhesion are associated with a nano-structuration of the silver surface.

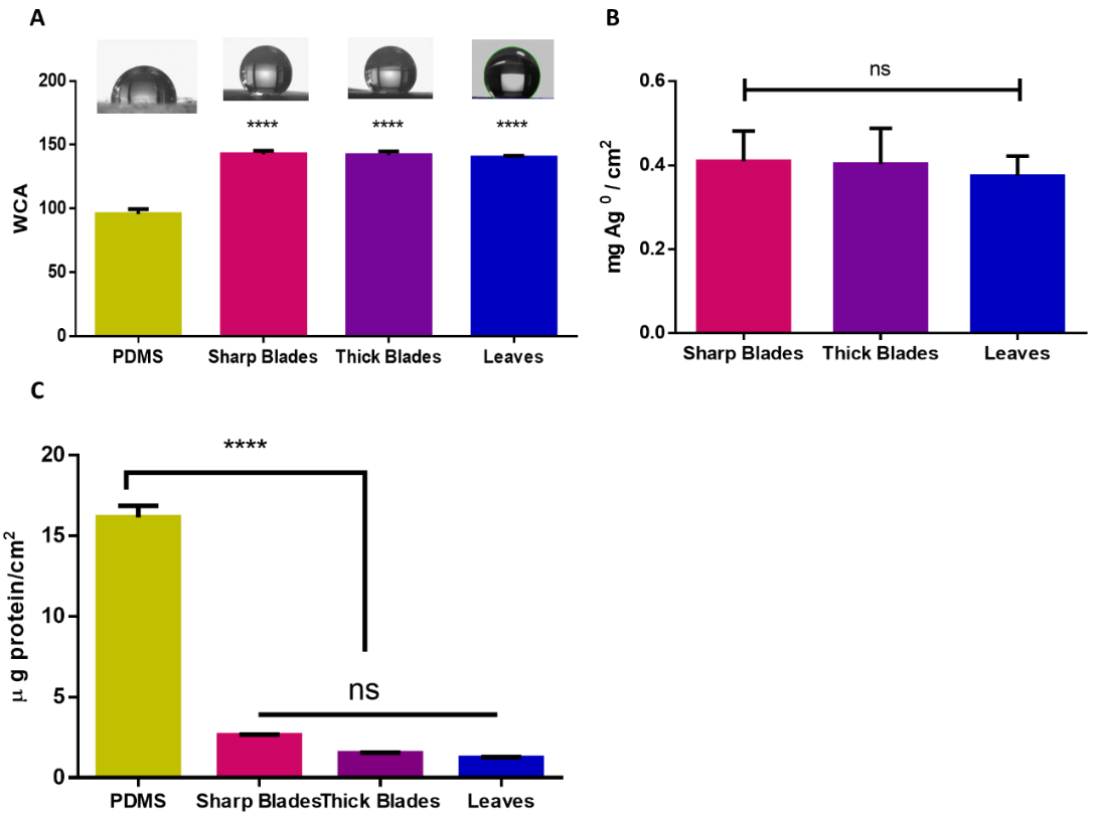

Figure III. 11. Characterization of three different surfaces based on PFM-silver coating. A. Water contact angle of the developed silver surfaces compared with uncoated PDMS. B. Silver quantification by cm^2 for each silver surface tested by ICP. C. Protein quantification from surfaces after 24 h of incubation with Fetal-Bovine Serum. Statistical analysis indicated a significative difference between control and all three surfaces, with a minimum p- value of < 0.05 (*) and a maximum p-value of < 0.001 (***).

To relate the superhydrophobic capacity with the repulsion of proteins present in complex media, the modified surfaces were put in contact with FBS and the protein adsorbed on them was quantified. As can be seen in the Figure III. 11 C, the amount of protein adsorbed by the PFM-silver modified surfaces was significantly reduced in all proposed samples. This low protein-adsorption is a highly desirable characteristic since, as demonstrated in the previous chapter by QCM-D experiments, a stable interaction of proteins with the surfaces of materials can promote bacterial adhesion in complex environments[24,49]. Therefore, it is expected that this low-protein interaction favours a more lasting bacteriophobic effect.

3.3.1.1 Silver ions release and its effect on bacterial growth.

The release of silver ions from the silver surfaces plays an important role in the bacterial adhesion mechanism and in the bacteriostatic/bactericide effect of the surface[16,21]. The amount

of silver released to bacteria medium can provide an idea of the contribution of silver ions to bacteria elimination, i.e., lower concentrations of silver ions would imply a major contribution of the surface nano-structuration on bacterial adhesion reduction. To evaluate the accumulated silver ion released in media from the three developed silver surfaces, 1 mL of each sample was taken from media (and replaced with fresh media) at different time points during 530 h and analysed by ICP, (Figure III. 12 A).

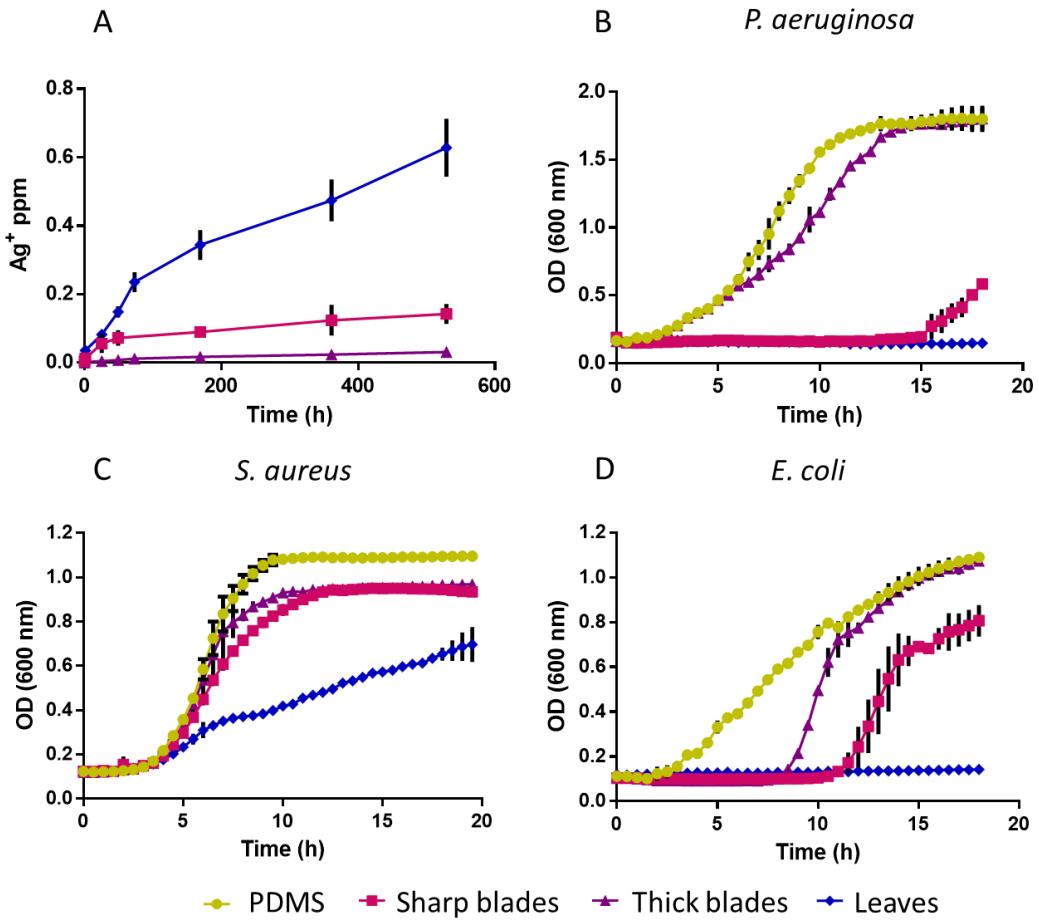

Figure III. 12. Accumulative release of silver ion from silver surfaces (A) and growth curves of *P. aeruginosa* PAO1 (B), *S. aureus* subs. aureus (C) and *E. coli* CFT073 (D) in contact with PDMS as a control surface and the three surfaces with "sharp blades", "thick blades" and "leaves".

It is interesting to note that the three silver surfaces with different nano-structuration present different profiles of silver ions release. On the one hand, the surface with "leaves" morphology revealed an initial burst release of 0.23 ± 0.03 ppm during the first 72 hours followed by a change

in the slope of the release profile. This behaviour may be explained through local oxidation reactions of silver leaves with the oxygen in the bacteria media which is promoted by the high specific surface that presents the leaves morphology. Hence, the first stage of the release would correspond with the silver release of poorly attached thin leaves (first 72 hours), followed by a sustained release of thicker leaves (from 72 h to endpoint). After 530 h of study (22 days) the release of silver ions does not reach a plateau indicating that silver leaves are a significant silver reservoir. On the other hand, “sharp blades” (Figure III. 12 A), showed an initial minimum burst release of 0.05± 0.02 ppm during the first 24 hours of incubation, followed by a sustained release that almost reaches the plateau. These differences can be explained because the “sharp blades” structure is less exposed to media than silver “leaves”, and therefore less exposed to local oxidation, presenting a sustained release of silver ions. Finally, the “thick blades” morphology showed a silver ion release below previous surfaces and being close to the quantification limit of the analytical method (10 ppb). This effect may be attributed to the blade thickness as well as to the tortuosity of the silver layer that protects the stability of silver blades making them more resistant to oxidation. Considering these results, it can be considered that the “thick blades” structure does not produce the release of silver ions in a significative way.

In addition, to exclude that silver ion release was caused by chemo-adsorbed silver during the Tollens reaction, silver release profiles were also obtained immersing the samples in acetic acid (Figure III. 13). Graphic shows the accumulative release of silver from the surface to media. The contribution of chemo-adsorbed silver is more present in complex structures such as known as “leaves”, stabilizing its release at 80 h. It is interesting to observe how the release profiles in acetic acid stagnate at the concentrations observed in the rapid release of the profiles made in aqueous medium. This phenomenon indicates that the chemosorbed silver is "washed" in the medium at first minutes, while the release effect over time is given by the oxidation of the metallic silver anchored to surface.

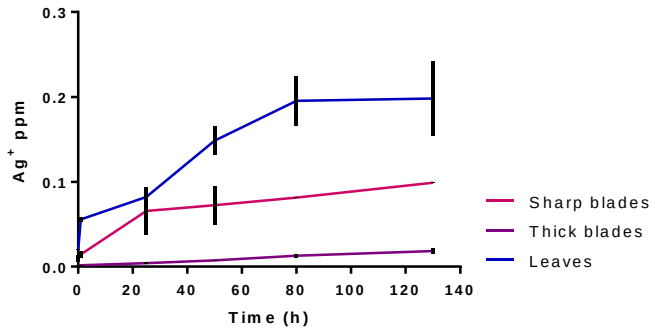

Figure III. 13. Silver release from surfaces using acetic acid as medium.

In order to evaluate the bactericidal or bacteriostatic effect of the different silver ion release profiles, the different silver surfaces samples were put in contact with three different bacterial strains to study their growth evolution: *Pseudomonas aeruginosa* PA01, *Staphylococcus aureus* subs. aureus and *Escherichia coli* CFT073 (Figure III. 12 B, C and D).

As it can be observed, bacterial growth profile showed several differences regarding on the exposed silver surface. The surface with the “leaves” morphology revealed a standard bacteriostatic behaviour on gram-negative strains (*P. aeruginosa* and *E. coli*) completely avoiding the bacterial growth (Figure III. 12 B and C), however, a delay on bacterial growth was observed on *S. aureus.* These behaviours are consistent with the silver release profile observed for the “leaves” morphology, where a high amount of silver ions was released into the medium, affecting bacterial duplication and viability. To demonstrate that the bacteriostatic effect observed with “leaves” surfaces is maintained over time, all the growth curves (gram-negative *P. aeruginosa*, *E. coli* and gram-positive *S. aureus)* were extended up to 50 h. No bacterial growth was observed in case of gram-negative and gram-positive *S. aureus* did not reach the stationary phase (absorbance values of end point measurements shown in supplementary materials, Figure III. 14). To demonstrate that the effect of surface with “leaves” on bacterial growth is bacteriostatic and non-bactericide, after 18 h of incubation, a bacterial sample was collected and cultivated in fresh medium overnight, measuring absorbance data without the presence of any surface, to evaluate if the bacteria were eliminated (antibacterial behaviour) or bacteria remained alive but without the ability to replicate (bacteriostatic effect).

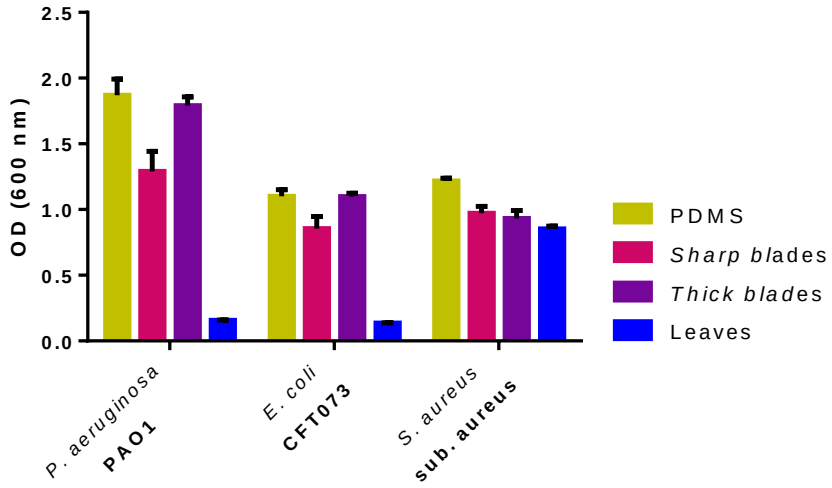

Figure III. 14. Representation of the end point of the growth curve at 600 nm and 50 h for each studied strain in contact with each of the proposed surfaces, using PDMS as a control surface.

Erratic bacterial growth profile was observed in the gram-negative species while gram-positive *S. aureus* was normally recovered (data not shown). This phenomenon indicates that the silver ion release of "leaves" samples dramatically reduced the population of gram-negative bacteria, but it was not eliminated, while gram-positive *S. aureus* was only inhibited and its viability was less affected. This effect is in complete consistency with the literature about silver ion affection on gram-positive strains[10,16] because gram-positive species present a bacterial wall composed of several layers of peptidoglycan with a thickness 15-80 nm that makes difficult for silver ions interact with respiratory chain, secretion systems or other components of inner membrane[61]. In this sense, the presence of this wall reduces the efficacy of antimicrobial effect of silver ions, as expected.

In contrast, the surface with "sharp blades" morphology presented different behaviour compared with the "leaves" morphology due to the general reduction of silver ion release profile. Thus, it was observed a delay on the beginning of the exponential phase in bacterial growth (Figure III. 12 B, C and D) that can be associated with the initial burst release of silver ion (Figure III. 12 A). This silver burst avoided the bacterial duplication, but it did not affected growth completely. Once the bacteria have replicated enough to overcome the silver ion effects, bacteria were able to overcome the effect of the released silver and began their exponential growth phase. It was observed that this effect is more attenuated in gram-positive species such as *S. aureus* (Figure III. 12 C). If the incubation times are extended to 50 h in *P. aeruginosa* and *E. coli*, the

growth curves reach the stationary phase, almost matching the PDMS control (Figure III. 14) which indicates that silver ion release is not able to kill bacteria, but it slows their growth.

Finally, the “thick blades” morphology did not present any effect on bacterial growth in any bacterial strain (Figure III. 12). However, it was observed a lengthening on the adaptation phase in *E. coli* but reaching a stationary phase at the same time as the control at 18 h period considering that profile a normal growth. These results are consistent with the provided with the silver ion release profile revealed in the Figure III. 12 A, where the “thick blades” morphology surface did not release significant silver ions once placed in medium. This result is especially interesting because any possible variations on bacterial adhesion obtained on this surface will not be able to be associated with the effect of silver ion but on the interaction between bacteria and the surface morphology.

*3.3.1.2 **Bacterial adhesion characterization.***

Characterization of how the nano-structured silver surfaces affect the bacterial adhesion after incubation with the developed samples, FE-SEM microscopy, Live and Dead staining and bacterial counts with the same bacterial strains studied in Figure III. 12 were performed.

First, samples were observed by FE-SEM after bacterial incubation (Figure III. 15). *E. coli* CFT073 was selected to show its attachment on metallic silver surfaces because it is a reference strain in the field of clinical pathogens due to its specific appendages that interacts with tissues and surfaces[4,62]. Non modified PDMS was used as a control (Figure III. 15 A) revealing a uniform, homogeneous and stratified layer of bacteria, indicating that bacteria have been adhered on the surface without difficulty. Bacteria were disposed randomly indicating that bulk PDMS surface topography does not produce a specific orientation effect on bacteria. Also, bacterial division could be observed indicating that bacteria were metabolically active on PDMS substrates. Signs of bacterial preference to be anchored on specific areas of the PDMS such as, a specific orientation of bacteria, bacteria-free areas or deformations in bacteria structure were not observed.

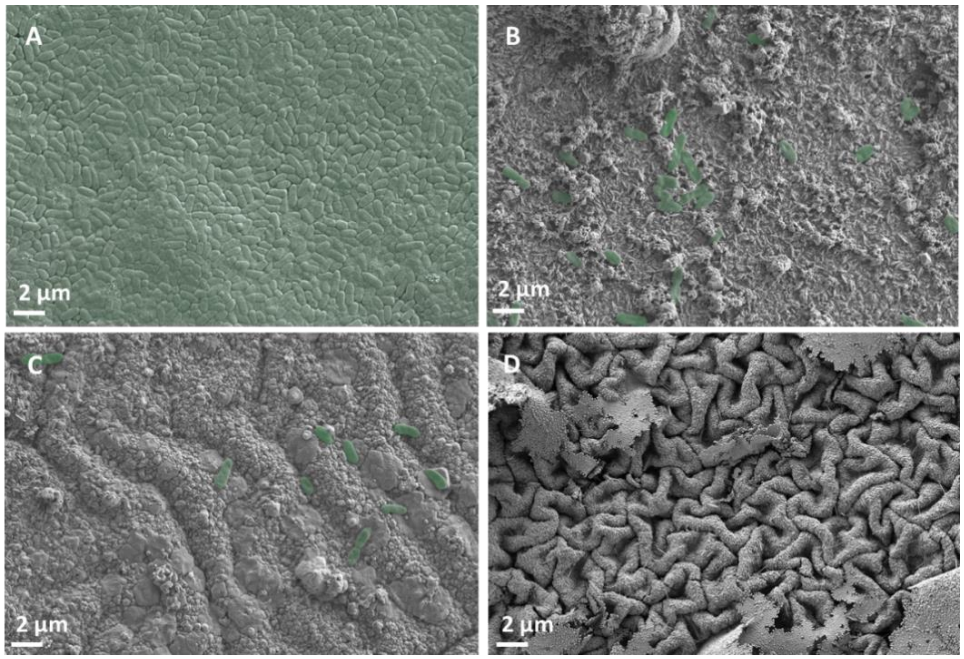

Figure III. 15. Field emission scanning electron microscopy images. PDMS as a control surface (A), surface with "sharp blades" (B), surface with "thick blades" (C) and surface with "leaves" (D) were incubated with *E. coli* CFT073. Bacteria were artificially painted in green to improve their visualization.

In contrast to PDMS behaviour, surface with "sharp blades" morphology (Figure III. 15 B) revealed significative less bacteria attached on the surface than PDMS control (p-value < 0.001, in bacterial adhesion quantification). Bacteria were randomly attached without showing a specific orientation. The morphology of the bacteria as well as their positions on the surface revealed some degree of membrane disruption which indicates that bacteria in the surface were dead. Considering that the formation of bacterial aggregates or microcolonies were not observed on all "sharp blades" studied samples, the anchored bacteria may be attributed to random bacterial attachment. In a similar way, surface with "thick blades" morphology (Figure III. 15 C) presented bacterial orientation according to the valleys of the grooves, preferring to anchor themselves to these grooves instead to the tops. These bacteria did not present structural membrane damage or affected volumes indicating no membrane disruption. Instead of that, bacteria seem to be not able to find a suitable anchoring site because it revealed significant less adhered bacteria than onto the PDMS control and similar to the "sharp blades" morphology. Considering that this surface does not present a release of silver ions, this effect can be attributed mostly to the bacteriophobic effect of the metallic silver nano-blades. Therefore, because of the nanostructure of the coating, bacteria are not able to be properly attached to the surface, being anchored by weak interactions. In this way, bacteria can be detached from the surface returning to the medium and avoiding the

adhesion process and the formation of biofilm. Finally, Figure III. 15 D, shows the image of "leaves" morphology surface after being incubated. As can be observed, the "leaves" structures were unhooked after the incubation with bacteria. Remains of these "leaves" structure can be seen on the surface, showing holes and eroded areas caused by medium exposition. The erosion also revealed the characteristic "mountainous" structure, where the grooves presented more tortuosity than the previously observed in the other metallic structures. This way, the "leaves" structures may have been formed through a nucleation process being an extension of the nano-blades present on the others surfaces. These leaves are weakly anchored to the main silver layer resulting in a dynamic surface where after exposition to a medium, silver "leaves" are detached producing an actively release of silver (in colloidal and ionic form). This massive release of silver affects the bacterial growth showing aberrant bacterial growth dynamics or inhibiting all strains as previously observed in the growth curves (Figure III. 12). Due to the structural changes produced on the surface after being exposed to bacteria media, FE-SEM images do not provide conclusive information about how bacteria interact with the "leaves" morphology. However, the surrounding bacterial behaviour to silver "leaves" detachment could be observed through confocal microscopy with the possibility to discern between living and dead bacteria (Figure III. 16).

In order to evaluate the behaviour of bacteria surrounding the "leaves" morphology surface, PDMS was used as a control with *P. aeruginosa* as a gold standard strain to study the bacterial attachment (Figure III. 16A). The surface with "leaves" morphology was incubated with, *E. coli* (Figure III. 16 B), *S. aureus* (Figure III. 16 C) and *P. aeruginosa* (Figure III. 16 D) to show total bacterial deposition discriminating between live attached bacteria, microcolonies and dead attached or deposited bacteria. PDMS (Figure III. 16 A) showed a layered and stratified biofilm, composed mostly of live bacteria (in green). Bacteria were attached to the surface extensively and, after adhesion, bacteria began to divide and secrete extracellular matrix, forming a microcolony, a platform where bacteria are promoted. These microcolonies with enough incubation time will form a structured biofilm.

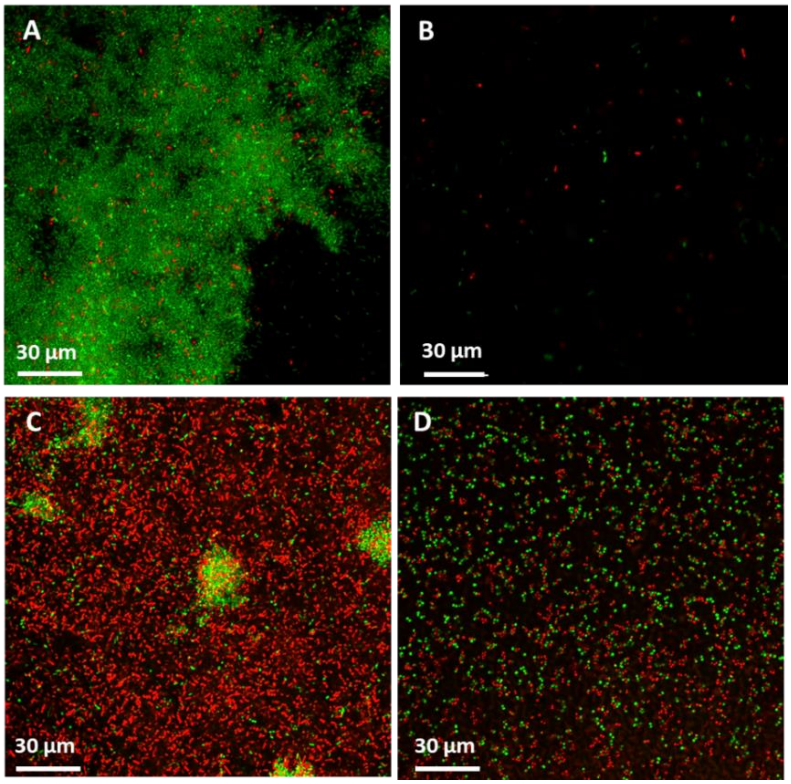

Figure III. 16. Confocal microscopy of PDMS incubated different studied bacteria strains. (A) *P. aeruginosa* and surface with silver "leaves" incubated with and *E. coli* (B), *S. aureus* (C) and P. *aeruginosa* (D). Samples were stained with Live&Dead cell staining kit: red dye shows dead bacteria with membrane damage and green dye shows live and metabolically active bacteria, biofilm matrix was not stained.

The structure with silver "leaves" presented a very different behaviour compared with the PDMS control. *E. coli* CFT073 and *P. aeruginosa* PAO1 had similar bacterial growth in the presence of silver ions, as previously mentioned on Figure III. 12, but showed different ability to be adhered the silver "leaves" surface. *E. coli* (Figure III. 16 B) revealed a clear surface without observing adhered bacteria. Despite *E. coli* presents a high amount of pili and specific adhesion mechanisms, once exposed to silver "leaves" structure, bacteria were unable to overcome the barrier of local release of silver ions and the potential effect of the surface morphology, where remaining leaves may produce a bacteriophobic effect in a similar way than observed in the other silver surfaces. By contrast, *P. aeruginosa* (Figure III. 16 C) was able to be adhered to the surface, as can be seen in the high concentration of bacteria in the image, but attached bacteria was found dead (red bacteria), probably due to the effect of silver ions released. As shown in Figure III. 16, bacteria were attached individually and showed no signs of biofilm formation. However, early stage microcolonies (green clusters) were observed among the dead bacteria. It seems that the

erosion of the surface reduces the surface ability to avoid bacterial attachment. Finally, *S. aureus* sub. aureus, shown in Figure III. 16 D, presented a homogeneous attachment of bacteria on the silver metallic surface, where the attached bacteria were partially live and dead almost in equal parts. This high number of attached bacteria was expected considering that *S. aureus* growth is less affected by the release of silver ions and therefore, more suitable to be adhered on the surface. Despite bacteria are localized on the top of silver surface through confocal microscopy, it is important to highlight that bacterial adhesion was punctual and reversible. Individual bacterium with no connection between them was observed and no indication of bacterial clusters formation was shown, therefore, the development of a biofilm on the surface was improbable.

The next step in the evaluation of the developed surfaces was the quantification of the total amount of living bacteria onto the surfaces in order to validate the ability of the coating to avoid the surface colonization. Samples were placed in medium with different bacterial strains and incubated to ensure bacterial growth and the ability to interact with the surfaces, and after that, samples were vigorously washed to remove weakly adhered bacteria. The remaining bacteria were plated and counted considering that each bacterium, alive and able to replicate, will generate a colony forming unit (CFU). Results are shown in Figure III. 17 for each strain used in this work: *E. coli* CFT073, *P. aeruginosa* PAO1 and *S. aureus* subs. aureus, growth in each proposed surface: “sharp blades”, “thick blades” and “leaves”, using PDMS as adhesion reference control surface.

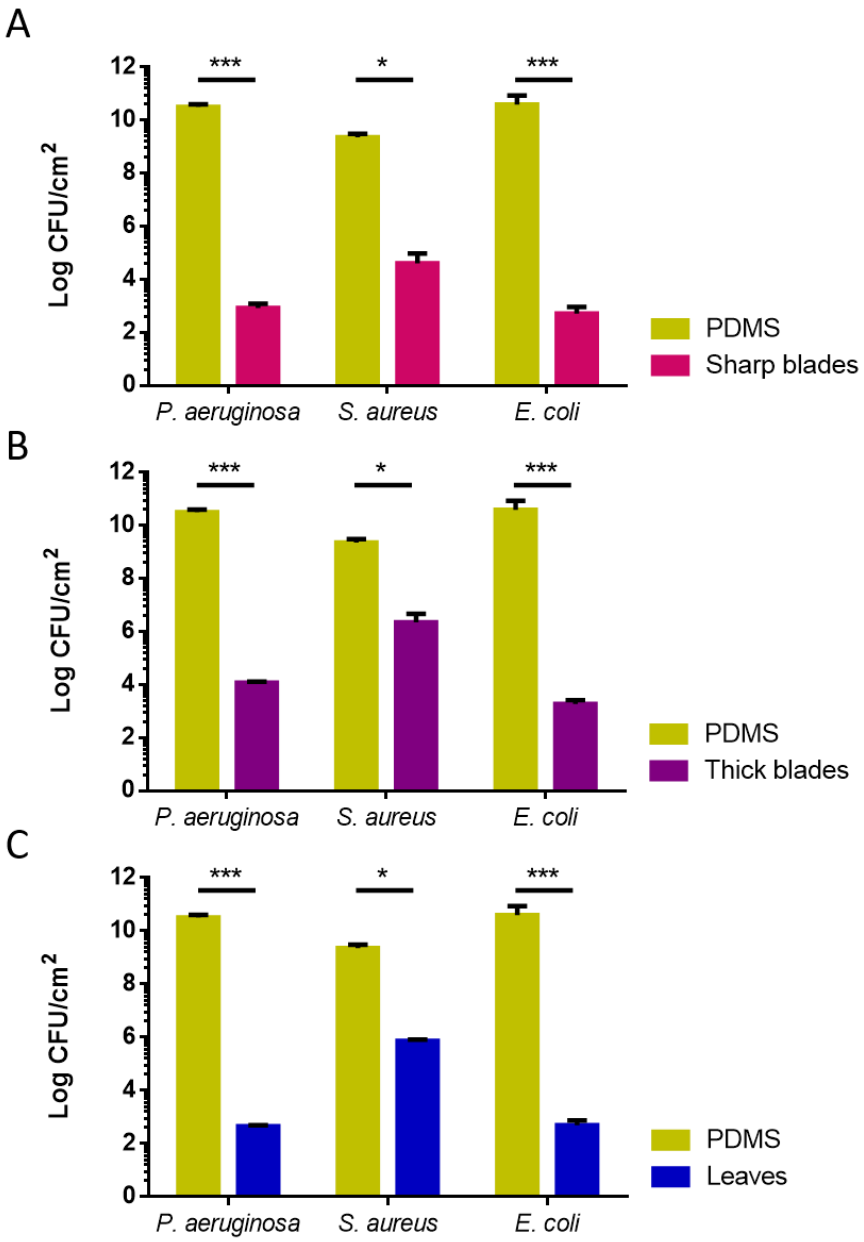

Figure III. 17. Bacterial counts on each surface (CFU/cm^2) with PDMS as a control. Three different bacterial strains were used in order to check that the behaviour shown does not depend on the species. The bacterial strains used were: *P. aeruginosa* PAO1, *S. aureus* subsp. aureus and *E. coli* CFT073 on surface with "sharp blades" (A), surface with "thick blades" (B) and surface with "leaves" (C). Statistical analysis indicated a significative difference between control and all three surfaces, with a minimum p- value of < 0.05 (*) and a maximum p-value of < 0.001 (***). Statistical analysis between the developed surfaces revealed no significant statistical differences with p-values from 0.056 (*P. aeruginosa*, "Leaves" vs "Thick blades" to 0.7 (*E. coli*, "Thick blades" vs "Sharp blades").

As can be seen in the Figure III. 17, the three developed surfaces showed a significative reduction of the adhered bacteria for each bacterial strain, where CFU per cm^2 revealing a reduction of 3 logarithms at least in the worst case (*S. aureus* on surface with “thick blades”) and 8 logarithms in the best case (*P. aeruginosa* on surface with “leaves”) in contrast with the uncoated PDMS control. Despite that silver surfaces present different mechanism to avoid bacterial adhesion as well as the intrinsic differences of bacterial strains, the bacterial adhesion reduction is similar for each case.

For the gram-negative strains (*P. aeruginosa* and *E. coli* CFT073) the presented surfaces represent a highly efficient method to avoid bacterial adhesion, reducing more than 6 orders of magnitude. This effect is mainly produced by a disruption of the bacterial outer membrane, achieved by the action of the surface morphology combined with the release of silver ion, which makes bacteria feel uncomfortable next to the surface. It is interesting to note that the surface with “thick blades” morphology (Figure III. 17 B), which do not present a ion release profile, reaches a similar adhesion reduction value similar to the other surfaces, indicating that the bacteriophobic effect developed, only with a surface based approach, can be as efficient as the release of silver ions, the bactericide surface.

Gram-positive bacteria (*S. aureus)* revealed higher adhesion on the silver surface. This behaviour can be explained due to the nature of *S. aureus* cell wall and membrane systems. *S. aureus* has a rigid peptidoglycan outer membrane that is harder to be disrupted than the gram-negative bacteria outer membranes[30]. This way, the silver ion released from the “sharp blades” and “leaves” structures (Figure III. 17 A and C) did not affect the growth of gram-positive *S. aureus*, increasing the bacterial population in the media offering more opportunities to bacteria to interact with the surface and to be adhered. However, “sharp blades” (Figure III. 17 A) is the surface which showed better *S. aureus* adhesion reduction, which may indicate that, the silver ions in combination with a nanostructured surface capable to disrupt the surface membrane is an optimal approach to avoid the bacterial adhesion.

At the end, modifying the properties of the pp-PFM thin film, structural changes were produced on the metallic silver coating affecting its morphology and therefore how bacteria interact and adheres to the surface. In this regard, by modifying the polymerization conditions of pp-PFM, three different silver morphologies with three different associated behaviour against bacteria were obtained. The three developed strategies against bacteria revealed an outstanding potential to avoid the bacterial adhesion, revealing more than 6 order of magnitude of CFU reduction on

bacterial counts compared with uncoated PDMS. This effect, along with the fact that these silver surfaces can be easily used to coat all kind of materials, including elastomeric ones which are more challenging to coat, represents an interesting solution to avoid bacterial colonization on medical devices.

3.3.2 Technology approach to a urinary catheter

Despite of the fact that the three developed surfaces ("sharp blades", "thick blades" and "leaves") showed an outstanding bacteriophobic behaviour based on their nanostructure, these interesting surfaces must be manufactured on the lumen of urinary catheters. Once the *in vitro* tests on flat silicone surfaces have been completed, it is necessary to start the tests in a real urinary device, to verify that the manufacture process is scalable.

The main physical characteristics of an urinary catheter are the length of the drainage tube and its external diameter. It depends on these characteristics that the patient drains the urine correctly with the greatest comfort and the least damage to the urethral epithelial tissue. Because of this, a medium-size urinary catheter for men (20 Fr or 6.7 mm diameter and 40 cm length) was used to adapt these surfaces to the device and check its operation.

First, 1 to 5 cm sections of urinary catheters were introduced into the reactor chamber, obtaining homogeneous pp-PFM polymerizations with a complete silver coating, equivalent to the previous studied ones. However, when introducing the complete urinary catheter, the pp-PFM films obtained were not homogeneous, showing a gradient from the ends of the tube towards the centre. This may be because the vacuum was not carried out completely inside the tube and the distribution of the PFM monomer was not uniform. This gradient polymerization resulted in not homogeneous silver deposition and uncoated areas. This fact caused a lack of nanostructured surface areas and the absence of metallic silver deposited homogeneously along the tube. This partial modification of the device did not avoid the bacterial attachment and biofilm formation correctly, not achieving the desired bacteriostatic or bacteriophobic effect in the urinary device. Furthermore, the manufacturing process was intended to be industrially scalable, so, eliminating cold vacuum plasma polymerization was a priority.

Due to the foregoing, alternatives to PFM and plasma polymerization were explored to achieve the same nanostructured surface effect with antibacterial properties using simple methodology, with a more industrialized vision.

In this context, the possibility of achieving an effective nanostructure on silicones, specifically on the entire urinary catheter, using dopamine arose. As explained before, dopamine as monomer

can polymerize in a wide range of conditions, coating surfaces homogeneously in a one-step reaction described between 2007 and 2018, being Polydopamine (PDA)[43,48]. PDA coating has been demonstrated to functionalize a wide array of material surfaces, including superhydrophobic surfaces such as silicones. Hence, PDA has opened a new route for surface modification and has garnered great interest, especially in biomaterials science.

3.3.3 Bacteriophobic nanostructured-silver coated surfaces based on dopamine polymers

Polydopamine (PDA) coating provides covalent and non-covalent bonding capabilities for a broad range of organic, inorganic and metallic substrates, offering potential applications in the challenging field of antibacterial coatings[52]. The main objective was to achieve a nanostructure with a behaviour similar to the structure called in previous section as "thick blades", which presented a powerful bacteriophobic effect, without affecting the bacterial growth, protecting the host microbiota.

Once dopamine polymerization process was optimized on PDMS substrates, the metallic silver coating was performed. The obtained surface was observed by FE-SEM (Figure III. 18 A-C). As can be noted, the surface showed a homogeneous coating filled with thin grooves less than 0.5 µm wide and a poor tortuosity. The nanostructure of the coating presented a set of structures with homogeneous shapes of about 100 nm wide, with some small insertions through the film. These structures had small inlays of metallic silver in a small proportion, smaller size and thicker than the previously studied ones.

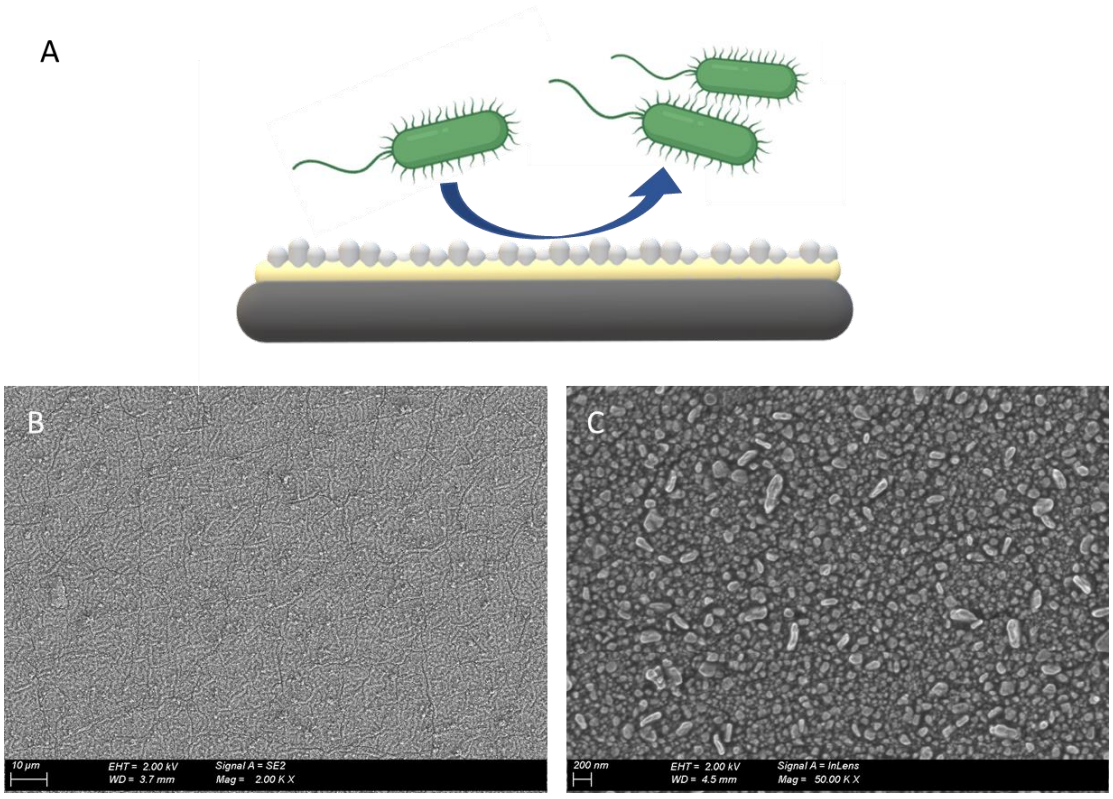

Figure III. 18.Nanostructured PDA-silver coated PDMS**.** A. Scheme of the metallic silver nanostructure. FE-SEM images of PDMS coupons modified with PDA and metallic silver coating at different zoom (B) magnification of 2.00K and C) magnification of 50.00K).

As explained before, it is shown that both wettability and surface morphology influence the bacterial adhesion, with neither super-hydrophobicity or low surfaces roughness alone sufficient for reducing initial retention of bacteria[35]. Super-hydrophobicity is the goal of these surface due to hydrophobic surfaces are friendly to bacterial attachment in complex environments, needing to avoid bacterial deposition by other methods such as antibiotic release. Hydrophobic or superhydrophobic strategies have not been addressed because these surfaces interact more with proteins present in a complex medium in flow. Hydrophilic surfaces are more susceptible to being covered by cellular debris and proteins, offering a platform for bacterial adhesion that is not of our interest[63].

To test the hydrophobic behaviour of the PDA-silver coated surfaces, WCA was measured and compared with PDMS as a standard grade of hydrophobicity in silicone-based medical devices (Figure III. 19 A). As expected, WCA measures of modified PDMS showed a super-hydrophobic coating with a statistical difference between control and modified samples. The super-

hydrophobic effect of the surface is given by the microstructure of the surface, which can trap air between its formations, giving anti-fouling properties to the material[49,64].

In order to study the amount of silver deposited on PDMS surfaces, after manufacturing, samples were digested with nitric acid and analysed by ICP (Figure III. 19 B). The total silver deposited per cm^2 was similar to the rest of the samples manufactured before with the plasma polymerization method. Therefore, the dip coating method for nano-structuring and silver coating of surfaces continues showing characteristics leading to bacteriophobic properties.

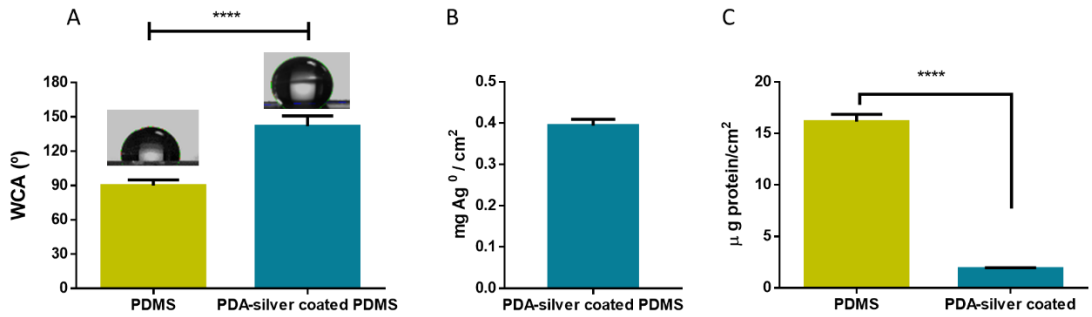

Figure III. 19. Characterization of PDA-silver coated PDMS. A. Water contact angle of PDMS and PDMS coupons modified with PDA-silver coating. B. Total silver was extracted from modified surfaces and quantified by inductively coupled plasma, showing a silver deposition on PDMS samples of 0.3938 mg ± 0.012 mg of metallic silver per cm2. C. Protein quantification from surfaces after 24 h of incubation with Fetal-Bovine Serum. Statistical analysis indicated a significative difference between control and modified surface, with a maximum p-value of < 0.001 (***).

As previous studies have shown in previous studies, avoiding adhesion of protein to the surface can help prevent bacterial adhesion. The protein repulsion capacity of the surface was studied by incubating with FBS for 24 h and quantifying the amount of protein adsorbed. As can be seen in the Figure III. 19 C, the amount of protein retained by the surface was more than 10 times less. This effect was similar to that presented by the rest of the antibacterial surfaces generated in the previous section, showing protein adhesion less than 5 µg protein per cm^2. Low protein adsorption in complex environments is a necessary feature when selecting the best approach to create bacteriophobic surfaces. Being able to repel proteins present in the urine will be key for patients with diabetes, heart attacks or other diseases that present proteinuria[24,65,66]. Since high protein adhesion to the surface of urinary catheters will favour interaction with bacteria and their subsequent infection[67,68].

The metallic silver layer deposited releases silver ions by located oxidation of the surface. This phenomenon will take place until the exhaustion, the blockade of the surface or the saturation of the medium. However, an unknown amount of silver may be chemo-absorbed by the surface during silver deposition reaction, in a non-reduce form. This kind of silver can release it in few seconds when samples come into contact with aqueous media, promoting a burst release of silver.

To test the silver release, samples were put in contact with different media for 22 days (529 h) at 37 ºC. Media were Mili-Q H_2O, as low complexity medium, PBS, as saline medium and acetic acid with the purpose of extract all chemo-absorbed silver and show it and then, silver was quantified using ICP (Figure III. 20 A and B).

The graphs of Figure III. 20 shown three profiles of silver release. First, the surface releases silver in a burst form when surface was in contact with media at first time, in all media tested. This effect may be due to the quickly release of chemo-absorbed silver from surface, producing a burst effect. To verify this hypothesis, the silver on acetic acid can be observed. Acetic acid washes the chemo-absorbed silver, and, as can be noted in the Figure III. 20 A, at short times of surface exposition to the medium, the amount of silver released reaches the same values than observed in H_2O and PBS. After first times, the tendency of the curve indicated that new amount of silver was not added to medium, so, all chemo-absorbed silver has been released in less than 10 h, left the surface completely clean. This effect is independent to the oxidation of metallic silver deposited on surface, which produces a constant silver ion release from it. After this first burst, the silver release is constant due to the local oxidation and it seems that it does not reach a liberation plateau. However, in comparation with the previous studied surfaces, the amount of silver and the tendency of the release are similar to the observed in the “thick blades” surface tested in previous section of this chapter (Figure III. 12 A). So, if graphs are viewed in normalize scale, the released silver from this surface will be showed as a stationary tendency in all media studied.

Furthermore, the differences observed between Mili-Q H_2O and PBS media were not significant. The differences showed may be due to the initial saturation of the media in case of PBS respect to Mili-Q H_2O, but, at long times of exposure, the amount of silver released was similar.

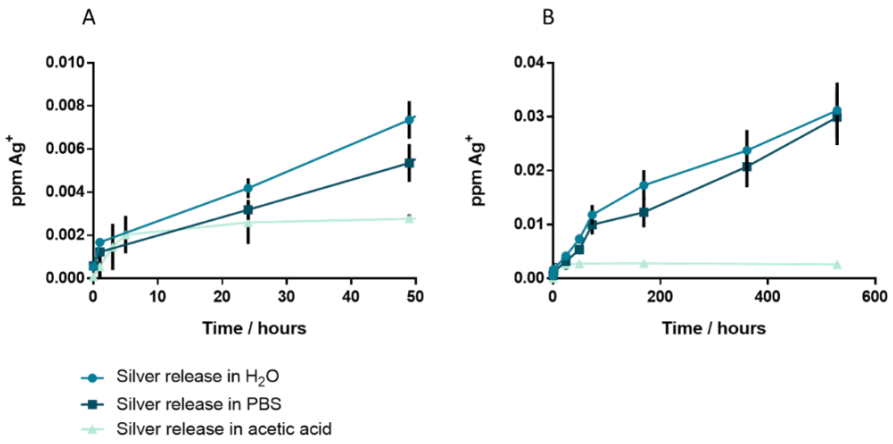

Figure III. 20. Accumulated silver release from modified PDMS surfaces in different media: Mili-Q H2O, PBS and acetic acid. The test was made at 37 ºC in static conditions for 529 h (approximately 22 days). A. Silver release at short times (until 49 h) to appreciate the initial burst of silver. B. Full test of silver release.

3.3.3.1 Coating characterization for continuous use applied on urinary catheters

In this section, with the aim of adapt this antibacterial strategy to real urinary catheters and to be able to carry out studies beyond the laboratory settings, the response of the surface to different stresses was studied. One of the most interesting tests to characterize the lifespan of materials, specially the medical-used ones, is the accelerated aging test. According to the guide ASTM F1980, applying 60 ºC during 3.7 weeks to polymer-based materials, the final effect on the material is equivalent to storage it during 1 year at room temperature. So, the samples of PDMS modified with PDA-silver coatings were put in a stove at 60 ºC and wet atmosphere into a glass vials during, at least, 26 days to test the coating stability.

In addition to this, the samples were exposed to mechanical stress, being sonicated to observe the effect on the coating. This test is not intended to simulate the wear of the coating in actual use. It is also not a reflection of the mechanical stress that the coating can be subjected to when applied to a urinary catheter. But the test can offer as a small approximation to be able to consider the coating as good candidate for the future application to medical devices or to discard it.

After these tests, samples were analysed by WCA (Figure III. 21 A), FE-SEM images (Figure III. 21 B) and ICP (Figure III. 21 C).

As shown in Figure III. 21 A, there are no significative differences between WCA measures. Stress effects also was observed by FE-SEM (Figure III. 21 B), where aged and sonicated surfaces are similar to the sample control (Figure III. 18). No loss of coating or breakage of it was seen and micro and nanostructure seem to hold up in good condition. Furthermore, the analysis of silver amount deposited on surfaces (Figure III. 21 C) revealed a non-significant difference between samples. Finally, it was possible to conclude that the coating is stable after being subjected to accelerated aging, which simulates its continuous use for more than a year. In addition, the coating resists aggressive sonication without detaching or losing its structure. Since the intention of the technology is to cover urinary catheters from the internal area, the coating will not suffer mechanical damage, it will not come off or lose its function during use.

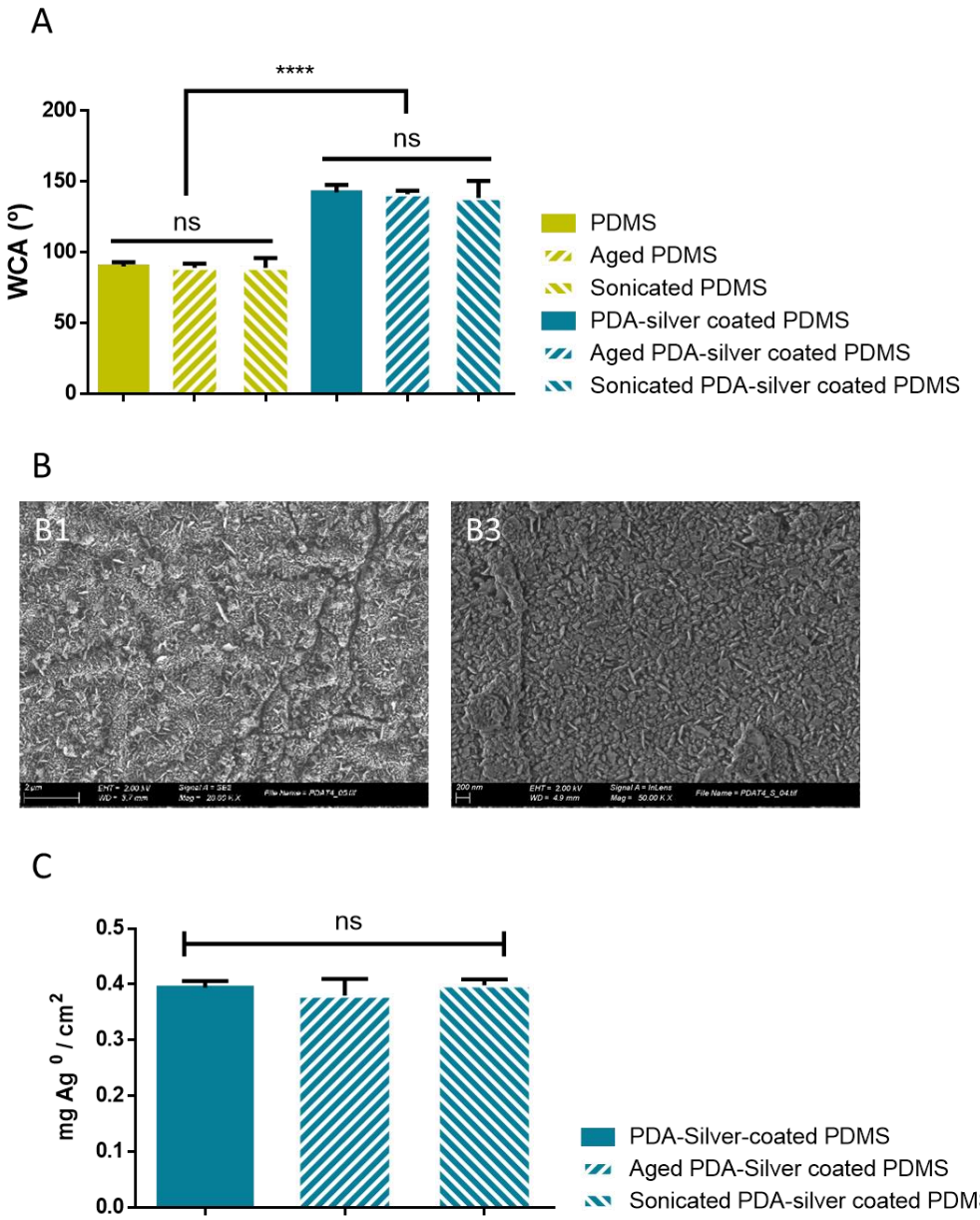

Figure III. 21. Stress test to characterize the coating after 1 year of simulated storage and physical pressure. A. Water contact angle measures after tests on PDMS samples as control and PDMS with PDA-silver coating samples. No significant differences were found between the modified samples B. FE-SEM images from surfaces of PDMS with PDA-silver coating after tests. B1. Aged surface. B2. Sonicated surface. C. Total silver extracted from surfaces of PDMS modified with PDA-silver coating after tests, analysed by inductively coupled plasma and normalized per area. No significant differences were found.

3.3.3.2 Bacterial viability and bacterial adhesion to proposed surface.

The release of silver ions from the surface affect to bacterial growth, depending on the amount of silver released, as studied in previous section (Figure III. 11). In this case, three bacterial strains were put in contact with the PDMS samples modified with PDA and a metallic silver coating to test the effect of the silver released in bacterial growth, using PDMS as a control material (Figure III. 22). The bacterial strains of the test were used in the previous study; *Escherichia* coli CFT073 (Figure III. 22 A), *Staphylococcus aureus* subspecies aureus (Figure III. 22 B) and *Pseudomonas aeruginosa* PAO1 (Figure III. 22 C). The bacterial growth was measured by spectroscopy at 600 nm during 18 h each 30 min and a final measure of these bacterial strains was read at end point (50 h), to ensure the stationary phase data were correct. Also, different bacteria of interest were tested at end point of growth (24, 36, 50 or 96 h) according to the optimal growth (Figure III. 22 D).

As can be noted, the growth profiles of the different bacterial strains were similar to the observed growth in contact with the surface called “thick blades”. These results were expected due to the similarities shown in silver release profiles. Gram-negative species such as *E. coli* (Figure III. 22 A) were more sensitive to the silver present in medium, but the growth reached the stationary phase 6 h later than the control. These species had a longer adaptation phase but did not show any other growth problems. In case of *P. aeruginosa* (Figure III. 22 C), despite of being gram-negative bacteria, or *S. aureus* (Figure III. 22 D), as gram-positive model, the observed growth was normal without differences between control and the samples.

Finally, different bacterial cultures were tested at their optimum time of growth and conditions to ensure the growth tendency and the surface behaviour were not strain-dependent. Differences between PDMS and modified PDMS with PDA-silver coating were not observed (Figure III. 22 D), so, the silver release from the surface did not affect any bacteria, regardless their nature. Among the strains shown, Lactobacillus genus are of special interest, in this case, several probiotic strains of the female genital tract. These species were not affected in their growth either, so, the technology does not affect the natural microbiota of the future host. This fact is of vital importance since, if natural microbiota is not affected, new niches for opportunistic pathogens will not release and the possibility of an infection can be reduced naturally by keeping the natural barriers of the organism intact.

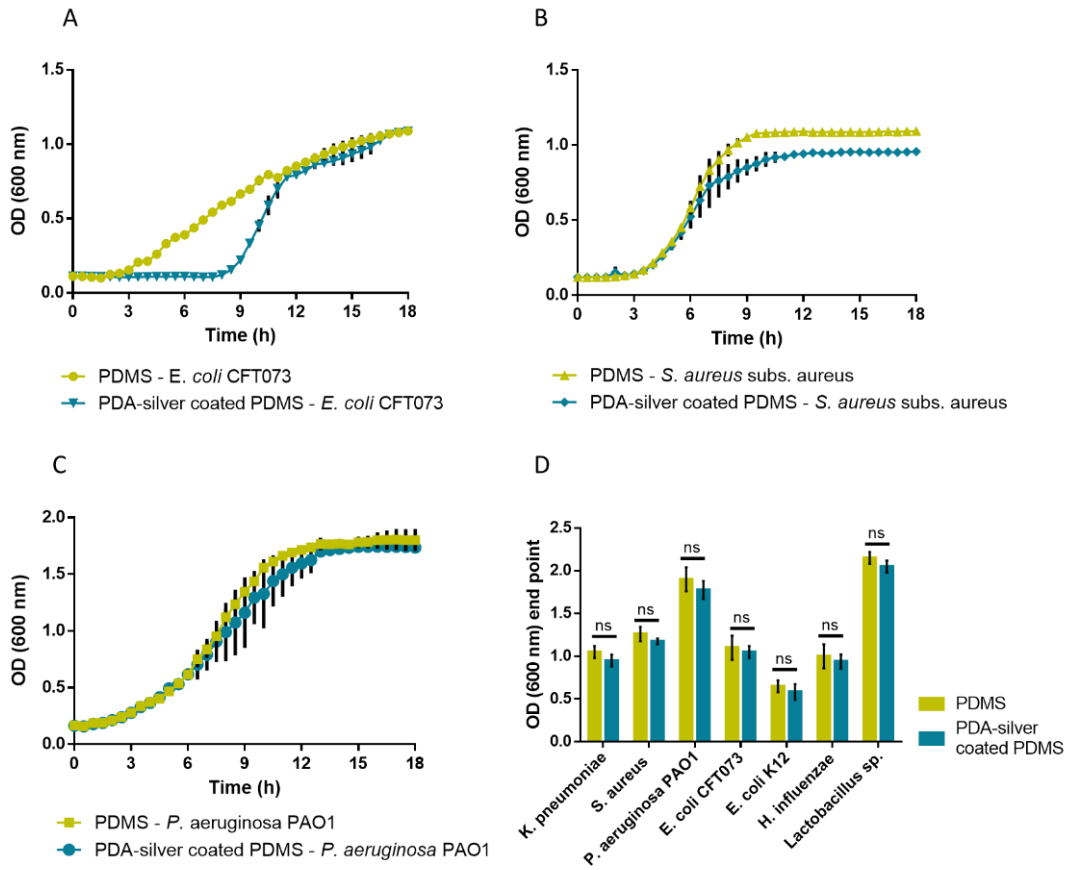

Figure III. 22. Bacterial viability. Growth curves of different bacterial species in contact with proposed surface and PDMS as a control surface. A. *E. coli* CFT073 growth curve. B. *S. aureus* sub. aureus growth curve. C. *P. aeruginosa* PAO1 growth curve. D. End point measure of different bacterial species after 36-48 or 50 h in contact with PDA-silver coated PDMS samples. Measures between PDMS and coated PDMS showed non-statistical differences.

These results indicated that the proposed surface in this section was not bacteriostatic or bactericide. The antibacterial behaviour, or not, given by this surface in advance will be due exclusively to the topography. Therefore, next step was to study bacterial adhesion to the surface, with the aim to observe a bacteriophobic behaviour before applying the technology to the urinary catheters.

Bacterial adhesion test was made using the three bacterial models previously mentioned, according to the protocols developed in previous chapter and briefly explained in MATERIALS and METHODS section. After samples incubation, washes and biofilm extraction, live bacteria

were quantified and represented as CFU per cm^2 (Figure III. 23). PDMS without modifications was used as control.

As shown in Figure III. 23, a reduction in bacterial adhesion to the surfaces of at least 4 orders of magnitude was observed in worst case, corresponding to *S. aureus*. A maximum of 7 logarithms was observed in case of *E. coli*. This test indicated that surfaces present a bacteriophobic behaviour, regardless of the bacterial species.

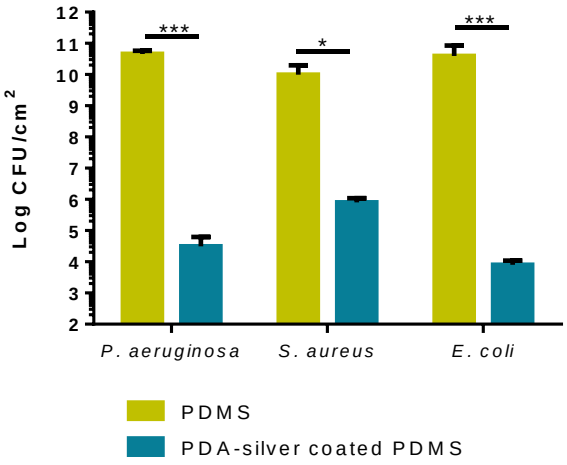

Figure III. 23. Bacterial adhesion to PDMS and PDA-silver coated PDMS surfaces. Different bacterial species were used, *Pseudomonas aeruginosa* PAO1, *Staphylococcus aureus* subs. aureus and *Escherichia coli* CFT073. Statistical significance was represented as (*) according to the p-value obtained.

All tests performed show a surface with bacteriophobic properties, capable of avoiding bacterial adhesion without affecting bacterial growth. This repulsion effect may be due to the observed topography. The nanostructure of the surface that does not offer a stable niche for the bacteria, and, at the same time, bacteria are disturbed by the local oxidation of silver and its release in amounts that are not considered harmful but constant. All these factors combine with the super-hydrophobicity, which prevents the deposition of elements that can serve as new anchored points for bacteria, camouflaging the nanostructure and the silver release effect at long times of exposure. Therefore, this technology can be useful to maintain a surface free of colonization and living organisms and free of biological remains for, almost, infinite times.

3.4 CONCLUDING REMARKS

A set of antimicrobial surfaces have been developed and characterized in this chapter. All of them have shown a super-hydrophobic characteristic due to the construction of a specific micro and nanostructure topography on the surface. These topographies avoided the protein adsorption, keeping clean the samples and avoiding a key factor to early bacterial attachment.

All the surfaces shown an antimicrobial effect, avoiding bacterial colonization by at least 4 orders of magnitude relative to uncoated samples, regardless of bacterial strain used. But, changes in the polymerization methodology led to obtaining different morphologies that have been shown to have different effects on bacteria: from bacteriostatic to only bacteriophobic effect. The bacteriostatic effect is promoted by a controlled silver release by the silver oxidation from the surface, that does not occur on the rest of surfaces.

Finally, the amount of total silver deposited per cm^2 on the surfaces, as well as the amount of silver released by the local oxidation of the coatings is well below the threshold considered cytotoxic. Therefore, all the proposals can be applied to silicone-based medical devices to give them antimicrobial properties without producing side effects.

3.5 REFERENCES

(1) Zaborowska, M.; Welch, K.; Branemark, R.; Khalilpour, P.; Engqvist, H.; Thomsen, P.; Trobos, M. Bacteria-Material Surface Interactions: Methodological Development for the Assessment of Implant Surface Induced Antibacterial Effects. *J. Biomed. Mater. Res. - Part B Appl. Biomater.* **2015**, *103* (1), 179–187. https://doi.org/10.1002/jbm.b.33179.

(2) Straub, H.; Bigger, C. M.; Valentin, J.; Abt, D.; Qin, X. H.; Eberl, L.; Maniura-Weber, K.; Ren, Q. Bacterial Adhesion on Soft Materials: Passive Physicochemical Interactions or Active Bacterial Mechanosensing? *Adv. Healthc. Mater.* **2019**, *8* (8), 1–8. https://doi.org/10.1002/adhm.201801323.

(3) Sabir, N.; Ikram, A.; Zaman, G.; Satti, L.; Gardezi, A.; Ahmed, A.; Ahmed, P. Bacterial Biofilm-Based Catheter-Associated Urinary Tract Infections: Causative Pathogens and Antibiotic Resistance. *Am. J. Infect. Control* **2017**, *45* (10), 1101–1105. https://doi.org/10.1016/j.ajic.2017.05.009.

(4) Terlizzi, M. E.; Gribaudo, G.; Maffei, M. E. UroPathogenic Escherichia Coli (UPEC) Infections: Virulence Factors, Bladder Responses, Antibiotic, and Non-Antibiotic Antimicrobial Strategies. *Front. Microbiol.* **2017**, *8* (AUG). https://doi.org/10.3389/fmicb.2017.01566.

(5) Adlhart, C.; Verran, J.; Azevedo, N. F.; Olmez, H.; Keinänen-Toivola, M. M.; Gouveia, I.; Melo, L. F.; Crijns, F. Surface Modifications for Antimicrobial Effects in the Healthcare Setting: A Critical Overview. *J. Hosp. Infect.* **2018**, *99* (3), 239–249. https://doi.org/10.1016/j.jhin.2018.01.018.

(6) Gilabert-Porres, J.; Martí, S.; Calatayud, L.; Ramos, V.; Rosell, A.; Borrós, S. Design of a Nanostructured Active Surface against Gram-Positive and Gram-Negative Bacteria through Plasma Activation and in Situ Silver Reduction. *ACS Appl. Mater. Interfaces* **2016**, *8* (1), 64–73. https://doi.org/10.1021/acsami.5b07115.

(7) Liao, S.; Zhang, Y.; Pan, X.; Zhu, F.; Jiang, C.; Liu, Q.; Cheng, Z.; Dai, G.; Wu, G.; Wang, L.; et al. Antibacterial Activity and Mechanism of Silver Nanoparticles against Multidrug-Resistant Pseudomonas Aeruginosa. *Int. J. Nanomedicine* **2019**, *14*, 1469–1487. https://doi.org/10.2147/IJN.S191340.

(8) Carvalho, I.; Dias, N.; Henriques, M.; Calderon V, S.; Ferreira, P.; Cavaleiro, A.; Carvalho, S. Antibacterial Effects of Bimetallic Clusters Incorporated in Amorphous Carbon for Stent Application. *ACS Appl. Mater. Interfaces* **2020**, *12* (22), 24555–24563. https://doi.org/10.1021/acsami.0c02821.

(9) Siedenbiedel, F.; Tiller, J. C. Antimicrobial Polymers in Solution and on Surfaces:

Overview and Functional Principles. *Polymers (Basel).* **2012**, *4* (1), 46–71. https://doi.org/10.3390/polym4010046.

(10) Lemire, J. A.; Harrison, J. J.; Turner, R. J. Antimicrobial Activity of Metals: Mechanisms, Molecular Targets and Applications. *Nat. Rev. Microbiol.* **2013**, *11* (6), 371–384. https://doi.org/10.1038/nrmicro3028.

(11) Mi, G.; Shi, D.; Wang, M.; Webster, T. J. Reducing Bacterial Infections and Biofilm Formation Using Nanoparticles and Nanostructured Antibacterial Surfaces. *Adv. Healthc. Mater.* **2018**, *7* (13), 1–23. https://doi.org/10.1002/adhm.201800103.

(12) Greulich, C.; Braun, D.; Peetsch, A.; Diendorf, J.; Siebers, B.; Epple, M.; Köller, M. The Toxic Effect of Silver Ions and Silver Nanoparticles towards Bacteria and Human Cells Occurs in the Same Concentration Range. *RSC Adv.* **2012**, *2* (17), 6981. https://doi.org/10.1039/c2ra20684f.

(13) Kubo, A. L.; Capjak, I.; Vrček, I. V.; Bondarenko, O. M.; Kurvet, I.; Vija, H.; Ivask, A.; Kasemets, K.; Kahru, A. Antimicrobial Potency of Differently Coated 10 and 50 nm Silver Nanoparticles against Clinically Relevant Bacteria Escherichia Coli and Staphylococcus Aureus. *Colloids Surfaces B Biointerfaces* **2018**, *170* (April), 401–410. https://doi.org/10.1016/j.colsurfb.2018.06.027.

(14) Colletta, A.; Wu, J.; Wo, Y.; Kappler, M.; Chen, H.; Xi, C.; Meyerhoff, M. E. S-Nitroso-N-Acetylpenicillamine (SNAP) Impregnated Silicone Foley Catheters: A Potential Biomaterial/Device to Prevent Catheter-Associated Urinary Tract Infections. *ACS Biomater. Sci. Eng.* **2015**, *1* (6), 416–424. https://doi.org/10.1021/acsbiomaterials.5b00032.

(15) Dave, R. N.; Joshi, H. M.; Venugopalan, V. P. Novel Biocatalytic Polymer-Based Antimicrobial Coatings as Potential Ureteral Biomaterial: Preparation and In Vitro Performance Evaluation. *Antimicrob. Agents Chemother.* **2011**, *55* (2), 845–853. https://doi.org/10.1128/AAC.00477-10.

(16) Jung, W. K.; Koo, H. C.; Kim, K. W.; Shin, S.; Kim, S. H.; Park, Y. H. Antibacterial Activity and Mechanism of Action of the Silver Ion in Staphylococcus Aureus and Escherichia Coli. *Appl. Environ. Microbiol.* **2008**, *74* (7), 2171–2178. https://doi.org/10.1128/AEM.02001-07.

(17) Dakal, T. C.; Kumar, A.; Majumdar, R. S.; Yadav, V. Mechanistic Basis of Antimicrobial Actions of Silver Nanoparticles. *Front. Microbiol.* **2016**, *7* (NOV), 1–17. https://doi.org/10.3389/fmicb.2016.01831.

(18) Silver, S.; Phung, L. T.; Silver, G. Silver as Biocides in Burn and Wound Dressings and Bacterial Resistance to Silver Compounds. *J. Ind. Microbiol. Biotechnol.* **2006**, *33* (7),

627–634. https://doi.org/10.1007/s10295-006-0139-7.

(19) Silver, S. Bacterial Silver Resistance: Molecular Biology and Uses and Misuses of Silver Compounds. *FEMS Microbiol. Rev.* **2003**, *27* (2–3), 341–353. https://doi.org/10.1016/S0168-6445(03)00047-0.

(20) Panáček, A.; Kvítek, L.; Smékalová, M.; Večeřová, R.; Kolář, M.; Röderová, M.; Dyčka, F.; Šebela, M.; Prucek, R.; Tomanec, O.; et al. Bacterial Resistance to Silver Nanoparticles and How to Overcome It. *Nat. Nanotechnol.* **2018**, *13* (1), 65–71. https://doi.org/10.1038/s41565-017-0013-y.

(21) Lansdown, A. B. G. Silver in Health Care: Antimicrobial Effects and Safety in Use Interactions between Skin and Biofunctional Metals. *Curr Probl Dermatol. Basel, Karger* **2006**, *33*, 17–34.

(22) Lansdown, A. B. G. A Pharmacological and Toxicological Profile of Silver as an Antimicrobial Agent in Medical Devices. *Adv. Pharmacol. Sci.* **2010**, *2010* (9), 1–16. https://doi.org/10.1155/2010/910686.

(23) Flores-Mireles, A. L.; Walker, J. N.; Caparon, M.; Hultgren, S. J. Urinary Tract Infections: Epidemiology, Mechanisms of Infection and Treatment Options. *Nat. Rev. Microbiol.* **2015**, *13* (5), 269–284. https://doi.org/10.1038/nrmicro3432.

(24) García-Bonillo, C.; Texidó, R.; Reyes-Carmenaty, G.; Gilabert-Porres, J.; Borrós, S. Study of the Human Albumin Role in the Formation of a Bacterial Biofilm on Urinary Devices Using QCM-D. *ACS Appl. Bio Mater.* **2020**, *3* (5), 3354–3364. https://doi.org/10.1021/acsabm.0c00286.

(25) Song, B.; Zhang, E.; Han, X.; Zhu, H.; Shi, Y.; Cao, Z. Engineering and Application Perspectives on Designing an Antimicrobial Surface. *ACS Appl. Mater. Interfaces* **2020**, acsami.9b19992. https://doi.org/10.1021/acsami.9b19992.

(26) Linklater, D. P.; Juodkazis, S.; Ivanova, E. P. Nanofabrication of Mechano-Bactericidal Surfaces. *Nanoscale* **2017**, *9* (43), 16564–16585. https://doi.org/10.1039/C7NR05881K.

(27) Damodaran, V. B.; Murthy, N. S. Bio-Inspired Strategies for Designing Antifouling Biomaterials. *Biomater. Res.* **2016**, *20* (1), 18. https://doi.org/10.1186/s40824-016-0064-4.

(28) Vadillo-Rodríguez, V.; Guerra-García-Mora, A. I.; Perera-Costa, D.; Gónzalez-Martín, M. L.; Fernández-Calderón, M. C. Bacterial Response to Spatially Organized Microtopographic Surface Patterns with Nanometer Scale Roughness. *Colloids Surfaces B Biointerfaces* **2018**, *169* (February), 340–347. https://doi.org/10.1016/j.colsurfb.2018.05.038.

(29) Watson, G. S.; Green, D. W.; Watson, J. A.; Zhou, Z.; Li, X.; Cheung, G. S. P.; Gellender,

M. A Simple Model for Binding and Rupture of Bacterial Cells on Nanopillar Surfaces. *Adv. Mater. Interfaces* **2019**, *6* (10), 1–8. https://doi.org/10.1002/admi.201801646.

(30) Elbourne, A.; Chapman, J.; Gelmi, A.; Cozzolino, D.; Crawford, R. J.; Truong, V. K. Bacterial-Nanostructure Interactions: The Role of Cell Elasticity and Adhesion Forces. *J. Colloid Interface Sci.* **2019**, *546*, 192–210. https://doi.org/10.1016/j.jcis.2019.03.050.

(31) Tripathy, A.; Sen, P.; Su, B.; Briscoe, W. H. Natural and Bioinspired Nanostructured Bactericidal Surfaces. *Adv. Colloid Interface Sci.* **2017**, *248*, 85–104. https://doi.org/10.1016/j.cis.2017.07.030.

(32) Anselme, K.; Davidson, P.; Popa, A. M.; Giazzon, M.; Liley, M.; Ploux, L. The Interaction of Cells and Bacteria with Surfaces Structured at the Nanometre Scale. *Acta Biomater.* **2010**, *6* (10), 3824–3846. https://doi.org/10.1016/j.actbio.2010.04.001.

(33) Jaggessar, A.; Shahali, H.; Mathew, A.; Yarlagadda, P. K. D. V. Bio-Mimicking Nano and Micro-Structured Surface Fabrication for Antibacterial Properties in Medical Implants. *J. Nanobiotechnology* **2017**, *15* (1), 1–20. https://doi.org/10.1186/s12951-017-0306-1.

(34) Serrano, C.; García-Fernández, L.; Fernández-Blázquez, J. P.; Barbeck, M.; Ghanaati, S.; Unger, R.; Kirkpatrick, J.; Arzt, E.; Funk, L.; Turón, P.; et al. Nanostructured Medical Sutures with Antibacterial Properties. *Biomaterials* **2015**, *52* (1), 291–300. https://doi.org/10.1016/j.biomaterials.2015.02.039.

(35) Lutey, A. H. A.; Gemini, L.; Romoli, L.; Lazzini, G.; Fuso, F.; Faucon, M.; Kling, R. Towards Laser-Textured Antibacterial Surfaces. *Sci. Rep.* **2018**, *8* (1), 1–10. https://doi.org/10.1038/s41598-018-28454-2.

(36) Modaresifar, K.; Azizian, S.; Ganjian, M.; Fratila-Apachitei, L. E.; Zadpoor, A. A. Bactericidal Effects of Nanopatterns: A Systematic Review. *Acta Biomater.* **2019**, *83*, 29–36. https://doi.org/10.1016/j.actbio.2018.09.059.

(37) Liu, L.; Ercan, B.; Sun, L.; Ziemer, K. S.; Webster, T. J. Understanding the Role of Polymer Surface Nanoscale Topography on Inhibiting Bacteria Adhesion and Growth. *ACS Biomater. Sci. Eng.* **2016**, *2* (1), 122–130. https://doi.org/10.1021/acsbiomaterials.5b00431.

(38) Hazell, G.; May, P. W.; Taylor, P.; Nobbs, A. H.; Welch, C. C.; Su, B. Studies of Black Silicon and Black Diamond as Materials for Antibacterial Surfaces. *Biomater. Sci.* **2018**, *6* (6), 1424–1432. https://doi.org/10.1039/c8bm00107c.

(39) Ponomarev, V. A.; Shvindina, N. V.; Permyakova, E. S.; Slukin, P. V.; Ignatov, S. G.; Sirota, B.; Voevodin, A. A.; Shtansky, D. V. Structure and Antibacterial Properties of Ag-Doped Micropattern Surfaces Produced by Photolithography Method. *Colloids Surfaces B*

Biointerfaces **2019**, *173*, 719–724. https://doi.org/10.1016/j.colsurfb.2018.10.040.

(40) Mas-Vinyals, A.; Gilabert-Porres, J.; Figueras-Esteve, L.; Borrós, S. Improving Linking Interface between Collagen-Based Hydrogels and Bone-like Substrates. *Colloids Surfaces B Biointerfaces* **2019**, *181* (June), 864–871. https://doi.org/10.1016/j.colsurfb.2019.06.046.

(41) Morent, R.; De Geyter, N.; Desmet, T.; Dubruel, P.; Leys, C. Plasma Surface Modification of Biodegradable Polymers: A Review. *Plasma Process. Polym.* **2011**, *8* (3), 171–190. https://doi.org/10.1002/ppap.201000153.

(42) Cifuentes, A.; Borrós, S. Comparison of Two Different Plasma Surface-Modification Techniques for the Covalent Immobilization of Protein Monolayers. *Langmuir* **2013**, *29* (22), 6645–6651. https://doi.org/10.1021/la400597e.

(43) Lee, H.; Dellatore, S. M.; Miller, W. M.; Messersmith, P. B. Mussel-Inspired Surface Chemistry for Multifunctional Coatings. *Science (80-.).* **2007**, *318* (5849), 426–430. https://doi.org/10.1126/science.1147241.

(44) Welch, R. A.; Burland, V.; Plunkett, G.; Redford, P.; Roesch, P.; Rasko, D.; Buckles, E. L.; Liou, S. R.; Boutin, A.; Hackett, J.; et al. Extensive Mosaic Structure Revealed by the Complete Genome Sequence of Uropathogenic Escherichia Coli. *Proc. Natl. Acad. Sci.* **2002**, *99* (26), 17020–17024. https://doi.org/10.1073/pnas.252529799.

(45) Texidó, R.; Borrós, S. Allylamine PECVD Modification of PDMS as Simple Method to Obtain Conductive Flexible Polypyrrole Thin Films. *Polymers (Basel).* **2019**, *11* (12), 2108. https://doi.org/10.3390/POLYM11122108.

(46) Horna, D.; Ramírez, J. C.; Cifuentes, A.; Bernad, A.; Borrós, S.; González, M. a. Efficient Cell Reprogramming Using Bioengineered Surfaces. *Adv. Healthc. Mater.* **2012**, *1* (2), 177–182. https://doi.org/10.1002/adhm.201200017.

(47) Francesch, L.; Borros, S.; Knoll, W.; Förch, R. Surface Reactivity of Pulsed-Plasma Polymerized Pentafluorophenyl Methacrylate (PFM) toward (1) Francesch, L.; Borros, S.; Knoll, W.; Förch, R. Surface Reactivity of Pulsed-Plasma Polymerized Pentafluorophenyl Methacrylate (PFM) toward Amines and Proteins. *Langmuir* **2007**, *23* (7), 3927–3931. https://doi.org/10.1021/la062422d.

(48) Ryu, J. H.; Messersmith, P. B.; Lee, H. Polydopamine Surface Chemistry - A Decade of Discovery. *ACS Appl. Mater. Interfaces* **2018**, acsami.7b19865. https://doi.org/10.1021/acsami.7b19865.

(49) Damodaran, V. B.; Murthy, N. S. Bio-Inspired Strategies for Designing Antifouling Biomaterials. *Biomater. Res.* **2016**, *20* (1), 18. https://doi.org/10.1186/s40824-016-0064-4.

(50) Wei, Q.; Zhang, F.; Li, J.; Li, B.; Zhao, C. Oxidant-Induced Dopamine Polymerization for Multifunctional Coatings. *Polym. Chem.* **2010**, *1* (9), 1430. https://doi.org/10.1039/c0py00215a.

(51) Zeng, R.; Luo, Z.; Zhou, D.; Cao, F.; Wang, Y. A Novel PEG Coating Immobilized onto Capillary through Polydopamine Coating for Separation of Proteins in CE. *Electrophoresis* **2010**, *31* (19), 3334–3341. https://doi.org/10.1002/elps.201000228.

(52) Zhou, P.; Deng, Y.; Lyu, B.; Zhang, R.; Zhang, H.; Ma, H.; Lyu, Y.; Wei, S. Rapidly-Deposited Polydopamine Coating via High Temperature and Vigorous Stirring: Formation, Characterization and Biofunctional Evaluation. *PLoS One* **2014**, *9* (11), 0–9. https://doi.org/10.1371/journal.pone.0113087.

(53) Gary Chinga, Per Olav Johnsen, Robert Dougherty, Elisabeth Lunden Berli, J. W. Quantification of the 3D Microstructure of SC Surfaces. *J. Microsc.* **2007**, *227* (December 2006), 254–265.

(54) Hohmann, S.; Neidig, A.; Kühl, B.; Kirschhöfer, F.; Overhage, J.; Brenner-Weiß, G. A New Data Processing Routine Facilitating the Identification of Surface Adhered Proteins from Bacterial Conditioning Films via QCM-D/MALDI-ToF/MS. *Anal. Bioanal. Chem.* **2017**, *409* (25), 5965–5974. https://doi.org/10.1007/s00216-017-0521-5.

(55) Cifuentes, A.; Borrós, S. Comparison of Two Different Plasma Surface-Modification Techniques for the Covalent Immobilization of Protein Monolayers. *Langmuir* **2013**, *29* (22), 6645–6651. https://doi.org/10.1021/la400597e.

(56) Nguyen, D. H. K.; Pham, V. T. H.; Truong, V. K.; Sbarski, I.; Wang, J.; Balčytis, A.; Juodkazis, S.; Mainwaring, D. E.; Crawford, R. J.; Ivanova, E. P. Role of Topological Scale in the Differential Fouling of: Pseudomonas Aeruginosa and Staphylococcus Aureus Bacterial Cells on Wrinkled Gold-Coated Polystyrene Surfaces. *Nanoscale* **2018**, *10* (11), 5089–5096. https://doi.org/10.1039/c7nr08178b.

(57) Xiaoxue, Z.; Ling, W.; Erkki, L. Superhydrophobic Surfaces for the Reduction of Bacterial Adhesion. *RSC Adv.* **2013**, *3*, 12003–12020. https://doi.org/10.1039/c3ra40497h.

(58) Marmur, A. From Hygrophilic to Superhygrophobic: Theoretical Conditions for Making High-Contact-Angle Surfaces from Low-Contact-Angle Materials. *Langmuir* **2008**, *24* (14), 7573–7579. https://doi.org/10.1021/la800304r.

(59) Lee, W. K.; Jung, W. Bin; Nagel, S. R.; Odom, T. W. Stretchable Superhydrophobicity from Monolithic, Three-Dimensional Hierarchical Wrinkles. *Nano Lett.* **2016**, *16* (6), 3774–3779. https://doi.org/10.1021/acs.nanolett.6b01169.

(60) Roach, P.; Shirtcliffe, N. J. J.; Newton, M. I. I. Progess in Superhydrophobic Surface

Development. *Soft Matter* **2008**, *4* (2), 224–240. https://doi.org/10.1039/b712575p.

(61) Kharisov, B.; Kharissova, O.; Ortiz-Mendez, U. *CRC Concise Encyclopedia of Nanotechnology*; 2016.

(62) Hagan, E. C.; Donnenberg, M. S.; Mobley, H. L. T. Uropathogenic Escherichia Coli. *EcoSal Plus* **2009**, *3* (2). https://doi.org/10.1128/ecosalplus.8.6.1.3.

(63) Wertz, C. F.; Santore, M. M. Effect of Surface Hydrophobicity on Adsorption and Relaxation Kinetics of Albumin and Fibrinogen: Single-Species and Competitive Behavior. *Langmuir* **2001**, *17* (10), 3006–3016. https://doi.org/10.1021/la0017781.

(64) Jaggessar, A.; Shahali, H.; Mathew, A.; Yarlagadda, P. K. D. V. Bio-Mimicking Nano and Micro-Structured Surface Fabrication for Antibacterial Properties in Medical Implants. *J. Nanobiotechnology* **2017**, *15* (1), 1–20. https://doi.org/10.1186/s12951-017-0306-1.

(65) Carter, J. L.; Tomson, C. R. V.; Stevens, P. E.; Lamb, E. J. Does Urinary Tract Infection Cause Proteinuria or Microalbuminuria? A Systematic Review. *Nephrol. Dial. Transplant.* **2006**, *21* (11), 3031–3037. https://doi.org/10.1093/ndt/gfl373.

(66) Wu, H. Y.; Huang, J. W.; Peng, Y. Sen; Hung, K. Y.; Wu, K. D.; Lai, M. S.; Chien, K. L. Microalbuminuria Screening for Detecting Chronic Kidney Disease in the General Population: A Systematic Review. *Ren. Fail.* **2013**, *35* (5), 607–614. https://doi.org/10.3109/0886022X.2013.779907.

(67) Ponche, A.; Ploux, L.; Anselme, K. Protein/Material Interfaces: Investigation on Model Surfaces. *J. Adhes. Sci. Technol.* **2010**, *24* (13–14), 2141–2164. https://doi.org/10.1163/016942410X507966.

(68) Knetsch, M. L. W.; Koole, L. H. New Strategies in the Development of Antimicrobial Coatings: The Example of Increasing Usage of Silver and Silver Nanoparticles. *Polymers (Basel).* **2011**, *3* (1), 340–366. https://doi.org/10.3390/polym3010340.

Chapter IV. New bacteriophobic nanostructured silver-based urinary catheter

ABSTRACT

In this chapter, silicone-based urinary catheters have been modified with the previously described polydopamine-silver coating. The properties of the new urinary catheter have been studied *in vitro*, simulating its use, and in an *in vivo* test using catheterized pigs for 15 days. The bacteriophobic effect of the new urinary catheter has been evaluated, being compared with commercial standards and with the antimicrobial gold standard urinary catheters.

4.1 INTRODUCTION

Once bacteriophobic surfaces have been developed, the next step is to evaluate the bacteriophobic coating on Foley urinary catheters with the aim to avoid catheter-associated urinary tract infections (CAUTIs).

Foley catheters are flexible tubes with two separated channels, or lumens, running down its length. The biggest lumen open at both ends, draining urine into a collection bag and the lumen with the smallest diameter has a valve on the outside end and connects to the balloon. Foley catheters are normally used for long-term catheterization, between 3 to 28 days or more, in seniors or patients with reduced mobility and physical damage, having affected the urinary tract or not, or with mental disabilities[1]. The use of these catheters for periods greater than 3-5 days carries risks. The most common side effects of having an urinary catheter, either occasionally or chronically, are urethral damage and inflammation of the lower urinary tract with the appearance of ulcers and micro-tears in the urothelium of the bladder, which can lead to rapid infection and sepsis[2,3]. Also, discomfort, pelvic and lower back pain are common effects of being catheterized[4,5]. All these effects coupled with the CAUTIs widely described previously, have a negative effect on the patient's life[6–9]. By this reason, currently commercialized urinary catheters for long-term catheterizations seek to offer solutions to the problems presented by this type of catheterization.

There are Foley urinary catheters focused on avoiding CAUTIs to improve the patient's quality of life. Focusing only on those antimicrobial urinary catheters that are currently on the market, Bard Medical® has the largest portfolio of urinary catheter products. Their antimicrobial proposal for Foley urinary catheters is based on silver-palladium-gold alloy coating technology, licensed

from Bactiguard® and called BARDEX®IC (Figure IV. 1 A), being a gold standard product. This coating technology releases silver ions, causing an antimicrobial effect on bacteria and, furthermore, describes a galvanic current phenomenon created by the alloy that prevents bacterial attachment on the catheter surface[17–19]. Other brand products on the market are based on silver salts, embedded in a hydrogel that degrades in contact with the patient. After degradation, silver oxidizes and releases silver ions, with an important bactericidal effect. However, these types of products, called Lubrisil® (Figure IV. 1 B), are not available in Europe. Another interesting antimicrobial catheter is the Strata-ReleaseNF® nitrofural catheter by Rochester Medical® (Figure IV. 1 C). Nitrofural has bactericidal properties and is a common antibiotic ointment. In one randomized clinical study in 2012, nitrofural catheters were shown to be more effective in preventing bacterial growth and biofilm formation on catheters than silver-based catheters in the first days of use[11,20].

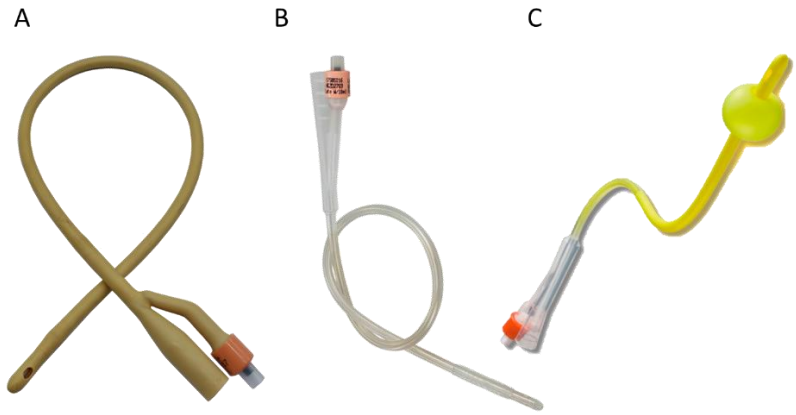

Figure IV. 1. Commercially available antimicrobial urinary catheters. A. BARDEX IC® silver-alloy based urinary catheter by BARD®. B. Lubrisil® urinary catheter, based on silver salts embedded on a hydrogel by BARD®. C. Strata-ReleaseNF®, a nitrofural coated catheter by Rochester Medical®. Images taken from the sales catalogue of the mentioned catheters.

Moreover, a multicentre clinical trial (over 7100 patients) compared two leading antimicrobial urinary catheters (BardexIC® silver alloy catheter and Strata-ReleaseNF® nitrofural catheter) with a standard uncoated urinary catheter for efficacy in preventing CAUTI, but found no clinically important reduction in the rate of symptomatic CAUTI beyond one week[10]. Two products were shown to have a short-term bactericidal effect, preventing infections between 3 and 8 days maximum. So, they proved being useful for short catheterizations, but not the definitive solution that is still being sought up until now.

The reason why these devices are not yet a solution is their strategy to avoid infections. The immobilization of substances to a surface that are released to acquire a function, is a strategy that has been widely accepted to treat diseases in a continuous and controlled way within a period. However, the release of antimicrobials such as silver or antibiotics, have a drawback: once the antimicrobial has been fully released, the surface is unprotected again. The existing reviews of clinical effect of coated urinary devices on the market have pointed out that many clinical studies are too limited in time to provide a solid basis for clear recommendations and indicate that the antibacterial claim can be discussed beyond day 7 of use[10,11,21].

For all these reasons, in this chapter a bacteriophobic coating will be implemented on the urinary Foley catheter, trying to overcome the deficiencies of current commercial catheters. From the set of bacteriophobic nanostructures generated, the coating selected to be applied to the urinary catheters was the PDA-silver coating, which is also an industrially scalable process. However, adapting the manufacturing process and maintaining the PDA-silver coating properties is a current challenge.

As explained above, the generation of the bacteriophobic environment on the device is due to the creation of a certain topography and roughness, building a super-hydrophobic micro- and nanostructure on the surface that avoids bacterial attachment. The process of adapting these micro- and nanostructures based on silver-coated polymeric films must consider the change of base material on which the coating is applied. Medical grade silicones, in addition to having demonstrated their biocompatibility, have subtle differences in mechanical properties regarding PDMS silicones. These properties must be considered and maintained after being modified with the coating. However, the greatest challenge is to adapt the coating to the morphology of the urinary catheter, going from building this micro- and nanostructure on flat surfaces to generating them inside a tube with diameters between 1.98 mm (6 Fr) and 7.92 mm (24 Fr) and between 10 and 40 cm in length homogenously.

Once the coating has been correctly implemented, it will be validated that the urinary catheter maintains the key parameters to be bacteriophobic: a super-hydrophobic micro- and nano-structured surface coated by a homogeneous metallic silver film. For this, *in vitro* bacterial adhesion tests will be carried out at different times, trying to simulate the conditions of use of the catheter and the environment of an urinary infection. Moreover, the bacteriophobic effect avoiding bacterial infection for long periods of time in a complex environment will be tested using catheterized pigs as animal model.

Pages have been removed from this version of the thesis as are protected under industrial property rights

4.3 RESULTS AND DISCUSSION

4.3.1 Implementation of the selected coating on the urinary catheter

After selecting the PDA-metallic silver coating to be implanted in urinary catheters, the manufacturing process was optimized to urinary catheters. The reproducibility and the scalability of the process were ensured, managing to manufacture batches from 50 to 200 pieces without needing to overly adapt the reactions, except by scaling quantities. The obtained coating was homogeneous in all devices, ensuring that the most complex parts of the catheter, the drainage eye and the port, were correctly coated. The final coated catheters are shown in the Figure IV. 7. The image shows the coated parts of the catheter: the entire drainage eye, the catheter tube without the appearance of bubbles, degraded areas or uncoated areas, and the port. In the port there are two areas: a covered area and another area with the bare silicone. The uncoated zone is intentionally, as the urine collection bag is attached to the port in this section and it does not need to be coated. This also allows us to appreciate the difference between the base and the coated catheter.

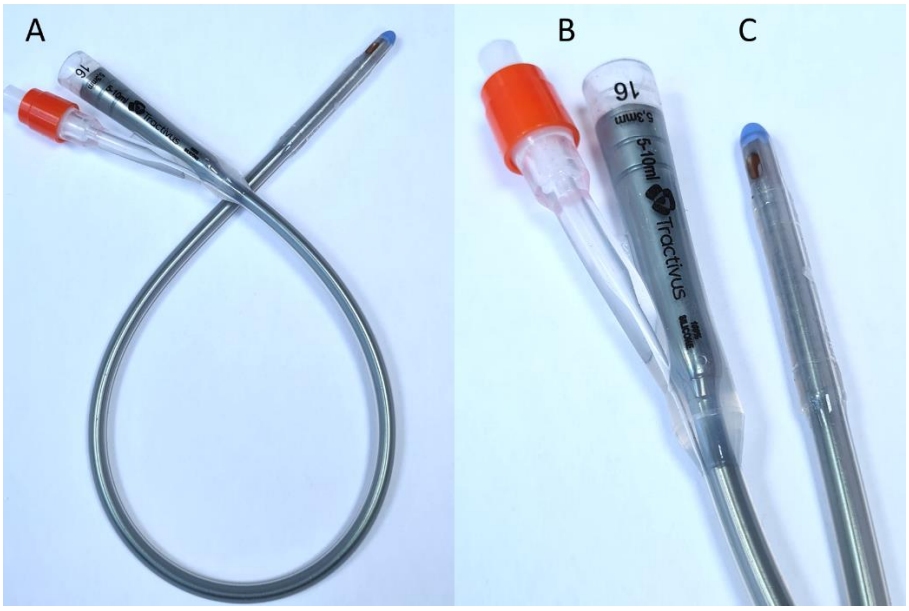

Figure IV. 7. PDA-silver coated Foley urinary catheter. A. Catheter appearance after manufacturing. B. End of drain tube, where collection bag is connected, and balloon valve (red). C. Drainage eye appearance.

Once implemented the coating on the urinary catheter in a homogeneous way with a scalable process, tests were carried out to verify the functionality of the device. The PDA-silver coated urinary catheters were tested according to ASTM F623 "*Standard performance specification for Foley catheters"* to ensure the meeting of the safety and effectiveness requirements despite of the modifications. The tests were made to obtain measures that determine parameters as: the flow rate through drainage lumen, the balloon integrity and the resistance to rupture, the response to traction and the balloon volume maintenance. In all the tests, data were in accordance with the regulation. Thus, the coating was well implemented in the medical device and its modification did not alter its function (data not shown).

To provide the catheter with bacteriophobic capacity, it was necessary to recreate the characteristics studied in the coatings developed in the previous chapter. Tests were performed to characterize the surface of the PDA-silver coated catheter (Figure IV. 8).

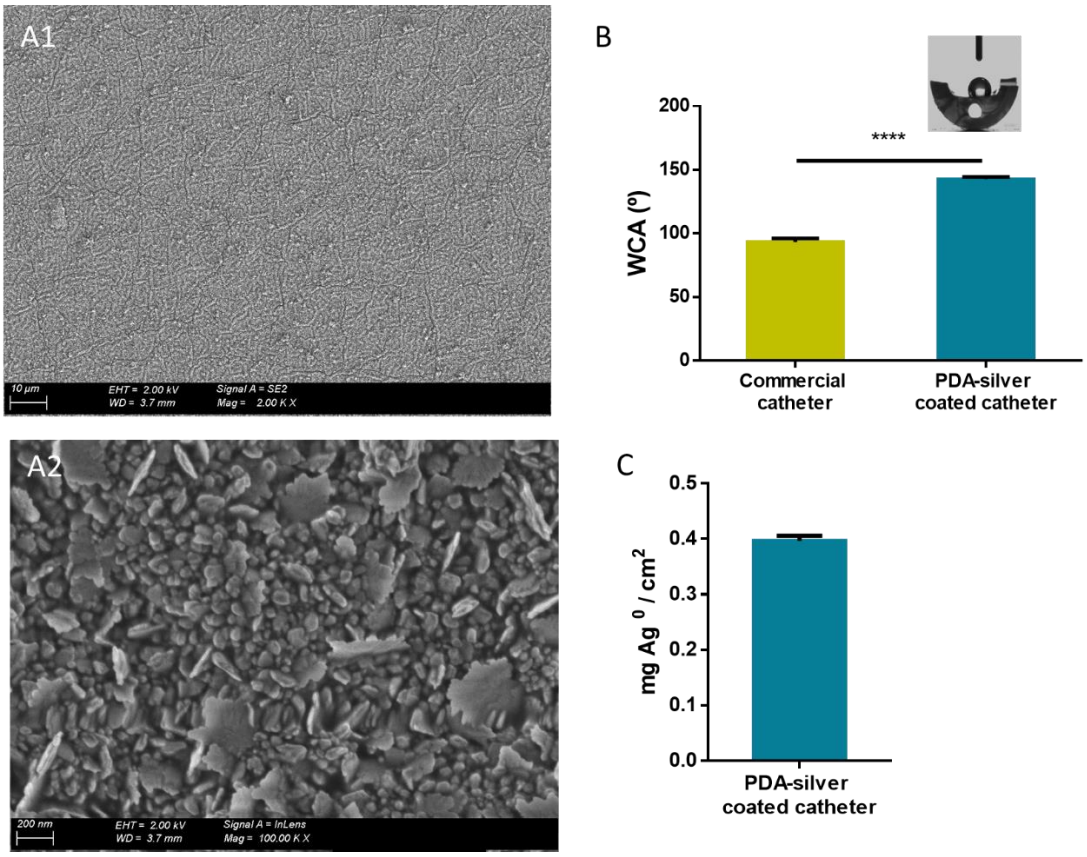

Figure IV. 8. Characterization of the coating applied on the urinary catheter. A. Field-Emission Scanning Electron Microscopy images from the surface after manufacturing at different at different magnification (A1, 2.00 K X, bars 10 µm

and A3, 100. 00 K X, bars 200 nm.). B. Water contact angle measures to determine the degree of hydrophobicity with regard to an uncoated catheter. C. Amount of total silver deposited on the urinary catheter analysed by Inductively Coupled Plasma.

Images from the surface of the catheter were taken by FE-SEM to appreciate the topography (Figure IV. 8 A1 – A2). The surface showed a microstructure with small and thin grooves less than 0.5 µm thick. By magnifying the image, the nanostructure of the surface was observed. Regular size 50-100 nm spheres could be observed with small pieces about 200 nm diameter attached homogeneously and distributed along the surface. These small pieces may be considered silver reservoirs created by nucleation during the reduction of the silver ions and they could be dislodged with the use. However, the surface maintains the topographic characteristics that we study in PDA-silver-based coatings. Also, WCA was measured to verify that the coating gave super-hydrophobic characteristics (Figure IV. 8 C). WCA measurements were made by cutting the curved part of the catheter and taking advantage of the flat area. This area of the lumen is flat because the airway passes through the tube to inflate the balloon. As shown in the figure, the coating produces an angle increase of 90 to 150 º approximately, which is considered super-hydrophobicity. This effect allows repelling protein adhesion and bacterial attachment to the surfaces, decreasing contact between proteins, bacteria and surface and greater shear stress due to interfacial slip between the superhydrophobic surface and the liquid[33,34]. Finally, total silver deposited onto the catheter surface was evaluated to compare values with the previously obtained in flat PDMS surfaces. As can be noted in the Figure IV. 8 C, the amount of silver deposited was 0.396 ± 0.009 mg Ag^0 per cm^2. The deposited silver had a difference of ± 0.0018 regarding the data obtained in flat PDMS-PDA-silver coated, being not statistically significant.

Thus, the coating was reproducible enough to be implemented in urinary catheters, maintaining all the properties previously studied in flat silicones: super-hydrophobicity, amount of deposited silver and a micro and nanostructured surface, guaranteeing the bacteriophobic properties of the device.

4.3.2 Silver release in comparison with current medical devices

Due to the strict European regulation of medical devices, it is important to consider if the amount of silver released by the urinary catheter is significant, not only for its active effect on cells, but also for the future classification of the device within regulatory standards. This study compared the release of silver from a urinary catheter with one of the only silver devices on the European market: the tracheostomy cannula. Silver cannulas have been widely used after a tracheostomy

to prevent the patient from closing the open pathway in the trachea for long periods. It was decided to compare the proposed coating of the urinary catheter with a silver cannula because commercial silver urinary catheters based their bactericidal activity on the release of silver in salt or ions form to the medium.

Measurements of silver present in the medium in contact with the devices were taken daily for 21 days (Figure IV. 9). Samples were obtained from the medium and analysed by ICP. No elevated initial burst release was shown. The amount of silver released by local oxidation at 15 days was about 0.01 µg / mm^2 (accumulated silver in the medium), which data were according to silver release tested in previous chapters from flat surfaces.

The silver release profile of the cannula was studied for 15 days in PBS medium, at 37 ºC under static conditions (Figure IV. 9). As can be seen in the figure, the amount of silver accumulated in the medium by the cannula was 7 times higher than the released by the catheter at the end of the study. The cannula showed a continuous silver release with an initial high burst of silver (at 30 min after contact with the medium reached 0.03 µg/mm^2). The urinary catheter showed a similar behaviour, an initial burst of silver perhaps due to the liberation of the chemo-adsorbed silver or the release of previously observed clumps of silver.

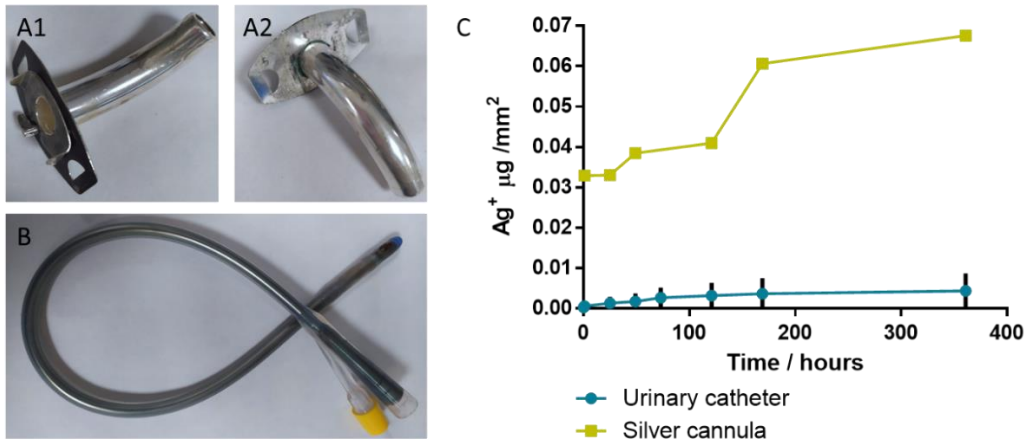

Figure IV. 9. Silver release of different medical devices. A. Silver cannula. B. PDA-silver coated urinary catheter. C. Silver release from a silver cannula and PDA-silver coated urinary catheters during 361 h (15 days) in phosphate buffer saline at 37 ºC. The study was carried out in continuous flow (1.38 mL/min) with the urinary catheter but not with the silver cannula. Silver cannula was tested in static conditions. The amount of silver accumulated in the medium was normalized by area for a better comparison between the devices.

The fact that the silver cannula, an implantable product approved for medical use, releases up to 7 times more silver than the urinary catheter serves as a benchmark for establishing acceptable free silver values. All these data are below the limit considered cytotoxic for humans, however, the fact that there is already a product on the market with values beyond those released by the catheter is a regulatory advantage.

4.3.3 Antimicrobial properties of new urinary catheter in vitro

To ensure the bacteriophobic effect of the new urinary device, an *in vitro* evaluation of the antimicrobial capacity was done. To test the non-bactericidal properties, different fragments of the catheter were incubated with bacterial culture medium with different bacterial strains. The bacteria chosen ranged from laboratory-use strains to clinical isolates and probiotics, to ensure the non-strain dependent effect of coating in bacteria. The bacteria were grown until they reached their maximum absorbance in appropriate culture media, atmospheric and temperature conditions according to each strain (Figure IV. 10 A). As expected, this test confirmed that the coating did not present antimicrobial activity. Each strain could reach its stationary phase despite of growing in contact with the coated urinary catheter embedded in the medium. The probiotic strains used in this study, mainly a *Lactobacillus* cocktail, also did not show a delay in their growth curves (data not shown) and reached their maximum at the same time as the bacteria in the absence of the coated urinary catheter. So, the coating did not affect to the natural urinary microbiota.

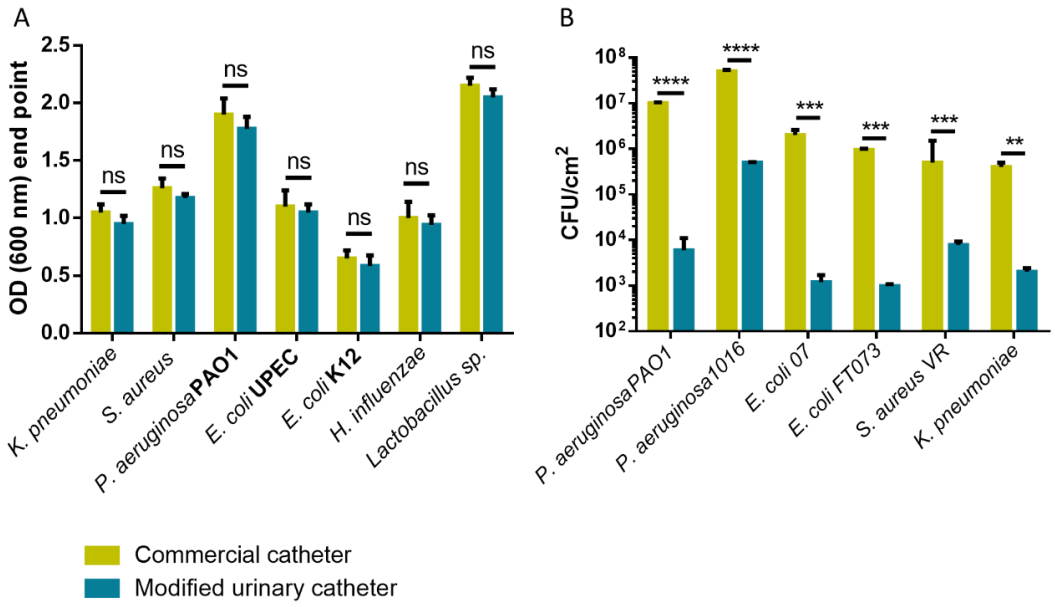

Figure IV. 10. Antimicrobial properties of PDA-silver coated urinary catheter. A. Absorbance at end point of bacterial growth in contact with commercial urinary catheters and modified catheters with PDA-silver coating in appropriate media and conditions for each bacterial strain. B. Bacterial adhesion counts on commercial urinary catheter and PDA-silver coated urinary catheter with PDA-silver coating after 18 h in contact. NS = not statistically significant. P-value was represented as: p-value < 0.01 (**), p-value < 0.001 (***) and p-value < 0.0001 (****).

To test the bacteriophobic effect of the catheter, being able to reduce bacterial adhesion, different bacterial strains were put in contact with the coated lumen of the catheter 18 h at least in complete media and 37 ºC. *Escherichia coli* CFT073 and 07 and *P. aeruginosa* PAO1 and 1016 were studied with special attention due to they are the most isolated urinary pathogens in patients with urinary infection (Figure IV. 10 B).

As can be noted in Figure IV. 10 B, all tested strains reduced their presence on PDA-silver coated catheter surfaces between 2 to 3 orders of magnitude regarding commercial urinary catheters. This result indicates a bacterial adhesion reduction between 99 to 99.9 %. The strain type, gram-positive or gram-negative, did not influence the decrease on bacterial adhesion. Moreover, despite of the different adhesion factors present in each strain, as the high expression of fimbria, the bacteriophobic effect was not lost.

To test the efficacy avoiding bacterial adhesion for long time, *E. coli* CFT073, a common uropathogen, was selected to be in contact with commercial and coated urinary catheters during

30 days (Figure IV. 11 A). During incubation time (overnight), bacteria could interact with the inner surface of the urinary catheter, adhere and multiply, beginning the first phases of the formation of a biofilm. Also, since the test was carried out under static conditions, the absence of flow helped the contact of bacteria on the catheter surface and could favour their irreversible adhesion. So, it was considered that this experiment used the most challenging conditions to submit the catheters. After first incubation, the catheters were emptied and filled only with fresh medium, without bacteria every day. This procedure aimed to observe how the anchored bacteria to the catheter surface proliferated, remained or were released, eliminating planktonic bacteria from the medium.

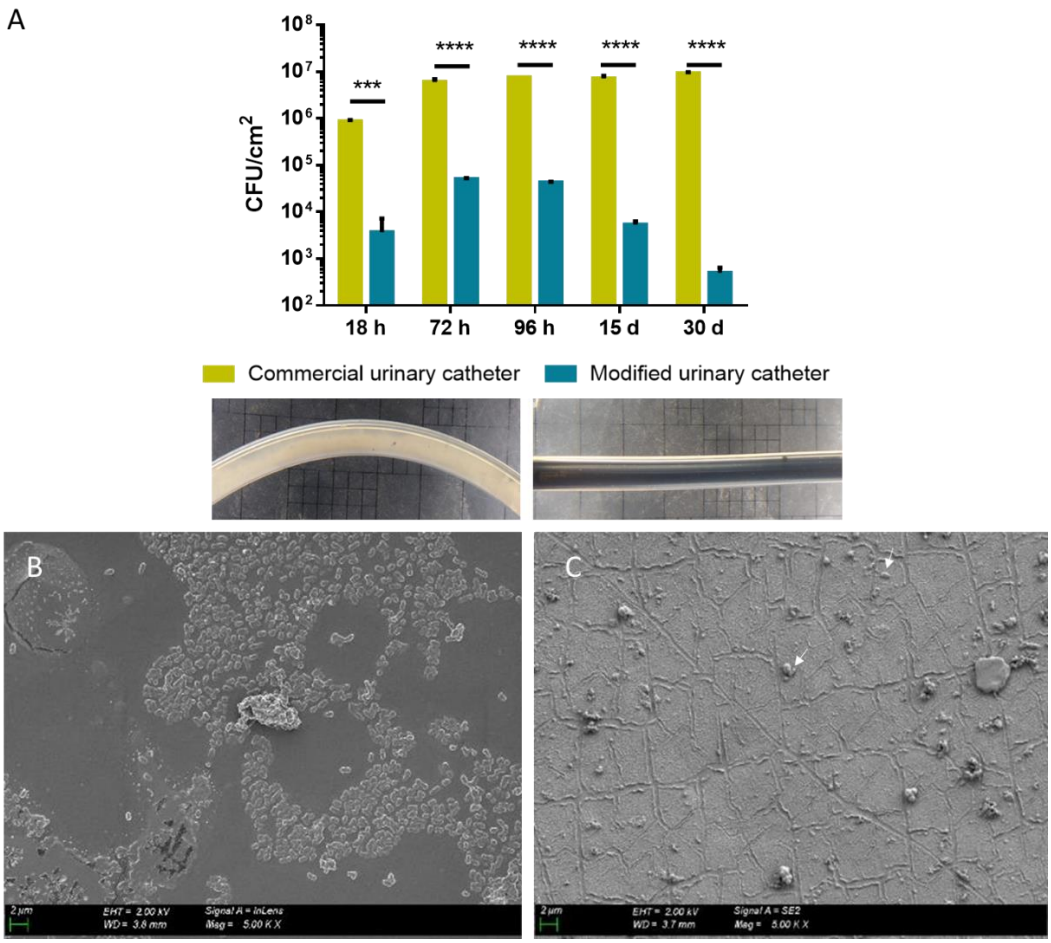

Figure IV. 11. Long-lasting bacteriophobic effect of PDA-silver coated urinary catheter. A. Bacterial adhesion quantification at 18 h, 3, 4, 15 and 30 days of attached bacteria on commercial urinary catheters (yellow) and PDA-silver coated urinary catheters (blue). Photographs correspond to 72 h of bacterial incubation on urinary catheters, control (left) and PDA-silver coated (right). Statistical analysis shown p-value < 0.001 at least. Field-emission scanning electron

microscopy images of commercial urinary catheters (B) and PDA-silver coated urinary catheters (C) after 96 h of bacterial culture. White arrows mark bacteria in picture C to better bacterial localization. Magnification of 5 K X with 2 µm bars.

As can be seen in the Figure IV. 11 A, after 18 h of incubation the control catheter showed 1E6 CFU / cm^2 adhered to the surface, while the PDA-silver coated catheter did not reach 1E4 CFU / cm^2. At day 3, bacterial counts showed an increase in the adhered bacteria to the internal surface of the control catheter, reaching 1E7 CFU / cm^2. Also, an increase in adhered bacteria to the PDA-silver coated catheter of almost one order of magnitude regarding the first time was observed. However, the population did not reach the levels of colonization detected in the control catheters. After 4 days of study, the number of adhered bacteria to the control catheter remains stable, reaching saturation. Also, the adhered bacteria to the PDA-silver coated catheter remains stable, without increasing despite having a free niche and availability of nutrients. Therefore, bacteria have reached a population equilibrium, where bacteria are not capable of dividing on the surface. In addition to being unable to duplicate, bacteria may not be able to adhere completely to the surface, so, they are released into the environment where they can divide until saturation levels. These bacteria try to colonize new points on the surface but without being able to establish mature populations. At day 15, attached bacteria population on PDA-silver coated urinary catheters decreased to 1E3 CFU / cm^2. Finally, the lowest adhesion values were observed at 30 days of incubation (1E02 CFU/cm^2). Control catheters kept adhering bacteria levels intact (1E07 CFU/cm^2). This difference could be due to the fact that the adhered bacteria were not permanently anchored or had formed resistance structures, but were instead anchored in a punctual or semi-permanent way, so, with the change of medium daily, bacteria were gradually eliminated and the living population was not able to proliferate on the surface of PDA-silver coated catheters. It is important to remember that the coating did not affect the growth of planktonic bacteria, therefore, the reduction in the bacterial population adhered to the catheter is exclusively related to the action of the coating against bacterial adhesion.

To show how bacteria were arranged on the catheter surface, samples were collected from the 96 h incubated catheters and observed with FE-SEM (Figure IV. 11 B - C). Bacteria anchored to commercial catheters showed a 3D structures, microcolonies that could give rise to a biofilm. By contrast, the surface corresponding to the PDA-silver coated urinary catheter was clean, with some loner bacteria adhered punctually, marked with white arrows in the Figure IV. 11 C. Furthermore, no deposition of salts or crystal constructions were observed on the surface, despite being in contact with saline media and biological debris. Thus, the coating was able to keep the surface clean for 30 days, without bacterial or biomass deposition on it.

4.3.4 Impact of use on catheter coating

After characterizing the PDA-silver coated urinary catheter ensuring that the bacteriophobic properties remained unchanged, it was decided to study the behaviour of the urinary device in a simulated-use environment. The objective of the study was to know the evolution and stability of the coating subjected to a continuous flow. To do this, an *in vitro* model of urinary tract was created to simulate the use of a complete urinary catheter working. Parameters such as urine flux through the urinary catheter, media and temperature were taken into consideration to mimicking the real conditions and wear of the device. An important point was that a full urinary catheter was used, unlike catheter fragment studies to date[25,35], so, it was possible to study the drainage port and drainage eyes behaviour, in addition to the catheter tube (Figure IV. 3). Therefore, a PDA-silver coated urinary catheter was connected to the system previously mentioned during 21 days at 37 ºC using artificial urine as medium. During the test, the coating was observed each day and no appreciable changes were seen, at naked eye. The coating appeared homogeneous, with no visible gradients or cracks. At the end of the test, a piece of the catheter was cut and observed by FE-SEM to analyse the surface state (Figure IV. 12). As can be noted in the Figure IV. 12, comparing the coating after manufacture process and after 21 days of use, no remarkable changes were found. The surface was clear after use, which suggest that the incrustations, the bigger ones observed at 5.00 K X, can be detached. Also, crystals were found with a size from 25 to 225 nm^2. The crystallization of the salts present on the medium on the surface may be due to drying of the samples before using FE-SEM, without relation with the urinary catheter working process. Therefore, within a controlled environment with no pH variations, controlled temperature and with a salt medium and constant flow, the coating lasted 21 days without presenting visual problems.

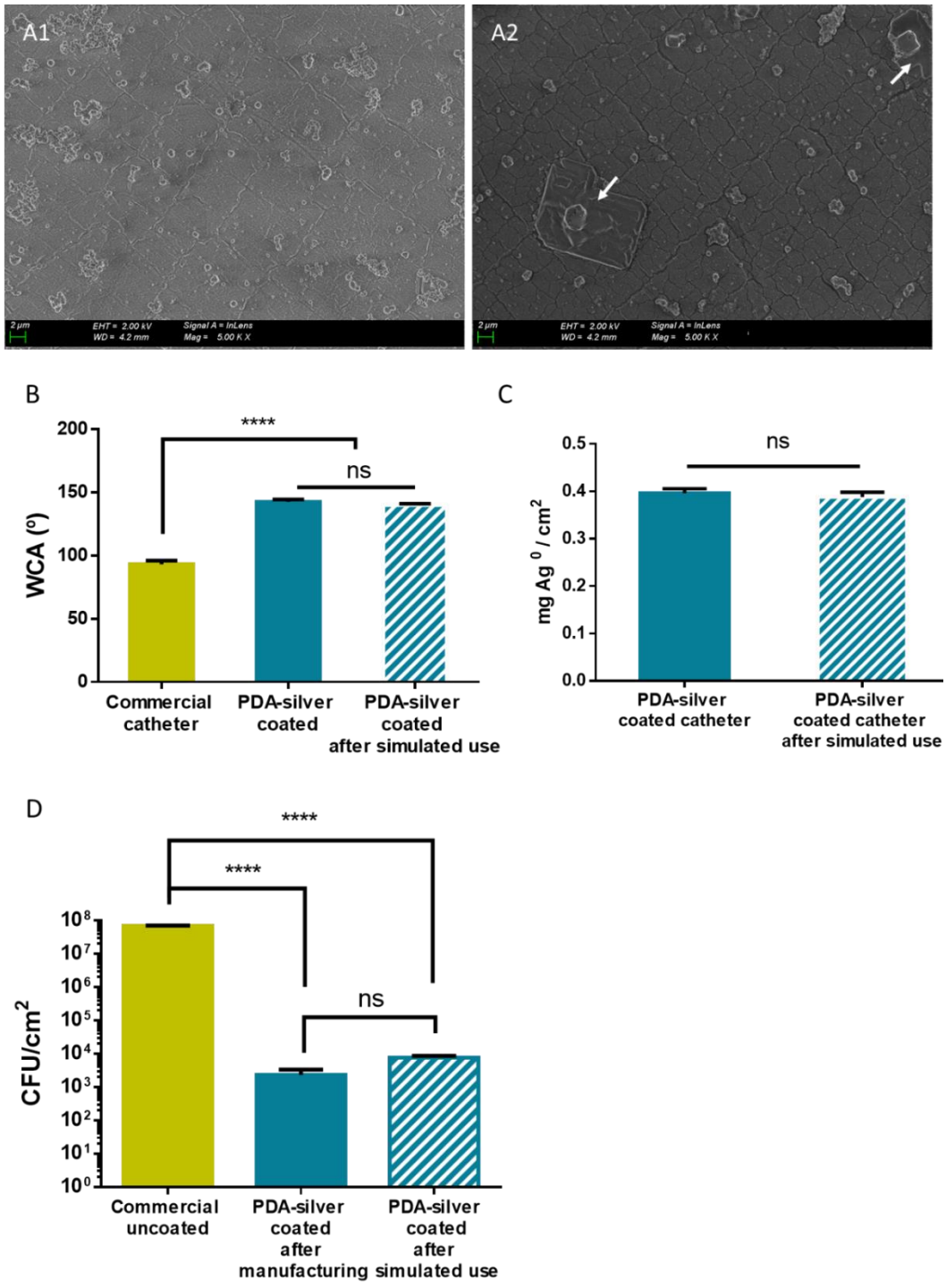

Figure IV. 12. PDA-silver urinary catheter characterization after 21 days of simulated use. A. Field-Emission Scanning Electron Microscopy of catheter surface. Catheter coating after manufacture process. (A1). Catheter coating after 21 days of simulate use (A2). White arrows mark the crystals deposited on the surface, generated by the medium used to the test,

based on salts. 5 K X Magnification and 2 µm bars. B. Water contact angle of commercial urinary catheters, after manufacturing and after simulated use. C. Total silver amount deposited on the catheter surface after manufacturing and the simulated use for 21 days analysed by ICP and normalised by internal area. D. Bacterial counts of *E. coli* CFT073 after being in contact with the urinary catheter after manufacturing and after simulating its use for 21 days.

To ensure the bacteriophobic behaviour of the new urinary catheter, one of the most interesting characteristics is its super-hydrophobicity. It is necessary to test if after simulating its use, the coating continues to show the same hydrophobicity values. Therefore, contact angle measurements were made after the simulated use test (Figure IV. 12 B). The results showed that, after simulated use, the surface loss a few degrees on average but not significant, maintaining the grade of hydrophobicity. Also, to ensure the coating remains intact after simulating catheter use, the total amount of silver deposited on catheter surface after manufacturing and the simulated use was quantified by ICP (Figure IV. 12 C). In this case, as expected, the amount of silver deposited on the catheter surface normalized by area, corresponds to the amount previously studied in previous chapters, 0.4 mg / cm^2. Therefore, the coating technology does not depend on the way it is applied, since the same surface structure and amount of silver per cm^2 was observed in PDMS flat silicones and urinary catheters. Furthermore, after simulating the use of the urinary catheter for 21 days, the amount of silver that remained on the surface did not represent significant or statistically differences enough. Moreover, to ensure the bacteriophobic capacity of the coating after a continuous use, *E. coli* CFT07 was put in contact with the urinary catheters after being manufactured and after 21 days of simulated use ((Figure IV. 12 D). Bacterial counts showed non-significant differences between catheters, maintaining a difference of 4 orders of magnitude regarding to the standard uncoated catheter. So, it could be concluded that the coating of the urinary catheter was stable and did not lose any of its properties with the continuous use.

The last experiment that was performed to characterize the urinary catheter using the use-simulation system was to measure the amount of free dopamine in the medium after 9 days. Free dopamine was measured using High Performance Liquid Chromatography (HPLC) using a method previously described in literature[23]. No dopamine residue was found, so the device was taken for granted. This fact was important as dopamine, as a monomer, is a neurotransmitter and a precursor of other substances including adrenaline. So, it was interesting to test that there were no unpolymerized dopamine residues in the device that could be released when using it.

Finally, it can be assumed that after exposing the catheter to a complex environment simulating the use of a urinary device, the coating is stable and maintains the properties that give it its bacteriophobic character.

4.3.5 Commercial antibacterial catheter compared to the new bacteriophobic catheter

Because the objective was to bring the PDA-silver coated catheter to a complex environment in vivo in order to validate its bacteriophobic capacity, it was decided to use the gold standard antimicrobial catheters as control catheters. One of the most widely used catheters with bacteriophobic properties based on the release of silver ions and the generation of a galvanic current is the BARD® latex catheters (BARD-IC®). To be able to compare the bacteriophobic effect of these commercial catheters with the catheter developed in this thesis, a small physical characterization was made between them to understand the catheters functioning.

Hydrophobicity of the coatings is a key parameter to discuss since, as previously shown, lower hydrophobic properties can favour bacterial adhesion to plastic surfaces[34,36,37]. On this occasion, the WCA on the inside and outside of the commercial antimicrobial catheter was measured to be compared with the commercial catheter silicone-based and the PDA-silver coated bacteriophobic catheter (Figure IV. 13 A). Low-hydrophobic behaviour could be observed by WCA in commercial antimicrobial catheters, being similar to the commercial silicone-based catheters. The antimicrobial silver embedded in the hydrogel that coats the internal and the external catheter surface did not show the expected hydrophilic behaviour, neither an increase of hydrophobic behaviour. Due to this result, it is assumed that the antimicrobial effect given by this device is exclusively due to the release of silver from its surface, and not by a physical effect of repulsion of the bacterial adhesion due to the creation of a super-hydrophilic or super-hydrophobic micro or nano-structured surface.

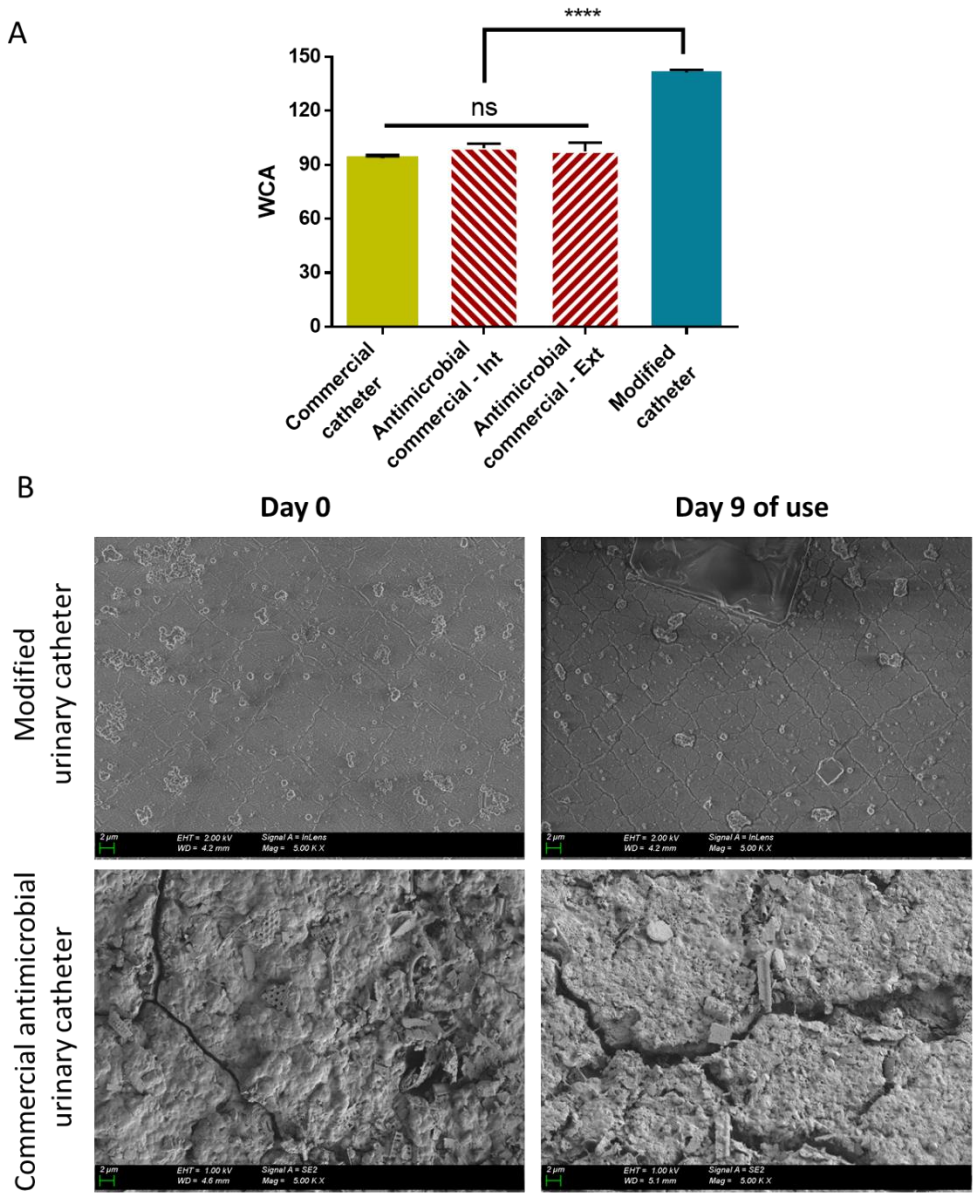

Figure IV. 13. Commercial antimicrobial urinary catheter characterization and comparison with PDA-silver coated urinary catheter proposed by this work. A. Water contact angle of commercial urinary catheter, antimicrobial catheter (internal and external face) and PDA-silver coated catheter. B. Field-emission scanning electron microscopy images taken after PDA-silver coated catheter manufacturing and after antimicrobial commercial catheter purchase (day 0). Images from the surface after 9 days of simulated use with artificial urine are shown in second column (day 9). Magnification 5 K X and bars = 2 µm.

In addition, the internal surface of the catheter was studied after 9 days of simulated use by FE-SEM (Figure IV. 13 C). As can be noted, the commercial antimicrobial urinary catheter surface was irregular and presented fragments of unidentified elements on its surface just after unpacked. Moreover, the surface presented cracks on its surface that could possibly be due to the collapse of the hydrogel after being subjected to the FE-SEM vacuum. However, these irregularities and cracks became more evident and deeper after simulating the catheter use with artificial urine at 37 ºC for 9 days, so the surface seemed to erode while catheter using, regardless of the effect that the vacuum of FE-SEM could have on it. The fact that these catheters had an irregular and degradable surface can favour bacterial adhesion and catheter occlusion, making it an interesting point to study.

It is possible that the antimicrobial effect of the commercial antimicrobial catheters was the result of the carry-over of attached bacteria with remains of the catheter walls because the surface erodes with during the use of the device. Since the patient's urine causes a carry-over effect, the catheter debris would not cause any harm to the host. So, this model together with the silver release, that is advocated in the product description, could grant the antimicrobial characteristics that make the catheter an antibacterial product.

To verify this, it was decided to perform a count of *E. coli* CFT073 adhered to the internal surface of the catheter, omitting the flow, for 96 h. The results can be seen in the Figure IV. 14.

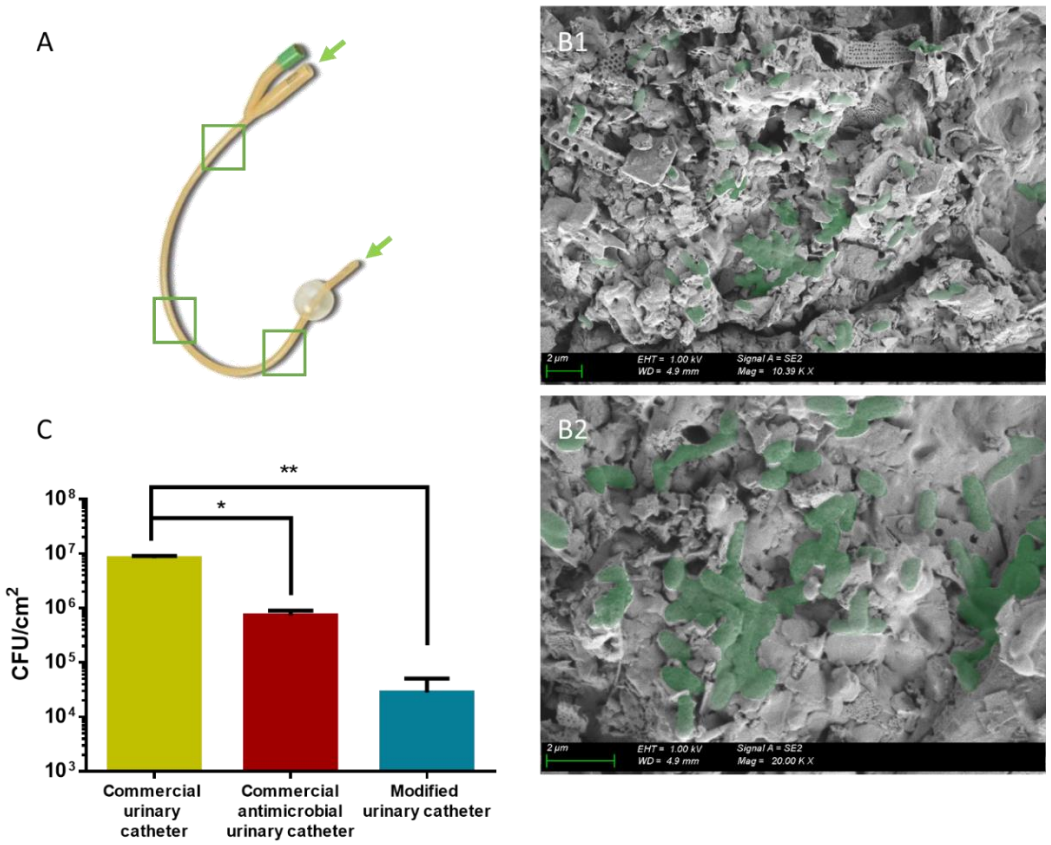

Figure IV. 14. Antimicrobial effect of antimicrobial commercial urinary catheter. A. Commercial antimicrobial urinary catheter scheme: the test was performed by filling the inside of the tube with culture medium and bacteria, keeping it under static conditions for 96 h at 37 ºC. Three fragments of each tested tube (3 per catheter type) was cut (green squares) and biofilm or bacteria was extracted and counted. B1 and B2. Field emission-scanning electron microscopy images from the commercial antimicrobial urinary catheter internal surface after 96 h of bacterial inoculum. Bacteria were painted artificially in green to improve their visualization. C. Colony forming units quantification per cm2, the statistical analysis indicated that there were significant differences between the catheters and the commercial control, represented as * (p-value < 0.05) and ** (p-value < 0.001).

As can be seen in the Figure IV. 14 C, the bacterial counts obtained in the commercial control were expected, according to those previously studied. In the case of the commercial antibacterial catheter, there was a decrease of approximately an order of magnitude with respect to the commercial antimicrobial catheter, which represents a considerable improvement in the ability to repel bacteria and the consequent infections. However, the bacterial adhesion observed on the surface of the catheter proposed in this thesis was considerably and significantly lower regarding the commercial antimicrobial. The PDA-silver coated catheter presented in this chapter

represents an improvement in bacteriophobic capacity of almost two orders of magnitude over the commercial antimicrobial catheter and near to three orders over the standard control, being a promising data.

To visualize how bacteria were deposited on the surface of the commercial antimicrobial catheter, catheter fragments were visualized by FE-SEM (Figure IV. 14 B1 and B2). The images that can be seen in the figure showed bacteria with a normal morphology on the surface, some of them in division process, so, metabolically active. Bacteria embedded in the catheter matrix could be observed, but it being unknown if this matrix was an early biofilm or a product of the catheter structure and the delamination phenomenon.

The study made it possible to compare the catheters under the same *in vitro* conditions, observing that the catheter PDA-silver coated with nanostructured PDA-silver offered advantages compared to commercial antimicrobial catheters currently available in the market.

4.3.6 New bacteriostatic urinary catheter *in vivo* test

Once the urinary catheter had been characterized and the bacterial adhesion to the catheter surface had been monitored under the worst possible conditions, an in vivo test was carry out to determine in a real setting if the proposed urinary catheter presents bacteriophobic activity and this effect is reflected in CAUTI-derived infections and animal welfare.

Throughout the study, unscheduled events occurred. Most relevant events can be observed in the event log (Figure IV. 15 A). During the night of day 3, a pig catheterized with a commercial antimicrobial catheter died spontaneously (black triangle). After performing the autopsy, an ulcer was discovered in the bladder (Figure IV. 15 B). The ulcer was caused by the catheter, showed the catheter passing through it. The loss of urine by this ulceration of the bladder invaded the abdomen, causing an acute infection and the death. Furthermore, the animals catheterized with the commercial antimicrobial catheters had problems urinating during the entire study. It was observed that the catheters from day 3 were occluded. Catheters were washed with sterile PBS when necessary (blue circle) to recover their function. It was observed that before the obturation of the catheters, the animals were apathetic, without hunger, and with abdominal pain (green triangle). Pain subsided once the catheters were washed, so the animals continued to participate in the study. Despite the washes, visible amounts of fibrinogen present in the bladder were shown after autopsies (Figure IV. 15 B).

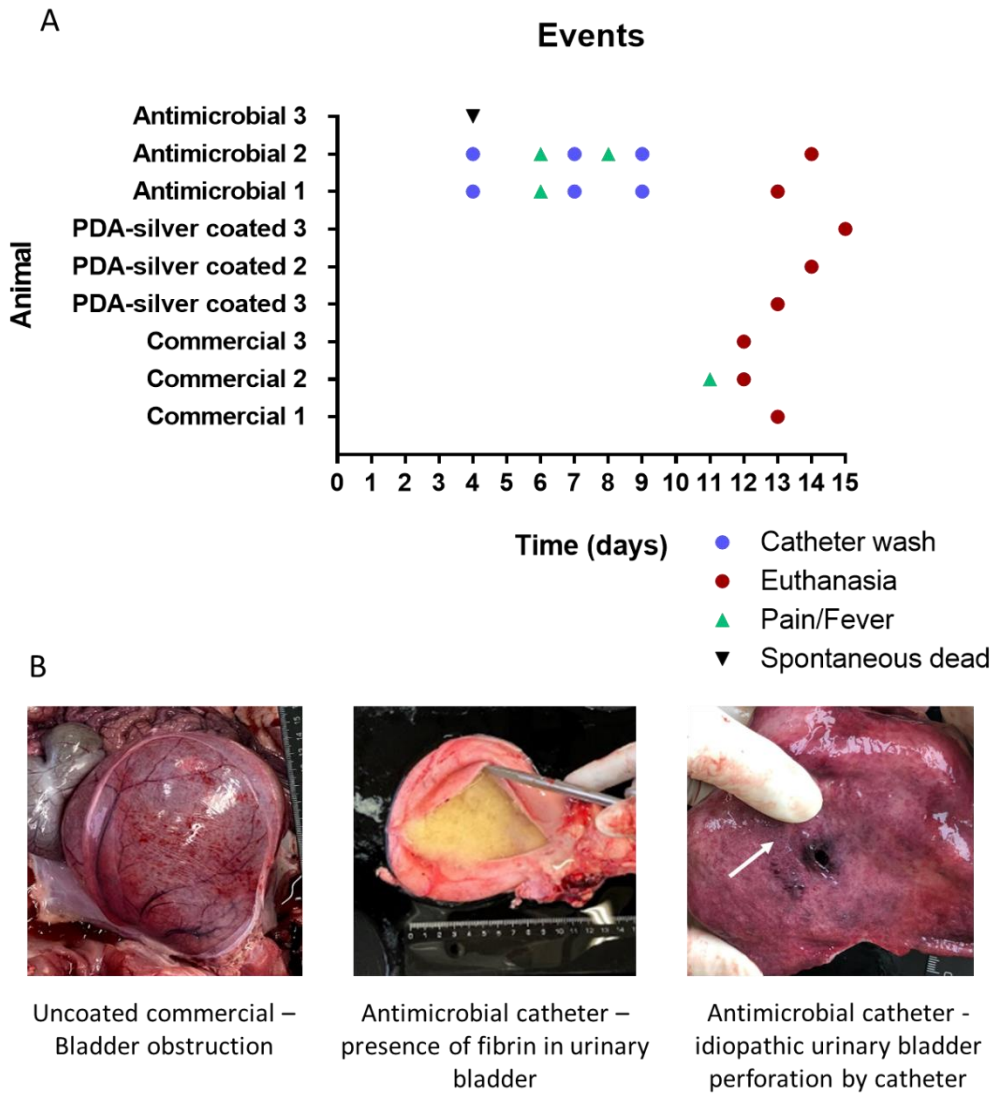

Figure IV. 15. Events occurred during the study in each of the catheterized animals. A. Events graph. Euthanasia events were scheduled in escalation, except in the case of having to advance the euthanasia day due to the condition of the animal. Catheter washes were performed with PBS or physiological saline solution. B. Images of some organs of pigs that had to be euthanized or were found spontaneously dead, probably explaining the cause of the deaths.

In the case of commercial uncoated catheters, by the end of the study several animals showed signs of fever and acute infection, apathy, and pain. It was decided to advance the date of euthanasia due to the suffering of the animals (Figure IV. 15 A, displaced red circles). Once the autopsy was carried out, the bladder was discovered about to collapse (Figure IV. 15 B), which could be the cause of its pain. Also, in pigs catheterized with antimicrobial commercial urinary

catheters, the advance of the euthanasia dates was due to the worsening of the health status of the animals or the obturation of the catheters and their loss of function.

On day 12, one of the animals catheterized with standard commercial urinary catheter suffered a rectal prolapse so the euthanasia of this animal was performed. It is assumed that the complete plugging of the catheter happened in the late afternoon on the day 12 and urine was accumulated in the bladder during the night. Failing to drain the urine properly, the pig's bladder was completely filled, and the animal had the urination reflex. By not urinating, the animal underwent overpressure and an anal prolapse occurred. On day 13 the prolapse was observed and euthanasia was carried out.

By contrast, the PDA-silver coated silicone catheters were able to pass the entire test without reporting pain, fever, or apathy by the pigs. The animals could also urinate correctly, without effort. The catheters were not blocked throughout the study and no washing was necessary. Euthanasia was performed to pigs within the set dates, only for the reason of completing the study. Because of this, the catheterization study was carried out between 12 and 15 days, depending on the healthy status of the animals. Moreover, after autopsy, no ulcers or bladder damage were observed. Fibrinogen or other substances were also not found. This result indicates that the PDA-silver coated catheters did not damage the tissue.

4.3.6.1 Silver biodistribution analysis and histopathology analysis

Once the events were analysed, the state of the animals after the study was checked to test the biocompatibility of the new urinary catheter. Several tests were carried out based on the detection of silver in urine and organs by ICP, to check the biodistribution of the metal and its possible side effects on the animals. Silver was searched in the following organs: brain, lungs, liver, kidneys, bladder and urethra. Furthermore, any damaged, necrotized or coloured area was analysed. The extracts were analysed by ICP and no silver positive samples were found within the range 1 ppb - 10 ppm / gram of organ (graph not shown). It was interesting not to find silver in the bladder of the pigs that were catheterized with the antimicrobial and PDA-silver coated catheters due to bladder was the organ most susceptible to presenting silver accumulation in the urothelium.

In addition to organs, silver was analysed in blood samples obtained every other day. Traces of silver were found in none of the blood samples. Also, the urine from animals catheterized with the PDA-silver coated catheter was analysed in order to find silver. As a control, urine from

animals catheterized with the commercial uncoated catheters was used. The results are shown in Figure IV. 16. As can be noted, the collected urine at day 0 (after the first urine), 2 and 5 showed detectable silver levels. The detected silver had similar results to silver release assays studied with the continuous *in vitro* systems. This release was expected since it corresponds to a primary wash of the surface. These burst-release events prevented bacterial adhesion in the first days of catheterization of the animals. However, these silver levels were under the silver cytotoxic levels (50 mg/day)[38] and under systemic silver levels in humans (2 ppm)[38–40]. So, despite finding traces of silver in urine, the levels of silver released do not pose a danger to the future patient.

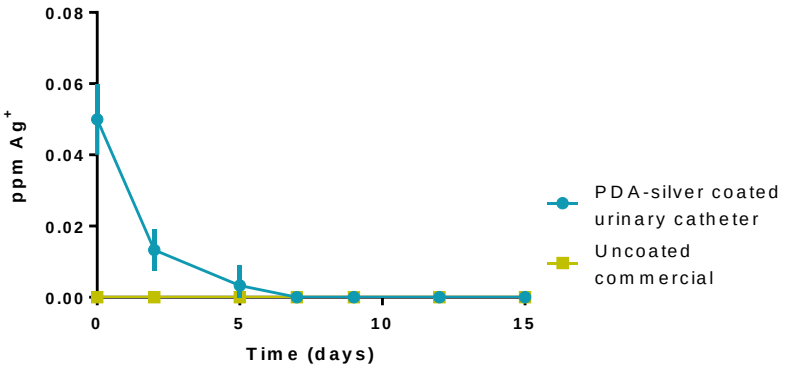

Figure IV. 16. Silver quantification in urine samples from PDA-silver coated and uncoated urinary catheters. The samples were treated with nitric acid between 2 and 4 h after collection and stored at 4 ºC. A silver standard between 1 ppb and 10 ppm was used for ICP.

Finally, tissue damage and inflammatory response caused by the implantation of catheters were studied through histopathology study. Deep inflammation, micro tears, ulcers, or presence of macrophages or other cells of the immune system were looked for indicating inflammation, tissue damage, or bacterial infection. All the images obtained can be consulted in the Annex IV section, but the most interesting images have been shown in Figure IV. 17.

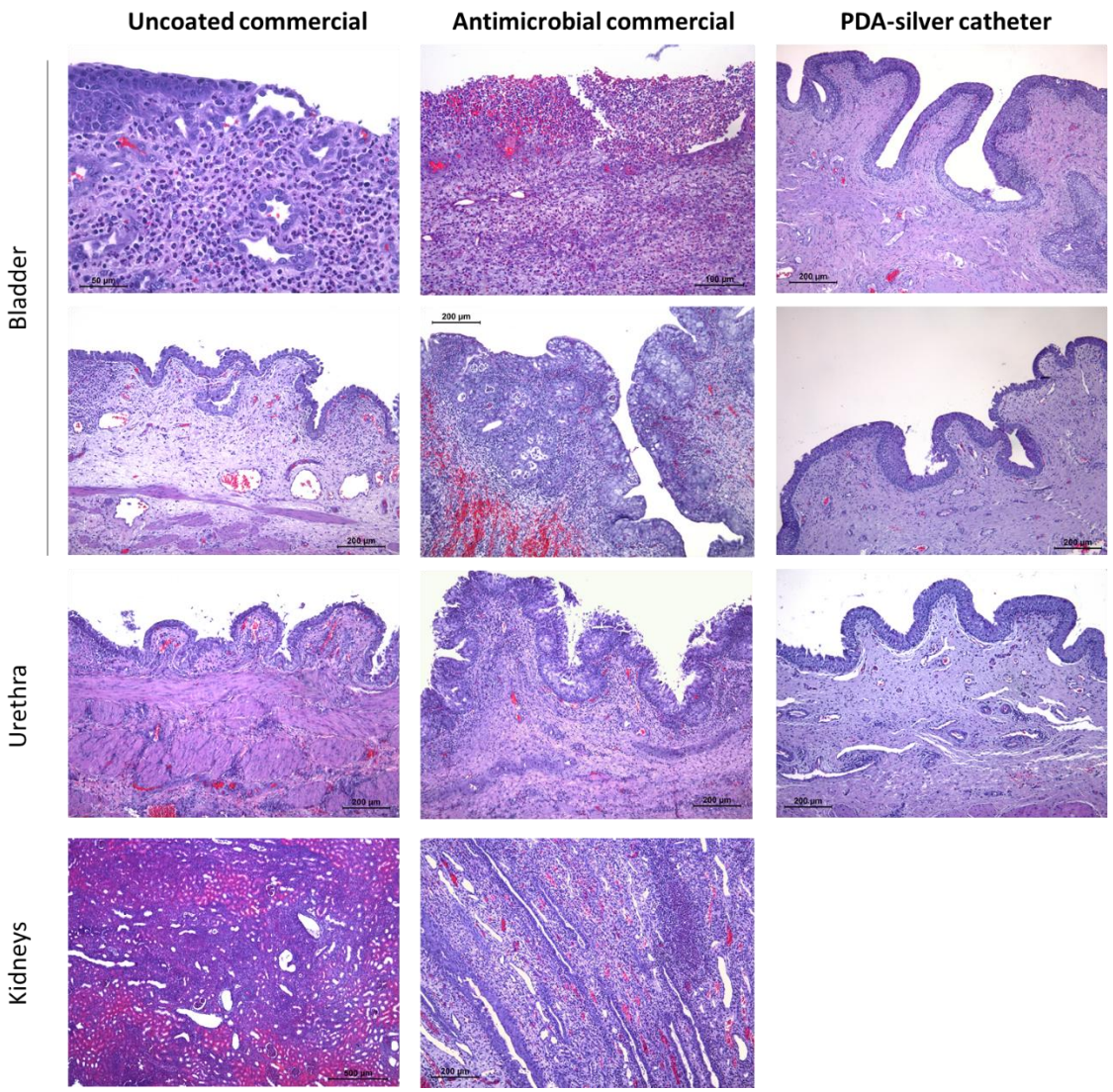

Figure IV. 17. Tissues from organs of catheterized pigs stained for histopathology study. Bladder vertex and trine and urethra were studied in all animals. Kidneys were analysed in animals with important tissue damage or necrosis. Bars: 200 µm. Test was carried out by the histopathology service of the Universitat Autónoma de Barcelona.

As can be noted in the histopathology analysis, the tissues in contact with commercial urinary catheters were seriously affected. Bladder presented purulent inflammation with epithelial exocytosis. Multifocal ulcers and intense vascular activation were observed, symptom of a strong bacterial infection present in the tissue. Urethra of uncoated commercial catheters showed also inflammation and accumulation of macrophages, reaching the conclusion that the bacterial infection was also lodged in the urethra. Kidneys showed multifocal inflammation and severe

tissue damage. One of the animals presented necrotized tissue that indicated severe kidney infection.

Conversely, the animals catheterized with the antimicrobial catheter showed similar damage to the bladder. Neutrophils were found in mucosa of bladder with an intense diffuse purulent-necrotizing inflammation that affected deep muscle layers and serous organs. Urethra presented an intense perivascular inflammation, which indicated the presence of bacterial population. By last, kidneys showed severe purulent character and severe inflammation with necrotized zones, warning of early kidney failure.

By contrast, pigs catheterized with the nanostructured silver-coated urinary catheter showed low inflammation affecting the mucosa with moderate exocytosis in bladder tissues. With respect to urethra, no apparent lesions were found as well as the rest of examined tissues. Images from kidneys were not provided.

4.3.6.2 Determination of bacteria present in urine

In order to monitor the urine tract infection evolution, throughout the study, urine was collected every 2 days through the catheter and urine culture was performed in complete media (blood agar (BA) and chocolate agar (CA)) and TSA. In addition, the urine was cultured in MacConkey medium (MA), selective for gastro-intestinal gram-negative bacteria, in order to identify species such as *E. coli*. Plates were incubated between 24 and 48 h to ensure the correct bacterial colonies growth at 35-37 ºC under normal atmosphere and in an incubator at 5 % CO_2. The results were graphed in the Figure IV. 18. Bacterial counts were averaged for each tested catheter group in different media (Figure IV. 18 A and B). To study each case individually and showing the evolution of the infection in urine, each animal was plotted individually (Figure IV. 18 C 1-3). An important point to highlight is that the urinary catheters remained open throughout the study, since the pigs did not allow the urine collection bag to be connected to the catheter. Therefore, the catheters were an open pathway to the bladder, so the animals were not inoculated with any pathogenic organisms and it was assumed that a natural infection would occur.

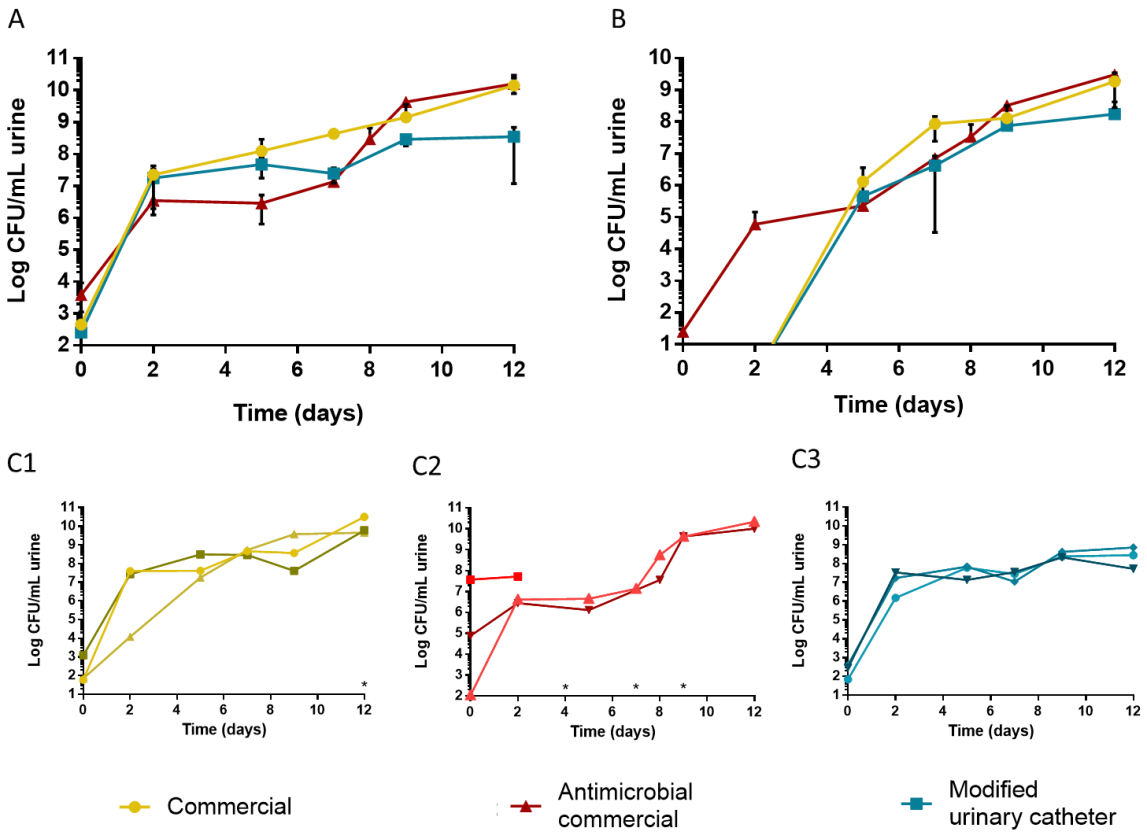

Figure IV. 18 Evolution of bacterial counts in urine. A. Urine culture in complete media (BA and CA), average of bacteria isolated every two days in urine, collected through the urinary catheters tested. B. Urine culture in Macconkey agar, average of gastro-intestinal bacteria. C1-3. Representation of individual bacterial counts in urine for each pig, average counts in complete media (BA and CA). Asterisks represent extraordinary events that happened to pigs (catheter obturation and catheter flushing). The uncompleted trends correspond to sacrificed animals before the end of the study due to acquired infection, damage to the urinary system or having exceeded the markers established in the animal welfare assessment table.

As can be seen in Figure IV. 18 A, at day 2, a bacterial population was detected in urine above 1E05 CFU / mL, which corresponds to a standard urinary infection. The detectable appearance of gastro-intestinal gram-negative bacteria arrived on day 2 in case of commercial antibacterial catheters, and they were detected on day 5 in case of standard commercial catheters and the PDA-silver coated catheters proposed in this thesis, as shown in the Figure IV. 18 B.

The evolution of bacterial infection in urine reflected 3 different behaviours depending on the catheter type. Standard commercial silicone catheters (Figure IV. 18 C1) showed infection from day 2 of the study. Bacterial counts were between 1E7 to 1E10 CFU / mL throughout the study,

without stabilizing. This indicated that the infection could continue to spread as it did not reach its maximum before finishing the study.

The profile shown by commercial antimicrobial catheters (Figure IV. 18 C2) was different from that shown by the commercial standard product; pigs showed infection on day 2, like the rest, but the number of isolated bacteria from the urine was stabilized from 2 to day 7. After, the urine infection increased considerably to reach the levels observed in the standard catheter (1E10 CFU / mL). Since it is a commercial antimicrobial catheter based on the release of silver, it is possible that the increase in the number of bacteria present in urine was due to the depletion of the antimicrobial product, losing its effect. Also, at the days marked with an asterisk (days 7 and 9), the urinary catheters were washed with sterile PBS 3 times each pig. The washes were performed because the catheters were plugged, and the animals were unable to urinate. These washes dragged biofilm and bacteria out of the urinary catheter, recovering its functionality until the end of the study. This procedure could reduce the number of bacteria present in the bladder. Catheter washes were not quantified.

Finally, the evolution of infection profile by the PDA-silver coated catheter showed infection in urine on day 2, like the rest of the catheters. However, the number of bacteria isolated from urine remained stable throughout the study, reaching a maximum concentration of 1E08 CFU / mL on the final day. Final bacterial concentrations showed two orders of magnitude less than those observed in the commercial catheter and antimicrobial catheters. Furthermore, no events occurred during the study, the catheters were not clogged, ensuring the continuous urine flow to the outside. The animals were not harmed leading to early euthanasia.

4.3.6.3 Bacteriophobic effect of PDA-silver coated urinary catheter

At the end of the study, FE-SEM images were taken to study bacteria directly adhered to catheter surface after *in vivo* study. First, the drainage eyes (the hole that allows the urine pass through the catheter) were cut and separated from the rest of the catheter. They were treated to fix the biofilm and they were visualized by FE-SEM (Figure IV. 19 B - D).

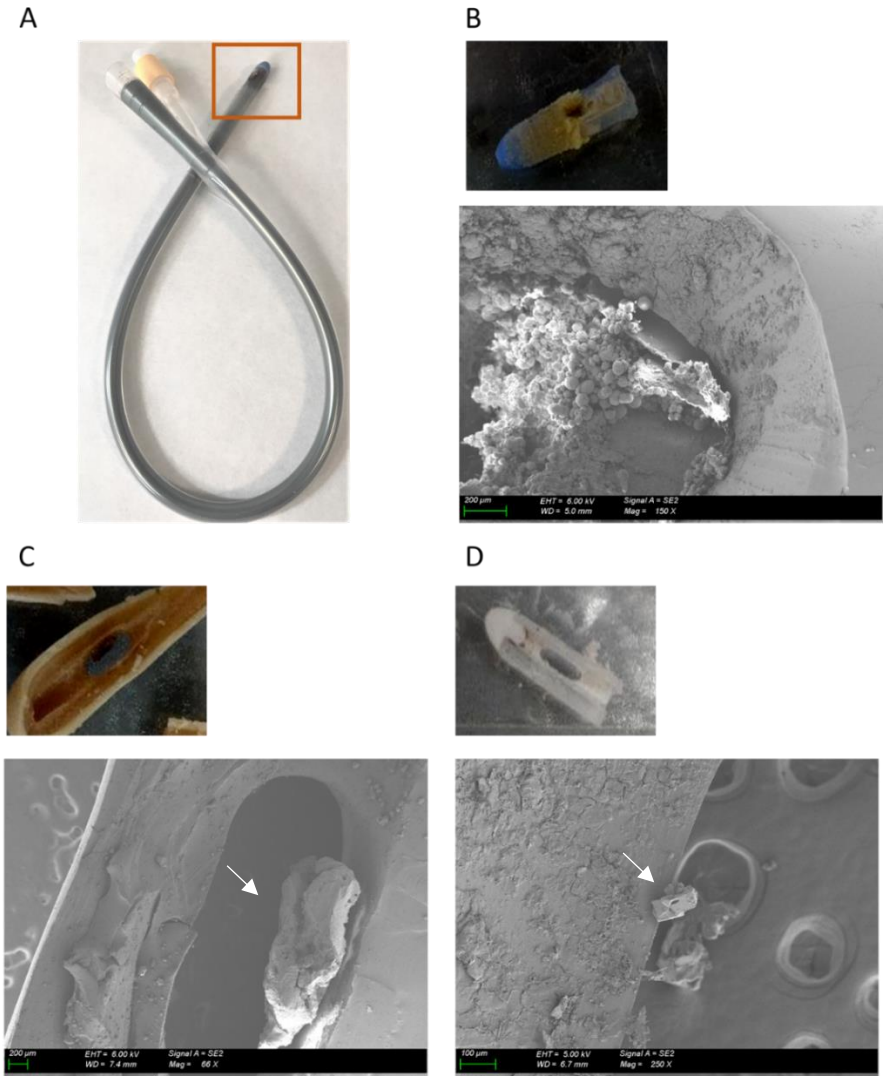

Figure IV. 19 Drainage eyes from urinary catheters after the end of the study. A. Photography of PDA-silver coated urinary catheters presented in this work with drainage eyes remarked. B. Drainage eye of commercial urinary catheter extracted from pigs. FE-SEM image from the drainage eye, almost occluded after 13 days of catheterization. C. Antimicrobial commercial urinary catheter, photography of drainage eye and FE-SEM image after 13 days of catheterization. White arrow: biomass detached from the surface. D. PDA-silver coated urinary catheter, photography of drainage eye and FE-SEM after 15 days of catheterization. White arrow: salt crystal attached on the surface. Dark zones with pores corresponded to the carbon tape where the catheter fragment was attached to visualize it.

Images showed differences between the three drainage eyes from each type of catheter studied. Figure IV. 19 B showed the silicone that forms the drainage eye where it is possible to visualize the biofilm attached on it. The eye was almost occluded by biofilm. As can be noted,

biomass had been structured by thick layers that grew to the eye centre and the composition was similar to mature biofilms, showing microcolonies and structured channels. The occlusion of the drainage eye causes a failure in the function of the urinary catheter, causing the urine not to flow properly and contributing to bacterial colonization in the bladder.

Secondly, the antimicrobial commercial catheter (Figure IV. 19 C) showed a biomass with high mucus content attached to the drainage eye walls that occluded the drainage hold. The eye was cut, and the biomass was dehydrated and fixed to visualize it by FE-SEM, due this process the biomass was detached from the walls, as can be noted in the Figure IV. 19 (white arrow). However, the eye remained partially occluded by the biomass and the interaction with the eye wall could be studied. The amount of mucosa and biomass adhered to the drainage eye caused its occlusion and it was the cause of the need to wash the catheters to perform their drainage function. The prolonged occlusion of the eye could cause the accumulation of urine in the bladder, inflammation and even damage together with a continuous urination reflex in the animal, causing discomfort and pain.

Finally, the image D in the Figure IV. 19 shows the drainage eye cut longitudinally of PDA-silver coated catheters presented in this thesis after 15 days of *in vivo* trial. The drainage eye presented absence of mucus and biomass and a large accumulation of salts was found. Salts crystals were found attached on the wall as simple structures (white arrow in Figure IV. 19 D), not like a salt-clusters. Structured biofilm or biomass were not found in the surfaces at magnificence between 60 to 250 X. An important result to highlight was the drainage eyes were not occluded during the test, so PDA-silver coated catheters with its intrinsic bacteriophobic effect avoided the occlusion of the drainage eyes for 15 days, at least.

Once drainage eyes were studied, catheters were prepared to observe the inside of the tube by FE-SEM and to perform the bacterial counts adhering to the catheter. Two segments of each catheter were observed by FE-SEM. One fragment corresponded to the middle area of the tube, and the second fragment to the area near the drainage eye. The port area, which was outside the animal's body, was not studied, as it was susceptible to external contamination. Images from uncoated commercial urinary catheters (Figure IV. 20), antimicrobial commercial urinary catheters (Figure IV. 21) and PDA-silver coated urinary catheters presented in this thesis (Figure IV. 22) are shown below.

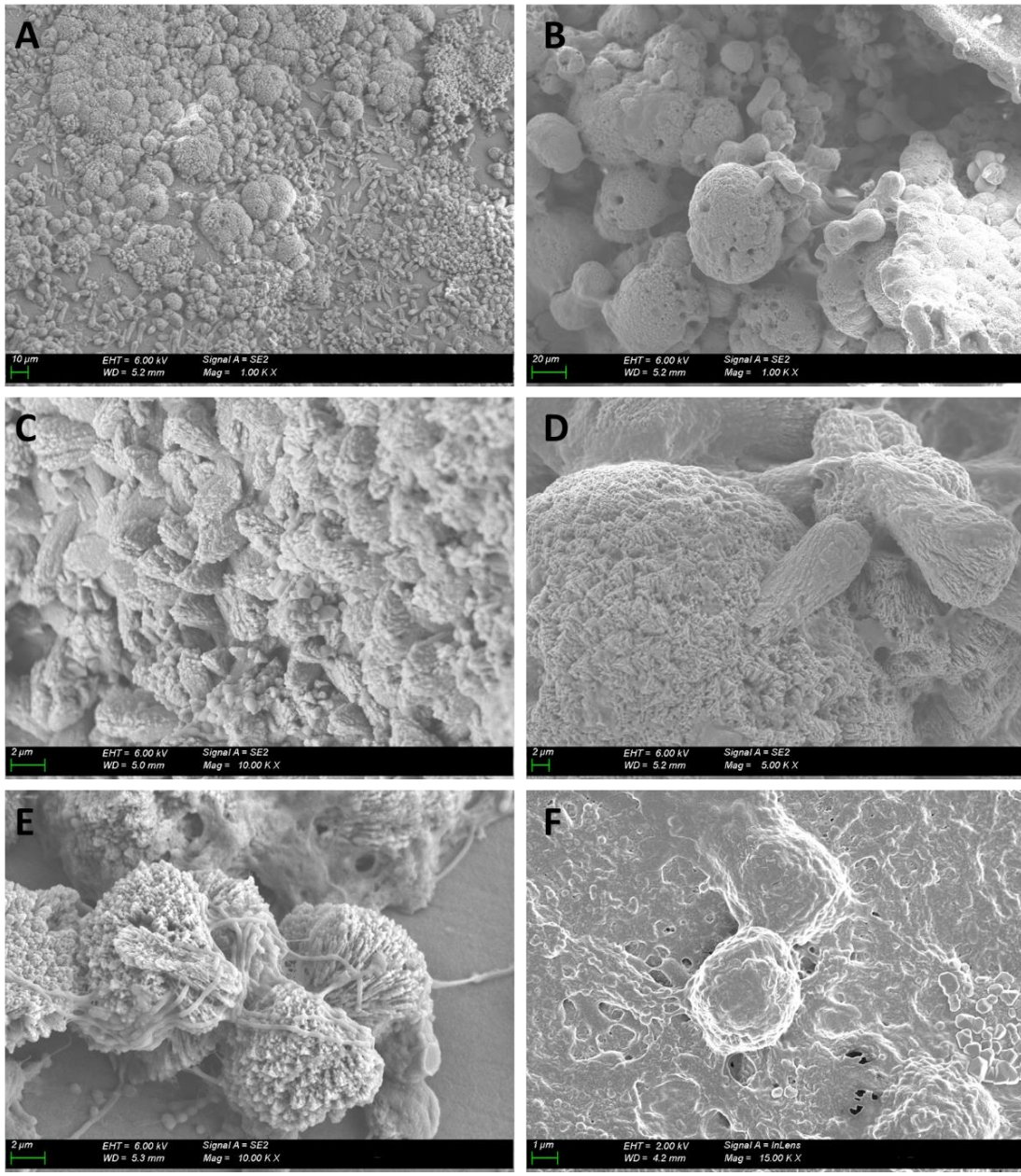

Figure IV. 20. Field-emission electron microscopy images of internal surface of commercial urinary catheters, untreated, between 12 to 13 days after implantation.

As can be noted, uncoated urinary catheters, used as a silicone 100 % control catheters (Figure IV. 20), presented a complex colonization of the surface. In none of the images the surface of the catheter could be seen free under the biomass. Mature biofilms anchored to the surface formed

by several different bacterial species were observed. It was also possible to observe areas colonized by structures similar to fungi. Between animals, a difference could be observed in the biofilms formed on the surface of the removed catheters: microbial prevalence, different biofilm structures, layers, channels and crystallization. Biofilms observed in catheters between Figure IV. 20 A to D were alike. These biofilms appeared to be highly laminated and layered, with great depth, where formed and structured channels could be seen. However, areas where colonization by fungi predominated were also seen (Figure IV. 20 E). Bacteria seemed to be less present without forming complex structures, they are seen anchored to the surface under the fungi but without developing further. It is possible that there were areas of the catheter completely colonized by fungi that competed for the niche with the bacteria. Finally, it was possible to visualize areas with a biofilm based on a matrix that contained bacteria visibly embedded in it (Figure IV. 20 F).

These images provided an overview of what was happening on the catheter surfaces. The devices were completely colonized by different species of microorganisms. The colonized urinary catheters became a reservoir of microorganisms that affected the functionality of the devices, preventing proper drainage of urine, and the health of the animals, being the obvious ones responsible for their infection.

After that, commercial antimicrobial catheters were studied by FE-SEM (Figure IV. 21). The images from the surface of the antimicrobial catheters were unexpected. As can be seen in the Figure IV. 21 A and B, different areas of the catheters in different animals were completely colonized by microorganisms. In no case could the catheter surface be observed.

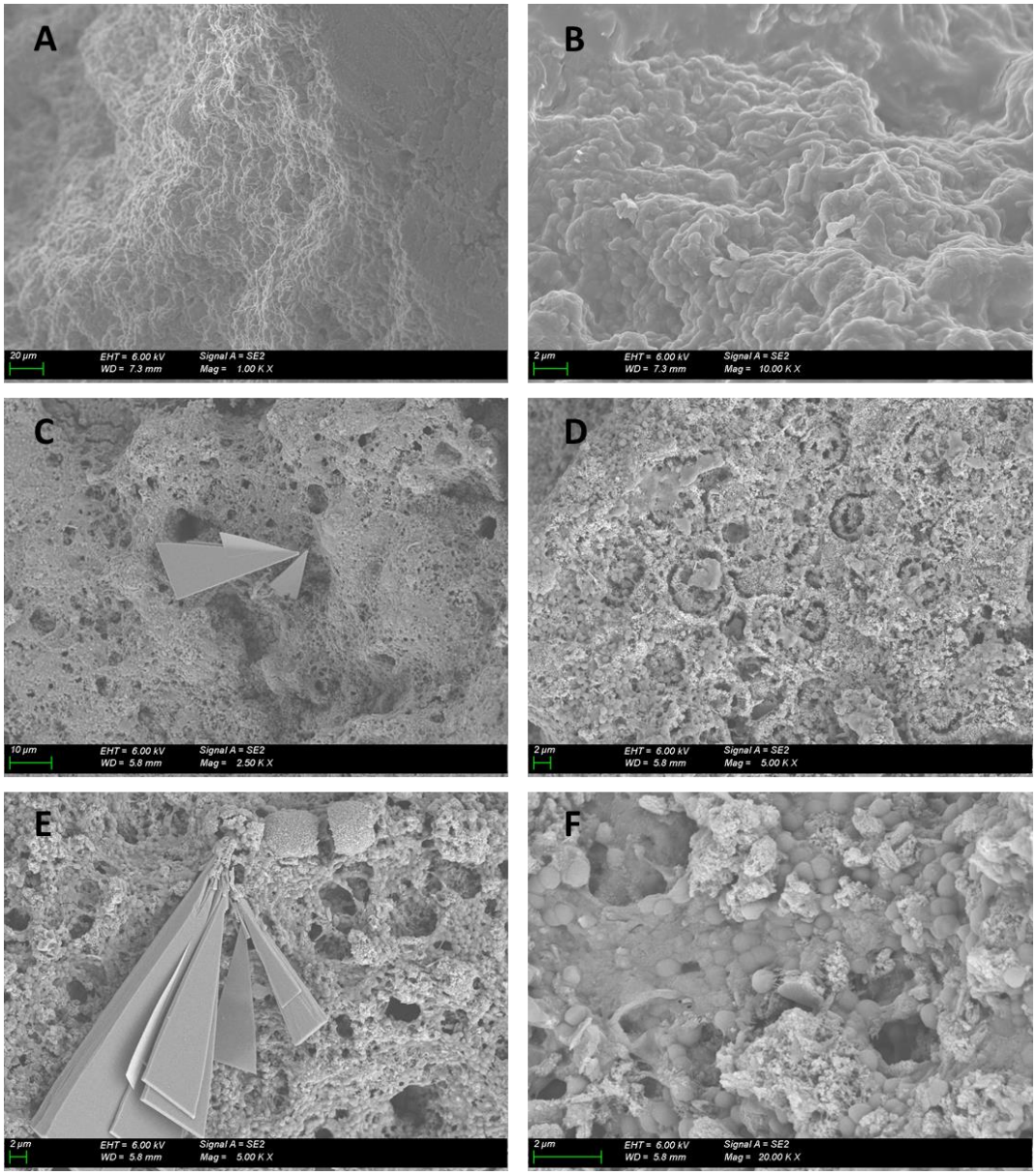

Figure IV. 21. Field-emission electron microscopy images of antimicrobial commercial urinary catheter surfaces between 13 to 14 days after implantation.

Moreover, as shown in Figure IV. 21, the surface was fully colonized, mostly based on bacteria, embedded in a deep, layered matrix. Exclusive colonization by one bacterial species was not observed, but rather various sizes and shapes of bacteria could be identified, which implies mixed colonization of the device. Also, different layers of mixed-population biofilm could be observed, with oxygenation and nutrient transport channels created with different textures, indicating

different degrees of hydration of the matrix. This high level of biofilm maturation indicated that bacterial colonization was well established on the medical device, having already built a stable population. In addition, different crystallizations could be observed in the samples (Figure IV. 21 C and E). One possibility to consider is that they are urea crystals, generated by urea deposition on the catheter surface. Urea crystals are usually shaped like a sharp flat triangle, which fits with what is seen in the images. The generation of urea crystals can be favoured by bacterial colonization, through a basification of the urine due to bacterial activity[41,42]. These crystals usually do not cause harm to patients if they do not reach sizes greater than 50 µm. In this case, crystals of this size and greater were observed, which could generate aggregates that block the lumen of the catheter tube, generating stones or causing micro-breaks. This bacterial colonization and biomass and crystals deposition on antimicrobial catheters revealed one of the great disadvantages of these kind of devices: their short half-life. Once the antimicrobial effectors were complete released from the catheter surface, it was colonized just as the commercial uncoated catheter did.

By last, samples from the PDA-silver coated catheters in this thesis were observed by FE-SEM (Figure IV. 22). The catheters of the three different animals presented a similar degree of colonization: very low. Bacteria were observed on the surface of the catheters in the different areas studied. These bacteria appeared to belong to a single species since they all had the same size and shape. The bacteria were, in all cases, showed on the surface individually and without surrounding biomass. Thus, bacteria were not embedded in a matrix nor had they developed biofilm.

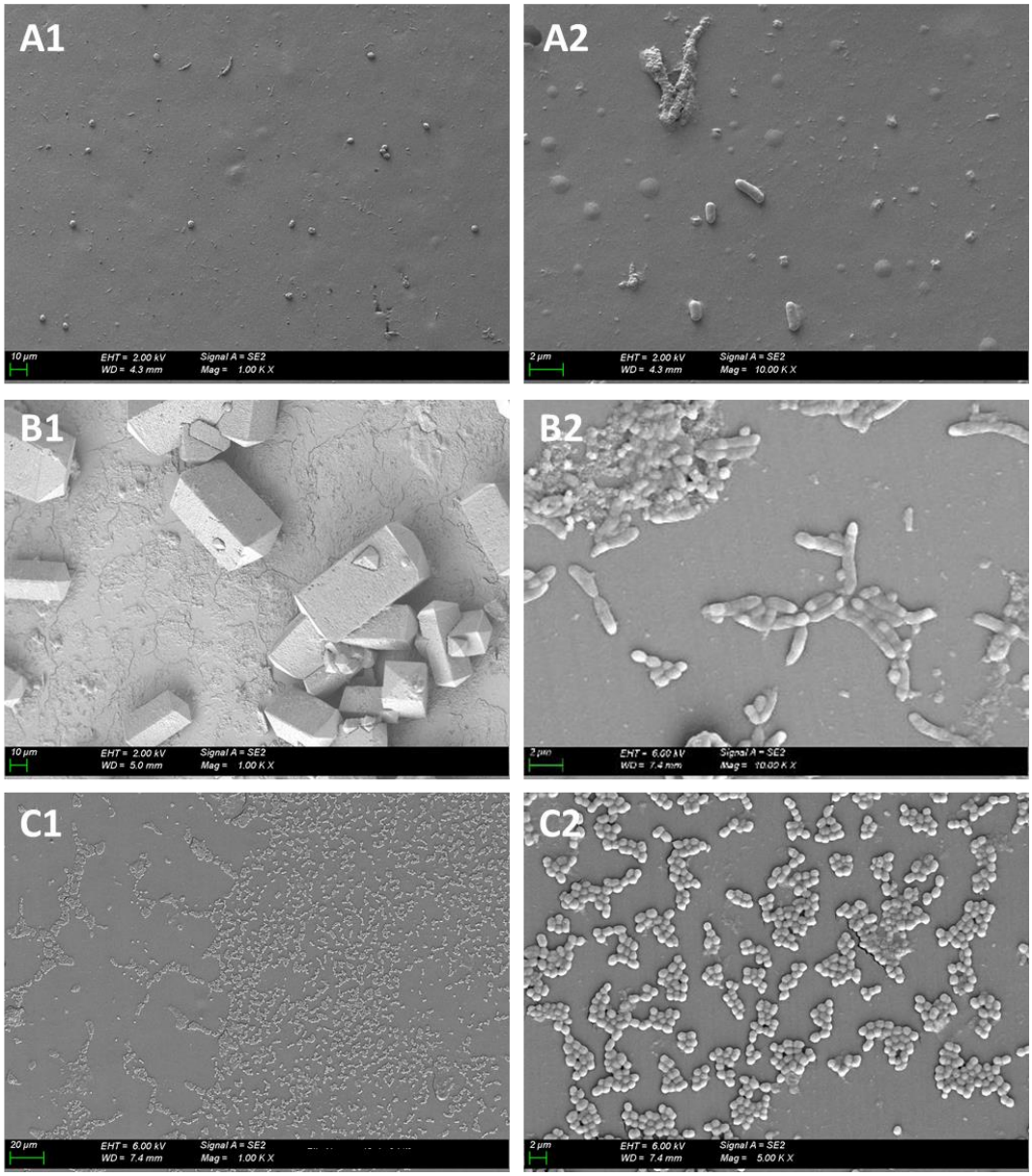

Figure IV. 22. Field-emission electron microscopy images of PDA-silver coated urinary catheter surfaces between 13 to 15 days after implantation. A2, B2 and C2 images are a zoom from A1, B1 and C1 images.

As can be seen, Figure IV. 22 A showed a punctual colonization of bacilli, like Figure IV. 22 B, and both bacterial species was different. The predominant species on the surface of Figure IV. 22 C, however, was a coco-like bacterium. This indicates that the surface does not have a bacteriophobic effect that works for a single type of cell membrane, but any bacterial species,

gram-negative or gram-positive can be avoided. There are bacteria capable of interacting to a greater or lesser extent with the surface, and this phenomenon is logical. Our surface does not have any antibacterial effect. It does not kill bacteria. However, the surface was able to permanently prevent the interaction of bacteria, the formation of microcolonies, the creation of biomass and the formation of biofilm on it. The bacterial-surface interaction observed was, presumably, due to the presence in higher numbers of this type of bacteria in the urine.

It is interesting to note the appearance of cubic crystals on the surface of the catheters. Crystals were not formed due to the treatment of the sample for FE-SEM and the dehydration processes, since they were colonized by bacteria (Figure IV. 22 B2, bacteria on the crystal of Figure IV. 22 B1). These crystals could correspond to precipitation of triple phosphate crystals, formed by phosphate, magnesium and ammonium salts, very common in urine[41,43]. The presence of these crystals in high concentrations warn of the presence of bacteria in urine, symptom presented by our animals.

Comparing the images obtained from the surface of the PDA-silver coated catheters with the uncoated control catheters and the antimicrobial catheters, it was possible to conclude that the interaction of the bacteria with the surface of the proposed catheters was much lower. The surface could avoid the colonization of the surface and the biofilm formation in any of its stages, for at least 15 days, without having performed any catheter washing.

In order to complete the study of the colonization of the different urinary catheters, an extraction and quantification of viable bacteria was carried out in different media and conditions (Figure IV. 23).

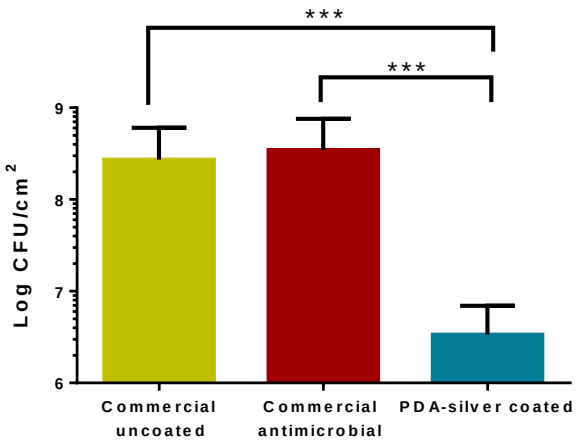

Figure IV. 23. Mean of bacteria extracted from urinary catheters 12 to 15 days after implantation. Bacteria were extracted and plated in optimized conditions (complete media (blood and chocolate agar) at 37 ºC in 5 % CO_2 or normal atmosphere during 24-48 h. Statistical analysis revealed p-value < 0.001 (***) for commercial uncoated and antimicrobial catheters vs. PDA-silver coated catheters data.

As can be seen, the mean of the bacterial counts obtained from the control catheters, uncoated and antimicrobial, was similar in both cases. The counts between the control catheters did not show statistically significant differences. However, the PDA-silver nanostructured catheter showed a reduction of two logarithms in bacterial adhesion regarding control catheters. In addition, the bacterial counts in control catheters would have been much higher if the washes would not have been performed on them. So, the difference between the controls and the PDA-silver coated catheter may have been much greater.

Despite this, the difference of bacterial adhesion corresponds to 99.99% reduction in bacteria present on the catheter surface, compared to uncoated and antimicrobials commercial catheters. Current commercial antimicrobial catheters, including those used in this study, claim between 45 to 90% reduction in bacterial adhesion[44]. Bacteria-surface interaction reduction percentages greater than 70% are considered successful and sufficient to prevent urinary tract infections associated with urinary catheter in patients hospitalized for more than 5 days[45–47].

4.4 CONCLUDING REMARKS

Throughout this chapter, bacteriophobic micro and nanostructured coating technology based on a PDA-silver film has been successfully implemented on urinary catheters. The coating can be applied homogeneously throughout the entire medical device, coating the most complex areas: the port and the drainage eye. After modifying the urinary catheter, its physical properties and its function have been verified, as specified in the ASTM F623 standard for urinary catheters. Tests showed no modifications that affected the catheter's function.

After implementing the coating, the antimicrobial efficacy was studied, determining the bacteriophobic properties against different bacterial species. Furthermore, the long-lasting effect of the coating was tested for 30 days in static conditions, maintaining the surface with a low bacterial colonization, with a difference between 3 to 4 orders of magnitude regarding the control catheters. Moreover, the coating is stable under flow conditions, sustaining its bacteriophobic properties after simulating 21 days of use with artificial urine.

To bring the catheter to a complex environment, an *in vivo* study was designed with catheterized pigs as an animal model. The biodistribution, histopathology and antimicrobial efficacy were evaluated comparing the gold standard commercial and antimicrobial catheters with the PDA-silver coated catheter. The PDA-silver coated catheter did not harm the animals. No-significant silver remains were found in organs or urine, proving that the catheter was completely biocompatible. Furthermore, during the study, the animals did not show signs of physical pain or discomfort, unlike animals catheterized with standard and antimicrobial control catheters.

Bacterial counts in urine were performed every two days and showed stabilization from day 2 in the animals catheterized with the PDA-silver coated catheter. The number of bacteria did not reach to the number of bacteria isolated from the control or the antimicrobial catheter at any time.

FE-SEM images obtained from the surface showed clear differences between the control catheters and the PDA-silver coated catheters. The commercial antimicrobial and control catheters showed a mature biofilm formed on the catheter surface, composed by different bacterial species and highly structured. While, the new catheter showed a low bacterial colonization. These results were corroborated by the bacterial quantification, extracted from the surface of the catheters, which showed a difference of up to 2 orders of magnitude between the control or antimicrobial catheters and the catheter proposed in this thesis.

4.5 REFERENCES

(1) Feneley, R. C. L.; Hopley, I. B.; Wells, P. N. T. Urinary Catheters: History, Current Status, Adverse Events and Research Agenda. *J. Med. Eng. Technol.* **2015**, *39* (8), 459–470. https://doi.org/10.3109/03091902.2015.1085600.

(2) Karchmer, T. B.; Giannetta, E. T.; Muto, C. A.; Strain, B. A.; Farr, B. M. A Randomized Crossover Study of Silver-Coated Urinary Catheters in Hospitalized Patients. *Arch. Intern. Med.* **2000**, *160* (21), 3294–3298. https://doi.org/10.1001/archinte.160.21.3294.

(3) Getliffe, K. A. Urinary Catheter Use in Older People. *Aging health* **2008**, *4* (2), 181–189. https://doi.org/10.2217/1745509X.4.2.181.

(4) Lui, M. M. S.; Thomas, R.; Lee, Y. C. G. Complications of Indwelling Pleural Catheter Use and Their Management. *BMJ Open Respir. Res.* **2016**, *3* (1), 1–8. https://doi.org/10.1136/bmjresp-2015-000123.

(5) Newman, D. K. The Indwelling Urinary Catheter: Principles for Best Practice. *J. wound, ostomy, Cont. Nurs. Off. Publ. Wound, Ostomy Cont. Nurses Soc.* **2007**, *34* (6), 655–661. https://doi.org/10.1097/01.WON.0000299816.82983.4a.

(6) Cortese, Y. J.; Wagner, V. E.; Tierney, M.; Devine, D.; Fogarty, A. Review of Catheter-Associated Urinary Tract Infections and in Vitro Urinary Tract Models. *J. Healthc. Eng.* **2018**, *2018*. https://doi.org/10.1155/2018/2986742.

(7) Andersen, M. J.; Flores-Mireles, A. L. Urinary Catheter Coating Modifications: The Race against Catheter-Associated Infections. *Coatings* **2019**, *10* (1), 23. https://doi.org/10.3390/coatings10010023.

(8) Sabir, N.; Ikram, A.; Zaman, G.; Satti, L.; Gardezi, A.; Ahmed, A.; Ahmed, P. Bacterial Biofilm-Based Catheter-Associated Urinary Tract Infections: Causative Pathogens and Antibiotic Resistance. *Am. J. Infect. Control* **2017**, *45* (10), 1101–1105. https://doi.org/10.1016/j.ajic.2017.05.009.

(9) Rognoni, C.; Tarricone, R. Healthcare Resource Consumption for Intermittent Urinary Catheterisation: Cost-Effectiveness of Hydrophilic Catheters and Budget Impact Analyses. *BMJ Open* **2017**, *7* (1), 1–12. https://doi.org/10.1136/bmjopen-2016-012360.

(10) Ramstedt, M.; Ribeiro, I. A. C.; Bujdakova, H.; Mergulhão, F. J. M.; Jordao, L.; Thomsen, P.; Alm, M.; Burmølle, M.; Vladkova, T.; Can, F.; et al. Evaluating Efficacy of Antimicrobial and Antifouling Materials for Urinary Tract Medical Devices: Challenges and Recommendations. *Macromol. Biosci.* **2019**, *19* (5), 1800384. https://doi.org/10.1002/mabi.201800384.

(11) Majeed, A.; Sagar, F.; Latif, A.; Hassan, H.; Iftikhar, A.; Darouiche, R. O.; Mohajer, M. Al. Does Antimicrobial Coating and Impregnation of Urinary Catheters Prevent Catheter-Associated Urinary Tract Infection? A Review of Clinical and Preclinical Studies. *Expert Rev. Med. Devices* **2019**, *16* (9), 809–820. https://doi.org/10.1080/17434440.2019.1661774.

(12) Wang, J.; Liu, Q.; Tian, Y.; Jian, Z.; Li, H.; Wang, K. Biodegradable Hydrophilic Polyurethane PEGU25 Loading Antimicrobial Peptide Bmap-28: A Sustained-Release Membrane Able to Inhibit Bacterial Biofilm Formation in Vitro. *Sci. Rep.* **2015**, *5* (Ldi), 8634. https://doi.org/10.1038/srep08634.

(13) Dave, R. N.; Joshi, H. M.; Venugopalan, V. P. Novel Biocatalytic Polymer-Based Antimicrobial Coatings as Potential Ureteral Biomaterial: Preparation and In Vitro Performance Evaluation. *Antimicrob. Agents Chemother.* **2011**, *55* (2), 845–853. https://doi.org/10.1128/AAC.00477-10.

(14) Olsson, A. L. J.; Wargenau, A.; Tufenkji, N. Optimizing Bacteriophage Surface Densities for Bacterial Capture and Sensing in Quartz Crystal Microbalance with Dissipation Monitoring. *ACS Appl. Mater. Interfaces* **2016**, *8* (22), 13698–13706. https://doi.org/10.1021/acsami.6b02227.

(15) Colletta, A.; Wu, J.; Wo, Y.; Kappler, M.; Chen, H.; Xi, C.; Meyerhoff, M. E. S-Nitroso-N-Acetylpenicillamine (SNAP) Impregnated Silicone Foley Catheters: A Potential Biomaterial/Device to Prevent Catheter-Associated Urinary Tract Infections. *ACS Biomater. Sci. Eng.* **2015**, *1* (6), 416–424. https://doi.org/10.1021/acsbiomaterials.5b00032.

(16) Schlenoff, J. B. Zwitteration: Coating Surfaces with Zwitterionic Functionality to Reduce Nonspecific Adsorption. *Langmuir* **2014**, *30* (32), 9625–9636. https://doi.org/10.1021/la500057j.

(17) Schoech, D. Bactiguard Technology Overview. **2008**, No. September, 1–12. https://doi.org/10.1093/acrefore/9780199975839.013.625.

(18) Hidalgo Fabrellas, I.; Rebollo Pavón, M.; Planas Canals, M.; Barbero Cabezas, M. Incidencia de La Infección Urinaria En Pacientes Postoperados de Cirugía Cardiaca: Estudio Comparativo Según El Dispositivo de Sondaje. *Enfermería Intensiva* **2015**, *26* (2), 54–62. https://doi.org/10.1016/j.enfi.2014.10.004.

(19) Magnusson, B.; Kai-Larsen, Y.; Granlund, P.; Seiger, Å.; Lindbo, L.; Sanchez, J.; Johansson, D. Long-Term Use of Noble Metal Alloy Coated Urinary Catheters Reduces Recurrent CAUTI and Decreases Proinflammatory Markers. *Ther. Adv. Urol.* **2019**, *11* (6),

175628721985491. https://doi.org/10.1177/1756287219854915.

(20) Pickard, R.; Lam, T.; MacLennan, G.; Starr, K.; Kilonzo, M.; McPherson, G.; Gillies, K.; McDonald, A.; Walton, K.; Buckley, B.; et al. Antimicrobial Catheters for Reduction of Symptomatic Urinary Tract Infection in Adults Requiring Short-Term Catheterisation in Hospital: A Multicentre Randomised Controlled Trial. *Lancet* **2012**, *380* (9857), 1927–1935. https://doi.org/10.1016/S0140-6736(12)61380-4.

(21) Al-Qahtani, M.; Safan, A.; Jassim, G.; Abadla, S. Efficacy of Anti-Microbial Catheters in Preventing Catheter Associated Urinary Tract Infections in Hospitalized Patients: A Review on Recent Updates. *J. Infect. Public Health* **2019**, *12* (6), 760–766. https://doi.org/10.1016/j.jiph.2019.09.009.

(22) Brooks, T.; Keevil, C. W. W. A Simple Artificial Urine for the Growth of Urinary Pathogens. *Lett. Appl. Microbiol.* **1997**, *24* (3), 203–206. https://doi.org/10.1046/j.1472-765X.1997.00378.x.

(23) De Benedetto, G. E.; Fico, D.; Pennetta, A.; Malitesta, C.; Nicolardi, G.; Lofrumento, D. D.; De Nuccio, F.; La Pesa, V. A Rapid and Simple Method for the Determination of 3,4-Dihydroxyphenylacetic Acid, Norepinephrine, Dopamine, and Serotonin in Mouse Brain Homogenate by HPLC with Fluorimetric Detection. *J. Pharm. Biomed. Anal.* **2014**, *98*, 266–270. https://doi.org/10.1016/j.jpba.2014.05.039.

(24) Kazan, Z.; Zumeris, J.; Jacob, H.; Raskin, H.; Kratysh, G.; Vishnia, M.; Dror, N.; Barliya, T.; Mandel, M.; Lavie, G. Effective Prevention of Microbial Biofilm Formation on Medical Devices by Low-Energy Surface Acoustic Waves. *Antimicrob. Agents Chemother.* **2006**, *50* (12), 4144–4152. https://doi.org/10.1128/AAC.00418-06.

(25) Hachem, R.; Reitzel, R.; Borne, A.; Jiang, Y.; Tinkey, P.; Uthamanthil, R.; Chandra, J.; Ghannoum, M.; Raad, I. Novel Antiseptic Urinary Catheters for Prevention of Urinary Tract Infections: Correlation of in Vivo and in Vitro Test Results. *Antimicrob. Agents Chemother.* **2009**, *53* (12), 5145–5149. https://doi.org/10.1128/AAC.00718-09.

(26) Pugach, J. L.; DiTizio, V.; Mittelman, M. W.; Bruce, A. W.; DiCosmo, F.; Khoury, A. E. Antibiotic Hydrogel Coated Foley Catheters for Prevention of Urinary Tract Infection in a Rabbit Model. *J. Urol.* **1999**, *162* (3), 883–887. https://doi.org/10.1097/00005392-199909010-00084.

(27) Shalom, Y.; Perelshtein, I.; Perkas, N.; Gedanken, A.; Banin, E. Catheters Coated with Zn-Doped CuO Nanoparticles Delay the Onset of Catheter-Associated Urinary Tract Infections. *Nano Res.* **2017**, *10* (2), 520–533. https://doi.org/10.1007/s12274-016-1310-8.

(28) Musk, G. C.; Zwierzchoniewska, M.; He, B. Catheterization of the Urethra in Female Pigs.

Lab. Anim. **2015**, *49* (4), 345–348. https://doi.org/10.1177/0023677215587637.

(29) Brown, C. Urethral Catheterization in the Female Guinea Pig (Cavia Porcellus). *Lab Anim. (NY).* **2011**, *40* (2), 42–43. https://doi.org/10.1038/laban0211-42.

(30) Li, D. P.; Zhang, W. H.; Yang, M. L.; Liu, C. Bin; Zhang, X.; Cai, C.; Li, J. J. An Improved Urethral Catheterization in Female Pigs : A Pilot Study. **2017**, *130* (15), 1880–1881. https://doi.org/10.3233/THC.

(31) Zak, O.; Sande A., M. *Handbook of Animal Models of Infection*; 2013; Vol. 53. https://doi.org/10.1017/CBO9781107415324.004.

(32) Price, T. K.; S, M.; Dune, T.; D, M.; Hilt, E. E.; S, M.; Thomas-white, K. J. The Clinical Urine Culture : Enhanced Techniques Improve Detection of Clinically Relevant Microorganisms. *J. Clin. Microbiol.* **2016**, *54* (March), 1216–1222. https://doi.org/10.1128/JCM.00044-16.

(33) Koc, Y.; de Mello, A. J.; McHale, G.; Newton, M. I.; Roach, P.; Shirtcliffe, N. J. Nano-Scale Superhydrophobicity: Suppression of Protein Adsorption and Promotion of Flow-Induced Detachment. *Lab Chip* **2008**, *8* (4), 582. https://doi.org/10.1039/b716509a.

(34) Zhang, X.; Wang, L.; Levänen, E. Superhydrophobic Surfaces for the Reduction of Bacterial Adhesion. *RSC Adv.* **2013**, *3* (30), 12003. https://doi.org/10.1039/c3ra40497h.

(35) Roe, D.; Karandikar, B.; Bonn-Savage, N.; Gibbins, B.; Roullet, J. baptiste. Antimicrobial Surface Functionalization of Plastic Catheters by Silver Nanoparticles. *J. Antimicrob. Chemother.* **2008**, *61* (4), 869–876. https://doi.org/10.1093/jac/dkn034.

(36) Wertz, C. F.; Santore, M. M. Effect of Surface Hydrophobicity on Adsorption and Relaxation Kinetics of Albumin and Fibrinogen: Single-Species and Competitive Behavior. *Langmuir* **2001**, *17* (10), 3006–3016. https://doi.org/10.1021/la0017781.

(37) Yuan, Y.; Hays, M. P.; Hardwidge, P. R.; Kim, J. Surface Characteristics Influencing Bacterial Adhesion to Polymeric Substrates. *RSC Adv.* **2017**, *7* (23), 14254–14261. https://doi.org/10.1039/c7ra01571b.

(38) Lansdown, A. B. G. A Pharmacological and Toxicological Profile of Silver as an Antimicrobial Agent in Medical Devices. *Adv. Pharmacol. Sci.* **2010**, *2010* (9), 1–16. https://doi.org/10.1155/2010/910686.

(39) Drake, P. L.; Hazelwood, K. J. Exposure-Related Health Effects of Silver and Silver Compounds: A Review. *Ann. Occup. Hyg.* **2005**, *49* (7), 575–585. https://doi.org/10.1093/annhyg/mei019.

(40) Lansdown, A. B. G. Silver in Health Care: Antimicrobial Effects and Safety in Use Interactions between Skin and Biofunctional Metals. *Curr Probl Dermatol. Basel, Karger*

2006, *33*, 17–34.

(41) Stickler, D. J.; Morgan, S. D. Observations on the Development of the Crystalline Bacterial Biofilms That Encrust and Block Foley Catheters. *J. Hosp. Infect.* **2008**, *69* (4), 350–360. https://doi.org/10.1016/j.jhin.2008.04.031.

(42) Grabe, M.; Bartoletti, R.; Johansen, T. E. B.; Associate, T. C. G.; Çek, M.; Associate, B. K. G.; Naber, K. G. Guidelines on Urological Infections. **2015**.

(43) Fogazzi, G. B. Crystalluria: A Neglected Aspect of Urinary Sediment Analysis. *Nephrol. Dial. Transplant.* **1996**, *11* (2), 379–387. https://doi.org/10.1093/oxfordjournals.ndt.a027276.

(44) Bactiguard. Bactiguard Infection Protection - BIP Foley Catheter. *www.bactiguard.com* **2016**.

(45) Verleyen, P.; De Ridder, D.; Van Poppel, H.; Baert, L. Clinical Application of the Bardex IC Foley Catheter. *Eur. Urol.* **1999**, *36* (3), 240–246. https://doi.org/10.1159/000068005.

(46) Verma, A. Differences in Bacterial Colonization and Biofilm Formation Property of Uropathogens between the Two Most Commonly Used Indwelling Urinary Catheters. *J. Clin. DIAGNOSTIC Res.* **2016**, *10* (6), PC01-3. https://doi.org/10.7860/jcdr/2016/20486.7939.

(47) Kart, D.; Kustimur, A. S.; Sağıroğlu, M.; Kalkancı, A. Evaluation of Antimicrobial Durability and Anti-Biofilm Effects in Urinary Catheters Against Enterococcus Faecalis Clinical Isolates and Reference Strains. *Balkan Med. J.* **2017**, *34* (6), 546–552. https://doi.org/10.4274/balkanmedj.2016.1853.

This page left blank intentionally.

Chapter V. Conclusions

With the objective to design new strategies to overcome the problem of bacterial colonization on urinary catheters, different techniques have been developed and optimized to evaluate the interaction of bacteria with materials commonly used in medical devices, to obtain robust protocols for their application in the study of antimicrobial surfaces.

- The replication of urinary environment, using artificial urine medium as well as bacterial strains similar to clinical strains present in urinary infections have demonstrated to be necessary to correctly extrapolate results.
- The most efficient protocol for extraction and quantification of adhered bacteria and biofilm was based on the physical disruption through a sonication process in an ultrasound bath, vortexing and a second sonication step. This protocol has been applied successfully for the extraction and quantification of bacteria and biofilm in different types of silicones (PDMS, NUSIL, tracheal stents and urinary catheters).
- The technique of counting viable bacteria that compose biofilm has been proven to be sufficiently sensitive and robust to be applied on complex biofilms formed in real environments, such as biofilms developed on tracheal stents implanted in pigs for 30 days or in urinary catheters after 15 days of use in pigs.
- A new methodology base on the dehydration of bacteria protocols using PBS-formaldehyde solution and a serial dehydration based on PBS-ethanol was evaluated to improve the quality of images obtained by Field Emission Scanning Electron Microscopy (FE-SEM), maintaining the morphology of biofilm and bacteria. This methodology allowed to visualize mature and complex biofilm structures after in vivo tests in both real medical devices: tracheal stents and urinary catheters.
- A methodology based on Quartz Crystal Microbalance with Dissipation monitoring (QCM-D) has been developed to study bacterial adhesion to hydrophobic surfaces under constant flow. This methodology allowed to study changes in a urinary model for the identification elements that affect bacterial adhesion.
- It was found that high concentration of human albumin dissolved in artificial urine was a key factor for bacterial adhesion. Thus, protein-rich fluids can make medical devices more susceptible to bacterial colonization, concluding that patients with proteinuria may be more susceptible to acquiring an infection while catheterized.

Once the study protocols have been stabilized, a set of new antimicrobial coatings was developed based on the immobilization of metallic silver on polymeric thin films. Four new coatings were applied on silicones based on plasma-polymerized pentafluorophenyl methacrylate (pp-PFM) or polydopamine (PDA).

- All samples modified with a nanostructured metallic surface presented a bacteriophobic behaviour, showing a reduction in bacterial adhesion of 4 orders of magnitude in tests with gram-positive and, at least, 6 orders of magnitude in gram-negative bacterial adhesion in vitro. This effect was led by a combination of super-hydrophobic properties, a specific roughness and morphology and a protein repulsion effect.
- Different effect on bacterial growth was observed according to the morphology of the silver deposited on the polymer film:
    - The “Thick blades” surface and the PDA-silver surface had not effect on bacterial growth.
    - The “Sharp blades” surface inhibited bacterial growth for 4 to 5 hours after being in contact with the medium, depending on the bacterial strain.
    - The “Leaves” surface showed a bacteriostatic effect on gram-negative bacteria and a slowdown on gram-positive bacterial growth during, at least, 50 h.

Once the antimicrobial technology was developed, it was implemented on a Foley-type urinary catheter to give it bacteriophobic characteristics.

- The PDA-silver coating was successfully implemented in Foley urinary catheter 100 % silicone. The catheter maintained its physical characteristics according to official international standards based on ASTM-F623 and ISO 20696 after being coated.
- The urinary catheter revealed the capacity to reduce bacterial adhesion by at least 3 orders of magnitude in vitro regardless the bacterial strain used.
- The long-lasting bacteriophobic effect of the modified urinary catheters was evaluated by a study of E. coli CFT073 adhesion and biofilm formation on the urinary catheter for 30 days, showing a bacterial adhesion reduction between 3 to 4 orders of magnitude throughout the test.
- The stability of the catheter was verified simulating a prolonged use of the urinary catheter for 21 days. The amount of total silver (0.4 mg/cm2) and the topography of the surface were maintained in vitro.

- The modified catheter did not affect to bacterial growth, protecting the local microbiota of the catheterized patient.

PDA-silver coated urinary catheters were evaluated in a *in* vivo test using pigs. Pigs were catheterized with commercial catheters, commercial antimicrobial catheters and with the new catheters for 15 days.

- None of the animals catheterized with the PDA-silver coated catheter suffered pain, discomfort, irritation or excessive inflammation, ulcers or occlusion of the catheter with inability to urinate. Unlike the animals catheterized with commercial catheters, which presented these problems.
- The study of silver accumulation did not found silver in any organ, showing, together with the histopathology studies, that the device is biocompatible.
- The count of present bacteria in urine showed that the PDA-silver catheter was able to reduce the presence of bacteria in urine during the study and the consequent infection of the pig due to the removal of bacterial reservoirs in the catheter surface, remaining the bacterial counts below of both commercial catheters throughout the study.
- Biofilm on the PDA-silver catheter showed a punctual bacterial attachment on the surface, while the control catheters showed mature, highly structured and multilayer biofilms, made up of mixed populations of bacteria, in either: standard or antimicrobial catheters.
- Finally, the PDA-silver coated catheter showed a bacterial adhesion reduction of, at least, 2 orders of magnitude (99%) regarding the uncoated and antimicrobial commercial catheters. Thus, this new bacteriophobic urinary catheter could potentially reduce the incidence of infections associated with the use of a urinary catheter (CAUTIs), being an alternative to current urinary devices.

Supplementary Information

ANNEX Chapter II

Overview of methods to grow and characterize biofilms, which includes different biofilm devices, methods to assess adhesion extent and strength, and techniques to measure biofilm biomass, viability and matrix composition.

Table S. 1. Techniques to grow and to study biofilm on surfaces. Data are based on the work of diverse authors, reviews and books[1,2,11–14,18,21,29,86,87].

	Advantages	Drawbacks
Biofilm growth methods		
Microtiter plates	Most commonly and inexpensive	Study of bacterial adhesion on polystyrene only Sensitive to sedimentation End-point measurement Exhaustion of nutrients Only short-term experiments Assessment possible only at a sufficiently high cell density Not suitable for investigating early stages of biofilm formation
Drip flow reactor	Visualization and quantification of biofilm formation on coupons at low shear stress	Poor reproducibility, heterogeneity of biofilm development on the coupons Expensive
Rotary biofilm reactors	A variety of materials can be com- pared in similar nutritional and hydrodynamic conditions Constant shear stress field	Low number of microbial strains can be analysed The geometry of the coupon is fixed and determined by the reactor design (coupon holder) Expensive
Flow chambers	Suitable for growing biofilms with continuous supply of fresh medium Can be used to study bacterial attachment and growth Allows nondestructive observation of developing biofilms	Low throughput Does not allow direct access to the biofilm cells Requires peristaltic pumps and special equipment
Microfluidic devices	Can be custom made for specific purposes Single cells analysis	Requires special equipment for manufacturing and running systems Can be expensive
Biofilm direct measurements		

Light microscopy	Simple sample preparation Cheap and easy to perform	Limited magnification and resolution Sample staining necessary Morphotype differentiation relatively gross Lacking discriminatory detail
Confocal laser scanning microscopy (CLSM)	Resolution compatible with single cell visualization Reconstruction of 3D images	Use of fluorophores is required Limited number of reporter molecules (no universal matrix probes exist) Interference of local properties of the biofilm with the fluorescence probes Natural auto-fluorescence may hide signal of interest
Field emission / Scanning electron microscopy (FE-SEM, SEM)	Resolution higher than other imaging techniques (resolves surface details) Good depth of field Ability to image complex shapes	Tedious and time-consuming sample preparation Lacks vertical resolution
Cryo-SEM	High resolution capability Sample viewed in fully hydrated state	Lower resolution than conventional SEM Melting and cracking of the frozen surface of the sample at high magnifications due to the heat generated by the focused electron beam
Biofilm indirect measurements		
Colony forming units counts (CFU)	Without restrictions, any strain can be studied Easy to perform and inexpensive	Only detects the culturable fraction of the biofilm population, underestimates the number of culturable cells due to microbial aggregation Time-consuming
Flow cytometry	Differentiating between total, dead and alive bacteria (actively dividing)	Need of fluorophores Specific protocol for each strain. Expensive
FISH techniques	Fast and accurate detection Able to detect non-actively dividing cells	Insufficient sensitivity Low probe permeability Poor probe hybridization efficiency Very limited number of different target organisms that can be detected simultaneously
qPCR	Assesses total number of cells indirectly	Expensive Overestimates the number of cells due to the presence of eDNA Not distinguish between live-dead bacteria.

Dye stanning	High throughput Does not require removal of the biofilm if it has been formed in microtiter plate	Lack of reproducibility Lack of sensitivity Overestimation or underestima- tion of biofilm biomass, depending on the washing step A standardized protocol is not available
Biofilm mass by phospholipid count	Versatile Can estimate viability because phospholipids are rapidly degraded in dead cells	Low sensitivity Sensitive to background lipid contamination Intracellular
Bacterial adhesion		
Quartz crystal microbalance w/wo dissipation module (QCM /-D)	Suitable for growing biofilms with continuous supply of fresh medium Can be used to study bacterial attachment and growth Allows non-destructive observation of developing biofilms	Requires peristaltic pumps and special equipment Requires equipment specialization and complex data processing Expensive materials Not available sensors of all materials
Atomic Force Microscopy (AFM)	Non-destructive technique Works under ambient conditions Same resolution along and perpendicular to the surface 3-D reconstruction Qualitative and quantitative assessment of living bacteria under physiological-like conditions	Inability to obtain a large area survey scan

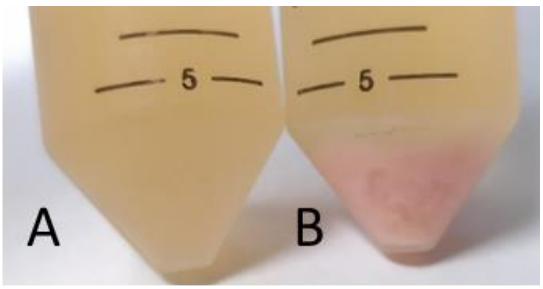

Figure S. 1. Real urine with and without human albumin . (A) Real urine from healthy donors after 18 h at room temperature and static conditions. (B) Real urine from healthy donors with 0.3 mg/mL HA after 18 h at room temperature and static conditions. It can be seen a pink precipitate that indicates the formation of complex between HA and unknown molecules from real urine. These aggregates may be the reason of erratic signals registered by QCM-D sensor surface.

Table S. 2. Bacterial identification by MALDI-TOF. Values between 0 to 1.700, unreliable identification (-), 1.700 to 1.999 probable gender identification (+), 2.000 to 2.299 high probability of gender identification (++) and up to 2.300 high probability of identification (up to +++).

Sample ID	Organism	Puntuation	Extra data
1	*Staphylococcus hyicus*	1.791	C2 ++ A
2	*Proteus vulgaris*	2.339	C4 ++ A
3	*Klebsiella pnemoniae*	2.222	C5 ++ A
4	*Actinomyces hyovaginalis*	2.142	C6 ++ A
5	*Staphylococcus chromogenes*	2.011	C7 +++ A
6	*Citrobacter koseri*	2.453	C8 ++
7	*Pseudomonas aeruginosa*	2.055	C9 ++++ B
8	*Klebsiella pnemoniae*	2.362	
9	*Pseudomonas aeruginosa*	2.122	C9 +++
10	*Pseudomonas aeruginosa*	2.335	C9 ++
11	*Citrobacter koseri*	2.385	C11 ++ A
12	*Pseudomonas aeruginosa*	2.691	C12 +++ A
13	*Pseudomonas aeruginosa*	2.777	D1 ++
14	*Citrobacter koseri*	2.518	D2 ++ A
15	*Trueperella aborisuis*	2.058	D3 +++ A
16	*Trueperella aborisuis*	1.998	D3 ++
17	*Actinomyces hyovaginalis*	2.313	
18	*Proteus mirabilis*	2.139	B9 ++ C
19	*Proteus mirabilis*	2.443	B10 +++ A
20	*Citrobacter koseri*	2.371	B11 ++++ A
21	*Citrobacter koseri*	2.158	C1 ++
22	*Pseudomonas aeruginosa*	2.081	C2 ++ A
23	*Pseudomonas aeruginosa*	2.035	C3 ++
24	*Proteus vulgaris*	2.271	C4 B
25	*Proteus vulgaris*	2.293	C5 +++ A
26	*Escherichia coli*	2.382	C6 +++ B
27	*Proteus vulgaris*	2.451	C8 ++
28	*Proteus vulgaris*	2.389	C9 +++ A
29	*Escherichia coli*	2.033	C10 +++ B
30	*Proteus vulgaris*	2.113	C11 ++ A
31	*Citrobacter koseri*	2.930	C12 +++ A
32	*Staphylococcus chromogenes*	1.999	D1 +++ A
33	*Proteus mirabilis*	1.982	D2 ++ A
34	*Staphylococcus chromogenes*	2.033	D3 ++++ A

35	*Klebsiella pnemoniae*	2.068	D5 ++
36	*Klebsiella pnemoniae*	2.129	D6 +++ A
37	Non-identify natural microbiota		D7
38	Non-identify natural microbiota		D8
39	Non-identify natural microbiota		D9
40	Non-identify natural microbiota		D10
41	Non-identify natural microbiota		D11
42	Non-identify natural microbiota		D12

ANNEX Chapter IV

Table S. 3. Exclusion criteria to mini pigs *in vivo* study.

GENERAL SIGNS	OBSERVATIONS
GENERAL APPEARANCE	0. Normal 1. Less activity than normal 2. Lesions/poor condition
BEHAVIOUR	0: normal, curious and active animal that has a normal response to manipulation 1: animal apathetic but responding in a normal way to manipulation 2: apathetic animal which also has an abnormal response to manipulation (no response or aggression)
SECRETIONS (BODY ORIFICES)	0: no secretions 1: mild secretions 2: severe/purulent secretions or haemorrhage
HYDRATION STATUS	0: hydrated animal 1: persistent skin crease 2: persistent skin crease and sunken eyes
MUCOUS COLORATION	0: normal 1: pale 2: extreme paleness
URINATION AND DEFECATION	0. Normal amount and appearance 2. Abnormal amount and appearance
VULVA/VAGINA APPEARANCE	0: normal 1: lightly redness 2: severe redness
WATER AND FOOD INTAKE	0: expected consumption, little food left 1: decrease in intake 2: no ingestion
BODY TEMPERATURE	0: Normal temperature (38 - 40ºC) 2: Fever> 40ºC

Table S. 4. Histopathology images, in vivo study with catheterized pigs for 15 days

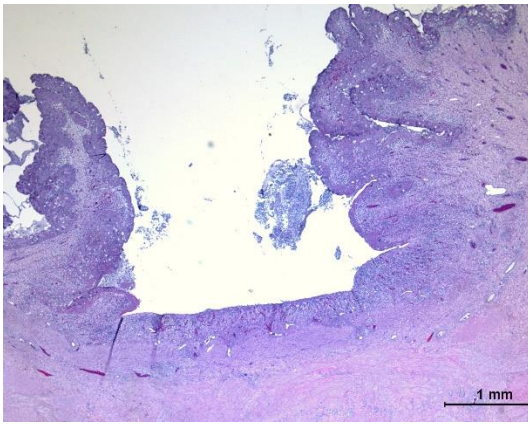

ID10 (Modified) Urinary bladder vertex

Focal ulcerative lesion crater form and very circumscribed. The rest of the mucosa is free of inflammation, so it is speculated that it is of traumatic origin during catheterization of the animal

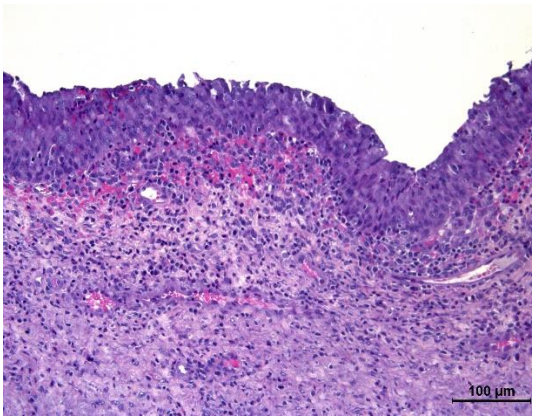

ID10 (Modified) Urinary bladder trine

Mixed inflammation mononuclear (MN) and polymorphonuclear (PMN) diffuse that affects the entire mucosa. Mild-moderate exocytosis. Presence of a very discrete microulceration.

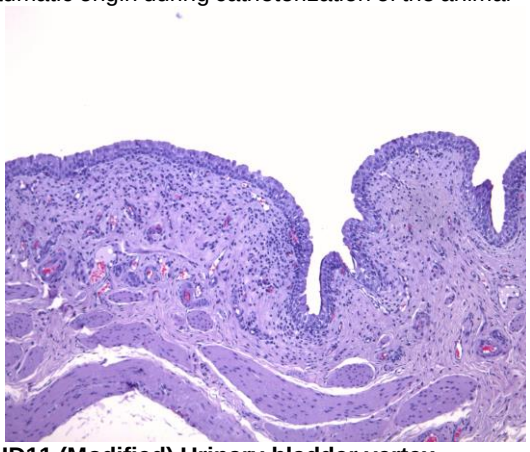

ID11 (Modified) Urinary bladder vertex

Mild multifocal inflammation. Slight discrete accumulations MNs (lymphoplasmocytic)

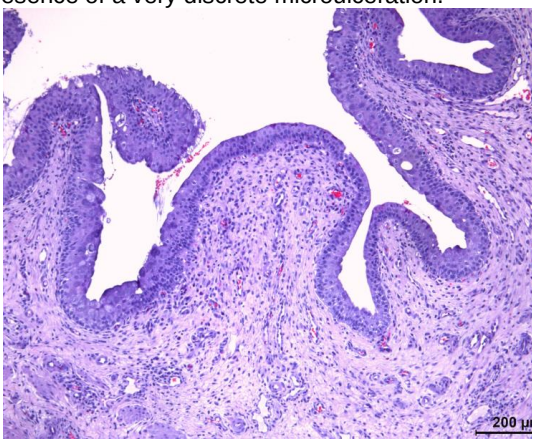

ID11 (Modified) Urinary bladder trine

Mild multifocal inflammation. Discreet accumulations MNs (lymphoplasmocytic) and dispersed PMNs, all of a mild nature

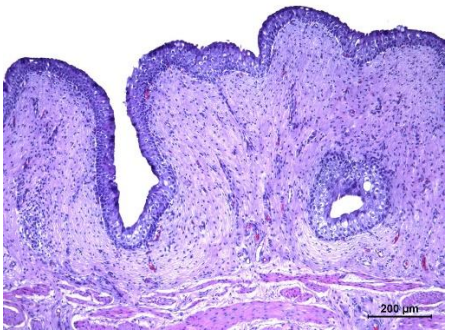

ID12 (Modified) Urinary bladder vertex
No apparent lesions

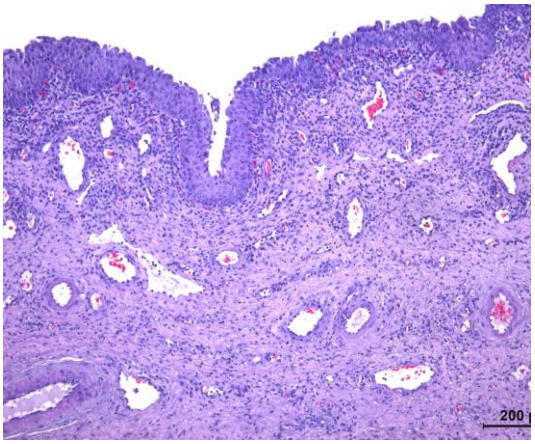

ID12 (Modified) Urinary bladder trine
Intense diffuse mononuclear inflammation with mild-moderate epithelial exocytosis. Focal Ulceration

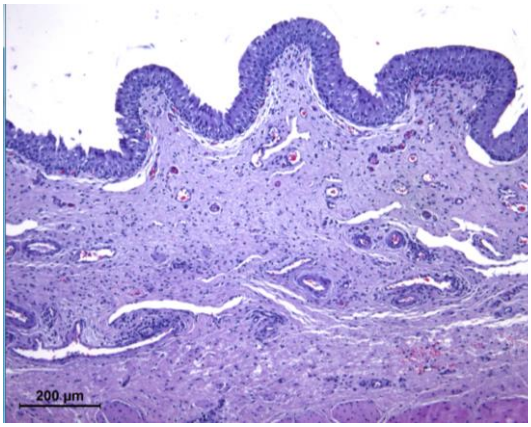

ID12 (Modified) Urinary urethra
No apparent lesions

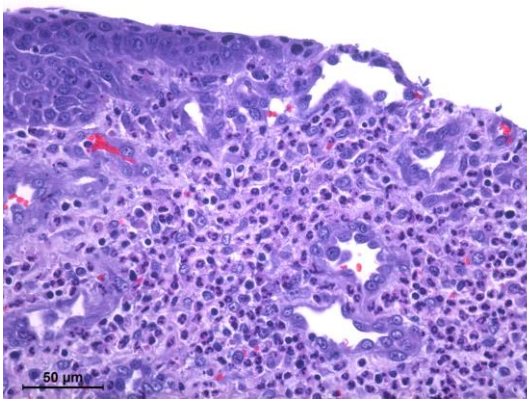

ID13 (Uncoated commercial) Urinary bladder vertex
Diffuse purulent inflammation with mild-moderate epithelial exocytosis. Probably multifocal ulcers. Intense vascular activation.

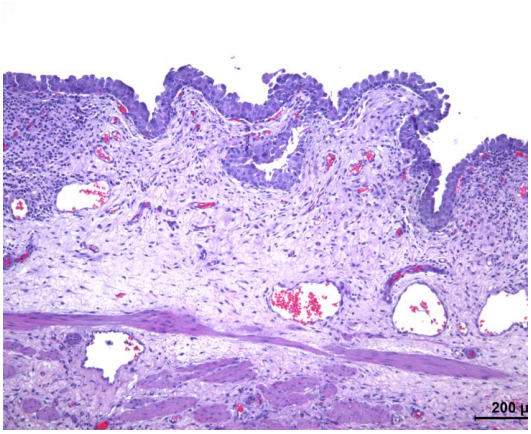

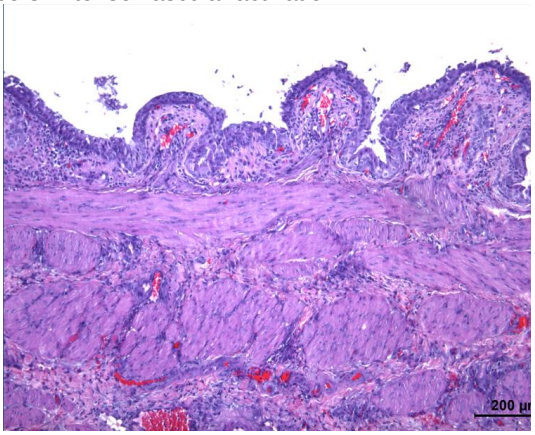

ID13 (Uncoated commercial) Urinary bladder trine

Mild discrete multifocal inflammation of character MN (lympoplasmocytic and macrophage). Intense congestion.

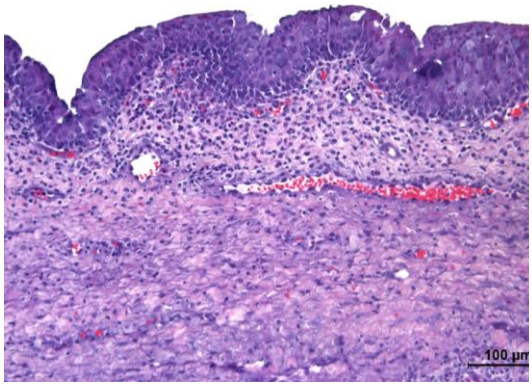

ID14 (Uncoated commercial) Urinary bladder Vertex

Perivascular to diffuse inflammation of predominantly MN character but with dispersed presence of PMNs.

Mild-Moderate Intensity.

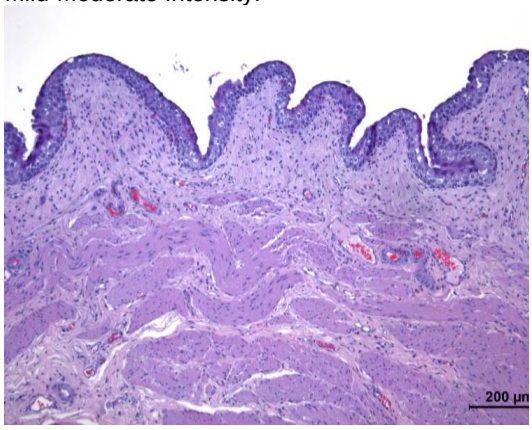

ID14 (Uncoated commercial) Urethra

Very discrete multifocal mononuclear aggregates.

ID13 (Uncoated commercial) Urethra

Mild scattered inflammation in which, eventually, scarce accumulations of PMNs are seen in the mucosa.

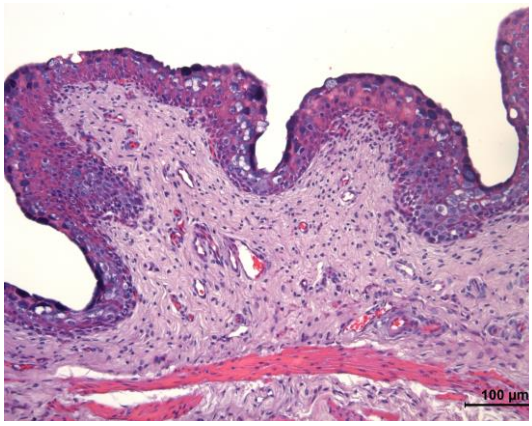

ID14 (Uncoated commercial) Urinary bladder trine

No apparent lesions.

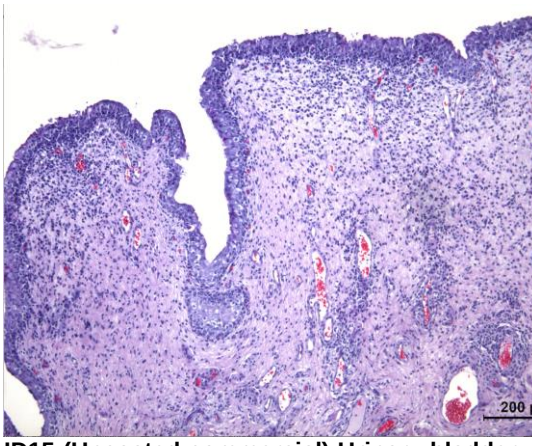

ID15 (Uncoated commercial) Urinary bladder vertex

Diffuse increase in mixed inflammatory cellularity (leukocytes, Mos, and PMNs). Moderate perivascular accumulations of mixed inflammation.

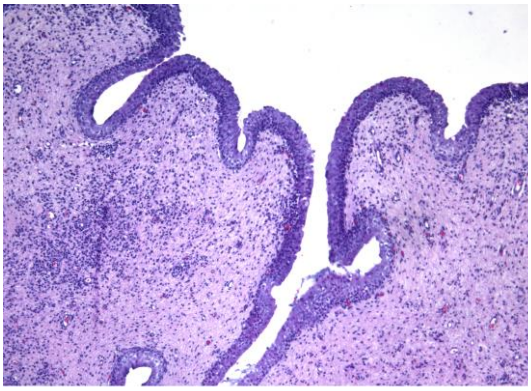

ID15 (Uncoated commercial) Urinary bladder trine

Mild perivascular inflammatory clusters of predominant MN character.

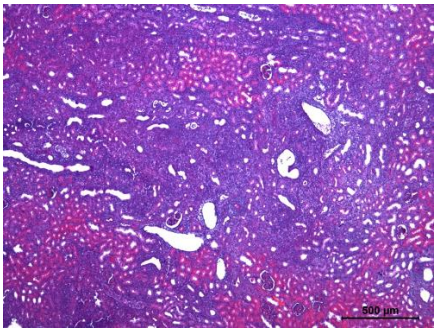

ID15 (Uncoated commercial) Kidneys

Moderate generalized multifocal segmental interstitial-segmental inflammation of predominant MN character. Presence of mild dispersed cellularity in renal pelvis.

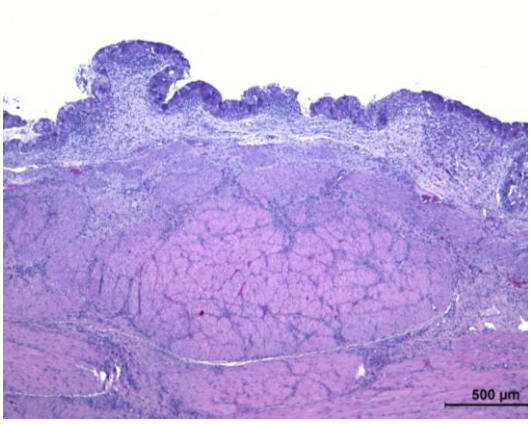

ID17 (Antimicrobial commercialex) Urinary bladder vertex

Mixed dispersed inflammation without obvious perivascular accumulations. Moderate-intense neutrophilic epithelial exocytosis.

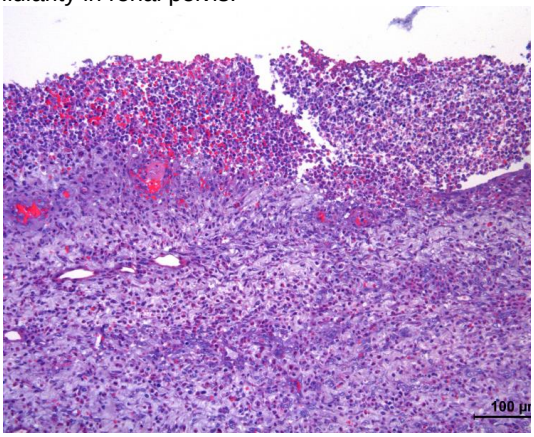

ID17 (Antimicrobial commercialex) Urinary bladder trine

Scattered presence of PMNs in the mucosa of a mild nature, but with neutrophilic evident epithelial exocytosis. Intense diffuse purulent-necrotizing inflammation that affects deep muscle layers and serous organ (probable traumatic fistulization).

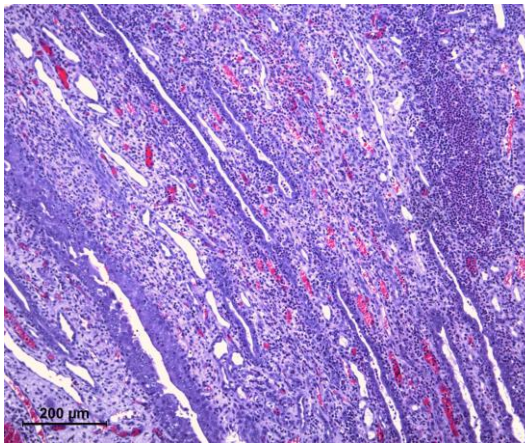

ID17 (Antimicrobial commercialex) Kidneys

Interstitial multifocal-segmental inflammation of predominant purulent character and severe intensity. Concomitant inflammation in the renal pelvis.

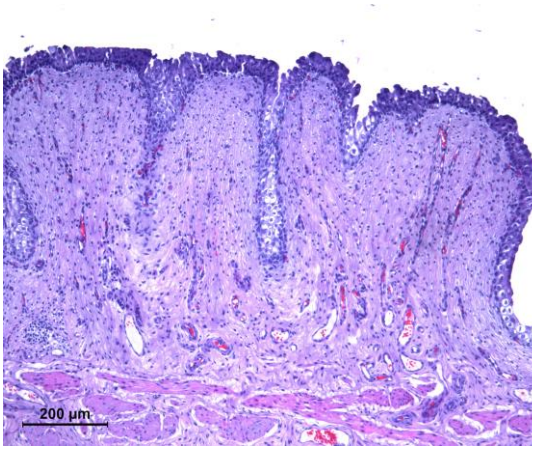

ID18 (Antimicrobial commercialex) Urinary bladder vertex

Very slight scattered perivascular inflammatory accumulations (almost negligible).

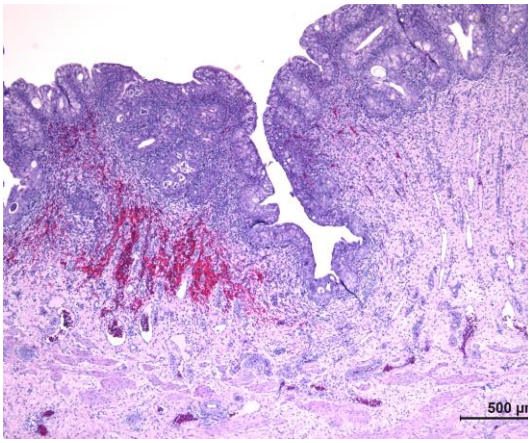

ID18 (Antimicrobial commercialex) Urinary bladder trine

Perivascular to diffuse mixed inflammation, focally intense with evident epithelial exocytosis -even intraepithelial microabscesses-.

The unaffected mucosa remains unscathed.

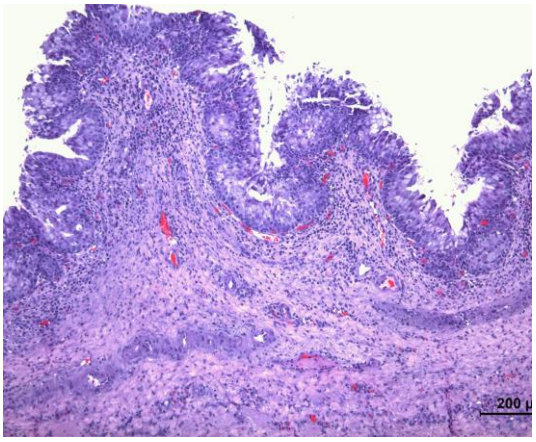

ID18 (Antimicrobial commercialex) Urethra

Intense perivascular-diffuse inflammation of the mucosa